Photodynamic inactivation – the role of ions and future application perspectives

Dissertation

Zur Erlangung des Doktorgrades der Naturwissenschaften (Dr. rer. nat.)

der Fakultät für Biologie und Vorklinische Medizin der Universität

Regensburg

Vorgelegt von

Daniel Bernhard Eckl

Aus

Oberviechtach

Im Jahr

2022

Diese Arbeit wurde von Januar 2019 bis April 2022 am Lehrstuhl für Mikrobiologie der Universität Regensburg sowie an der Klinik und Poliklinik für Dermatologie am Universitätsklinikum Regensburg durchgeführt.

Das Promotionsgesuch wurde eingereicht am 14.04.2022

Diese Arbeit wurde von den Mentor*innen Dr. Harald Huber, Prof. Dr. Wolfgang Bäumler und Prof. Dr. Dina Grohmann angeleitet.

Prüfungsausschuss:

Vorsitzender: Prof. Dr. Stephan Schneuwly

1. Gutachterin: Prof. Dr. Dina Grohmann

2. Gutachter: Prof. Dr. Wolfgang Bäumler

3. Prüfer: Prof. Dr. Winfried Hausner

Unterschrift:

Daniel B. Eckl

Photodynamic inactivation – the role of ions, the search for resistances and future application perspectives

Dissertation

For achieving the doctoral degree of natural sciences (Dr. rer. nat.) at the faculty of Biology and Preclinical Medicine at the University of Regensburg

By

Daniel Bernhard Eckl

From

Oberviechtach

2022

This work was carried out from January 2019 to April 2022 at the Department of Microbiology at the University of Regensburg and at the Clinic and Polyclinic for Dermatology at the University Hospital Regensburg.

The doctoral application was submitted on 14.04.2022.

This work was supervised by the mentors Dr. Harald Huber, Prof. Dr. Wolfgang Bäumler and Prof. Dr. Dina Grohmann.

Examination board:

Chairman: Prof. Dr. Stephan Schneuwly

1st reviewer: Prof. Dr. Dina Grohmann

2nd reviewer: Prof. Dr. Wolfgang Bäumler

3rd examiner: Prof. Dr. Winfried Hausner

Signature:

Daniel B. Eckl

Index

Scientific contributions

Published manuscripts

Manuscripts before PhD program

Daniel Bernhard Eckl[*], Linda Dengler[*], Marina Nemmert, Anja Eichner, Wolfgang Bäumler, Harald Huber[†]: A Closer Look at Dark Toxicity of the Photosensitizer TMPyP in Bacteria. Photochem Photobiol. 2018 Jan;94(1):165-172. doi: 10.1111/php.12846.

Manuscripts during PhD program

Maja Schreiner, Wolfgang Bäumler, **Daniel Bernhard Eckl**, Andreas Späth, Burkhard König, Anja Eichner[†]: Photodynamic inactivation of bacteria to decolonize meticillin-resistant Staphylococcus aureus from human skin. Br J Dermatol. 2018 Dec;179(6):1358-1367. doi: 10.1111/bjd.17152.

Anja Eichner, Thomas Holzmann, **Daniel Bernhard Eckl**, Florian Zeman, Michael Koller, Michaela Huber, Sylvia Pemmerl, Wulf Schneider-Brachert, Wolfgang Bäumler[†]: Novel photodynamic coating reduces the bioburden on near-patient surfaces thereby reducing the risk for onward pathogen transmission: a field study in two hospitals. J Hosp Infect. 2020 Jan;104(1):85-91. doi: 10.1016/j.jhin.2019.07.016.

Daniel Bernhard Eckl[†], Harald Huber, Wolfgang Bäumler: First Report on Photodynamic Inactivation of Archaea Including a Novel Method for High-Throughput Reduction Measurement. Photochem Photobiol. 2020 Jul;96(4):883-889. doi: 10.1111/php.13229.

Daniel Bernhard Eckl[*†], Stefanie Susanne Eben[*], Laura Schottenhaml, Anja Eichner, Rudolf Vasold, Andreas Späth, Wolfgang Bäumler, Harald Huber: Interplay of phosphate and carbonate ions with flavin photosensitizers in photodynamic inactivation of bacteria. PLoS One. 2021 Jun 11;16(6):e0253212. doi: 10.1371/journal.pone.0253212.

Wolfgang Bäumler[†], **Daniel Bernhard Eckl**, Thomas Holzmann, Wulf Schneider-Brachert: Antimicrobial coatings for environmental surfaces in hospitals: a potential new pillar for prevention strategies in hygiene. Critical Reviews in Microbiology. 2021. Doi: 10.1080/1040841X.2021.1991271

Larissa Kalb, Pauline Bäßler, Wulf Schneider-Brachert, **Daniel Bernhard Eckl**†: Antimicrobial Photodynamic Coatings Reduce the Microbial Burden on Environmental Surfaces in Public Transportation - a Field Study in Buses. Int. J. Environ. Res. Public Health 2022, 19(4), 2325; https://doi.org/10.3390/ijerph19042325

Submitted manuscripts

Daniel Bernhard Eckl†, Nicole Landgraf, Anja Karen Hoffmann, Laura Schottenhaml, Julia Dirscherl, Nina Weber, Stefanie Susanne Eben, Pauline Bäßler, Anja Eichner, Harald Huber, Wolfgang Bäumler: Inhibitory effects of calcium or magnesium ions on PDI. Submitted to Journal of Photochemistry and Photobiology

Daniel Bernhard Eckl, Nicole Landgraf, Anja K. Hoffmann, Anja Eichner, Harald Huber, Wolfgang Bäumler: The influence of citrate on photodynamic inactivation of bacteria in the presence of bivalent cations, tap water, and synthetic sweat. Submitted to Photochemistry and Photobiology

Preprints

Daniel Bernhard Eckl†, Anja Karen Hoffmann, Nicole Landgraf, Larissa Kalb, Pauline Bäßler, Susanne Wallner, Anja Eichner, Harald Huber, Wolfgang Bäumler: On a photodynamically active hydrogel capable of killing bacteria on the human skin; bioRxiv; 2022; https://doi.org/10.1101/2022.04.10.487760

Conference proceedings

Conference proceedings before PhD program

Poster – Maximilian Mora, **Daniel Bernhard Eckl**, Michael Mauermeier, Christine Moissl-Eichinger: ARBEX - Archaeal and bacterial extremophiles onboard the International Space Station ISS, EANA 2014, Edinburgh

Poster – **Daniel Bernhard Eckl**[1], Linda Dengler[1], Marina Nemmert, Anja Eichner, Wolfgang Bäumler, Harald Huber: New insights into the „dark toxicity“ of the photosensitizer TMPyP in bacteria, 5th Joint Conference of the DGHM & VAAM 2017, Würzburg

Conference proceedings during PhD program

Poster – **Daniel Bernhard Eckl**, The role of ions in photodynamic inactivation, 6th Joint Conference of the DGHM & VAAM 2020, Leipzig

Poster – **Daniel Bernhard Eckl**, Anja K. Hoffmann, Nicole Landgraf, Anja Eichner, Harald Huber, Wolfgang Bäumler: Decolonization of human skin by application of a photodynamically active hydrogel, 19th Congress of the European Society for Photobiology 2021, Salzburg

Poster – **Daniel Bernhard Eckl**, Anja K. Hoffmann, Nicole Landgraf, Anja Eichner, Harald Huber, Wolfgang Bäumler: Decolonization of human skin by application of a photodynamically active hydrogel, 19th Congress of the European Society for Photobiology, 73. DGHM-Jahrestagung 2021, Berlin

Talk – **Daniel Bernhard Eckl**, Anja K. Hoffmann, Nicole Landgraf, Anja Eichner, Harald Huber, Wolfgang Bäumler, Decolonization of human skin by application of a photodynamically active hydrogel, 6th International Conference on Prevention & Infection Control (ICPIC) 2021, Geneva

*: contributed equally

†: corresponding author

Abstract

The careless use of antibiotics led to the emergence of multi-resistant bacteria responsible for 700,000 deaths annually, estimates even predict 50 million annual deaths as of 2050 - especially since new antibiotics are unlikely to be introduced. To counteract this development, new approaches are urgently needed. In both medicine and hygiene, photodynamic inactivation (PDI) can make its contribution in the treatment of human skin or the use of antimicrobial surfaces. In PDI, highly reactive singlet oxygen ($^1O_2$), responsible for the antimicrobial effect, is formed based on a photosensitizer (PS). PDI shows excellent activity in a controlled laboratory environment, but applications under real live conditions require considerably higher PS concentration or light doses. This hampers the application and requires purposeful research to unfold these obstacles. The aim of this work was to elucidate which substances and processes are involved in this effect to overcome those obstacles, in particular for PDI on human skin. Investigated substances were Na^+, Ca^{2+} or Mg^{2+} as well as CO_3^{2-} and PO_4^{3-}, especially relevant for applications under real life conditions. It was hypothesized, if citrate might circumvent detrimental effects via complexation in artificial solutions containing Ca^{2+} or Mg^{2+} and in tap water or synthetic sweat. The synthetic sweat contained several ions and organic molecules like histidine. Lastly, the results were transferred to the human skin with a PS-hydrogel.

Initially, a procedure was established for an efficient investigation of the physical and chemical processes of PDI using SAPYR, a phenalene-based PS as well as the porphyrin TMPyP on *Halobacterium salinarum*, which requires high NaCl concentrations for growth. It was found that the PS did not change in the high salt environment, still generated $^1O_2$, and were able to induce a reduction of viable cells of at least 99.9%. In the next part of this work, it was found that flavin derivatives FLASH-02a and FLASH-06a undergo a chemical reaction with CO_3^{2-} or PO_4^{3-}. Consequently, the PS stops generating $^1O_2$, accompanied by a quasi-absence of PDI. Similarly, it was shown that regardless of the PS Ca^{2+} and Mg^{2+} have drastic effects on antimicrobial potential. Although the tested PS (methylene blue, TMPyP, SAPYR, FLASH-02a and FLASH-06a) remained chemically intact and generated $^1O_2$ a reduced efficacy was demonstrated. Based on this, citrate as chelator was used to circumvent the negative influence of Ca^{2+} and Mg^{2+} and at least for Gram-negative bacteria efficacy was improved. In this context, experiments were also carried out in tap water and synthetic sweat. It was observed that especially histidine in sweat is primarily responsible for an inhibitory effect on PDI. As a final step, the knowledge about inhibitory substances in PDI

was used to develop a SAPYR-hydroxyethyl cellulose hydrogel. The hydrogel also contained citrate to circumvent the detrimental effects of Ca^{2+} and Mg^{2+}. In all cases, bacterial reduction on human skin was greater than or close to 99.99%. Apoptosis and necrosis did not occur in the skin tissue despite treatment with the PS-hydrogel.

The results of this work are of great relevance for the transfer of PDI from laboratory to applications under real life conditions. The data obtained can be used to adapt the application of PDI in Ca^{2+} and Mg^{2+}-rich environments like tap water and skin. In the field of dentistry, where PDI is already used, it is advisable to possibly add a washing step with citrate solution to existing protocols to increase effectiveness. The PS-hydrogel could have the greatest contribution to solving the problems mentioned above with multidrug-resistant germs, since it has been shown that good efficacy can be achieved on the skin under acceptable treatment conditions. Finally, many currently used antibiotics or antiseptics in the treatment or prevention of SSTIs already show resistances to the substances used. However, PDI is unlikely to provoke resistance in bacteria because the generated $^1O_2$ damages almost all biomolecules via oxidative mechanisms. In this way, the PS-hydrogel described in this thesis may possibly provide a partial answer to the questions of the post-antibiotic age that is upon us.

Zusammenfassung

Der sorglose Umgang mit Antibiotika führte zur Entstehung multiresistenter Bakterien, welche jährlich für 700.000 Todesfälle verantwortlich sind, Schätzungen gehen sogar von 50 Millionen jährlichen Todesfällen ab 2050 aus - zumal die Entdeckung neuer Antibiotika unwahrscheinlich ist. Um dem entgegenzuwirken, werden dringend neue Ansätze benötigt. Sowohl in der Medizin als auch in der Hygiene kann die photodynamische Inaktivierung (PDI) ihren Beitrag zur Behandlung menschlicher Haut oder beim Einsatz antimikrobieller Oberflächen leisten. Bei der PDI wird hochreaktiver Singulett-Sauerstoff ($^1O_2$), der für die antimikrobielle Wirkung verantwortlich ist, auf der Basis eines Photosensibilisators (PS) gebildet. Experimente mit PDI zeigen eine ausgezeichnete Aktivität in kontrollierter Laborumgebung, aber Anwendungen unter realen Bedingungen erfordern wesentlich höhere PS-Konzentrationen oder Lichtdosen. Dies erschwert die Anwendung und erfordert gezielte Forschung, um diese Probleme zu beseitigen. Ziel dieser Arbeit war es, herauszufinden, welche Substanzen und Prozesse an diesem Effekt beteiligt sind und wie ein Umgehen dieser möglich ist, insbesondere für PDI auf der menschlichen Haut. Bei den untersuchten Substanzen handelte es sich um alltagsrelevante Ionen wie Na^+, Ca^{2+}, Mg^{2+}, CO_3^{2-} und PO_4^{3-}. Es wurde die Hypothese aufgestellt, ob Citrat die inhibierende Wirkung durch Komplexierung umgehen kann, insbesondere in Leitungswasser oder synthetischem Schweiß, welche Ca^{2+} oder Mg^{2+} enthalten. Der synthetische Schweiß enthielt dabei verschiedene Ionen und organische Moleküle wie Histidin. Letztlich wurden die Ergebnisse mit Hilfe eines PS-Hydrogels auf die menschliche Haut übertragen.

Zunächst wurde ein Versuchsablauf zur effizienten Untersuchung der physikalischen und chemischen Prozesse von PDI entwickelt. Unter Verwendung von SAPYR, einem Phenalenon, sowie des Porphyrins TMPyP wurde auch die antimikrobielle Wirksamkeit auf *Halobacterium salinarum* untersucht, welches hohe NaCl-Konzentrationen für sein Wachstum benötigt. Daraus resultierte, dass sich die PS auch bei hoher Salzkonzentration nicht veränderten, immer noch $^1O_2$ generieren und in der Lage waren, die lebensfähigen Zellen um mindestens 99,9 % zu reduzieren Der nächste Teil dieser Arbeit zeigte, dass die Flavine FLASH-02a und FLASH-06a eine chemische Reaktion mit CO_3^{2-} oder PO_4^{3-} eingehen. Infolgedessen erzeugten die PS kein $^1O_2$ mehr, was mit einem Ausbleiben der PDI einhergeht. Ebenso wurde gezeigt, dass unabhängig vom PS Ca^{2+} und Mg^{2+} drastische Auswirkungen auf das antimikrobielle Potenzial besitzen. Obwohl die getesteten PS (Methylenblau, TMPyP, SAPYR, FLASH-02a und FLASH-06a) chemisch intakt blieben und $^1O_2$

erzeugten, wurde eine geringere Wirksamkeit nachgewiesen. Daraufhin wurde Citrat als Chelator eingesetzt, um den negativen Einfluss von Ca^{2+} und Mg^{2+} zu verringern. Dabei wurde zumindest für Gram-negative Bakterien eine bessere Wirksamkeit erzielt. In diesem Zusammenhang wurden auch Versuche in Leitungswasser und synthetischem Schweiß durchgeführt. Es zeigte sich, dass vor allem Histidin im Schweiß für eine hemmende Wirkung auf PDI verantwortlich ist. In einem letzten Schritt wurde das Wissen über hemmende Substanzen eingesetzt, um ein SAPYR-Hydroxyethylcellulose-Hydrogel zu entwickeln. Das Hydrogel enthielt zusätzlich Citrat, um die nachteiligen Auswirkungen von Ca^{2+} und Mg^{2+} auszugleichen. In allen Fällen lag die bakterielle Reduktion auf menschlicher Haut bei über oder nahe 99,99 %. Apoptose und Nekrose traten im Hautgewebe trotz der Behandlung mit dem PS-Hydrogel nicht auf.

Die Ergebnisse dieser Arbeit sind von großer Bedeutung hinsichtlich der Übertragung von PDI aus dem Labor auf Anwendungen unter realen Bedingungen. Die hierbei gewonnenen Daten können genutzt werden, um die Anwendung von PDI in Ca^{2+} und Mg^{2+}-reichen Umgebungen wie Leitungswasser oder Haut anzupassen. Im Bereich der Zahnmedizin, wo PDI bereits Anwendung findet, ist es ratsam, den bestehenden Protokollen möglicherweise einen Waschschritt mit Citratlösung hinzuzufügen, um die Wirksamkeit zu erhöhen. Das PS-Hydrogel könnte großen Beitrag zur Lösung der oben erwähnten Probleme mit multiresistenten Keimen leisten. Hierbei zeigte sich, dass auf der Haut unter akzeptablen Behandlungsbedingungen eine gute Wirksamkeit erzielt werden kann. Schließlich existieren bereits gegen viele der zur Behandlung oder Vorbeugung eingesetzten Antibiotika oder Antiseptika Resistenzen. Dass PDI bei Bakterien eine Resistenz hervorruft, gilt als unwahrscheinlich, da das erzeugte $^1O_2$ fast alle Biomoleküle über oxidative Mechanismen schädigt. Auf diese Weise könnte das in dieser Arbeit beschriebene PS-Hydrogel möglicherweise eine Teilantwort auf die Fragen des post-antibiotischen Zeitalters geben, das uns bevorsteht.

General Introduction

Infectious diseases

Over the course of mankind, severe bacterial infectious diseases have emerged quite often. A prominent example is also the plague – a disease caused by the Gammaproteobacterium *Yersinia pestis* [1] that leads, untreated, to death in most cases. In the 14th century, it is estimated that the plague was responsible for 50 million deaths in Europe alone [2]. Thankfully, days in which an infection with *Y. pestis* posed a dramatic problem are nowadays in modern societies a thing of the past. It should be noted that some *Y. pestis* infections still occur in some low-income countries with impeded access to population wide medical care – between 2010 and 2015 around 3,248 cases were reported [3].

As luck would have it, it was mainly due to the discovery of penicillin by Alexander Fleming [4–6] that made it possible for humanity to treat most of the bacterial infections for more than six decades now easy, cheap, efficiently and quick. There is a vast amount of data supporting this statement as infectious diseases became rarer since the discovery of antibiotic therapy. In the pre-antibiotic era, a quarter of all deaths in Germany was caused by infectious diseases [7], 75% that suffered from an infectious disease died unless a chirurgical intervention took place quite immediately after infection [8].

Even in 1930, over 300,000 US citizens died of pneumonia and tuberculosis, accounting for 22% of the annual deaths in the US that year [9]. After the distribution of antibiotics, death rates caused by infections in general dropped down to 6% in 1953 [9] and 4.6% in 1989 [10]. Since the late 90's, this rate stayed more or less constant, only few deaths are nowadays accounted to bacteria, most of the infectious disease fatalities are caused by viral infections [11]. Humanity therefore was in a convenient position when it came to the treatment of bacterial infections. Yet, already Fleming warned researchers in his Nobel prize speech that bacteria will develop resistances, if the administration of antibiotics is not carefully pondered [4]. However, Fleming's warning found only little hearing. Although from 1940 to 1962 over 20 chemical classed of novel antibiotics were discovered or synthesized [12], resistances emerged soon after the introduction to the market [13]. Figure 1 displays major cornerstones in antibiotic research history by the discovery of novel antibiotic classes. Accordingly, the first emergence of the corresponding resistance to that antibiotic class is given. It becomes obvious that resistances inevitably emerge in the bacterial population sooner or later. While for a long time the arms race between researchers and bacteria was balanced,

at least as new types of antimicrobial substances were discovered, the situation has changed dramatically in the past three decades as no new antibiotics were discovered.

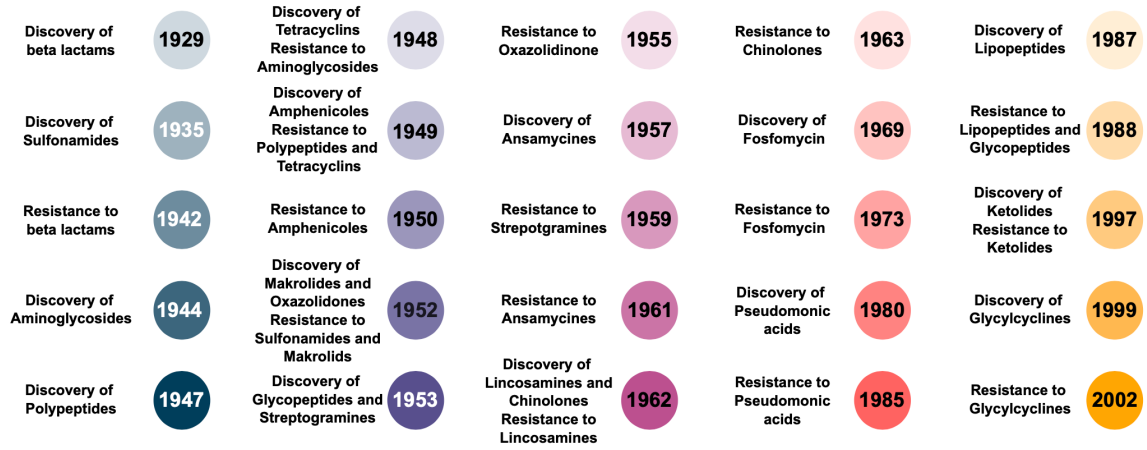

Figure 1: Important cornerstones of antibiotic research and first emergence of an antibiotic resistance. The years are derived from either the first report of the antibiotic from the respective class or from the first scientific report of the emerged resistance. Figure based on [14–48].

Meanwhile, the situation is more severe than ever. In 2017, the WHO published a priority list displayed in figure 2 in order to encourage science and industry to research and develop novel antibiotics, innovative processes or creative alternatives [49]. Most urgent needs in R&D are necessary – concerning the published list – with carbapenem-resistant *Acinetobacter baumanni*, causing wound infections, pneumonia, and meningitis. As equally urgent the WHO assessed multiresistant *Pseudomonas aeruginosa* strains and representatives of the *Enterobacteriaceae*. Further intensive research should be dedicated to *Enterococcus faecium*, *Staphylococcus aureus*, *Helicobacter pylori*, *Campylobacter* spp., *Salmonella* spp. and *Neisseria gonorrhoeae*. Due to the extensive use of antibiotics, the WHO published a list that contains important last resort antibiotics that should consequently only be used in life-threatening cases [50].

Figure 2: Detailed WHO Priority List of Pathogens for the research and development of antibiotics. The list is comprised out of three categories, namely critical, high, and medium. Figure based on the official information of the WHO [49].

The problems that are caused by antibiotic resistant microorganisms have reached tremendous extents and are a serious threat to public health [51]. In Europe, estimates of the ECDC (European Centre for Disease Control) account up to 33,000 deaths annually to multi-drug resistant bacteria [52], which is in good agreement with a study conducted by independent researchers [53] but doubted by other researches estimating the number of deaths to be lower [54]. For the US on the other hand, the CDC attributes 35,000 deaths to multi-drug resistant bacteria [55] which some researchers have found this to be a critically underestimation stating that around 150,000 deaths are caused by such organisms per year [56]. Worldwide, the World Health Organization estimates that yearly 700,000 people die due to multi-drug resistant bacteria [57]. A bold and admittedly discussed prediction stated that in 2050 over 50 million people might die annually due to antimicrobial resistant bacteria [58]. However, decision makers in politics and health economy rather tend to adjudicate based on economic measurements which shall be briefly taken into consideration here as well. Hospital acquired infections, often caused by multi-drug resistant bacteria [59–61], cause bloodstream infections, pneumonia, surgical site infections and urinary tract infections. One case of a patient with bloodstream infection causes expenses of up to 45,814 USD leading to annual costs of 3.3 billion USD in the US alone – all hospital acquired infections

associated expenditures combined cause costs of nearly up to 10 billion USD annually [62]. Estimations from Europe suggest that HAIs cause a financial loss in all EU countries of 7 billion EUR [63], in Germany alone for the year 2011 1.55 billion EUR [64]. It is clear that this situation is going to get more dramatic over time as the antibiotic innovation gap is far from closing, several authors around the world stated numerous times that the antibiotic innovation pipeline is dry, partly also due to the consideration of economic aspects [65–71].

Attempts to solve the antibiotic crisis

Based on this dramatic situation, scientists, and physicians all over the world have come up with methods to cope with hospital acquired infections and multidrug resistant bacteria. General measures to be taken as soon as possible are for instance the reduction of antibiotics used in food industry and livestock as part of the one health approach [72] and the so-called antibiotic stewardship, which includes for example restricting the sale of antibiotics to prescriptions [73]. Besides these two more general measures, in the following further innovative examples shall be mentioned. These more or less novel approaches can be split up roughly in two major categories, which complement each other in synergistic ways: the development of novel treatment strategies and hygiene-based approaches.

Examples of alternative treatments for multi drug resistant bacteria

Concerning treatment alternatives, several approaches might tackle the current situation appropriately. First, there is the development of vaccines to be mentioned. For example, Valneva is currently working on a *C. difficile* vaccine that passed phase 2 trials [74], Pfizer had a vaccine against *S. aureus* in a rather unsuccessful phase 2 trial [75] and Intercell in cooperation with the university of Vienna tries to tackle *P. aeruginosa* based on a vaccine [76]. Vaccination approaches more of a scientific nature are researched for example concerning *E. coli* [77,78].

Another well-known alternative to antibiotics is the administration of antibodies against the pathogens itself or the toxins they produce. These antibodies have been investigated intensively on the academic level [79–83], mostly targeted against *C. difficile* [84,85], *S. aureus* [80,84] and *P. aeruginosa* [83]. Furthermore, probiotics of non-toxic *C. difficile* strains might help to cope with these infections, several probiotic preparations are in development right now [86]. Lysins that hydrolyze the bacterial murein of for example *S. aureus* are being developed by iNtRON and ContraFect [87,88].

A less promising approach is the attempt to stimulate the immune system of patients by bacterial extracts [89], phenylbutyrate [90] or vitamin D3 [91]. However, immune stimulation might pose some synergistic effects with other mentioned applications in the future. The stimulation of the immune system comes besides that also with various contraindications as it cannot be successfully administered in patients with immune system deficits.

The therapy of patients with bacteriophages seems to be very promising but are in the urgent need for further research. Currently, the use of wild-type phages is investigated on *P. aeruginosa* and *S. aureus* by Armata Pharmaceuticals [92]. Modern molecular biology has additionally opened the door for genetically engineered phages, currently studied in a pre-clinical phase study against *P. aeruginosa* [93].

Lastly, there is also great effort put into the development of novel antimicrobial peptides as they have, compared to most of the latter mentioned methods, a much broader therapeutic spectrum. Several of these antimicrobial peptides are in the focus of research and just a few years away from transition to clinical trials [94–98].

Besides these mentioned alternatives, photodynamic inactivation might represent a promising method as it has been found to be useful for decolonization of the human skin from *S. aureus* [99]. Photodynamic approaches were also proven to be effective in animal models for example in the treatment of burn wounds [100,101].

Hygiene based improvements concerning hospital acquired infections

The second category to focus on are advances made in hygiene in general as well as in respect to hospital acquired infections. The fact that environmental contamination, hospital acquired infections and hospital hygiene are closely entwined is nowadays widely accepted [102–104]. When it comes to hygiene in general or hospital hygiene in specific, the most obvious measure is thorough cleaning. While this seems like a trivial note, it is in fact not. For example disposable wipes with the addition of further disinfecting chemicals achieves highly efficient logarithmic reduction of the bacterial load on surfaces [105–107], but reusable cloth does not yield as efficient results as for example due to insufficient laundry practice [108,109]. In general, several researchers [110,111] recommended a so-called bundle approach in reducing the environmental contamination in hospitals. This approach includes exact instructions for cleaning staff as well as the standardization of processes as SOPs. Further, the correct choice of the disinfecting agent is of utter importance. The properties that an ideal disinfectant has to fulfil were proposed by several authors and include

for example a broad activity against a variety of microbes as well as good action even in the presence of other substances that are common within the clinical daily business [110,112,113]. However, for hygiene specialists there are helpful tools besides scientific literature that allow to choose appropriate disinfectants for specific uses such as the VAH-list relevant for Germany, providing detailed information concerning the correct application of (commercial) disinfectants [114]. An additional monitoring of cleaning compliance that also includes feedback has also shown to have positive impact on the cleanness of the environment [115–122]. A tutoring led by scientists or physicians specialized in hygiene seems urgently necessary as cleaning staff measures its output most likely by macroscopic cleanness [123]. However, alternative measurement methods besides the removal of macroscopic smut include techniques like ATP-measurement or contact plates come with their own limitations. In general, a microbiologically safe surface should exhibit not more than 2.5 or 5 CFU cm^{-2}, in case of pathogens less than 1 CFU cm^{-2} [124,125]. These values of clean surfaces in general have been introduced by researchers in order to establish benchmarks. These benchmarks of clean surfaces are for example 2.5 CFU cm^{-2} in hospital settings, while in food industry a surface can be considered as clean with 5 CFU cm^{-2} or lower [125,126]. Lastly modern technologies that do not require humans to conduct cleaning seem to be another promising approach as supplemental strategy. In brief, two methods are available here and include automated UV based irradiation [127] or peroxide based vapor [128–130]. However, these methods also come with several drawbacks as for example UV irradiation needs to cope with distance, room geometry, and dust potentially leading to dead zones without sufficient bacterial reduction [131]. Furthermore, UV disinfection is inefficient against endospores and needs to act upon several hours. Drawbacks of peroxide based disinfection are for instance the harmful action towards eyes and skin and its corrosive properties [132].

Especially in the light of the COVID-19 pandemic, antimicrobial coatings started to attract the attention of researchers. Such coatings may be capable of closing hygiene gaps in hospitals and high touch surfaces outside of the hospital. For antimicrobial coatings quite a variety of modes of action are known such as surfaces that reduce the adhesion of bacterial cells [133] or contact-active surfaces that influence in some ways membrane integrity of the cells like cooper [134] or covalently bound quaternary ammonium compounds [135]. Further, there are antimicrobial surfaces known that rely on the release of biocidal substances such as silver [136,137], copper [138], zinc [139], quaternary ammonium compounds [140], iodocarb [141] or isothiazolinone [142] among others. Titanium dioxide surfaces however use photocatalytic reactions to produce oxygen radicals and hydrogen peroxide in

order to inactivate bacteria [143–145]. However, these commonly used antimicrobial surfaces come with some drawbacks as for example they sometimes only show antimicrobial efficacy when the testing is performed under wet conditions or do not show antimicrobial efficacy under real life conditions [146]. Lastly, there are also photodynamically active surfaces known that generate singlet oxygen under visible light and thereby oxidizes bacteria and organic matter [147]. These photodynamically active coatings have been applied successfully just recently in a hospital associated environment [147] as well as in public transportation [148].

History of Photodynamic inactivation and photodynamic therapy

Although the use of photodynamic inactivation on human skin or in self-sanitizing surfaces emerged just recently, the roots of photodynamic inactivation long back to the at least 3,500 BC to ancient Egypt, where plant extracts containing furanocoumarins of *Ammi majus* were used to treat pigmentation defects of the skin [149,150]. Similar treatment approaches seem to have developed independently in ancient India and China as well as in Rome, Greece, and the Near East [149,151,152].

However, the first scientific literature report for photodynamic inactivation longs back to the year 1900 where in Munich Oscar Raab conducted experiments in the lab of Hermann von Tappeiner, studying the toxicity of acridine towards to the protozoon *Paramecium caudatum* [153]. They recognized that the toxicity varied and they speculated about some sort of light-dependent mechanism, finally validated by data generated by Raab, von Tappeiner and Jodlbauer [154,155]. However, von Tappeiner wrongly attributed this toxicity effect to florescence-based mechanisms, and not, as known today, to the generation of reactive oxygen species. Despite this flawed explanation on the cause of the toxicity, they were already aware of the potential that their discovery might bear [156]. Already in its earliest days, the photodynamic research split up in two major categories namely the application of the method towards bacteria [157] and the treatment of carcinoma [158]. However, the discovery of Raab and von Tappeiner did not spark greatly within the scientific community by that time as only few further reports are known, maybe also owed to the two world wars that forced science rather to focus on the research on antibiotics [159]. Cyanine based photosensitizers however found use in wound disinfection in the first world war, whereas it is not clear if the researchers at that time were aware of the photodynamic processes that facilitated the antiseptic effect [160]. Phenothiazine based photosensitizers were among the first photosensitizers that were used for the photodynamic inactivation of viruses, first reports long back

to the year 1928 [161]. One note from 1948 by Figge and co-workers described tumors in mice that specifically take up and accumulate porphyrins [162], further described in a study from 1955, where intravenously administered hematoporphyrin led to selective fluorescence in cancerous tissue [163]. The findings of Figge and co-workers were later in the 1960s validated by another independent workgroup rather focusing on the diagnostic possibility of the described specific accumulation [164,165]. A group from the University of California was the first one in 1972 to be really capable of showing cytotoxicity in cell culture as well as in *in vivo* experiments with hematoporphyrin [166]. From a nowadays perspective, one might speculate that this preliminary communication of Ivan Diamond *et al.* facilitated the establishment of the term photodynamic therapy, in short PDT, for the described method towards malignant tumors. Phenothiazines were found to be effective against Herpes simplex viruses in laboratory situations as well as in a clinical study since the 1970s [167,168]. However, significant scientific progress in the field of photodynamics was made by Thomas Dougherty in the 1970s. Dougherty's lab started with experiments of hematoporphyrin successfully destroying murine cancerous tissue [169] and moved soon on to experiments in humans [170] with prosperous advances in treating breast cancer [171].

Dougherty also postulated some properties photosensitizers should possess [170,172], which still apply in nearly all its cornerstones up to today [173]. First, a photosensitizer should not be toxic to cells in therapeutic doses. Second, the dye should accumulate either somewhere inside or in the vicinity of the targeted cells. Third, the substance used for photodynamic processes, must be, of cause, photodynamically active. Last, within the scope of tumor therapy, the wavelength of the light should be around 600 nm due to the deeper penetration depth of the light into human tissue. This last-mentioned point however is only crucial when inactivation aims for antitumoral therapy, for most antimicrobial applications the wavelength of the light and the matching absorption spectrum of the photosensitizer is only of minor importance, as penetration depth is not as crucial. While Dougherty and colleagues made outstanding progress in the area of PDT, the photodynamic inactivation of bacteria or short PDI started to emerge slowly as its own field of research. Bertoloni and co-workers were looking for alternative models to study the efficacy of hematoporphyrins and suggested the use of various *Candida* sp. as fungal organism and *E. coli*, *K. pneumoniae*, *S. aureus* and *Enterococcus hirae* [174]. However, while Gram-positives were readily inactivated, Gram-negatives just were not inactivated as efficiently and many efforts focused on *S. aureus* as an organism to investigate the effects of PDI [175–178]. First attempts in optimizing the PDI towards Gram-negatives were then attempted by Ehrenberg and colleagues by the utilization of lipid vesicles

to which derivatives of hematoporphyrin were attached [179]. It was the same researchers that recognized the problem in antibacterial photodynamic inactivation is the Gram-negative envelope as *E. coli* spheroplasts behaved in similar manners as intact *S. aureus* cells. Further, polymyxin b nonapeptide [180,181] in combination with hematoporphyrin made the Gram-negative envelope permeable for the hydrophobic photosensitizer [182].

In the 1990s, further advances were made in clinical treatment to counteract the degeneration of the macula [183]. Interestingly, also within the 1990s, interests seemed to shift a little away from the clinic to the wet lab as researchers aimed to investigate the biological reasons, why the tumoral cells die. Agarwal *et al.* made progress in this case as they initially observed cell death by apoptosis induced through photodynamic treatment [184]. More in detail, Kim *et al.* as well as Xue *et al.* identified bcl-2 as major target in photodynamic therapy that induces cell death [185,186]. Besides apoptosis, autophagy and other pathways seem occur but are rather unrepresented [187–189].

While long time PDT used hematoporphyrin administered via injection, in 1987 researchers found that application of 5-aminolevulinic acid led to the formation of endogenous porphyrins such as protoporphyrin IX [190]. While Kennedy, Pottier and Pross made first significant success in the clinical application [191] further advances in application were made as scientists and physicians began to develop the photodynamic therapy against basal cell carcinoma and actinic keratosis with 5-aminolevulinic acid [192,193]. The substance thereby accumulates mostly in the cancerous tissue and gets thereby metabolized to protoporphyrin IX which then acts as the photodynamic substance. Since then, research in photodynamic therapy – which addresses the specific use of the method towards cancer cells – was pushed forward as a promising therapy method. Finally, this led to the approval of another photodynamically active drug, namely Photofrin®, basically a hematoporphyrin derivative where its use is indicated for treatment of esophagus carcinoma, endobronchial carcinoma and dysplasia of the esophagus [194]. Between 1995 and 1996, the photodynamic inactivation of *Plasmodium falciparum* [195] and *Trypanosoma cruzi* [196,197] was demonstrated using phthalocyanine based photosensitizers. Photodynamic inactivation of bacteria on the other hand made a giant leap forward in 1996 as Jori and co-workers demonstrated the efficient inactivation of Gram-positives as well as Gram-negatives by utilizing cationic porphyrins [198]. Similar effects were shown in the same year for cationic phthalocyanines [199]. As it was now known, photodynamic inactivation with cationic photosensitizers was possible against both, Gram-positives as well as Gram-negatives, research started to flourish around PDI.

Although photodynamic inactivation has been shown throughout history that nearly all forms of life such as fungi, protozoa, Gram-positive bacteria, Gram-negative bacteria, and viruses may be readily inactivated, the scientific literature lacked evidence for archaea until 2019.

Physics of Photodynamic inactivation

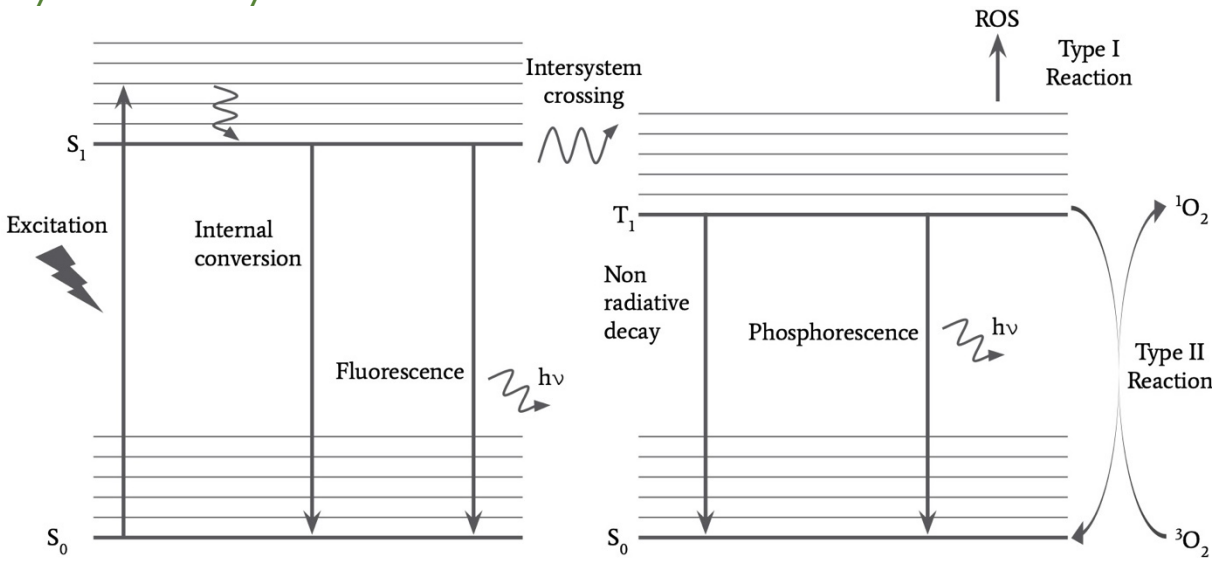

Figure 3. Jablonski-Scheme of the underlying physical processes of photodynamic inactivation. Initial excitation of the photosensitizer from S_0 to S_1 occurs due to the absorbance of a photon, the S_1 state either decays via internal conversion or fluorescence or undergoes intersystem crossing to T_1. The triplet state photosensitizer then returns to the S_0 ground state either via non-radiative processes, phosphorescence, type I or type II reactions. Both latter mentioned produce the biocidal substances.

For efficient photodynamic inactivation, one needs in principle three components. Light, triplet oxygen and a photosensitizer molecule. The photosensitizer molecule absorbs a photon, the molecule gets excited from its S_0 ground state either to the S_1 or S_2 state. These singlet states are generally characterized by electrons of antiparallel spin in their binding orbitals. Depending on the energy supplied by the absorbed photon, the electron is present in a specific vibration niveau within the multiplicity according to the Franck-Condon principle [200,201]. However, according to Kasha's rule, the steps described further can only happen from the lowest excited state of any given multiplicity [202], which is reached after a few picoseconds after excitation [203]. From the lowest vibration of the S_1 state of the photosensitizer, within a lifetime of the S_1 state of some nanoseconds [204], three different and competing effects occur. First, the photosensitizer returns to its S_0 state by the release of a photon, termed fluorescence. Second, the energy might also be converted to heat energy, so-called internal conversion, with the photosensitizer again present in its S_0 state. It should

be kept noticed that both mechanisms do not lead to photodynamic inactivation and are therefore considered disadvantageous. As a third possibility, the molecule can undergo intersystem crossing, where due to a change in the electron spin the photosensitizer is then present in its triplet state T_1. Again, from that triplet state, four different mechanisms might be observed. Just as for the return to the S_0 state, emittance of light is one way to release the energy. In this case, the emission of a photon is termed phosphorescence. Second, the release of the energy in the form of non-radiating intercombination is possible. Just as the intersystem crossing, this transition is a forbidden mechanism in quantum mechanics [205], but can nevertheless occur due to several effects that in return make these processes possible [206]. This leads consecutively to long lifetimes of the triplet state in the magnitude of microseconds [207]. Another option for the photosensitizer leaving its triplet state is the collision act of the photosensitizer with another molecule. Such a collision implies an overlap of molecules or a close vicinity at least. In that moment, charge or energy can be transferred from the excited photosensitizer to an acceptor molecule, leaving the photosensitizer un-excited behind. When charge is transferred from the photosensitizer to an acceptor molecule a so-called type-I-reaction takes place. Thereby, Fenton-like reactions transmit the energy to water or other substrate molecules in the form of an electron or proton. Consequently, this leads to the formation of reactive oxygen species such as hyperoxide anions, hydroxyl-radicals, perhydroxyl-radicals, peroxyl-radicals or alkoxyl-radicals that subsequently are capable of destructing organic matter [208–211]. Lastly, and most importantly, the photosensitizer can also undergo type-II-reactions, where the photosensitizer transfers the energy to triplet oxygen via spin permitted energy transfer resulting in the formation of singlet oxygen [212,213] that is highly reactive towards organic matter, especially unsaturated carbon bonds. One of the most important characteristics of a photosensitizer is its singlet oxygen quantum yield Φ defined as the number of singlet oxygen molecules produced divided by the number of absorbed photons [214]. A detection of the amount of the produced singlet oxygen is most accurately possible via luminescence of the radiative transition from singlet oxygen to triplet oxygen at 1270 nm [215–221]. However, due to the complexity of these measurements, some chemicals are available that specifically react with singlet oxygen such as DPBF [222] or Singlet Oxygen Sensor Green, a fluorescein-anthracene derivative [223]. These chemicals are especially useful to researchers in the wet lab as this offers a quick and easy method to roughly determine a photosensitizer's efficacy with present resources. Besides the two mentioned reaction types that generate singlet oxygen, just recently Michael Hamblin and Heidi Abrahamese proposed oxygen independent type-III-reaction occurring in psolarens,

tetracyclins and in combination with inorganic salts [224]. However, this proposal remains to be discussed by the literature until now.

Photosensitizers

In general, in photosynthesizer research it is one of the major aims to minimize fluorescence, phosphorescence and internal conversion as undesired side effects. More importantly, photosensitizers should generate either reactive oxygen species or singlet oxygen in significant quantum yield proportions. The properties a potent PDT photosensitizer must fulfil were mentioned earlier. Although these principles apply mostly for PDI, PACT or aPDT as well, the photosensitizer properties were specified by Maisch in 2014 adding that a high binding affinity to microbial live and low affinity for mammalian cells is necessary [225]. Nowadays, researchers mainly focus on photosensitizers that produce chiefly singlet oxygen as a reactive agent, as type-I-reactions come with one major drawback: due to the likelihood of the occurrence of radicals in this reaction steps, hard to control chain reactions might occur, even after illumination in the dark. type-II-reactions and the singlet oxygen generated on the other hand are capable of reacting much more specifically in the vicinity of the binding site of the photosensitizer, as singlet oxygen possesses a dramatically small reaction range of 20 nm [226,227]. By this fact, an optimization of the photosensitizer's binding behavior can also influence the specifity, allowing chemical alterations of photosensitizers to target semi-specific components of the cell. In general, for photodynamic inactivation of bacteria, one or more positive charges are required so that the photosensitizer accumulates at negatively charged bacterial structures such as the outer membrane or teichoic acids or is even taken up by the bacterial cell [228–230]. Antimicrobial photosensitizers generate singlet oxygen, which most likely damage preferably the outer structures of bacteria and cause irreversible oxidative damage consequently leading to the inactivation of the bacteria [219].

Azines and phenothiazine-based photosensitizers

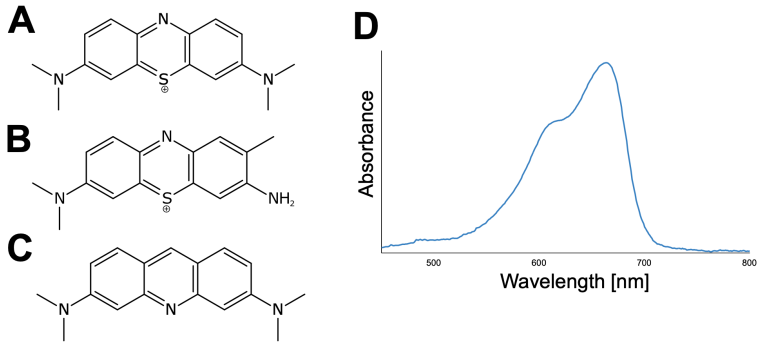

Figure 4: (A) displays the cationic dye methylene blue containing a positively charged sulfur atom and two dimethylamine groups. (B) shows the chemical structure of toluidine blue, which differentiates from methylene blue by its side chains. Both latter mentioned belong to the class of the phenothiazines. (C) displays the chemical structure of acridine orange, which does not contain a sulfur atom in contrary to (A) and (B). Additionally, acridine orange is neutrally charged. (D) depicts a typical absorption spectrum of the phenothiazines, here the spectrum for methylene blue is shown. It is a major characteristic of phenothiazine dyes that λ_{max} is at the upper end of the visual spectrum.

One of the oldest substances in use for photodynamic inactivation are the tricyclic azines. These include also the very first photosensitizer ever used, namely the beforehand mentioned acridine orange Fig 4C. However, these tricyclic azines are, without sophisticated chemical modifications of potential side chains not charged rendering them nearly useless for modern broad spectrum antimicrobial activity as Gram-negatives are not targeted.

More specifically, phenothiazines are nowadays the most important subclass to mention. Phenothiazines are specified by a sulfur atom at position 5 and a nitrogen atom at position 10. The two most prominent representatives from this group are methylene blue (Fig 4A) and toluidine blue (Fig 4B). The maximum absorption λ_{max} for methylene blue is at 660 nm (Fig 4D) while toluidine blue O has its λ_{max} at 625 nm. This wavelength comes with a great advantage in human application as light of longer wavelength can penetrate human tissue much deeper than visible light of shorter wavelength. Naturally, phenothiazines have a positive charge and attach therefore readily to most bacterial envelopes and show therefore effective killing against several microorganisms [231]. Now, although phenothiazines like methylene blue or toluidine blue are well known photosensitizers, their properties are far from optimal. On the one hand, their singlet oxygen quantum yield is around 0.5 [232]. On the other hand, the side chains of phenothiazines offer a variety of possibilities to optimize the photosensitizers. This was shown for example for the derivatives dimethyl methylene blue, new methylene blue and methylene green [233–235]. Späth and colleagues demonstrated that

ammonium side chains of methylene blue derivatives can lead to improved microbial killing, most likely due to increased attachment or uptake of the photosensitizer [236].

Cyanines

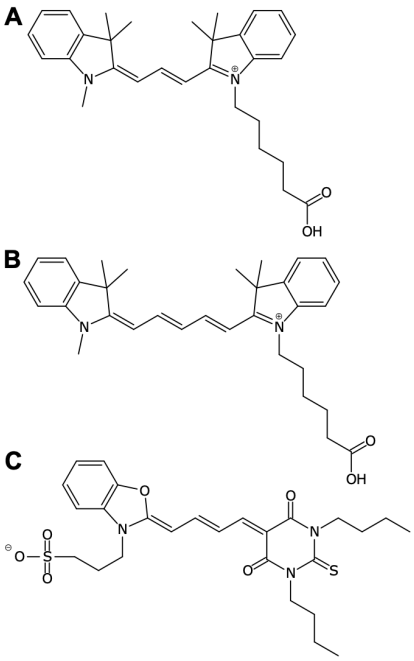

Figure 5: (A) displays the chemical structure of Cy3 and (B) of Cy5, two dyes commonly used as fluorescence-based dyes. (C) depicts the chemical structure of the photosensitizer merocyanine 540.

Cyanines are commonly used as dyes with a positively charged quaternary ammonium group and a tertiary amino group connected via a polyene bridge structure. While nowadays, cyanines like Cy3 (Fig 5A) or Cy5 (Fig 5B) are commonly used as fluorescence dyes in life sciences especially in molecular biology, the antimicrobial use of this dye class longs back to the first world war where these dyes were partly used for treatment of wounds [160]. Nowadays, cyanine dyes that are used as fluorescence markers, they are also available as derivatives with increased fluorescence quantum yield, i.e. with adjacent azide groups. The negatively charged Merocyanine 540 (Fig 5C) with a λ_{max} at 535 nm was shown to efficiently inactivate viruses [237]. However, although some cyanine dyes have a positive charge and are therefore capable of inactivating various microorganisms, they come with various drawbacks concerning their use in photodynamic inactivation. First, most of the cyanine dyes are mainly fluorescent dyes, and therefore also optimized in lower singlet oxygen quantum yield as well as ROS. Secondly, due to their chemical structure they tend to photoisomerization although this effect can be circumvented at a certain extent utilizing the heavy atom effect that also facilitates the singlet oxygen production of the cyanines [238,239]. The

treatment of blood plasma and blood serum was shown elsewhere with cyanine photosensitizers utilizing the heavy atom effect [240]. An optimization of cyanine photosensitizers has been attempted to increase the binding capability of the photosensitizers to bacteria and enveloped viruses [237]. Although these dyes can serve as efficient photosensitizers, they are to the state of the art not widely used anymore mostly due to their drawbacks compared to other available photosensitizers.

Porphyrins

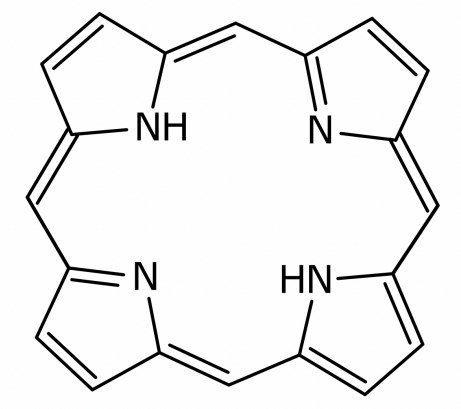

Figure 6: The porphin molecule. This is the basic structure that all porphyrins have in common. The porphin molecule consists out of 4 pyrrole rings and is capable of complexing different divalent ions.

Porphyrins are chemically based on the porphin molecule and are common naturally occurring substances with important functions in blood transportation in vertebrates or photosynthesis in many photoautotrophic organisms. The chemical core of porphyrins contains four pyrrol rings connected with methine bridges. This basic structure, which is a molecule on its own called porphin (Fig 6), is the backbone of all other porphyrins. Furthermore, porphyrins exhibit a very specific photometric spectrum showing several peaks with the global λ_{max} termed Soret band while the other local λ_{max} are called Q bands. A typical absorption spectrum of a phorphyrin based photosensitizer is shown in Fig. 7 However, when experimenting with porphyrins in various solutions, one should be aware that due to their chemical structure, porphyrins are pristine chelators of divalent ions which have impact on their photophysical behavior and the measured absorption spectrum [241,242].

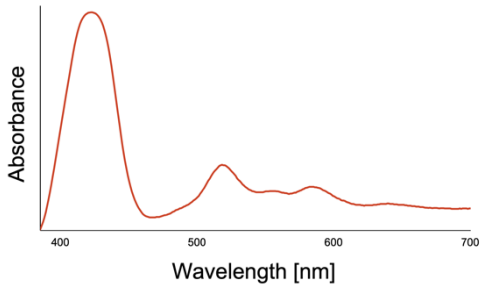

Figure 7: Absorption spectrum of a commercially used porphyrin-based photosensitizer, in this case TMPyP. Typically, the spectrum of a porphyrin has its global absorption maximum in a range of around 400 to 436 nm. This global maximum is also named Soret band after the French scientist Jaques-Louis Soret, initially describing this band in diluted blood samples [243]. Besides this maximum caused by S_0 to S_2 transition, the local maxima are derived from S_0 to S_1 transitions and are termed Q bands, most likely somewhere between 490 and 650 nm [244].

Porphyrins such as HpD or Deuteroporphyrin can efficiently kill Gram-positive bacteria but do not affect Gram-negatives due to a lack of a positive charge [245]. In order to improve binding to Gram-negatives, cationic porphyrins were developed to broaden the use of this photosensitizer class as an antimicrobial substance [198]. In general, porphyrin based photosensitizers are efficient against Gram-negatives when they contain at least one positive charge [198]. Even more efficiently porphyrin based photosensitizers are fourfold positively charged with alkyl side chains up to 14 C-atoms long [246]. Porphyrins have also been shown to be efficient against viruses most likely due to damage on the viral envelope [247–249].

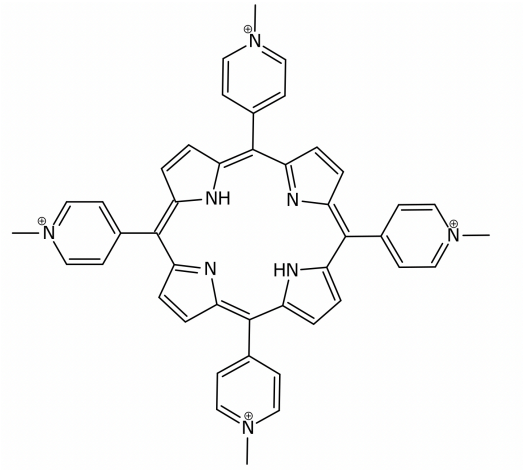

Figure 8: Chemical structure of TMPyP (α,β,γ,δ-Tetrakis(1-methylpyridinium-4-yl)porphyrin p-toluenesulfonate). The molecule is based on a porphyrin structure but has four cationic charges due to its methylpyridinium moeites which enable close attachment to bacterial cells.

One of the most studied photosensitizers in general is α,β,γ,δ-Tetrakis(1-methylpyridinium-4-yl)porphyrin *p*-toluenesulfonate – or in short TMPyP (Fig 8). Due to its four positive charges, it

attaches greatly to Gram-positive as well as Gram-negative cells and inactivates both upon light exposure. Further, TMPyP has excellent light absorption characteristics with a tremendously high absorption cross section. However, this somehow limits its use as high concentrations of this photosensitizer lead to a self-inhibitory effect that reduces the light penetration into a suspension containing the targeted bacteria. Furthermore, TMPyP has a singlet oxygen quantum yield of 0.77 [250] and therefore produces in combination with good absorption characteristics high amounts of singlet oxygen in the vicinity of the bacterial cells.

Another prominent porphyrin-based photosensitizer is the twofold positively charged molecule XF73. Due to its positively charged quaternary ammonium component the molecule can attach well to Gram-positive as well as Gram-negative bacteria [251] but might also possess a certain toxicity in the absence of photons just as other quaternary ammonium compounds. Chlorin e6, another porphyrin derivative with several side chain alterations is also often used for antimicrobial photodynamic inactivation [252] – however the molecule has no positive charge due to its carboxy-side chains but for example antibody coupling allows also the inactivation of Gram-negatives [253]. Further, embedding chlorin e6 in a poly-L-lysine conjugate showed good efficacy against *E. coli* [254].

Overall, porphyrins have excellent properties as photosensitizers. They are chemically stable, well researched and allow for a tremendous chemical variation of side chains that enables their use in a vast number of potential applications.

Phtalocyanine

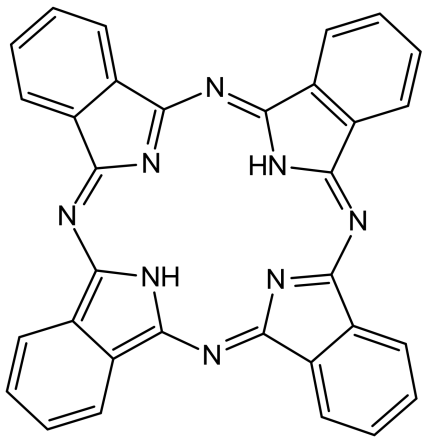

Figure 9: Basic structure of phthalocyanine. Potential alterations such as cationic charges are often introduced at the nitrogen atom in the crosslinking region.

Phthalocyanines in general are macrocyclic compounds with aromatic properties, more specifically they are tetra-benzotetraazaporphyrines (Fig 9). Due to their excellent quantum yield [255] these photosensitizers have been successfully applied in a wide variety of organisms. It has been shown that coated as well as uncoated viruses are efficiently inactivated [256–258] even in blood products [259].A major advantage of phthalocyanines is their high capability in producing singlet oxygen – exceeding the quantum yield obtained for methylene blue [255]. Optimizations concerning special central atoms such as silicon containing residues have been shown to bear potential in the inactivation of HIV in infected red blood cells [260]. Furthermore, such modified phthalocyanines have been shown to be efficient also against *Plasmodium falciparum* - the main cause for Malaria [195]. Of cause, phtalocyanines especially with aluminum as a central atom, are also efficient against *Streptococcus sanguinis* as well as MRSA [261,262]. Embedding of phtalocyanines in tetra(tert-butyl) polymer films was also successful in inactivating *S. aureus* [263]. Again, only cationic phtalocyanines are efficient against Gram-negative bacteria [199]. Cationic Phtalocyanines with Zn ions as a central atom represent also efficient photosensitizers with a broad antimicrobial activity [199,264,265].

Fullerenes

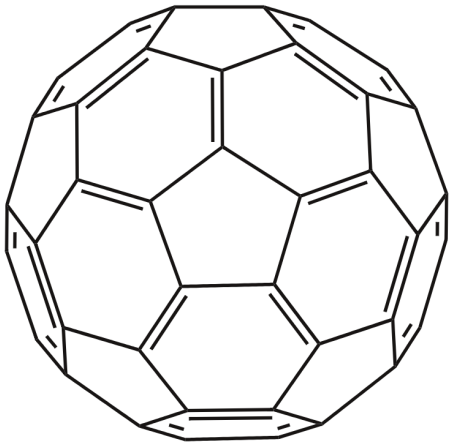

Figure 10: A C60 Buckminsterfullerene. At one of the various carbon atoms of the molecules, side chains can be introduced that improve their applicability for attachment or embedding in several media.

Fullerenes are molecules which were initially described in the 1970s by Eiji Osawa and have a ball-shaped structure (Fig 10) [266]. Most often, in photodynamic C_{60}-Fullerens, also known as Buckminsterfullerene, are used that are coupled with cationic structures such as quaternary pyrrolidiniums that are positively charged allowing the attachment of the molecule to Gram-negative bacteria as well [267]. Again, as for porphyrins increased cationic charge leads to better

photodynamic inactivation [268]. For fullerenes it was shown that it is dependent on the solvent weather the type I or type II mechanism is preferred [268–270]. Furthermore, due to the structural properties such fullerene based photosensitizers might also counterintuitively allow oxygen independent use in the presence of sodium azide [271].

Perinaphtenones

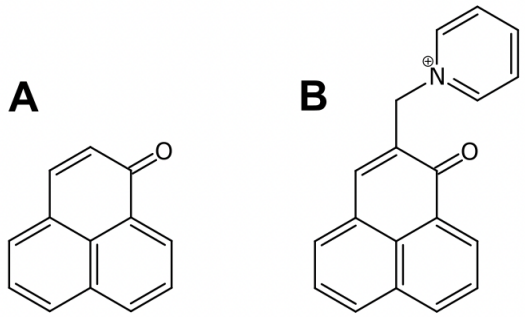

Figure 11: (A) shows the chemical structure of 1-H-phenalen-1-one which is neutrally charged and (B) displays the molecule SAPYR with a positively charged pyridinyl moiety.

Ester Olivieros and her colleagues made an interesting discovery in 1991: a molecule named 1-H-phenalen-1-one or perinaphtenone (Fig 11A) which can produce singlet oxygen with a quantum yield of around 0.97 which is compared to most other photosensitizers extraordinary. The molecule is soluble in water as well as in non-polar solvents with good photostability [272]. Nonell and co-workers were able to push the boundaries of singlet oxygen production even further as they synthetized 1-H-phenalen-1-one-sulfonic acid, capable of producing singlet oxygen with a quantum yield close to unity. However, this molecule is anionic, therefore not suitable for a broad antimicrobial activity [220]. The synthesized molecule (2-((4-pyridinyl)methyl)-1-H-phenalen-1-one – briefly called SAPYR (Fig 11B) – showed a singlet oxygen quantum yield of 0.99, additionally with a cationic charge in the pyridinyl group, making it a highly efficient photosensitizer for antimicrobial approaches [230]. It is also speculated that SAPYR possesses biofilm-disruptive properties just as other compounds with pyridinium groups [230,273].

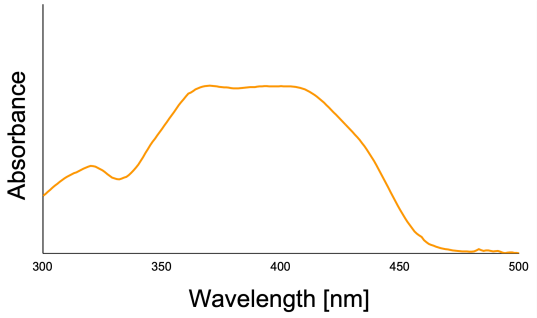

Figure 12: Absorption spectrum of SAPYR. Clearly visible is the large maximum of the photosensitizer from around 360 to 425 nm.

Besides the pristine singlet oxygen generation properties, phenalenones come with several other advantages on the chemical side. On the one hand, they have a broad absorption maximum in the visible spectrum (Fig 12). This favors their use especially when planning for environmental approaches as the light source must not excite the photosensitizer at a specific wavelength. Therefore, singlet oxygen can also be generated efficiently under ambient light conditions. Furthermore, the photosensitizers are chemically stable. Solutions stored in the dark at low temperatures, no loss of concentration is observed even after three years of storage.

Riboflavin and its derivatives

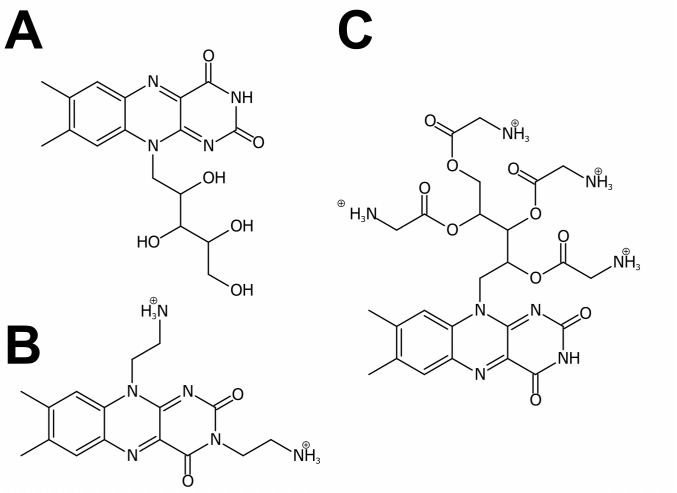

Figure 13: (A) Riboflavin, also known as vitamin B2 comprised out of a ribityl moiety and the isoalloxazine scaffold. (B) shows the structure of FLASH-02a two positive charges located at the end of two side chains to avoid steric hinderance and (C) displays the photosensitizer FLASH-06a with four positive charges [274].

Chemically speaking, flavins are heterocyclic 7,8-dimethylisoalloxazine compounds [275,276]. Flavins such as the riboflavin, vitamin B2 (Fig 13A), flavin mononucleotide as well as the flavin adenine dinucleotide fulfil important functions in various biochemical pathways [276–279].

Furthermore, flavins as natural molecules are considered to be biodegradable and safe for human use [280,281]. In the late 1940s it was shown that riboflavin can oxidize indoleacetic acid in plants in the presence of oxygen and photons [282]. Indoleacetic acid, which is also a common phytohormone and also known as auxin fulfils highly important functions of plant growth, therefore, the oxidation of these molecules led to dramatic changes in plant growth [282]. It was also shown that flavins can produce ROS in vivo to a certain extent but observed no intracellular damage, most likely due to protective flavin binding proteins [283]. Subsequently, the light-induced triplet state as well as the generation of singlet oxygen via light was shown elsewhere *in vitro* [284,285]. Although endogenous flavins were shown to produce efficiently singlet oxygen and other ROS [286–289], a sufficient bacterial inactivation due to the lack of a cationic charge is not observed [290,291]. Later on, it was shown that cationic riboflavin molecules with $-NH_3^+$ moieties possess a broad activity spectrum against several bacteria [225,280]. Examples of flavins modified in this way include the in this work used FLASH-02a (Fig 13B) or FLASH-06a (Fig 13C). Flavin derivatives still remain a major class in photodynamic inactivation and are of utter importance, a recent preprint reports on the possibility of enhancing the chemical properties of flavin based photosensitizers [292].

Curcumins

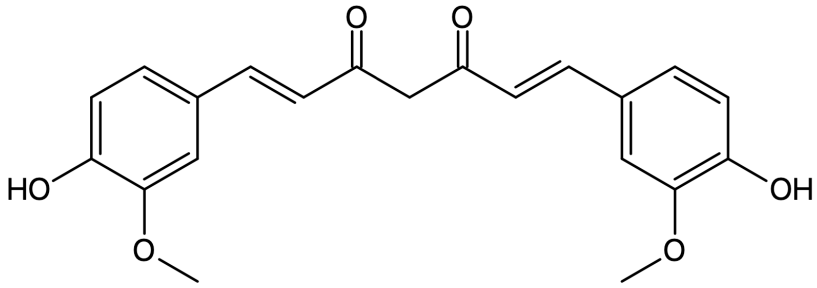

Figure 14: Chemical structure of curcumin. The molecule itself is neutrally charged and therefore only capable of killing Gram-positives.

The large group of curcumins is mostly known by the main representative curcumin in combination with curcumas properties as spice – mainly used in Indian and Thai cuisine. These secondary plant substances are chemically speaking diarylheptanoids, more in detail two 2-Methoxyphenoles are connected via an unsaturated C7 bridge with 2 keto-residues (Fig 14). One of the most important characteristics of curcumin-based photosensitizers is that they tend to generate rather ROS via type I reactions than singlet oxygen via type II reactions [293]. When applying curcumin based photosensitizers, one should be aware that these molecules are chemically not really stable and

degradation reactions such hydrolysis, oxidation or photodegradation are likely to occur [294]. Curcumins have been proven to have a antimicrobial photodynamic efficacy against MRSA [295], *Streptococcus mutans* and *Lactobacillus acidophilus* [296]. Cationic curcumin derivatives have also been synthesized and showed good efficacy against *E. coli* [297]. However, due to the fact that curcumin is a well-known food additive, this molecule group might be well suited for applications in food industry [298,299].

Cationic BODIPY derivatives

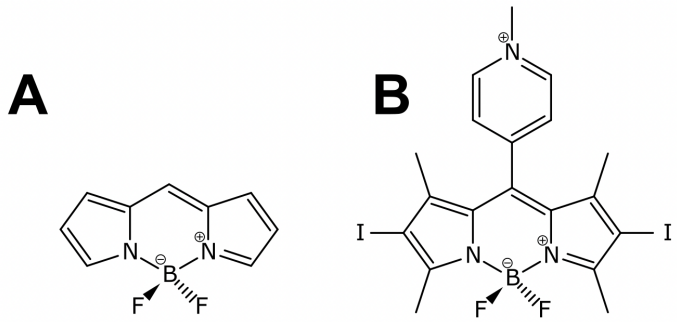

Figure 15: (A) Displays the BODIPY molecule, (B) shows a cationic BODIPY derivative as reported elsewhere [300,301].

The technical term BODIPY refers to the basic chemical structure of those molecules. They consist of a **bo**ron difluoride moiety which is connected to 2-2'-**dipy**rromethene (Fig 15A). The introduction of a pyridinium moiety and therefore a positive charge make it possible that the photosensitizer can attach to Gram-positive as well as Gram-negative bacteria (Fig 15B) [300]. However, with BODIPY photosensitizers several issues need to be addressed in the future such as an optimization of the singlet oxygen quantum yield as well as agglomeration problems.

Photosensitizers used in this thesis

A brief summary with some properties of the different photosensitizers is given in table 1. Generally, all uncharged or negatively charged photosensitizers were not considered relevant for this study as a positive charge is required for efficient broad spectrum antimicrobial activity. Furthermore, cyanines were not used due to their low singlet oxygen quantum yields, fullerenes were not studied as positively charged fullerenes as photosensensitizers are relatively new to the field and there is not much experience with these in terms of application and curcumins were excluded as they produce mainly ROS and not singlet oxygen and because they are heavily subjected to

photobleaching. Due to their structural similarity to porphyrins, phthalocyanines were not considered further and BODIPY photosensitizers were not investigated as there are still ongoing debates how good photosensitizers for antimicrobial photodynamic inactivation should look like [302]. Methylene blue (Fig 4A) and TMPyP (Fig 8) were chosen as one of the best studied representatives of the phenothiazines and porphyrins, respectively. From the group of the perinaphtenones, the cationic dye SAPYR (Fig 11B) was investigated closer because its pristine singlet oxygen generation rates and its light-yellow color, which does not lead to undesired staining in the region of application. Furthermore, the flavins FLASH-02a (Fig 13B) and FLASH-06a (Fig 13C) were studied as they are one of the few positively charged flavins available. Additionally, flavins in general are considered safe for application as they can be degraded easily by the human body.

Table 1: Brief summary of some of the most important characteristics of the different photosensitizer classes. Min. MW indicates the minimum molecular weight of the respective photosensitizer class, the absorption represents a range in which most of the molecules used as photosensitizers have their maximum and Φ is showing the singlet oxygen quantum yields for photosensitizers in the corresponding class. However, especially both latter mentioned values given within this table should only be used as rough indications as they are at least to a certain extent depending on the solvent the measurements were conducted in.

PS class	**Charge**	**Min. MW [g mol-1]**	**Absorption [nm]**	**Φ**	**Color**
Phenothiazines	Positive	200	600 - 700	0.31 - 0.5 [303]	Intensive blue or green
Cyanines	Neutral, positive or negative	714	490 - 743	0.003 - 0.12 [303,304]	varies
Porphyrins	Neutral or positive	310	400 – 450	0.27 - 0.85 [305]	Intensive red-brown
Phthalocyanines	Neutral or positive	515	600 - 700	0.13 - 0.62 [255]	Intensive blue or green
Fullerenes	Neutral or positive	720	300 – 400	0.76 - 0.84 [306]	Intensive violet to brown
Perinaphtenones	Neutral or positive	180	350 - 400	0.99 - 1.00 [220,230]	Light yellow
Flavins	Neutral or positive	242	350 – 500	0.51 - 0.54 [288]	Light yellow
Curcumins	Neutral or positive	368	350 - 500	0.011 - 0.11 [293]	Yellow to orange
BODIPY	Neutral or positive	192	507 - 766	0.10 - 0.78 [307,308]	Yellow to red-brown

Applications of photodynamic inactivation

Over the decades, photodynamic inactivation has been proven to be highly efficient under laboratory conditions against a variety of organisms in all kinds of experimental parameters. However, photodynamic inactivation as a platform technology is predestined for the leap out of the wet lab into real life conditions. Due to its simplicity as well as the major advantage that the formation of resistances has not been observed yet [309], photodynamic inactivation finds possible applications nowadays in a vast number of areas. In the following, several examples are given where photodynamic inactivation finds its use in different areas.

Dental applications

In general, in dentistry there is also an urgent need for alternatives to conservative disinfectants as there are reports that resistances against chemicals used as gold standard such as chlorhexidine seem to emerge [310,311]. The main photosensitizers currently investigated in dentistry are methylene blue [312], toluidine blue [313,314], curcumin [314,315], rose bengal [316], and chlorin e6 [317]. In general, photodynamic inactivation in dental applications has been studied in a vast extent on an academic level. One of the first broad screenings by Wilson *et al.* investigated on eight different photosensitizers against their bactericidal potential on *Streptococcus sanguinis*, *Porphyromonas gingivalis*, *Fusobacterium nucleatum* and *Aggregatibacter actinomycetemcomitans* [318]. S. *sanguinis* is a commensal of the oral cavity [319] but can also lead to endocarditis after oral surgery [320]. *P. gingivalis* [321], *F. nucleatum* [322] as well as *A. actinomycetemcomitans* [323] play a major role in periodontal disease . Therefore, the four chosen organisms are of high relevance in dentistry in general. Especially toluidine blue O as well as methylene blue showed a bactericidal effect against all of these organisms [318]. The causative agents for dental caries *Streptococcus mutans*, *S. sobrinus*, *Lactobacillus casei* and *Actinomyces viscosus* are also susceptible to photodynamic inactivation with a phthalocyanine derivative [324]. *S. mutans* was also shown to be susceptible to toluidine blue in demineralized dentine as well as collagen [325].

While prior mentioned studies focused on *in vitro* experiments, there is also evidence for a good efficacy in modelled environments or *in vivo*. Cieplik and colleagues for example used a tooth model with human premolar and molar teeth that were inoculated with *Enterococcus faecalis* in phosphate buffered saline. As photosensitizers, they used methylene blue and TMPyP in a concentration of 10 µmol l^{-1}, applying light doses of 4.54 J cm^{-2} and 2.4 J cm^{-2}, respectively. With these conditions, an inactivation efficacy of around 5 $\log_{10}$ steps was shown [326]. Chitosan-hydroxypropyl methylcellulose-toluidine blue O gels were found to be efficient in inactivating *Staphylococcus*

aureus, *A. actinomycetemcomitans* and *P. gingivalis* in a 3D gingival model using tryptic soy broth as a solvent. Toluidine blue was applied in a concentration of around 20 µmol l^{-1} and light had to be applied in dosages between 10.8 and 108 J cm^{-2} to lead to efficient reductions [327]. Researchers from the Friedrich Schiller University in Jena demonstrated in a beagle dog model, that chlorine e6 as well as its derivative BLC 1010 [328] significantly reduced *P. gingivalis* and *F. nucleatum* infected sites applying a total of 12.7 J cm^{-2} in intervals of several days [329]. A clinical study on humans compared a conservative scaling and root planning treatment of periodontitis with a phenothiazine-based photosensitizer therapy. The researchers applied 0.6 J cm^{-2} of light to the teeth to be treated and compared both methods in the light of several clinical parameters such as plaque and gingival index. The comparative study revealed that the conservative method in comparison with the photosensitizer-based method did not differ significantly in treatment success based on the parameters taken into account [312]. It should be stated that some researchers in general suggest that only the conservative mechanical treatment method of periodontitis consequently leads to positive outcomes in the long term [330–332]. Similar results were obtained in a rat model, efficient inactivation with toluidine blue at 3.27 mmol l^{-1} in combination with 12 J cm^{-2} were just as efficient as conventional treatment [313]. Fontana and colleagues investigated on biofilms that were derived from dental plaque samples. As a photosensitizer, methylene blue was used in a concentration of 156.32 µmol l^{-1} dissolved in brain heart infusion by applying 30 J cm^{-2} of appropriate light leading to a bacterial reduction of 32% [333]. A study from Germany did research on artificial biofilms of *Streptococcus mutans*, demonstrating efficient inactivation with a pharmaceutically ready-to-use formulation with a phenothiazinium dye dissolved in a buffer medium and hydroxypropyl methylcellulose at 12 J cm^{-2} [334]. A multispecies biofilm consisting of *S. mutans* and *L. acidophilus* in a dentine caries model was reduced in viability by 70% by 13.5 mmol l^{-1} curcumin with a light dose of 5.7 J cm^{-2}. However, in the same study the researchers achieved a viability reduction of the biofilm by more than 90% in *in vitro* experiments [296]. The application of 100 to 300 µmol l^{-1} chitosan-rose bengal-nanoparticles has been shown to reduce the viability of *E. faecalis* cells and to disrupt biofilms of the latter. Furthermore, the researchers found positive influences of the novel nanoparticles towards the dentin-collagen structure. More remarkably, the study also investigated on the presence of bovine serum albumin which was shown to have detrimental effects on photodynamic inactivation [316]. Swiss researchers investigated on the influence of curcumin, eosin Y as well as rose bengal not only towards *Lactobacillus* isolates derived from caries lesions but also towards murine odontoblast-like cells, dental pulp cells as well as human embryonic stem cells,

proving that much higher PS concentrations are needed to kill eukaryotic cells compared with bacterial ones [335]. Voos *et al.* choose the uncommon PS safranin O with 10 µmol l^{-1} for their studies, in which they inactivated on the one hand planktonic cells of *Streptococcus gordonii*, *S. mutans*, *F. nucleatum*, *A. actinomycetemcomitans* and *P. gingivalis* in comparison with 0.2% chlorhexidine. Additionally, the researchers used *ex vivo* biofilms derived from plaque and saliva samples for their investigations. Remarkably, the researchers found that the photodynamic treatment was in most cases equally or more efficient than the conservative chlorhexidine treatment [336]. The potential applicability of photodynamic inactivation towards deep caries lesions has been demonstrated via the use of 370 µmol l^{-1} toluidine blue O and 94 J cm^{-2} in a study that included 45 human individuals, reduce the bacterial load up to 1.7 $\log_{10}$ steps [337]. Interestingly, there is also a report that finds excellent killing efficacy of toluidine blue towards several Gram-positive as well as Gram-negative bacteria whereas the application of riboflavin as a photosensitizer did not lead to efficient inactivation [338]. Just recently, phenothiazinium chloride was successfully used for decontamination of oral surgical sites [339]. Peri implants in combination with photodynamic inactivation seem also to be capable of improving the prognosis [340]. However, when it comes to dental applications it is also important to note that color changes of the dentin might occur depending on the different staining properties of the photosensitizer [341]. In root canal treatments, sterility of the root canal is of paramount importance to avoid reinfection consequently leading to better healing [342,343]. Compared to the conservative use of bleach for disinfection, photodynamic inactivation with methylene blue has shown to be at least as efficient [344,345]. A typical but severe disease pattern in dentistry is also periapical periodontis, which consecutively leads to cyst formation as the inflammation is often without symptoms and therefore only diagnosed by chance in most patients [346]. While the therapy gold standard is repeatedly applied calcium hydroxide rinsing [345], photodynamic inactivation has been shown to be efficient in a clinical study with 20 patients [347]. Caries is a disease of the teeth based on increased rates of demineralization [348,349], mostly caused by *S. mutans* [350,351]. The disease begins as dental plaque that then slowly penetrates deeper regions of the infected dental material. Therefore, the removal of dental plaque and consequently also the caries causing bacteria mostly organized in biofilms is the main treatment approach [352,353]. It has been shown that *S. mutans* biofilm formation can be efficiently inhibited by the application of toluidine blue after irradiation with 18 J cm^{-2} [354]. Although implants in dentistry are often used, sometimes inflammatory responses due to bacterial contamination occur, possibly leading to severe complications [355]. While conservative treatment includes several

decontamination techniques [356], photodynamic inactivation might complement the toolbox in treating such infections. A clinical study on 15 patients with inflammatory complications derived from implants investigated on the efficacy on toluidine blue, in which a significant reduction of bacteria was reported [357]. Indeed, concerning the usefulness of photodynamic inactivation there is also another study that contradicts the findings latter mentioned. In this study, the researchers could not report on a more positive outcome when patients were subjected to a commercially available system utilizing photodynamic inactivation compared to conventional treatment options [358].

However, while these results from other researchers seem to be very promising for future approaches there is still tremendous potential for optimization as *in vivo* experiments do not reach efficacies of *in vitro* studies. Photodynamic inactivation in the vicinity of teeth must cope with various substances like calcium ions or saliva which contains proteins and different ions and up to date, it is still not known how for instance different ions interact with photodynamic processes, especially as *in vitro* experiments most often use phosphate buffered saline as solvent. The research, which is presented in this thesis, tries to clarify especially the role of calcium and magnesium ions in the light of photodynamic inactivation and aims for an optimization under high calcium and magnesium ion concentrations.

Dermal application

The effective action of photodynamic inactivation against standard skin bacteria has been shown *in vitro* to a vast extent with various photosensitizers. Typical bacteria causing skin infections include *S. aureus*, Streptococci, *P. aeruginosa* [359] and members of the genus *Propionibacterium* [360]. Against all these pathogens *in vitro* data exist demonstrating that these bacteria are readily inactivated [361–366]. However, most studies on skin or wound treatment were conducted using animal models. Probably the first *in vivo* study investigating photodynamic inactivation on skin was published by Berthiaume and colleagues. The researchers used chlorine e6 anti-*Pseudomonas* monoclonal antibodies as described by Xiao-Ming *et al.* [367] and injected this conjugate i.c. intro *Pseudomonas aeruginosa* infection sites introduced before. The researchers finally reported an bacterial reduction of around 86 to 88% [253]. A similar study from the Wellman Laboratories of Photomedicine introduced wounds in mice and infected those wounds with bioluminescent *E. coli* cells. The treatment was then carried out with 100 µmol l^{-1} chlorine e6 dissolved in PBS with a total fluence of 160 J cm^{-2}, the success of the method was measured as luminescence intensity of

the wounds of the mice. The photodynamic inactivation in this study led to a reduction of the luminescence signal by 99% and was therefore considered to be effective by the authors, additionally the wound healing was not inhibited in the treated wounds [254]. Of cause, *in vivo* studies were also conducted with one of the most important pathogens for the human skin: MRSA. To study this organism, Zolfaghari *et al.* introduced excisional wounds in mice and infected those wounds with MRSA. Subsequently, 312 µmol l^{-1} MB and 360 J cm^{-2} were applied as treatment which was able to reduce the median cell count of around 1.5 log_{10} steps. Furthermore, it should be noted that the researchers were not able to detect any histological changes of the treated skin [368]. Recently, wound models in mice were also found to deliver effective inactivation with curcumin-based photosensitizers. At an applied light dose of 60 J cm^{-2}, the commercially available curcumin formulation S. aureus were reduced between 2 and 4 log_{10} steps [369]. Qui and co-workers were able to manufacture highly complex gold nanoparticles with chlorin e6 as photosensitizer that showed good efficacy in a murine wound model against *S. aureus* as well as *E. coli*. While the concentration of the photosensitizer was around 250 µmol l^{-1}, the researchers applied tremendously high light doses of 480 J cm^{-2} to the mice. Additionally to a photodynamic effect, the researchers also described a so-called photothermal effect, which might lead to additional killing of the bacteria [370]. Curcumin based photodynamic inactivation was also reported recently to be efficient against VRSA in an *in vivo* rat model [371].

Besides those mentioned studies investigating on mechanically introduced wounds, there are also several studies that deal with thermally introduced burn wounds. A group of Chinese scientists used a cationic porphyrin conjugate to treat infected burn wounds in rats. The burn wounds were infected with either MRSA, *E. coli* or *P. aeruginosa* and treated with 500 µmol l^{-1} of the conjugate and 60 J cm^{-2} light dose. Over the course of 17 days, the rats that were treated with photodynamic inactivation showed a significantly higher wound healing rate than the control group [372]. Similar has also been demonstrated for methylene blue and *P. aeruginosa* [373,374], chlorine e6 conjugates and *A. baumanii* [375], TMPyP and *S. aureus* [101], and many more in various combinations and modifications [376–379].

While animal models were investigated quite frequently providing a good database, evidence for research on the human skin are scarce. One of the few studies dealing with the effects of photodynamic inactivation of bacteria on the human skin is a work from a research group at the University Hospital Regensburg. In the respective study, human as well as porcine skin was used *ex vivo* to analyze the potential of a phenalenone-based photosensitizer. For concentrations of 500

to 1000 µmol l^{-1} of the PS and up to 60 J cm^{-2} applied energy, a logarithmic reduction of around 3 to 4 log_{10} steps for MRSA was measured. Interestingly, the researchers did not find any changes in mitochondrial activity based on an NBTC histological staining of the skin, which indicated that PDI did not provoke collateral damage in skin cells [99]. However, also PDT methods have been proven to be efficient on the human skin. There are several clinical reports, in which the application of 5-ALA – which was initially used for treatment of actinic keratosis as mentioned earlier – was successful in acne treatment caused by *P. acnes* [380–384]. A recently published case report suggests that 5-ALA might also be used as treatment against infections with fungi of the genus *Candida* [385].

In sum, only few evidence exists about the efficacy of photodynamic inactivation on human skin although *in vitro* evidence against common skin pathogens are frequently reported. However, *in vitro* experiments with skin pathogens were mostly carried out in artificial solvents such as PBS or culture medium. These experimental environments do not reflect the situation on the human skin as there is mostly sweat present. Additionally, *in vitro* experiments are most often carried out in aqueous environments and not on dry surfaces such as the human skin. Therefore, the effects of synthetic sweat on photodynamic inactivation as well as the photodynamic inactivation on human skin are up to date still open questions, which will be tackled within this thesis.

Water treatment

The first report, in which water treatment with photodynamic inactivation was demonstrated longs back to the year 1977 where Gerba *et al.* used methylene blue to reduce viral and bacterial load in waste waters. Successfully, they were able to reduce the coliform load of up to 8 log_{10} steps and the viral load of up to 2 log_{10} steps in their study [386]. However, especially photosensitizers with their absorption maximum around 400 nm are pristine photosensitizers for their use in water as blue light penetrates water much deeper than red light [387]. With an efficacy of up to 8 log_{10} steps it was possible to remove *E. coli*, *P. aeruginosa*, *A. baumannii* as well as *S. aureus* from hospital waste waters with TMPyP [388]. Interestingly, the researchers also analyzed the antibiotic profile of the waste water as such substances might interfere with the proper usage of photodynamic inactivation [388]. Similar reduction was also observed in waste waters in combination with TMPyP and *E. coli* as well as *Enterococcus* sp. [389]. Furthermore, the photodynamic inactivation could also reduce the concentration of chemical pollutants in waste water such as phenol [389]. Other porphyrin-based derivatives have also been shown to be efficient against coliforms by nearly 3 log_{10}

steps [390] and T4 like phages by over 6 $\log_{10}$ steps [391]. Beyond, the photodynamic inactivation of wastewater has also already been optimized with the addition of potassium iodide and a combination of five different cationic porphyrins towards their efficacy in viral inactivation [392]. A commercially available cationic porphyrin, AquaFrin, has been successfully used to reduce *Edwardsiella ictaluri* and *Flavobacterium columnare* [393], two major pathogens in catfish aquaculture [394,395]. The same photosensitizer and method was used to reduce the load of *Saprolegnia parasitica* in trout aquaculture [396]. The fact that artificial light is not always necessary in photodynamic inactivation was proven in studies conducted in Tunisia where AquaFrin was able to reduce the coliform count of 5 $\log_{10}$ steps as well as significant amounts of parasitic worm eggs in wastewater under the influence of sunlight [397,398]. Last but not least, cationic porphyrins might also find its use in the control of algae, at least in aquaristic uses [399].

This thesis tries to investigate the impact of several, common ions which are found in water and their impact on photodynamic inactivation. While the beforehand mentioned literature clearly shows that notable efficacies with photodynamic inactivation can be achieved in water treatment applications, the impact of ions or water itself was not closely investigated yet.

Hygiene

It is recognized recently that hospital acquired infections might be closely entwined with contaminated environmental surfaces [102–104]. When inanimate surfaces are touched, they might become contaminated and might then subsequently be transferred to other individuals [104,400]. Bacteria, fungi and viruses can persist on contaminated inanimate surfaces for prolonged periods of several days and months [401–405] without proper disinfection. Therefore, hygiene measures targeting contaminated fomites in hospitals are inevitable and of great importance. Standard hygiene measures include various physical and chemical interventions [110,406] but the success of those measures are greatly depending on the compliance and execution of the implementing staff [407,408]. It was reported that the hand hygiene compliance among health care workers is around 41% [409] and for hygiene interventions on surfaces 48% [410]. Furthermore, disinfection measures are only active to the time they are applied and the surfaces become recontaminated again [126]. Antimicrobial coatings in general might therefore be capable of permanently reducing the microbial burden on inanimate surfaces leading to the closing of hygiene gaps occurring due to low compliance or incorrect execution [411–414]. It is in general important to note that such antimicrobial coatings do not intend to replace standard hygiene but rather fulfils complementing function in order to

decrease potential transmission risks [126,415]. While there are quite some reports on antimicrobial coatings based on copper [416–420], silver [137,421,422] or quaternary ammonium compounds [135,415], reports for photodynamically active coatings are quite scarce. In a field study that was conducted over three months in two different hospitals, photodynamically active antimicrobial coatings were implemented at frequently touched surfaces. The study showed that the implementation of such a coating was able to reduce the risk of high microbial load by 48% for values above 2.5 colony forming units per cm^2 and even by 67% for 5 colony forming units per cm^2 and above [147]. Further, there are reports on a methacrylated hyaluronic acid coating with embedded methylene blue but the coating was until now only tested *in vitro* with *S. aureus* [423]. In the light of the COVID-19 pandemic, researchers also developed a polyvinyl alcohol-based coating with TMPyP, methylene blue or rose bengal and could efficiently eradicate viruses as well as *S. aureus* [424]. However, also for the latter study just *in vitro* studies were performed [424].

Food technology

Food waste is another major task of the upcoming decades humanity must face. It is estimated that a quarter of all produced food worldwide is lost due to microbial spoilage [425]. To reduce such losses, to improve overall food quality and microbial safety as well as potential development of antibiotic resistances [426], photodynamic inactivation might also represent an important cornerstone in the future. Although food processing often has sophisticated protocols in cleaning which are also implemented in HACCP concepts, the contamination of environmental surfaces is a critical concern [427], pathogen load on surfaces should be reduced to minimal levels [428]. A major advantage of photodynamic inactivation in the context for example of meat is that this method is likely to avoid detrimental changes in sensory and nutritional properties [426,429]. *In vitro* studies of several researches and colleagues demonstrated an efficacy of several log_{10} steps of photodynamic inactivation towards typical food associated pathogenic bacteria with a variety of photosensitizers [430–436]. However, when talking about contaminated food, viruses should also be considered as those are in most cases pathogens of paramount importance [437]. Concerning food related pathogenic viruses, the literature is scarce with only one major study published by Randazzo *et al.*, successfully inactivating murine norovirus as well as feline calicivirus with curcumin [438].

In food industry, experimental data exist for the successful application of photodynamic inactivation on various fruits and vegetables such as strawberries [439,440], tomatoes [298,441], cucumbers [298,442,443], peppers [442], papaya [444], pineapples [445], lettuce [298] and blueberries [446].

Besides this, *E. coli* contaminated fenugreek seeds as well as mung beans could be successfully decontaminated with a curcumin derivative [298]. As an alternative to pasteurization of milk, photodynamic inactivation with methylene blue in milk has been carried out successfully by Srimagal and coworkers [447]. On the contrary, there are also reports that photodynamic inactivation in milk is drastically hindered [448]. Furthermore, the importance of the turbidity of the medium to be treated was pointed out, problems are here rather caused by the penetration depth of light [432,449]. Photodynamic inactivation has also been applied to smoked salmon with riboflavin as a photosensitizer [450] or oysters and curcumin [451] in terms of seafood. Further, poultry meat – more specifically chicken thighs – have been efficiently decontaminated from *S. aureus* with curcumin based photosensitizers [442]. Now, just as mentioned in the section that dealt with the application of photodynamic inactivation in hygiene, surfaces are also in food industry critical key points. Most studies that deal with photodynamic inactivation of surfaces in food industry dealt with polyolefins such as PP or PE. Experiments here were successful with sodium chlorophyllin as a photosensitizer and *B. cereus* [452,453] as well as *L. monocytogenes* [454]. A recent study also reported on the successful fabrication of a biodegradable chitosan-riboflavin composite packaging material that could hinder spoilage and therefore potentially prolong the shelf-life of products [455]. However, it is to be welcomed in food industry that novel, innovative approaches are in the pipeline. This is especially important, as standard techniques such as quaternary ammonium compounds in sublethal concentrations might lead to more tolerant or even resistant strains of *L. monocytogenes* [456–458] or *Salmonella* sp. [459]. Moreover, sanitizers or inappropriate UV treatment might lead to further undesired dissemination of antimicrobial resistance genes [460,461].

Aims of the present work

We can now conclude that photodynamic inactivation is a potentially suitable method for solving certain problems caused by bacteria, antibiotic resistances, or HAIs. Moreover, in a modern, technological world, the method can contribute to increasing the quality and safety of various products. As can be seen from the previously mentioned findings, photodynamic inactivation has been extremely well studied, both in *in vitro* studies and in the actual field of application. What strikes the attentive reader of the literature, however, is the enormous discrepancy in the physical, biological, and chemical parameters that the individual studies reveal. In table 2, some of these discrepancies exemplarily for methylene blue and TMPyP are listed as those provided the best

database for this comparison. To provide sufficient comparability of the following table, only studies were included that used comparable light sources. Additionally, logarithmic bacterial reduction should be taken with a grain of salt as the outcome of this measurement greatly depends on the number of bacteria that are applied in the experiment. Similar divergence was also demonstrated for experiments that were conducted with a phenalenone-based photosensitizer *in vitro* and on the human skin [99]. The tests in this study were conducted with two *S. aureus* strains as well as *E. coli* and *P. aeruginosa*. While *in vitro* experiments clearly showed a reduction of 5 $\log_{10}$ steps with 50 µmol l^{-1} photosensitizer and 0.2 J cm^{-2} for the Gram-positive organisms and 1.2 J cm^{-2} for the Gram-negative organisms, *in vivo* experiments needed up to 2000 µmol l^{-1} photosensitizer and 60 J cm^{-2} light intensity to achieve $\log_{10}$ reductions from 3.5 to 5 [99].

Table 2: Examples of studies and their applied physical, biological and chemical parameters of methylene blue and TMPyP as examples.

Methylene blue					
Organism	c [µmol l^{-1}]	Dose [J cm^{-2}]	$\log_{10}$ reduction	Medium	Ref.
S. aureus	42	15	6.8	0.45 % saline	[462]
S. aureus	27	15	7.9	0.45 % saline	[462]
E. coli	180	40	7.8	0.45 % saline	[462]
P. aeruginosa	200	40	3.5	0.45 % saline	[462]
S. aureus	5	30	1.2	0.9 % saline	[463]
E. coli	20	30	3.5	0.9 % saline	[463]
E. coli	6.25	11.2	1.4	Phosphate buffer	[464]
E. coli	35.2	6	3.5	0.85% saline	[465]
S. aureus	35.2	6	4.0	0.85% saline	[465]
S. aureus	312	360	1.5	skin	[368]
E. faecalis	10	4.54	5.8	teeth	[326]
TMPyP					
E. coli	11	6	6	PBS	[466]
E. coli	10	0.5	6	H_2O	[467]
B. atrophaeus	5	0.5	6	H_2O	[467]
E. coli	3.7	5	9	Culture medium	[468]
A. baumannii	3.7	9	9	Culture medium	[468]
S. aureus	5	30	1	Culture medium	[469]
S. aureus	5	30	1	Culture medium	[469]
S. aureus	10	10	6	PBS	[436]
E. coli	100	10	1	PBS	[436]
B. atrophaeus	1	10	6	PBS	[436]
E. faecalis	10	2.4	6.5	teeth	[326]
S. aureus XEN 8.1	1.56	1.5	4.8	PBS	[101]
S. aureus XEN 8.1	500	200	1.7	Burn wounds	[101]

Based on these findings in literature, initial experiments were conducted that indicated a certain influence of the ions contained in the reaction. These findings represent a clear hurdle for the implementation of PIB in practical, especially clinical application. It is therefore hypothesized that ions as well as small organic molecules might inhibit the photodynamic inactivation, especially as based on the evidence presented in table 2 on some photosensitizers indicate that the efficiency of PIB can be significantly influenced or even blocked by the simultaneous presence of different substances.

It was the first aim of this thesis to implement a high-throughput method and a set of experiments, which allow an investigation of the chemical, physical and biological parameters of PIB. Such an efficient method to analyze the photodynamic system in certain environments is urgently needed as a variety of parameters with different concentrations need to be analyzed and current experimental flows are too time consuming.

Second, with an established methodology it was aimed to investigate on the efficacy of PIB under high sodium chloride concentrations. As an organism living in such high sodium chloride concentrations *Halobacterium salinarum* – an archaeon – was used as up to date no report on photodynamic inactivation towards this domain of life was reported.

At present, it can be assumed that cationic photosensitizers interact with other ions, which led to the third aim of the thesis, which was the investigation of the impact of phosphate and carbonate ions on flavin based photosensitizers and the consequences of potential interactions on photodynamic inactivation efficacy.

Fourth aim was then to evaluate the chemical, physical and biological impact of calcium and magnesium ions towards several photosensitizer classes (phenalenones, phenothiazines, flavins, porphyrins), which are used as photosensitizers for PIB partly *in vitro* or already clinically in humans (methylene blue).

As such divalent cations can react with sequestering agents, it was the fifth aim to try to optimize the efficacy of PIB using citrate in solutions containing different concentrations of calcium and magnesium. Many of these ions that were mentioned in this chapter are ubiquitous under real environmental conditions and are present in high concentrations on the skin. Not only there, but also in other potential application areas (aqueous environments), they could significantly hinder the efficiency of PIB.

Therefore, the sixth aim of the project was to transfer the results obtained for the optimization with citrate in calcium and magnesium ion containing solvents to more realistic solvents, namely

tap water and synthetic sweat. In case of synthetic sweat, it was also tried to evaluate the influence of amino acids like histidine, which are well-known singlet oxygen quenchers.

Lastly, as demonstrated in table 2, the skin seems to be one of the most daunting tasks photodynamic inactivation can cope with now. Therefore, the obtained results were used to optimize the photodynamic process for applications on the human skin. The preclinical project aims to show that it is possible to effectively kill bacteria on the skin surface using PIB (decolonization) without damaging the epidermis underneath. For this purpose, skin surfaces were inoculated *ex vivo* with various bacteria and treated photodynamically with a hydrogel that contains a photosensitizer. To optimize decolonization, all results from the previous work is considered. The investigations in the present project form the important basis for future projects, namely the first clinical testing of PIB for the decolonization of pathogenic bacteria on human skin.

Manuscripts

Overview

This dissertation contains 5 manuscripts. 2 manuscripts were already published, 2 have been submitted to the Journal of Photochemistry and Photobiogy and Photochemistry and Photobiology, respectively. The last manuscript is available as a preprint on the preprint sever bioRxiv. All manuscripts printed in the following were authored by the PhD candidate Daniel B. Eckl as first author. The work contains the manuscripts printed with figures and tables as submitted. The digital appendix of this work (Supplementary data and supplementary figures) can be accessed at https://drive.google.com/drive/folders/1-on6u7rIgvbJoWiDo0dmHgHkCeiIWKIu?usp=sharing.

For convenience reasons, the style of the references was changed to provide a uniform picture within the dissertation itself and are identical with the ones cited in the published manuscripts. Further, the indexing of the figures and tables was adjusted to the style of this dissertation. The author roles are indicated at the end of each chapter according to CRediT [470].

First Report on Photodynamic Inactivation of Archaea Including a Novel Method for High-Throughput Reduction Measurement

Daniel Bernhard Eckl[1], Harald Huber[1], Wolfgang Bäumler[2]

1: Department of Microbiology, University of Regensburg, Regensburg, Germany

2: Department of Dermatology, University Hospital Regensburg, Regensburg, Germany

Correspondence: Daniel B. Eckl, email: Daniel.eckl@ur.de

Manuscript information:

Photochemisty and Photobiology, 2020, 96: 883-889

Received 21 November 2019

Accepted 16 December 2019

DOI: 10.1111/php.13229

Abstract

Archaea are considered third, independent domain of living organisms besides eukaryotic and bacterial cells. To date, no report is available of photodynamic inactivation (PDI) of any archaeal cells. Two commercially available photosensitizers (SAPYR and TMPyP) were used to investigate photodynamic inactivation of *Halobacterium salinarum*. In addition, a novel high-throughput method was tested to evaluate microbial reduction *in vitro*. Due to the high salt content of the culture medium, the physical and chemical properties of photosensitizers were analyzed via spectroscopy and fluorescence-based DPBF assays. Attachment or uptake of photosensitizers to or in archaeal cells was investigated. The photodynamic inactivation of *Halobacterium salinarum* was evaluated via growth curve method allowing a high throughput of samples. The presented results indicate that the photodynamic mechanisms are working even in high salt environments. Either photosensitizer inactivated the archaeal cells with a reduction of 99.9% at least. The growth curves provided a fast and precise measurement of cell viability. The results show for the first time that PDI can kill not only bacterial cells but also robust archaea. The novel method for generating high-throughput growth curves provides benefits for future research regarding antimicrobial substances in general.

Introduction

At the very beginning of the 20th century, Oskar Raab and Hermann von Tappeiner discovered that *Paramecium* cells can be inactivated by simultaneous application of light and acridine dyes by a process called photodynamic mechanism [153,154,156]. Now, it is well known that light is absorbed by such a photosensitizer molecule, which thereby generates reactive oxygen species (ROS). These ROS can destroy cells via oxidation of various cellular structures. Meanwhile, the photodynamic mechanism found its way into different medical fields termed photodynamic therapy of tumors (PDT) [471].

Another promising application of the photodynamic mechanism is PDI of microorganisms that has been proven efficient against viruses, bacteria and fungi. In PDI, a cationic photosensitizer is usually attached to the surface or taken up by the cell and ROS kill the cells or viruses via oxidative mechanisms [309]. A variety of molecules were successfully tested as photosensitizers to be used in PDI like porphyrins, phthalocyanines, phenalenones, phenothiazines or flavins [309].

Photodynamic inactivation (PDI) is efficient in killing bacteria regardless their types or resistances to antibiotic substances [280,472]. The photodynamic inactivation of antibiotic-resistant bacteria like methicillin-resistant *Staphylococcus aureus* (MRSA) was successfully shown on human skin *ex vivo* [99]. When immobilizing photosensitizers as antimicrobial coating, a clinical study provided evidence that generated singlet oxygen can kill bacteria on near-patient surfaces [147]. PDI was also successfully applied to inactivate different viruses [473–478]. Also, fungi [479–483] can be killed with ease with different photosensitizers. Furthermore, photodynamic inactivation is capable of efficiently treating certain protozoa [484].

Thus, PDI can be applied to various pathogenic and non- pathogenic organisms spanning nearly all parts of known living matter. However, the scientific literature remains without any prove that this principle applies to archaea. This might be explained by the fact that there are no discrete pathogens within the archaea so far. However, scientists start to understand the importance of a healthy human microbiome that also contains archaea [485–487] although archaea are typically found in various extreme environments such as black smokers or hydrothermal vents. These organisms are called hyperthermophiles with optimal growth temperatures above 80°C. Some archaea have also been reported to be extremely tolerant to ionizing radiation such as the anaerobic Euryarchaeon *Thermococcus gammatolerans* [488]. *Picrophilus oshimae* on the other hand is an organism that was isolated from a solfataric field in Hokkaido, Japan, that naturally has a pH of 2.2 and is therefore considered an acidophilic organism [489]. Recently, archaeal signatures have

been discovered on board the international space station that is the latest prove for archaea in artificial, human-inhabited environments [490].

Since PDI requires oxygen to generate ROS, such research in archaea is hampered since the majority of these organisms is considered anaerobic. Aerobic archaea usually require pH values at which photosensitizers are chemically destroyed [491].

Therefore, in this study the extremely halophilic organism *Halobacterium salinarum* [492], which grows aerobically at neutral pH values was investigated. Cells of the genus *Halobacterium* are rods or disk-shaped cells that stain Gram-negative and often contain gas vacuoles [493]. The present study shows PDI of an Archaeum (*Halobacterium salinarum*) for the first time. Another goal of this study was the application of growth curves in order to evaluate the logarithmic reduction of viable cells like archaea. The application of growth curves allows a much higher throughput of samples compared to other methods such as pour plate, spread plate or drop plate methods [494,495].

Materials and Methods

Photosensitizers

The Photosensitizer TMPyP was purchased from Sigma-Aldrich with a minimum dye content of 97%, while SAPYR, an exclusively singlet oxygen producing photosensitizer, was purchased from TriOptoTec GmbH, with a minimum dye content of 97%. Photosensitizer solutions were prepared in adequate concentrations of 2, 10, 20, 50 and 100 µmol l^{-1} in sterile sodium chloride solution (10% w/v).

Organism and cultivation

For inactivation, *Halobacterium salinarum*^{T} DSM 3754 was used. It was cultivated at 37°C for 48 h in a modified Halobacterium medium containing per liter 5 g yeast extract (Becton, Dickinson and Company, Sparks), 5 g casamino acids (Becton, Dickinson and Company), 1 g sodium glutamate (Merck KGaA, Darmstadt, Germany), 2 g potassium chloride (Carl Roth GmbH+Co. KG, Karlsruhe, Germany), 3 g sodium tetra citrate (Merck KGaA), 20 g magnesium sulfate heptahydrate (Merck KGaA) and 200 g sodium chloride (Carl Roth GmbH+Co. KG). Besides the organic compounds, all substances were provided in analytic grade. The medium was autoclaved at 121°C for 20 min in 50 mL Erlenmeyer flasks containing 20 ml medium.

Cell preparation

Cells were harvested via centrifugation of 10 ml medium transferred into sterile 15 ml reaction tubes. Centrifugation took place for 7 min at 4,500 g. The supernatant was discarded, and the pellet was suspended in 5 mL of sterile sodium chloride solution (10% w/v). These steps were repeated thrice in order to remove remaining culture medium. After harvesting, the optical density measured at 600 nm of the cells was adjusted to 0.6.

Photodynamic inactivation

The assays were conducted in 96-well plates. Column 1 of the plate contained 25 µl of archaeal cells with 25 µl of sodium chloride solution (10% w/v). Next five columns contained TMPyP as a photosensitizer in ascending concentration, namely 1, 5, 10, 25 and 50 µmol l^{-1} and 25 µl of archaeal cells. Columns 7–12 were prepared accordingly with SAPYR. Experiments were conducted at low ambient light conditions as described elsewhere [496]. The assays were illuminated beneath a commercial blue light source (blue_v, Waldmann GmbH, Villingen-Schweningen, Germany) with a radiant exposure of 10.8 J cm^{-2}. Additionally to the illuminated sample, a dark control was

treated in the same manner without irradiation for dye concentrations of 0 and 50 µmol l^{-1}. After illumination, 20 µl of the cell suspension were immediately transferred into 180 µl of prewarmed (37°C) culture medium in 96-well plates. Twelve wells of the well plate contained medium without cells and served as blank control. These so prepared well plates were placed in a spectral photometer (CLARIOStar, BMG LABTECH GmbH, Ortenberg, Germany). Internal incubator was set to 37°C, while the internal shaker was turned on every 5 min shaking at 200 rpm for 30 s. After every 5 min, the spectral photometer measured the optical density at 600 nm of all wells. In total, the measurement was carried out for 2245 min with an additional last measurement carried out at 4115 min in order to increase the limit of detection to around 3 orders of magnitude. As each experiment was performed in triplicates, mean values of the optical density values were calculated and plotted via SigmaPlot against the incubation time.

Calculation of microbial reduction

The method used in this report for calculation of the microbial reduction was performed in accordance with another report in a modified manner [497]. Therefore, doubling time of the archaeal cells was calculated as Δt_D between an optical density of 0.1 and 0.2 in early exponential growth phase. The doubling times were calculated for the untreated control. The time difference in reaching the optical density of 600 nm of 0.1 of the control and illuminated cells was calculated and is further on called Δt. The logarithmic reduction shortly called ρ was subsequently calculated as described in the formula below.

$$\rho = log2^{\frac{\Delta t}{\Delta t_D}}$$

Attachment of photosensitizers to cells

In order to investigate the attachment of the photosensitizer to the cell surface, a culture grown as mentioned before was centrifuged at 4,500 g for 7 min and final optical density at 600 nm was adjusted to 0.6. The supernatant was discarded and the cells were suspended in 500 µl of 10% (w/v) NaCl and 500 µl of 20 µmol l^{-1} of photosensitizer solution. Cells were mixed thoroughly and centrifuged again. The supernatant was measured in a photometer at a wavelength of 421 nm for TMPyP and 370 nm for SAPYR, resembling the corresponding absorption maxima. As blank, a 10% (w/v) NaCl solution was used. Control consisted of 5 µmol l^{-1} in a 10% (w/v) NaCl solution.

DPBF (1,3-Diphenylisobenzofuran) assays

For analyzing the production of singlet oxygen production under high salt concentrations, photosensitizer in final concentrations of 1, 5, 10, 25 and 50 µmol l^{-1} and sodium chloride (20% w/v) were mixed and resuspended with the DPBF reagent with MeOH as a solvent to a total volume of 200 µl. Final concentrations were 1, 5, 10, 25 and 50 µmol l^{-1}, 500 µmol l^{-1} DPBF and 10% (w/v) NaCl. DPBF was excited in a spectral photometer (CLARIOStar, BMG LABTECH GmbH) at 411 nm while emission was detected at 451 nm. Relative fluorescence was calculated from a control without PS as $\frac{Fluorescence_{PS}}{Florescence_{Control}}$. Data were plotted via SigmaPlot V14. Control measurement was performed with a nonilluminated sample. The generation of singlet oxygen was then initiated via illumination beneath the light source blue_v applying a fluence of 0.018 J cm^{-2}, and fluorescence was measured as mentioned above. The illumination and measurements were repeated four times with the same sample. A final illumination with the same sample was performed applying another 0.09 J cm^{-2}. The applied fluence was equal to 1, 2, 3, 4, 5 and 10 s of illumination time in total.

Measurement of absorption spectra

Photosensitizer concentrations were prepared and mixed with an equal volume of 10% (w/v) NaCl solution in 96-well microreaction plates with a total volume of 100 µl. Spectra were recorded from 300 to 700 nm. Measurements took place with the illuminated and nonilluminated samples. The applied radiant exposure was 10.8 J cm^{-2} corresponding to 10 min of illumination.

Results

Under high salt concentrations (10% [w/v] NaCl), no alterations of TMPyP absorption spectrum were detectable after irradiation (10.8 J cm^{-2}) (Fig. 16a). In contrast, SAPYR showed photobleaching after an applied radiant exposure of 10.8 J cm^{-2} (Fig. 16b). The data of the reference spectra with the photosensitizer dissolved in ultrapure water are not shown, as the curves did not differ from the nonirradiated sodium chloride controls.

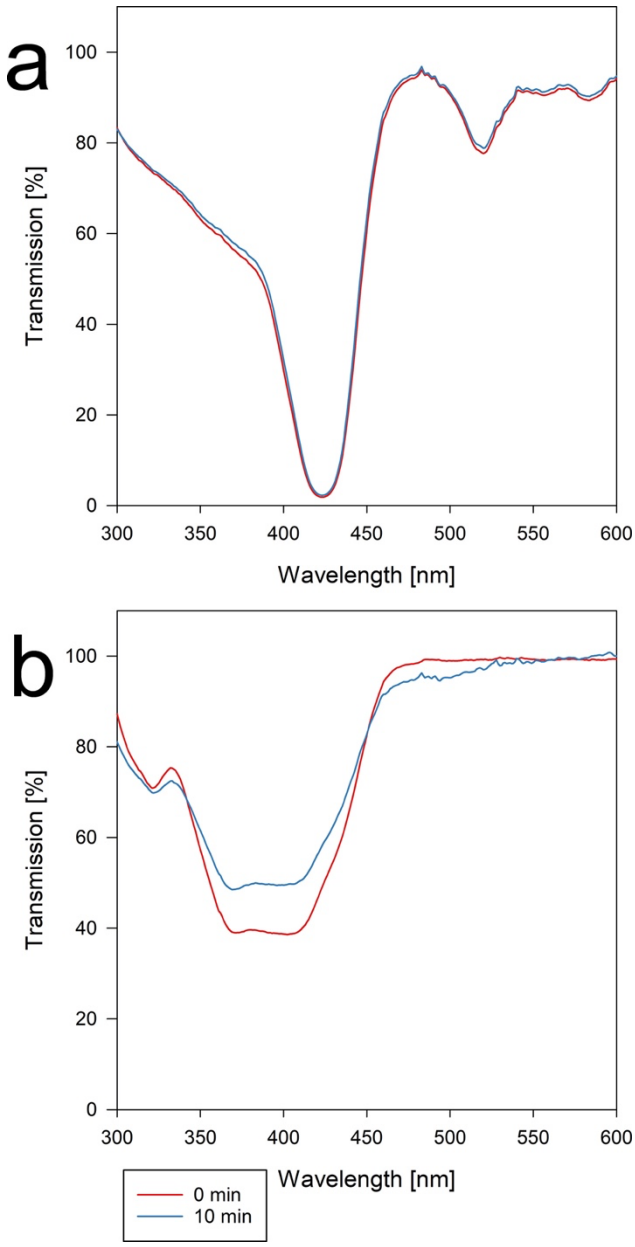

Figure 16: Transmission spectra for TMPyP (a) and SAPYR (b) dissolved in 10% (w/v) NaCl. Red lines refer to the nonilluminated control, while blue lines refer to photosensitizer solution after illumination at a radiant exposure of 10.8 J cm^{-2}.

Attachment assays showed that TMPyP binds much more efficient to the tested archaeal cells than SAPYR does. 73 % of TMPyP (3.62 µmol L^{-1}) attached to cells at a concentration of 5 µmol L^{-1}. In case of SAYPR, only 14 % (0.70 µmol L^{-1}) attached to the cells.

DPBF assays indicate that the production of singlet oxygen takes place with both dyes under high sodium chloride concentrations (Fig. 17). TMPyP generated more singlet oxygen when compared to SAPYR under the experimental conditions. For the highest concentration of 50 µmol L^{-1}, the same fluorescence is observed, indicating that either the same amount of oxygen was produced or all the available oxygen was depleted within the reaction. After 10 s of illumination, 50 µmol L^{-1} TMPyP (Fig. 17a) yielded a relative fluorescence of 10.3% and 11.0% for 50 µmol L^{-1} SAPYR (Fig. 17b), respectively. 25 µmol L^{-1} of photosensitizer showed a relative fluorescence of 10.2% for TMPyP and 55.6% for SAPYR, respectively. At 10 µmol L^{-1}, barely reduced relative fluorescence for TMPyP after 10 s was detected (10.5%) while SAPYR exhibited a tremendously higher relative fluorescence with 80.3%. 32.9% for 5 µmol L^{-1} TMPyP and 75.1% for 5 µmol L^{-1} SAPYR were the measured relative fluorescence values for mentioned concentration. 1 µmol L^{-1} of photosensitizer led to a relative fluorescence of 80.7% for TMPyP and 102.4% for SAPYR. Water controls after 10 s of illumination for SAPYR (data not shown) showed values of 22.6% for 50 µmol L^{-1}, 39.9% for 25 µmol L^{-1}, 64.2% for 10 µmol L^{-1}, 76.9% for 5 µmol L^{-1} and 107.4% for 1 µmol L^{-1}. Water controls for TMPyP showed after 10 s of illumination: 10.2% for 50 µmol L^{-1}, 10.3% for 25 µmol L^{-1}, 10.5% for 10 µmol L^{-1}, 16.5% for 5 µmol L^{-1} and 84.5% for 1 µmol L^{-1}. Fig. 17c compares the relative fluorescence for SAPYR and TMPyP after 10 s of illumination in dependence of the concentration of the photosensitizer.

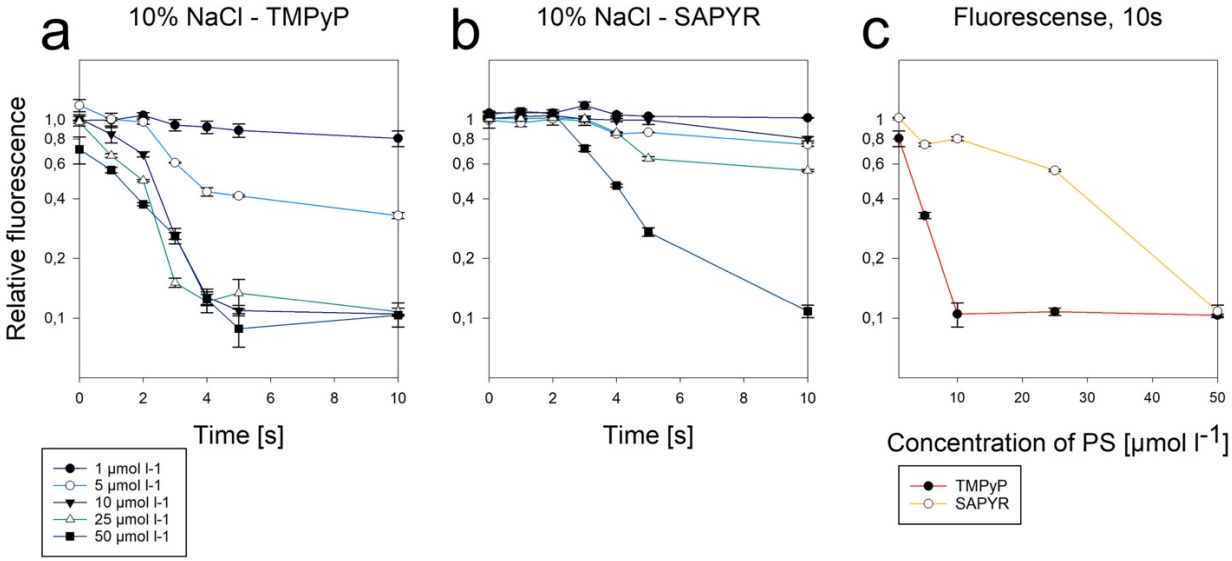

Figure 17: DPBF assays for TMPyP (a) and SAPYR (b) carried out in a 10% NaCl solution. Relative fluorescence is displayed logarithmically on the y-axis, and illumination time in seconds is plotted on x-axis. A comparison of the relative fluorescence (y-axis) for different photosensitizer concentrations (x-axis) is shown after 10 s of illumination equal to a total applied radiant exposure of 0.018 J cm^{-2} (c).

The growth curves displayed in Fig. 18a clearly show that for the highest concentrations of SAPYR (25 and 50 µmol L^{-1}), no growth of *H. salinarum* was detected. Even after 4115 min of incubation, optical density values have not reached values above 0.1 (data not shown). The calculated $\log_{10}$ reductions for SAPYR are displayed in Fig. 18b. Significant $\log_{10}$ reductions were obtained for photosensitizer concentrations of 25 and 50 µmol L^{-1}. The illuminated control without photosensitizer exhibited a logarithmic reduction of 0.05.

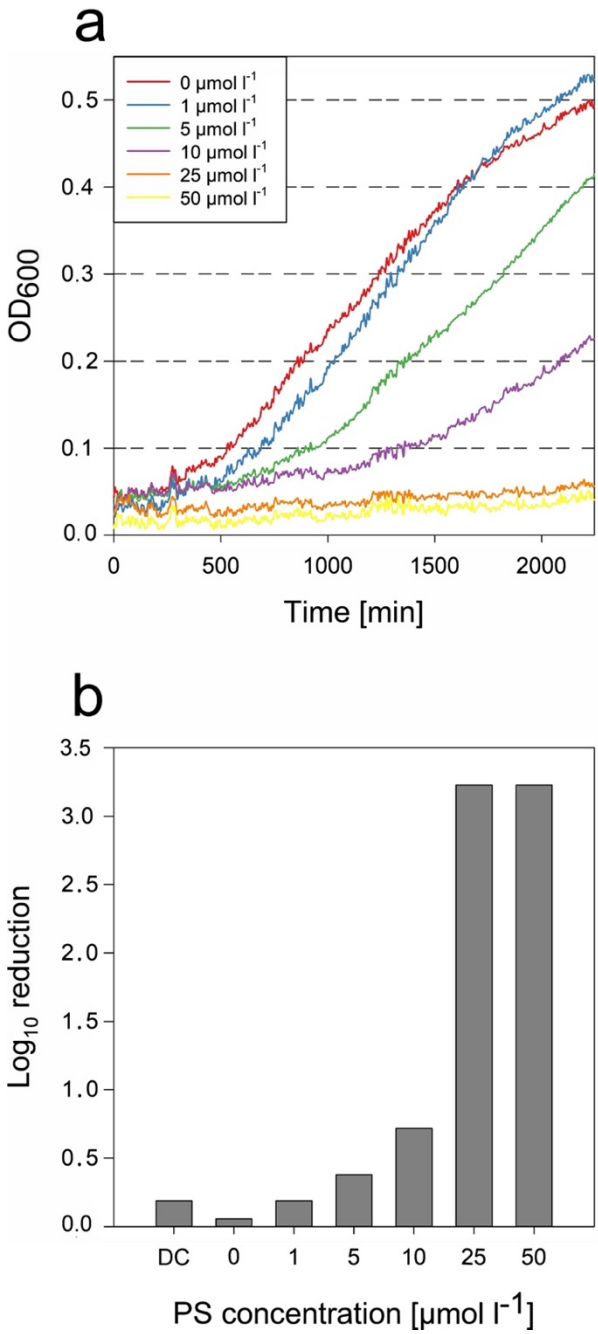

Figure 18: (a) Growth curves of *H. salinarum* after PDI treatment with SAPYR as photosensitizer. Different colors reflect the different SAPYR concentrations used for PDI treatment. Y-axis indicates the optical density measured at 600 nm. X-axis indicates the time in minutes. (b) Calculated $\log_{10}$ reduction displayed as bar chart diagram.

When using the same concentrations of TMPyP and radiant exposure, the inactivation of *H. salinarum* was more efficient as shown by the growth curves in Fig. 19a compared to SAPYR (Fig. 18). The lowest photosensitizer concentration was 5 µmol L^{-1} to achieve maximal logarithmic reduction of 3.22. At 4115 min, TMPyP concentrations from 5 to 50 µmol L^{-1} showed that optical density did not exceed values above 0.1 resulting in a microbial reduction of at least 3 orders of magnitude. Dark control for TMPyP at 50 µmol L^{-1} showed no relevant logarithmic reduction with a calculated value of 0.09. The logarithmic reduction values are displayed as a bar chart in Fig. 19b.

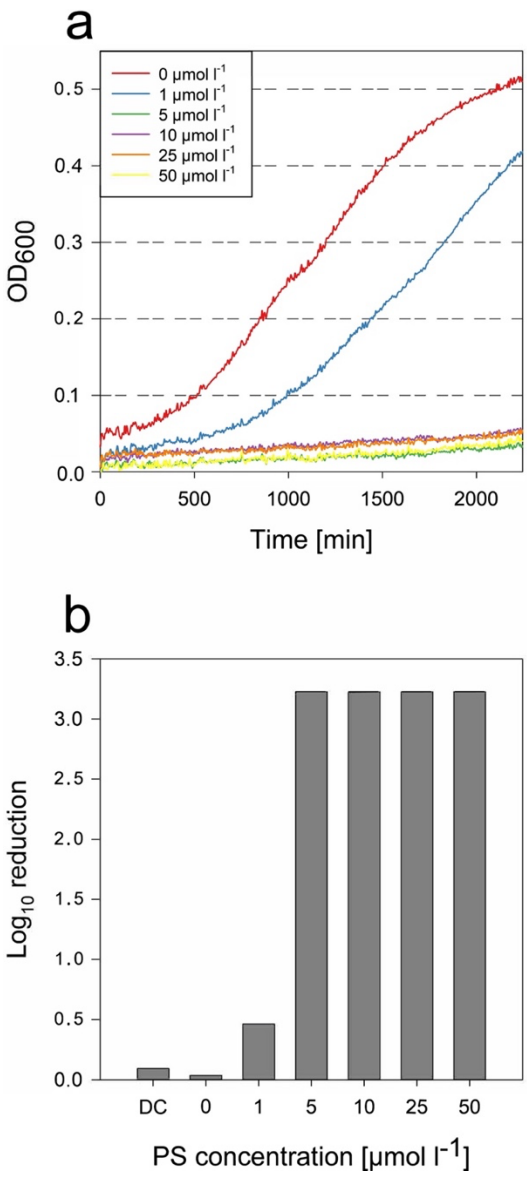

Figure 19: (a) Growth curves of *H. salinarum* after PDI treatment with TMPyP as Photosensitizer. Different colors reflect the different photosensitizer concentrations used for PDI treatment. Y-axis indicates the optical density measured at 600 nm. X-axis indicates the time in minutes. (b) Calculated $\log_{10}$ reduction displayed as bar chart diagram.

Discussion

The presented results clearly show that the Archaeum *Halobacterium salinarum* can be efficiently inactivated (>99.9%) using PDI with either photosensitizer at low concentrations. The results also show that high concentrations of sodium chloride, for example, 10%, did not lead to a chemical alteration of the photosensitizers used. The loss of concentration after illumination for SAPYR is a general feature of the molecule, observed even in water without further substances present.

The structure of archaeal cells shows significant differences when compared to eukarya or bacteria. One of the most striking differences is their outer structure. Besides an S-Layer, which is also known for some bacteria, archaea are characterized by their extraordinary membrane structure. The phospholipid bilayer membrane consists of side chains of 20 carbon atoms built from isoprene attached with an ether linkage to glycerol compared to eukarya and bacteria that form ester bonds with fatty acids [498,499]. Another obvious feature of halophilic archaea is the pink-to-purple color of the cells due to retinal bound to rhodopsin-like molecules named bacteriorhodopsin [500]. Bacteriorhodopsin is an integral membrane protein with seven near-parallel alpha helices, whereas between the helices a retinal molecule is integrated as ligand forming a trimer composed of 21 helices and three retinal molecules [501]. This protein functions as a light-driven proton pump contributing to the formation of a pro- ton gradient for energy conservation [502]. As rhodopsin and bacteriorhodopsin are structurally and chemically very similar, the singlet oxygen-quenching rate constant for rhodopsin should be quite similar to bacteriorhodopsin, at least within the same order of magnitude. The reported value for the quenching rate is 1.1×109 L mol^{-1} s^{-1}, therefore being similar to the ones found in literature for the azide ion [503–506]. The presented results clearly show that archaeal structures compared to bacteria should have an impact on the efficiency but do not lead to a certain resistance or tolerance. Recently, van der Oost and coworkers engineered an *E. coli* cell capable of producing and incorporating archaeal lipids into the cell membranes [507]. The impact of archaeal lipids concerning the susceptibility toward ROS could be studied in a sophisticated manner in future research utilizing the mentioned *E. coli* with the hybrid membrane. This study also showed that archaeal structures like S-layer, rhodopsin or ether lipids did not prevent binding of the photosensitizer. It should be noted that the present investigation cannot differentiate whether photosensitizer molecules are taken up by the archaeal cells or are attached to the cellular wall only. The amounts of photosensitizer bound to the cells differ for both photosensitizers used. This difference might be explained by the different charges of the photosensitizers. SAPYR molecule exhibits only one positive charge while TMPyP four. Thus,

TMPyP should attach much better to negatively charged outer structures of cells in general. As for bacterial cells, the S-layer of *Halobacterium* is negatively charged as the charge also maintains the lattice of the S-layer [508–510].

DPBF assays in general are sufficient to detect the generation of singlet oxygen. Our data suggest that under the experimental conditions, TMPyP produced more singlet oxygen than SAPYR. However, the different extinction coefficients along with emission spectrum of the light source and the photosensitizer concentrations must be considered. The impact of the absorbed photons on photosensitizers was thoroughly investigated elsewhere [511]. According to that publication, the amounts of absorbed photons per second were compared. Additionally, the different singlet oxygen quantum yields were considered which are 0.77 for TMPyP [512] and 0.99 for SAPYR [230]. Under present experimental conditions, SAPYR generates 94% or 62% less singlet oxygen than TMPyP for 1 or 50 µmol L^{-1} photosensitizer concentrations, respectively. These data should explain to some extent the difference in singlet oxygen production (DPBF assays; Fig. 2) and consequently also in PDI of *Halobacterium salinarum* for both photosensitizers (Figs. 3 and 4). Nevertheless, a reduction of viable cells is achieved for both photosensitizers with more than 3 $\log_{10}$ at 5 µmol L^{-1} (TMPyP) or 25 µmol L^{-1} (SAPYR). Our study showed that photodynamic inactivation of archaea works well and efficiently even at high salt concentrations. However, when compared to other model organisms like *E. coli*, *B. atrophaeus* or *E. faecalis*, *Halobacterium salinarum* seems to be less susceptible to PDI [230,496,511].

Various studies concerning photodynamic inactivation focus primarily on pathogenic bacteria causing severe skin infection [99,297,513,514]. Nevertheless, the contribution of archaea to the human health in general is highly debated and highlighted [515–517]. Up to date, there are no representatives known within the archaea that can cause pathogenic infections. However, it is known that archaea are able to colonize the human body [486,515,518–520]. The role of *Methanobrevibacter oralis* in gingivitis and brain abscesses has been described [521,522].

When looking at the second goal of the present study, the data indicate that the presented method for high-throughput measurement of the antimicrobial potential can be applied to any microorganisms in liquid medium. The presented method offers several advantages compared to other methods like spread plating, pour plating or drop plating. First, the method offers huge time saving as the process of measuring and partly evaluation is automated. Compared to plating methods, a dilution series is not necessary, as well as plating is obviously not performed. Furthermore, the method is much cheaper than plating methods as no agar medium is necessary

and the experiments can be performed within the microvolume range. Drop plating methods have some issues like accuracy and limitations to certain cells; however, the problems were mentioned and tried to optimize elsewhere [495].

Conclusions

The presented results are the first record for the photodynamic inactivation of archaea, therefore proving the applicability of PDI toward all domains of life. The novel method for generating high-throughput growth curves will prove useful in the future concerning research of antimicrobial substances in general, as the method is applicable for all organisms that grow in liquid media. Our future research concerning photodynamic inactivation of archaea will focus on the role of archaeal lipids concerning photodynamic inactivation.

Acknowledgements

Technical help of G. Gmeinwieser is highly appreciated. This work was supported by the German Research Foundation DFG [grant number 415812443].

Contributions

DBE: Conceptualization, methodology, validation, formal analysis, investigation, writing – original draft, visualization; WB: Resources, writing – review and editing, supervision, project administration, funding acquisition; HH: Resources, writing – review and editing, supervision, project administration, funding acquisition

Interplay of phosphate and carbonate ions with flavin photosensitizers in photodynamic inactivation of bacteria

Daniel Bernhard Eckl[1*], Stefanie Susanne Eben[1*], Laura Schottenhaml[1], Anja Eichner[2], Rudolf Vasold[3], Andreas Späth[4], Wolfgang Bäumler[2], Harald Huber[1]

1: Department of Microbiology, University of Regensburg, Regensburg, Germany

2: Clinic and Policlinic of Dermatology, University Hospital Regensburg, Regensburg, Germany

3: Department of Organic Chemistry, University of Regensburg, Regensburg, Germany

4: TriOptoTec GmbH, Regensburg, Germany

*: Contributed equally

Correspondence: Daniel B. Eckl, email: Daniel.eckl@ur.de

Publication information:

PLoS ONE 16 (6): e0253212

Received 22 January 2021

Accepted 29 May, 2021

DOI: 10.1371/journal.pone.0253212

Abstract

Photodynamic inactivation (PDI) of pathogenic bacteria is a promising technology in different applications. Thereby, a photosensitizer (PS) absorbs visible light and transfers the energy to oxygen yielding reactive oxygen species (ROS). The produced ROS are then capable of killing microorganisms via oxidative damage of cellular constituents. Among other PS, some flavins are capable of producing ROS and cationic flavins are already successfully applied in PDI. When PDI is used for example on tap water, PS like flavins will encounter various ions and other small organic molecules which might hamper the efficacy of PDI. Thus, the impact of carbonate and phosphate ions on PDI using two different cationic flavins (FLASH-02a, FLASH-06a) was investigated using *Staphylococcus aureus* and *Pseudomonas aeruginosa* as model organisms. Both were inactivated in vitro at a low light exposure of 0.72 J cm^{-2}. Upon irradiation, FLASH-02a reacts to single substances in the presence of carbonate or phosphate, whereas the photochemical reaction for FLASH-06a was more unspecific. DPBF-assays indicated that carbonate and phosphate ions decreased the generation of singlet oxygen of both flavins. Both microorganisms could be easily inactivated by at least one PS with up to 6 log_{10} steps of cell counts in low ion concentrations. Using the constant radiation exposure of 0.72 J cm^{-2}, the inactivation efficacy decreased somewhat at medium ion concentrations but reached almost zero for high ion concentrations. Depending on the application of PDI, the presence of carbonate and phosphate ions is unavoidable. Only upon light irradiation such ions may attack the PS molecule and reduce the efficacy of PDI. Our results indicate concentrations for carbonate and phosphate, in which PDI can still lead to efficient reduction of bacterial cells when using flavin based PS.

Introduction

Flavins in general are based on a heterocyclic 7,8-dimethylisoalloxazine and appear as yellow substances with excellent water solubility [275,276]. The most important flavin taken up by the animal digestive tract is riboflavin, also known as vitamin B_2 or as food additive E101 [523]. Unlike riboflavin, FMN (flavin mononucleotide) and FAD (flavin adenine dinucleotide) are commonly associated to proteins as cofactors. The first isolation of a flavin, called lactochrome, was executed in 1879 from cow's milk by the English chemist A. W. Blyth [275,524].

FMN fulfills for example important functions in biochemical pathways [277] as a coenzyme for oxidoreductases [276] and plays a major role in aerobic cellular respiration. FMN functions as an electron carrier in the complex I of the respiratory chain [278]. In addition, flavins play an important role in the bioluminescence of *Aliivibrio fischeri* [279]. In 1949 Arthur W. Galston discovered that riboflavins are capable of oxidizing indolacetic acid in plants by the requirement of oxygen and light, which also led to growth deficits in plants [282].

Flavins are also well known for forming several redox states. They either occur in oxidized form, as semiquinone or hydroquinone. Each redox state of the flavins has a distinct absorbance spectrum that can be used to differentiate between each state [275]. Flavin semiquinones as well as hydroquinones are likely to react with molecular oxygen resulting in the oxidized form that is known to be stable in standard atmospheric condition [275].

The oxidation of flavin molecules via generation of a light-induced triplet state was shown elsewhere [284] as well as singlet oxygen generation of riboflavin [285]. Eichler *et al.* observed that endogenous flavins are capable of producing ROS intracellularly [283]. In this case, the authors could not detect harmful effects and discussed a protective effect of flavin binding proteins. Although such endogenous flavins like riboflavin are capable of efficiently producing singlet oxygen [286–289], a sufficient inactivation of bacteria was not observed [290,291].

The measurement of the quantum efficiency of singlet oxygen generation (Φ_Δ) of riboflavin, FMN and FAD by Baier *et al.* in 2006 [288] paved the way for the application of riboflavin as a new photosensitizer (PS) in photodynamic inactivation of microorganisms (PDI).

Thus, the same research group decided to change the disadvantage of riboflavin, namely the lack of a positive net charge hampering the attachment of riboflavin to bacterial cells. The synthesis of cationic riboflavin molecules enabled a highly effective PDI for different bacterial strains [225,280]. A close cell attachment or cellular uptake of a PS is mandatory because singlet oxygen shows a short diffusion range of less than 100 nm in cellular environments [219,226].

Flavins, either cationic or not, are molecules with interesting properties as PS. These molecules are biodegradable and therefore considered safe for human use [280,281]. Limited water solubility hinders gastrointestinal uptake [525] and high doses do not lead to side effects [526]. These properties allow flavins to be used in a wide range of applications ranging from humans to animal products as well as applications in the environment. However, potential fields of application for flavin PS like the human skin, the oral cavity, water disinfection and inanimate surfaces show the presence of different cations such as sodium ions as well as potassium ions and anions like chloride, carbonate and phosphate.

Thus, the present study aimed to investigate PDI with cationic flavin PS, exemplarily regarding the potential impact of sodium carbonate and sodium phosphate in four different concentrations. To unveil the potential effects of such ions, the experiments were performed at low light exposure of 0.72 J cm^{-2}. Biological logarithmic reduction data were supplemented with assays of PS attachment towards cells, chemical analysis and physical measurements.

Material and methods

Bacterial strains

Bacterial strains were purchased from the German Collection of Microorganisms and cell culture lines (DSMZ, Braunschweig, Germany). As a Gram-positive representative *Staphylococcus aureus* DMZ 1104 was used, as Gram-negative model organism *Pseudomonas aeruginosa* DSMZ 1117. All organisms were grown on Mueller-Hinton-Agar [527] at 37° C.

Preparation of the ionic solutions

Solutions were prepared as stock solutions with a concentration of 150, 15, 1.5 and 0.15 mmol l^{-1}. As a solvent ultra-pure water with a conductance > 18 Ω was used, hereafter called H_2O. After preparation, solutions were stored in plugged, sealed, gas tight serum bottles under nitrogen atmosphere in the dark at room temperature. pH value was adjusted to 7 with phosphoric acid for sodium phosphate solutions while for sodium carbonate HCl was used for adjustment. Sodium phosphate (Na_3PO_4) was obtained from Merck KGaA, Darmstadt, Germany while sodium carbonate (Na_2CO_3) was bought from Sigma-Aldrich, St. Louis, MO, USA, both in analytical grade.

Photosensitizer

The PS were flavin derivatives designated as FLASH-02a and FLASH-06a [26]. Both PS were purchased from the TriOptoTec GmbH (Regensburg, Germany) with a minimum dye content of 97%. The structure of the PS is displayed in Fig 20A for FLASH-02a and Fig 20B for FLASH- 06a, FLASH-02a is a doubly charged cation with a rather small side chain compared with the fourfold charged cationic PS FLASH-06a with remarkably larger side chains. The positive charge of both PS allows the molecules to be located in the vicinity of bacteria enabling efficient inactivation.

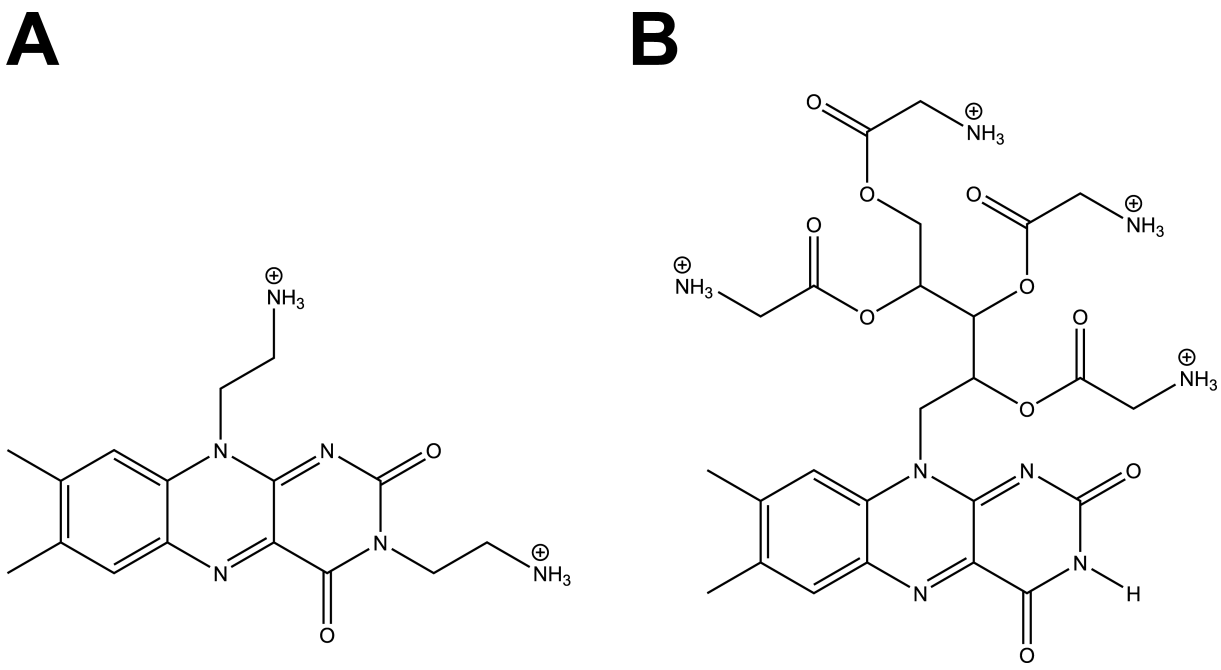

Figure 20: Structure of the used PS. (A) shows the structure of FLASH-02a, (B) shows the structure of FLASH-06a. The counterions of the substances were in both cases chloride anions.

Spectroscopy

In order to investigate the chemical interactions of ions and PS at various concentrations, absorption spectroscopy in the visible spectral range (VIS) was performed. Assays were composed out of a total volume of 200 µl with PS concentrations ranging from 0 to 50 µmol l^{-1} and ionic solutions in concentrations of 0.075 mmol l^{-1} to 75 mmol l^{-1}. Spectra measurement took place in 96-well plates utilizing a BMG Labtec plate reader (BMG Labtec, Ortenberg, Germany). Spectra were measured prior and after irradiation with up to 10.8 J cm^{-2}, equivalent to 10 min of irradiation. The obtained percentage transmission was plotted with OriginLab 2019b (Northampton, USA). In order to analyse isosbestic points, the apparent coefficient of variation was calculated as follows

$$CV = \frac{\sigma(\lambda)}{A(\lambda)} \times 100$$

CV: Apparent coefficient of variation

$\sigma(\lambda)$: Standard deviation at wavelength λ

$A(\lambda)$: Absorption at wavelength λ

Whenever an intersection of the spectra occurred and the apparent coefficient was below 2.5% [528], an isosbestic point was assumed.

DPBF-assays

DPBF-assays aimed for a qualitative statement whether the photophysical properties of the dye are hindered in the presence of ions. 1,3-Diphenylisobenzofurane (DPBF) was purchased from Sigma-Aldrich with a minimum dye content of 97%. Each assay was composed as follows:

200 µl in dark 96-well plates (Sarstedt AG & Co. KG, Nuembrecht, Germany) contained a concentration of 0 to 50 µmol l^{-1} PS, 75, 7.5, 0.75 or 0.075 mmol l^{-1} of the corresponding ion and 500 µmol l^{-1} DPBF (dissolved in 99% methanol, analytical grade). The DPBF solution was prepared immediately before each experiment. Controls consisted out of 100 µl ionic solution in appropriate concentration and 100 µl methanol. Internal references contained 100 µl H_2O and 100 µl methanol with 500 µmol l^{-1} DPBF. Each value for each condition was obtained as the mean value of three independent replicates. The assays were measured after 0, 1, 2, 3, 4, 5 and 10 s of irradiation with the beforehand mentioned light source utilizing a fluorescence plate reader, purchased from BMG Labtech. Excitation wavelength was set to 411 nm while emission was detected at 451 nm. Values obtained for the internal reference were set to 1, relative fluorescence was calculated as ratios to the control and displayed in per cent via OriginLab 2019b. A statistical analysis of the retrieved values was performed afterwards as explained in S1 File.

Light source

Irradiation of all samples was performed with a blue light emitting prototype containing a neon tube with an emission range from about 380–470 nm (BlueV, Medizintechnik Herbert Waldmann GmbH & Co. KG, Villingen-Schwenningen, Germany). Intensity was measured with a thermal sensor (Nova 30 A-P-SH, Ophir-Spiricon, North Logan, UT, USA). All irradiation steps were carried out at a light irradiance of 18 mW cm^{-2}.

Photodynamic treatment of bacteria

Bacteria were taken from the agar plates and suspended in H_2O. Optical density was adjusted to 0.6 at 600 nm utilizing a photometer (Ultrospec 10, Amersham Biosciences, Little Chalfont, UK). After density adjustment, 1 ml of the bacterial suspension was transferred to 1.5 ml reaction tubes and centrifuged at 13,000 x g for 7 min. Subsequently, supernatant was discarded and the pellet was resuspended in H_2O. Centrifugation was repeated and mixed thoroughly with 1000 µl of ionic solution prepared as mentioned above. 25 µl of the prepared suspension were then mixed with 25 µl of PS-solution in ascending concentrations, incubated for 10 min in absolute darkness and

irradiated with a constant energy of 0.72 J cm^{-2} (corresponding to an illumination time of 40 s) afterwards.

20 µl of this reacting solution were transferred to 180 µl preheated Mueller-Hinton bouillon and cultivated at 37° C for 48 h. A plate reader measured the optical density at 600 nm which was used to calculate the bacterial reduction as described in detail elsewhere [467]. In principle, the applied method concerning cultivation and evaluation of the microbial reduction is a adaption of a method initially described by Bechert and co-workers [497] and has been successfully used for example by Bruenke *et al.* [529]. Doubling time was calculated for an optical density of 0.2 and 0.4. All light sensitive parts of the procedure were conducted at low light conditions as investigated elsewhere [496]. Obtained inactivation values, which were obtained from three independent measurements, were analyzed statistically as mentioned in S2–S4 Files.

Binding assays

To investigate binding of flavins to bacteria, optical density at 600 nm was adjusted to 0.6. 500 µl cell suspensions were placed in 1.5 ml reaction tubes, centrifuged as mentioned before and washed in H_2O. The pellet was suspended in 500 µl of ionic solution and 500 µl of PS with a concentration of 100 µmol l^{-1} and incubated for 10 min in the dark. After incubation, the cells were centrifuged at 4,500 x g for 10 min. The supernatant was transferred into a cuvette and measured against a control. Measurements were carried out at 444 nm for FLASH-02a and 446 nm for FLASH-06a, respectively. Each condition was tested independently thrice leading to three independent values. A statistical analysis of the binding assays was performed and is shown in S5 File.

Statistical analysis

Data from DPBF-assays were collected in three independent replicates, while values of the binding assays and logarithmic reduction rates from the photodynamic inactivation experiments were obtained from three biological replicates of each tested condition. In order to investigate the data statistically the values of the replicates were compared between the tested conditions and p-values were calculated via unpaired, two-tailed t-tests assuming normal distribution. Events were considered statistically significant for $p < 0.05$. When p was < 0.01, events were considered highly significant, $p < 0.001$ indicated extremely significant events. The calculated p-values are given in S1-S5 Supporting information, the values of the replicates are given in the S3–S7 Datasets.

Results

Photochemical alterations of the PS

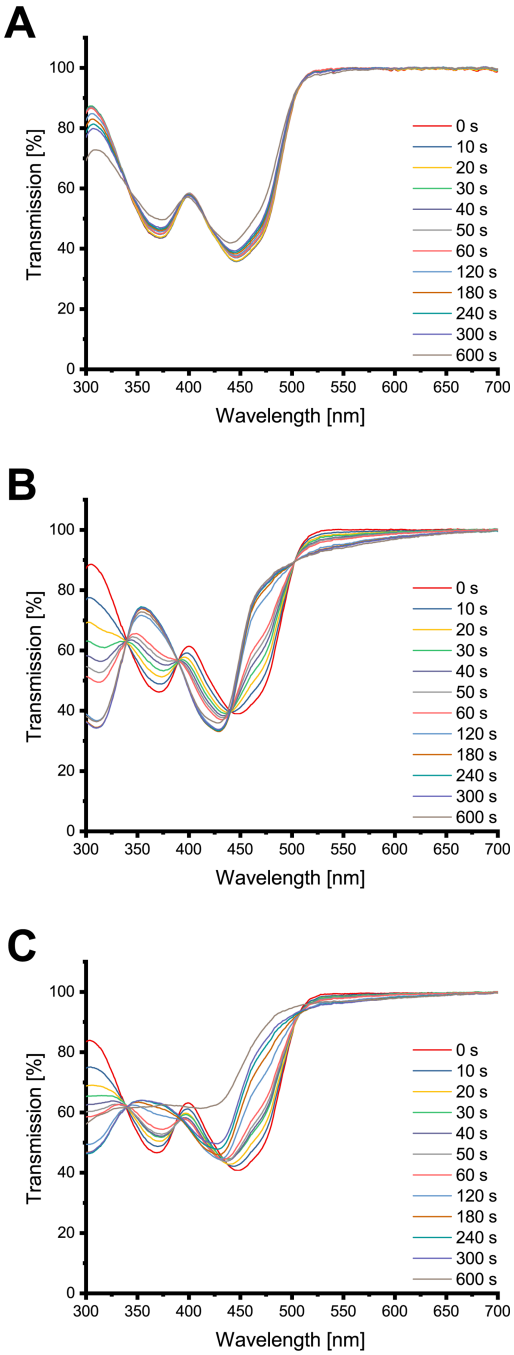

Figure 21: Transmission spectra of FLASH-02a. Y axes indicate the transmission in per cent, x axes the wavelength in nm. Various colors of the spectra indicate different irradiation times. (A) shows the results for H_2O, (B) for 75 mmol l^{-1} sodium phosphate and (C) for 75 mmol l^{-1} sodium carbonate.

FLASH-02a showed photodegradation upon light exposure as indicated by measuring the transmission of the PS in H_2O after the application of 10.8 J cm^{-2} (equal to 10 min of irradiation), equivalent to a loss of concentration of about 17% (Fig 21A). The presence of phosphate and carbonate ions in solutions caused an alteration of the spectra depending on ion concentration and

irradiation time. The photochemically changed flavins show isosbestic points at 339 nm (CV = 1.55%), 389 (CV = 0.96%), 440 (CV = 2.25%) and 503 nm (CV = 1.24%) for isosbestic points at 348 (CV = 1.24%), 389 (CV = 0.68%) and 405 nm (CV = 0.83%) (Fig 3B). Interestingly, the isosbestic points for carbonate were about the same wavelength as for phosphate with 346 nm (CV = 1.17%), 393 nm (CV = 1.75%) and 402 nm (CV = 1.95%) (Fig 22C). However, chemical reaction was more pronounced with less light exposure for carbonate. The transmission data are shown in the S2 Dataset.

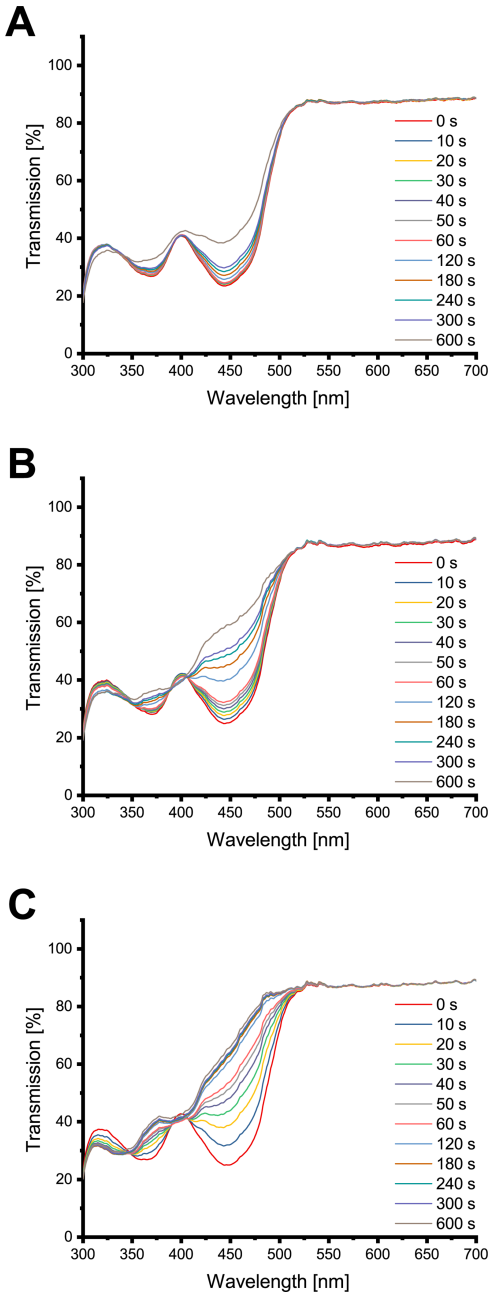

Figure 22: Transmission spectra of FLASH-06a. Y axes indicate the transmission in per cent, x axes the wavelength in nm. Various colors of the spectra indicate different irradiation times. (A) shows the results for H_2O, (B) for 75 mmol l^{-1} sodium phosphate and (C) for 75 mmol l^{-1} sodium carbonate.

Singlet oxygen production with and without ions

The singlet oxygen production was monitored by relative fluorescence of DPBF. Without the addition of ions, relative DPBF fluorescence decreased after 10 s of irradiation with 18 mW cm^{-2} (equal to 0.18 J cm^{-2}) and reached values below 1% for the maximum concentration of 50 µmol l^{-1} FLASH-02a (Fig 23A). The results for the H_2O control of the DPBF assays carried out with FLASH-02a diverge all significantly from each other–except for a comparison of the highest two PS concentrations (detailed results are displayed in S1 File).

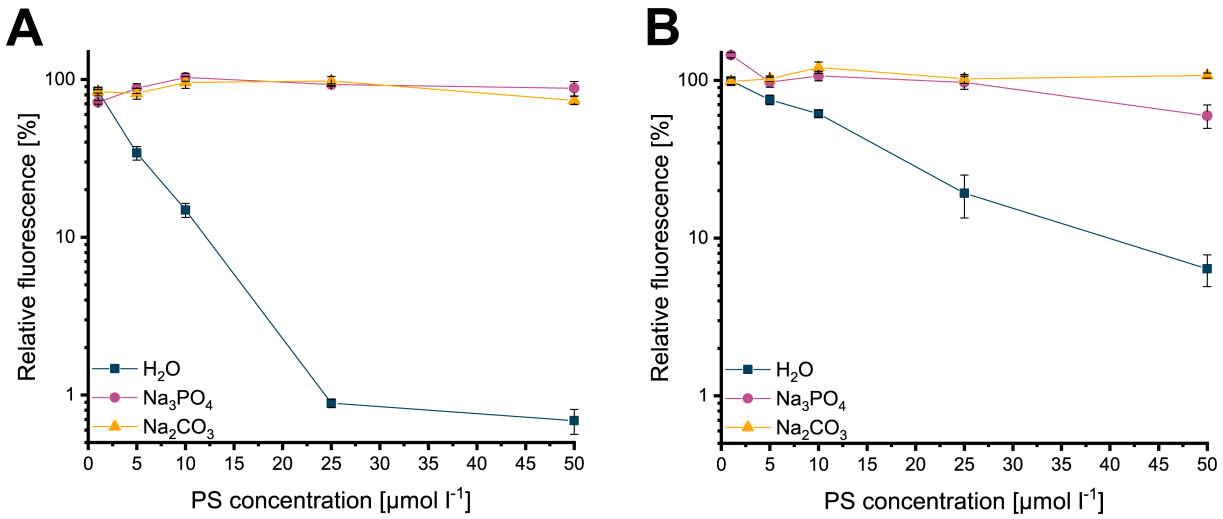

Figure 23: Results for the DPBF assays. Relative fluorescence in presence of FLASH-02a is shown in (A) and FLASH-06a in (B) after 10 s of irradiation. Different colors of the lines and symbols indicate the used environment. In this experiment, 75 mmol l^{-1} of sodium phosphate or sodium carbonate were applied. Y axes indicate the relative fluorescence in percent referenced to the DPBF control, X axes indicate the PS concentration in µmol l^{-1}. Error bars display the calculated standard deviation of the triplicates.

However, with increasing concentrations of sodium phosphate or sodium carbonate, less singlet oxygen was generated as indicated by the constant relative DPBF fluorescence. The statistical analysis also showed in nearly all compared conditions non-significant events, whereas the detailed results are given in S1 File. When using FLASH-06a without the addition of ions, relative DPBF fluorescence decreased after 10 s of irradiation with 18 mW cm^{-2} (0.18 J cm^{-2}) and reached minimum values below 7% for the maximal concentration of 50 µmol l^{-1} FLASH-06a (Fig 23B). Again, a comparison of all tested conditions showed that all values were significantly distinct from each other, with the comparison of the highest two PS concentrations being the only exception. With increasing concentrations of sodium phosphate, less singlet oxygen was generated. However, the obtained values for 1 and 5 µmol l^{-1} of FLASH-06a differ from the other PS concentrations significantly (S1 File). The same result was observed for increasing concentrations of sodium

carbonate, in which none of the tested conditions does vary significantly from each other (S1 File). Values above 100% indicate that the photobleaching effect due to residual light of the control exceeded the decrease in fluorescence caused by singlet oxygen production of the photosensitizer. Measured values, means and standard deviation are shown in the S3 Dataset.

Photodynamic inactivation of bacteria with and without ions

PDI experiments in H_2O revealed a higher inactivation efficiency for *Pseudomonas aeruginosa* (Fig 24C and 24D) compared to *Staphylococcus aureus* for both PS (Fig 24A and 24B). In general, FLASH-06a was less efficient in the inactivation of bacterial cells, for *S. aureus* the inactivation did not exceed four orders of magnitude (Fig 24B). However, besides the treatment of *S. aureus* with FLASH-06a, both bacteria could be inactivated to the lower limit of detection of six orders of magnitudes. Each obtained logarithmic reduction value for each experiment is displayed in the S4 Dataset. All tested conditions diverge significantly from each other except for concentrations of FLASH-06a below 5 µmol l^{-1} for *P. aeruginosa*. Detailed statistics are given in S2 File.

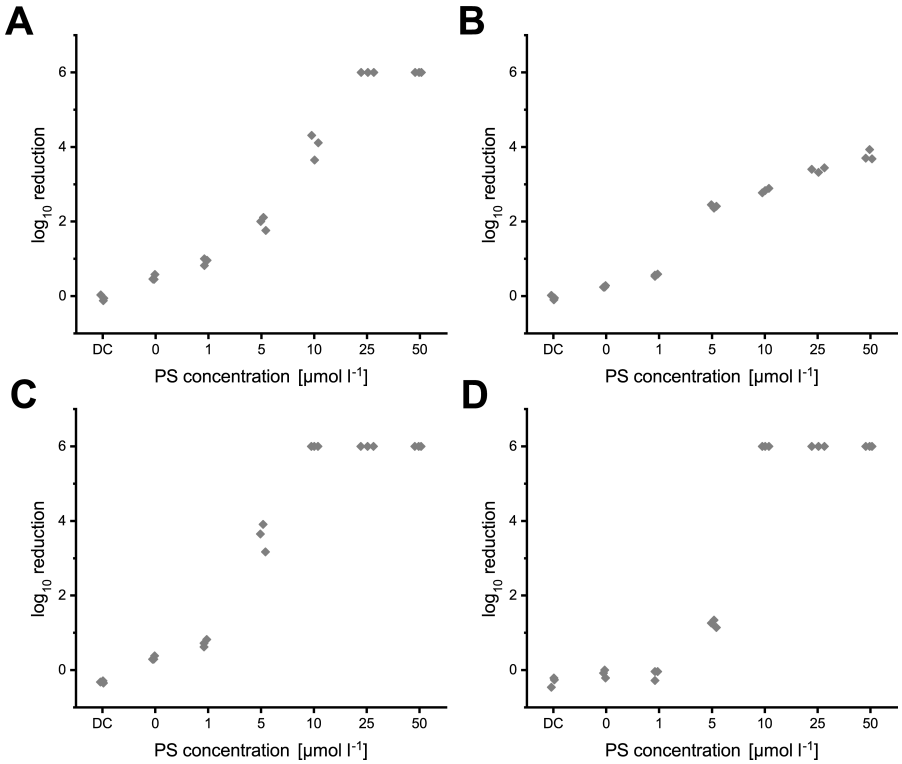

Figure 24: Results for the photodynamic inactivation without the application of ions.

Logarithmic reduction values of *S. aureus* with FLASH-02a (A) and FLASH-06a (B) compared to the logarithmic reduction of *P. aeruginosa* treated with FLASH-02a (C) and FLASH-06a (D). Y axis of the graphs indicate the decadic logarithmic reduction while the x axis displays the different concentrations of the applied PS with DC indicating the dark control (no irradiation, 50 µmol l^{-1} PS). As each experiment was carried out by n = 3, each dot represents one single value from a single experiment.

When comparing the photodynamic inactivation for *S. aureus* in H_2O, sodium carbonate and sodium phosphate, dark control (DC), light control (0 µmol l^{-1}) and 1 µmol l^{-1} of any PS, no noteworthy reduction of the number of viable bacterial cells was obtained. Even with increasing PS concentrations up to 50 µmol l^{-1}, no efficient inactivation was achieved for 75 and 7.5 mmol l^{-1} of the ions at the constant light exposure of 0.72 J cm^{-2} (40 s of irradiation). Only if concentrations of sodium phosphate were reduced to at least 0.75 mmol l^{-1} and

5 µmol l^{-1} of FLASH-02a (Fig 25A) or FLASH-06a (Fig 25C), logarithmic reduction started to exceed one order of magnitude. For sodium carbonate and FLASH-02a, this critical point was reached for 10 µmol l^{-1} of respective PS with 0.75 mmol l^{-1} of sodium carbonate. Therefore, PDI had a better efficiency with phosphate, while carbonate seemed to have a much more detrimental effect on the system (Fig 25A and 25C vs. Fig 25B and 25D). For *S. aureus*, the best inactivation results were obtained when ion concentrations were as low as possible with PS concentrations from 25 to 50 µmol l^{-1}. A statistical analysis of the logarithmic reduction values of the various applied conditions is given in S3 File. Measured logarithmic reduction values for each experiment are displayed in the S5 Dataset.

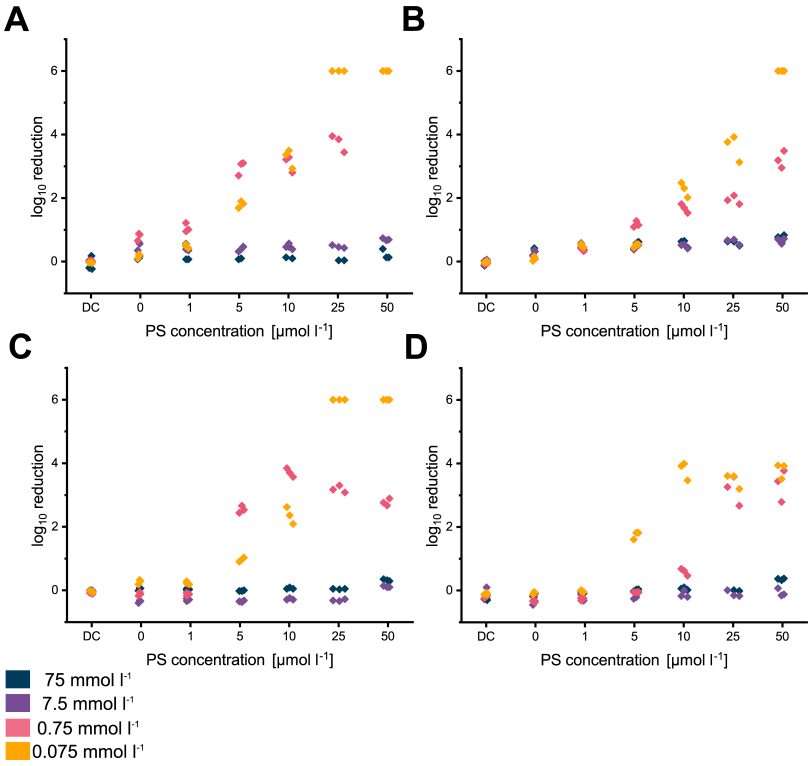

Figure 25: Logarithmic inactivation for *S. aureus* data obtained for each experiment displayed as scatter plot. (A) shows results for sodium phosphate and FLASH-02a, (B) displays the results for sodium carbonate and FLASH-02a. Obtained values for FLASH-06a are displayed in (C) for sodium phosphate and (D) for sodium carbonate. Y axes indicate the decadic logarithmic reduction and x axes indicate the PS concentration in µmol l^{-1} or the dark control (DC). Different colors of the dots indicate the various sodium carbonate or sodium phosphate concentrations.

The observations were quite similar for the Gram-negative organism *P. aeruginosa*. H_2O, sodium carbonate and sodium phosphate did not lead to a reduction of the dark control (DC), light control (0 µmol l^{-1}) and 1 µmol l^{-1} exceeding one order of magnitude. Again, increasing PS concentrations did not result in an efficient inactivation exceeding three orders of magnitude for 75 and 7.5 mmol l^{-1} of both tested solutions. In contrast to the results obtained for *S. aureus*, the Gram-negative strain was eradicated with more than 6 orders of magnitude for 0.075 mmol l^{-1} of sodium phosphate (Fig 26A and 26C) with PS concentrations as low as 10 µmol l^{-1}. The results of the statistical analysis of the obtained logarithmic reduction values for *P. aeruginosa* are included in S4 File. Inactivation of *P. aeruginosa* in the presence of sodium carbonate was less efficient than for sodium phosphate which was in good agreement with results obtained for *S. aureus* (Fig 26B and 26D). In general, inactivation with FLASH-02a was more efficient (Figs 25A, 25B, 26A and 26B) than with FLASH-06a (Figs 25C, 25D, 26C and 26D). Measured logarithmic reduction values for each experiment are deposited in the S6 Dataset.

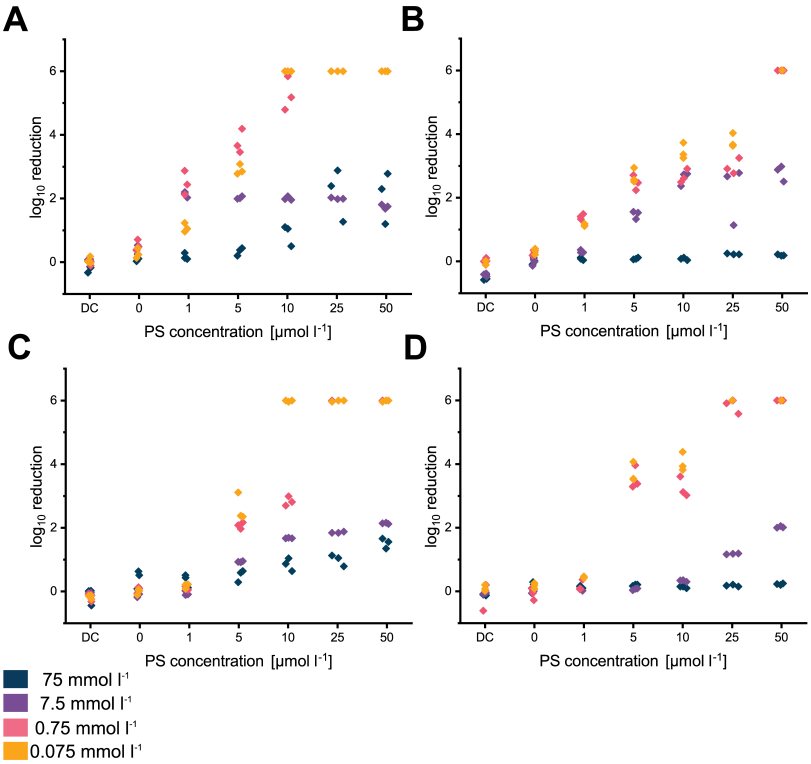

Figure 26: Logarithmic inactivation for *P. aeruginosa* data obtained for each experiment displayed as scatter plot. (A) shows results for sodium phosphate and FLASH-02a, (B) displays the results for sodium carbonate and FLASH-02a. Obtained values for FLASH-06a are displayed in (C) for sodium phosphate and (D) for sodium carbonate. Y axes indicate the decadic logarithmic reduction and x axes indicate the PS concentration in µmol l^{-1} or the dark control (DC). Different colors of the dots indicate the various sodium carbonate or sodium phosphate concentrations.

Additionally, the presence of carbonates and phosphates did not alter the binding behavior of the PS in a detrimental manner, the amount of PS attached to bacterial cells did either not diverge significantly from the H_2O control or was in some cases significantly higher when ionic solutions were applied. The results of a statistical analysis are included in S5 File. The mean calculated amounts and the corresponding standard deviation of bound PS to the respective cells are shown in Table 3. The results of each measurement are included in the S7 Dataset.

Table 3: Results of the binding assays.

PS	Ions	c (salt) [mmol l^{-1}]	c(PS) bound to *S. aureus* [µmol l^{-1}]	Standard deviation	c(PS) bound to *P. aeruginosa* [µmol l^{-1}]	Standard deviation
FLASH-02a	H_2O		31.29	0.91	30.90	0.29
	Na_2CO_3	75	31.77	1.72	28.51	1.09
	Na_2CO_3	0.075	33.11	1.41	35.40	0.66
	Na_3PO_4	75	31.39	0.35	39.68	0.50
	Na_3PO_4	0.075	32.67	1.38	35.60	0.42
FLASH-06a	H_2O		25.76	1.02	27.71	1.13
	Na_2CO_3	75	27.53	1.41	28.29	0.49
	Na_2CO_3	0.075	29.11	0.98	29.96	0.75
	Na_3PO_4	75	28.12	1.01	27.64	1.93
	Na_3PO_4	0.075	29.76	0.97	31.28	0.32

https://doi.org/10.1371/journal.pone.0253212.t001

Discussion

The results of the present investigation show some obstacles as ions like carbonate and phosphate can hamper PDI of flavin PS. Ions in combination with the herein used PS change the mechanism in chemical, physical and biological manners.

The spectra without ions showed a photobleaching effect that was more pronounced for FLASH-06a compared to FLASH-02a, most likely due to the chemical nature of the molecules due to larger side chains of FLASH-06a. Degradation effects without involvement of ions have been described for other flavins previously [530,531].

However, the presented study showed that phosphate and carbonate react by a light-based mechanism with the used flavin PS altering the chemical structure. Time dependent spectra showed isosbestic points under addition of carbonate and phosphate. Isosbestic points in general are strong hints at mass conservation, indicating a variety of compounds, most likely even the involvement of just two substances [532].

Even though all ion treated PS with isosbestic points meet the requirement according to the definition of Thomas and Burgess [528] the isosbestic points are not sharp and clearly defined in a strict sense. Shifts in isosbestic points are either caused by different molar extinction coefficients due to the experimental condition or the contribution of a third, unknown substance [533], experimentally shown by Harris and Bashford [534].

It is known that riboflavin derivatives undergo chemical changes upon light irradiation, resulting in several isosbestic points in the absorption spectra [535–537]. We tentatively assume that degradation of FLASH-02a in the presence of phosphate occurs via cleavage of the side chain to lumichrome [530] possibly followed by an unspecific degradation as observed for example in dairy products [538]. However, for carbonate the transmission spectra are quite distinct from the ones of phosphate, indicating the involvement of more than one substance. Therefore, it is speculated that in this specific case after the side chain cleavage additionally to lumichrome lumiflavin is produced. Neither of the both assumed molecules are capable of producing singlet oxygen. Organisms encounter such degradation products on a daily basis without being harmed, as shown for example for human keratinocytes where no [280] or very low [281] toxicity was found. Although the structural discussion of FLASH-02a is more of a speculative nature, FLASH-06a presents with a clearer situation. It is hypothesized that the ester bonds of the side chains are at least partially hydrolyzed. The remaining scaffold of the former PS might then undergo a cyclization comparable to cyclodehydroriboflavin CDRF–similar to the photoaddition of riboflavin [530,539]. It has been

described elsewhere that both carbonate and phosphate facilitate such processes [539]. However, carbonate promotes the cyclisation more than phosphate, which is also supported by the data shown in this publication. The work of Vaid *et al.* shows that the cyclization of riboflavin is depending on the ionic concentration of are in good consistency with the results presented here. The proposed CDRF-like end product is just as lumichrome or lumiflavin no longer capable of producing singlet oxygen as it was observed in this study by DPBF assays. Again, we observed a less detrimental effect of phosphate for singlet oxygen production compared to carbonate which is also supported by work from other researchers [539].

Additionally, this publication may impact PDI in general as well. Ubiquitous ions as well as other small molecules are frequently present when PDI is applied outside a laboratory setting. These substances may initiate photochemical reactions of the PS leading to the usage of the absorbed light energy for chemical reactions rather than for singlet oxygen production. Such effects decrease the efficacy of killing bacteria as shown here for flavin PS by reducing the amount of generated singlet oxygen. However, e.g. Kainz *et al.* demonstrated the formation of zinc(II)-cyclen-flavin complexes in combination with Fe/C nanoparticles [540]. The use of such methods could protect flavins from harmful effects caused by ions.

It is crucial to understand how ions influence PDI since a major aim is the application of photodynamic inactivation in environments outside the laboratory. Future fields of application include the treatment of wastewater [390,398], the disinfection of drinking water [541,542], decontamination of food [298], the reduction of the bacterial load on surfaces [147] or the decolonization of skin [99]. However, ions are not only included in environmental photodynamic inactivation, but sometimes even *in vitro* studies often use phosphate buffered saline or culture medium for PDI experiments that contain various ions or inhibitory substances [543–545]. Tap water or wastewater may contain various ions like Na^+, Ca^{2+}, Mg^{2+}, and HCO_3^- with a concentration to a few mmol l^{-1}, whereas these ions can also be found on animal or human skin, in particular HCO_3^- with concentrations of up to 4 mmol l^{-1} [546,547]. A literature screening concerning PS concentration and applied fluence reveals divergent parameters that were chosen for efficient inactivation. On the one hand, PDI was efficient of up to four orders of magnitude at low light doses and low porphyrin PS concentrations under ambient light conditions [496]. Yang *et al.* successfully inactivated *Propionibacterium acnes* with a curcumin PS by applying 0.09 J cm^{-2} and PS concentrations as low as 1.5 µmol l^{-1} [548]. Efficient inactivation was also shown with flavin PS at a concentration of 10 µmol l^{-1} and a light exposure of 1.5 J cm^{-2} [280]. Jemli and co-workers

showed an efficient reduction of five orders of magnitude by using 10 µmol l^{-1} of methylene blue, rose bengal or TMPyP with a light dose of 0.13 J cm^{-2} in an wastewater environment [398].

On the other hand, some studies used elevated PS concentrations and/or high light exposures [230,549,550]. Bactericidal action in wastewater for example was achieved with different PS in the µmol l^{-1} range at high light exposures up to a few hundred J cm^{-2} [388,398,541]. Carvalho *et al.* studied the application of PDI in the context of wastewater treatment, achieving a logarithmic reduction of three orders of magnitude. The study used a porphyrin PS at a concentration as low as 5 µmol l^{-1} and a light dose of 145.8 J cm^{-2} [390].

A review article [100] listed 19 animal studies in which bacteria were treated in wounded skin using different PS. It is striking that the light exposure shows high values ranging from 6–423 J cm^{-2} with a mean value of 163 J cm^{-2}. Another study showed the difference of in vitro and in vivo application of PDI. When using a cationic Zn(II) phthalocyanine PS, MRSA was efficiently inactivated *in vitro* using PS concentrations of less than 1 µmol l^{-1} and a 48 J cm^{-2} light exposure [551]. For inactivation of MRSA in an animal wound model *in vivo* the authors had to increase PS concentration to 7.8 µmol l^{-1} and light exposure to about 300 J cm^{-2}. Another research group showed the inactivation of clinically relevant organisms with polycationic PS in nutrient broth. Possibly due to inhibitory substances in the culture medium, light doses of up to 40 J cm^{-2} had to be applied [549].

In a publication concerning a phenalenone PS, organisms with importance in dentistry like *Enterococcus faecalis*, *Actinomyces naeslundii* or *Fusobacterium nucleatum* were efficiently inactivated. These experiments were carried out in PBS buffer with PS concentrations of 100 µmol l^{-1} and light doses of 72 J cm^{-2} [230]. Another study used quite similar organisms and PS in concentrations of up to 250 µmol l^{-1} applying light doses of up to 150 J cm^{-2} [550].

Therefore, the major problem behind these studies is that all used different PS, bacteria, PS concentrations, light sources, light irradiance and light doses. Although some adaptions are necessary when using different photosensitizers or bacteria, it is obvious that there are further elements impacting PDI. Higher light exposure and PS concentrations might be applied to counteract detrimental effects of various substances that are inevitably present in environmental settings. Four studies also assumed a connection between the presence of inhibitory substances and reduced inactivation efficacy [299,448,552,553]. Besides only inhibitory effects there are also enhancing substances known such as EDTA [448], sodium azide [554] and potassium iodine [555,556].

Conclusion

The success of PDI as a new treatment against pathogens requires a successful application beyond standardized laboratory experiments. The impact of ubiquitous ions on the photodynamic mechanism may complicate the application under environmental conditions. As shown in this study, carbonate and phosphate alter the chemical structure of the PS leading to less singlet oxygen generation and hence reduced inactivation of bacteria. The lower the amount of additional material in PDI and the higher the applied light dose is, the better the inactivation. This study provides practical advice for future studies with flavin PS in the presence of phosphate and carbonate. Furthermore, this study stresses the inevitable importance of chemical analysis, physical measurements and investigations concerning bacterial inactivation prior to the application outside the laboratory.

Acknowledgements

We thank G. Gmeinwieser and E. Kowalewski for their great technical assistance and D. Grohmann, L. Dengler and A. Böllmann for fruitful discussions.

Contributions

DBE: conceptualization, formal analysis, investigation, methodology, validation, visualization, writing – original draft; SSE: conceptualization, investigation, validation, writing – original draft, writing – review and editing; LS: investigation, validation, writing – review and editing; AE: conceptualization, investigation, methodology, supervision, validation, writing – review and editing; RV: validation, writing – review and editing; AS: writing – review and editing; WB: conceptualization, formal analysis, funding acquisition, project administration, supervision, validation, writing – original draft, writing – review and editing; HH: conceptualization, formal analysis, funding acquisition, project administration, supervision, validation, writing – review and editing

Inhibitory effects of calcium or magnesium ions on PDI

Daniel Bernhard Eckl[1], Nicole Landgraf[1], Anja Karen Hoffmann[1], Laura Schottenhaml[1], Julia Dirscherl[1], Nina Weber[1], Stefanie Susanne Eben[1], Pauline Bäßler[2], Anja Eichner[2], Harald Huber[1], Wolfgang Bäumler[2]

1: Department of Microbiology, University of Regensburg, Regensburg, Germany
2: Clinic and Polyclinic of Dermatology, University Hospital Regensburg, Regensburg, Germany

Correspondence: Daniel B. Eckl, email: Daniel.eckl@ur.de

Manuscript information:

Journal of Photochemistry and Photobiology (submitted, in review)

Received 08 February 2022

Abstract

Photodynamic inactivation of microorganisms (PDI) finds use in a variety of applications. Several studies report on substances enhancing or inhibiting PDI. In this study, we analyzed the inhibitory potential of ubiquitous salts like $CaCl_2$ and MgCl2 on PDI against *Staphylococcus aureus* and *Pseudomonas aeruginosa* cells using five cationic photosensitizers methylene blue, TMPyP, SAPYR, FLASH-02a and FLASH-06a.

TMPyP changed its molecular structure when exposed to $MgCl_2$, most likely due to complexation. $CaCl_2$ substantially affected singlet oxygen generation by MB at small concentrations. Elevated concentrations of $CaCl_2$ and $MgCl_2$ impaired PDI up to a total loss of bacterial reduction, whereas $CaCl_2$ is more detrimental for PDI than $MgCl_2$. Binding assays cannot not explain the differences of PDI efficacy. It is assumed that divalent ions tightly bind to bacterial cells hindering close binding of the photosensitizers to the membranes. Consequently, photosensitizer binding might be shifted to outer compartments like teichoic acids in Gram-positives or outer sugar moieties of the LPS in Gram-negatives, attenuating the oxidative damage of susceptible cellular structures.

In conclusion, $CaCl_2$ and $MgCl_2$ have an inhibitory potential at different phases in PDI. These effects should be considered when using PDI in an environment that contains such salts like in tap water or different fields of food industry.

Introduction

PDI nowadays has a wide range of possible applications. There is plenty of experimental applications in development for example in wastewater treatment [386,388–390,392,398,542,557], implementation in antimicrobial coatings [147,558], lowering the microbial load of food and crops [298,299,559,560], decolonization of human skin [99] or in dentistry [326,561,562]. Furthermore, Majiya and colleagues demonstrated sunlight driven water disinfection with a porphyrin immobilized in a chitosan membrane. The researchers successfully reduced the bacterial load by three orders of magnitude and therefore demonstrate a cost-efficient and sustainable method for drinking water disinfection [563]. Further successful advances in the application of PDI were recently made using an *ex vivo* human skin model. A successful decolonization of the human skin concerning methicillin-resistant *Staphylococcus aureus* could be achieved with a phenalenone based photosensitizer SAPYR [99].

The herein cited examples for applied PDI make use of several photosensitizer classes, ranging from well-known photosensitizers such as methylene blue (MB), porphyrins (5,10,15,20-Tetrakis(1-methyl-4-pyridinio)-porphyrin tetra(p-toluene sulfonate, briefly called TMPyP), new substances that exclusively produce singlet oxygen (SAPYR [230]) to curcumins or flavins (FLASH-02a and FLASH-06a [564]). Especially curcumins are considered safe for food applications [298].

The efficacy of PDI is frequently studied under laboratory conditions using media like PBS, which are rather uncommon when considering PDI applications under real life conditions. Thus, when comparing PDI efficacies of environmental photodynamic applications with ones from *in vitro* laboratory studies, it is not surprising that the results of such studies seem to diverge tremendously in some cases.

As mentioned, several fields of application are conceivable for photodynamic inactivation, in which a wide variety of substances, including divalent ions, will inevitably be present. An example of a potential future application outside the laboratory is the antimicrobial treatment of water [399,563,565,566]. Exemplarily for tap water, water hardness is calculated based on the concentration of calcium carbonate and has the following definition according to the US Geological Service. A concentration of 0 – 0.6 mmol l^{-1} is considered as soft water, 0.61 – 1.2 mmol l^{-1} moderately hard water, 1.21 – 1.80 mmol l^{-1} hard water, and above 1.8 mmol l^{-1} very hard water [567]. In Germany, water hardness is divided in three categories termed soft for <1.5 mmol l^{-1}, medium from 1.5 to 2.5 mmol l^{-1} and hard is > 2.5 mmol l^{-1} measured as total $CaCO_3$ [568]. Worldwide, concentrations of calcium and magnesium ions vary greatly depending on the geological

background the water originates from. The concentration of calcium ions in drinking water derived from ground water generally ranges from about 0.025 mmol l^{-1} to 2.5 mmol l^{-1} with values reported up to nearly 10 mmol l^{-1} [569–574]. Magnesium in drinking water is found all around the world and varies greatly depending on the geographical region. Studies from Sweden found magnesium ion concentrations in drinking water of around 0.065 up to 0.62 mmol l^{-1} [575–577], reports from Norway mentioned concentrations up to 0.1 mmol l^{-1} [578] with a median of around 0.2 mmol l^{-1} [579]. Research from England measured values up to 4.56 mmol l^{-1} [580] and another study from South-Africa reported on magnesium concentrations up to 2 mmol l^{-1} [581].

Another application of PDI is the inactivation of microorganisms in food production and processing [582–584]. Approaches of applying PDI towards milk [448] should be taken into focus as divalent ions are inevitably present. The calcium content of milk depends to a certain extent also on the breed of the milked cow [585] or the diet of the cow itself [586]. The various milks commercially available today have quite similar calcium concentrations between 29.5 and 31.56 mmol l^{-1}. Yoghurt on the other hand varies in a range of 34.62 to 45.62 mmol l^{-1}. The calcium concentration of raw cheese varies between 98.02 to 299.40 mmol l^{-1} [587].

A future promising approach is the treatment of the human skin based on photosensitizer solutions. Although this has been proven to show good initial results, the obtained inactivation values are still lower than when experiments are conducted in controlled liquid environment with H_2O. For example, within this study, good efficacy of at least 6 orders of magnitude was achieved for SAPYR for 0.72 J cm^{-2} and 50 µmol l^{-1}. However, on *ex vivo* skin experiments at least 100 µmol l^{-1} were applied in combination with at least 30 J cm^{-2} in order to achieve sufficient inactivation [99]. Similar was found by another research group where harsher parameters for efficient inactivation had to be applied in an *in vivo* model [588]. The differences in the efficacy of these experiments are to a certain extent based on slight experimental differences. However, experiments on skin in general or sweat in particular are by no means similar to pure water. Much more, they resemble complex environments with a variety of substances, even in literature, the found compositions vary greatly [589,590]. Sweat also contains various amounts of calcium and magnesium that inhibit the PDI at least to a certain extent.

Even though the commercial application of PDI in various environments is one of the major aims, it is frequently not sufficiently explored whether or to which extent various ubiquitous substances in these environments may hamper PDI efficacy when using such photosensitizers. Among others, up to date the effects of abundant substances such as calcium or magnesium ions or complex

biological molecules remain mostly uninvestigated. Of course, it is known for some photosensitizer that certain chemicals inhibit [564,591] or enhance [554–556] the photodynamic process. One of the most prominent molecules in this context is sodium azide acting as a potent physical singlet oxygen quencher [591]. In contrast, there are also studies investigating on effects that promote the photodynamic action in presence of sodium azide [554]. Furthermore, it was recently shown that carbonate and phosphate ions, which are two prominent molecules in most environments, have detrimental effects on the chemical structure of flavin based photosensitizers [564]. Additionally, some research data concerning the photodynamic treatment of milk suggested that calcium and magnesium ions pose some issues in efficacy [448].

Therefore, we hypothesize that ubiquitous bivalent ions might affect the photodynamic process at different stages. In this study, we investigated five different cationic PS with various chemical structures such as a porphyrin, a phenothiazine, two flavins and a phenalenone. The biocidal potential of the different photosensitizers towards several bacteria was evaluated under the influence of various aqueous solutions containing calcium and magnesium in ascending concentrations resembling concentrations found in possible areas of future applications.

Material and Methods

Photosensitizers

Methylene blue was purchased from SERVA Electrophoresis GmbH with a minimum dye content of 96%. Methylene blue has a singlet oxygen quantum yield of around 0.50 depending on the applied measurement method [232], providing a mixture of ROS and singlet oxygen that is generated. TMPyP was brought from Sigma-Aldrich with a minimum dye content of 97%. The quantum yield of the porphyrin based photosensitzer is around 0.77 [250], producing chiefly singlet oxygen with minor amounts of other ROS. Besides, an exclusive singlet oxygen producing photosensitizer shortly called SAPYR with a quantum yield of 0.99 [230] was purchased from the TriOptoTec GmbH.. Additionally, two different flavin based photosensitizers were included with a quantum yield of around 0.75 that was also purchased from TriOptoTec GmbH, the chemical structure of the molecules has been published elsewhere [564]. In general, all light sensitive parts of the procedures were conducted at low light conditions with a maximum radiant flux of 55 µW cm^{-2} as described elsewhere [496].

Bacteria

The used bacterial strains were obtained from the German Collection of Microorganisms and cell culture lines DSMZ (Braunschweig, Germany). As a Gram-positive representative *Staphylococcus aureus* F-182 (DSM 13661) was used. The strain was derived from a clinical isolate from Kansas and exhibits resistance towards methicillin and oxacillin, therefore also considered as MRSA. The Gram-negative organism tested in this study was *Pseudomonas aeruginosa* Boston 41501 (DSM 1117) initially isolated from a blood culture. As universal culture medium Mueller-Hinton-Bouillon [527] was used on which the bacteria grew over night at 37°C at 100 rpm.

Ionic solutions

Stock solutions of calcium chloride ($CaCl_2$) and magnesium chloride ($MgCl_2$) were prepared with stock concentrations of 150, 15, 1.5 and 0.15 mmol l^{-1}. As a solvent and control served ultra-pure H_2O with a conductance of 0.056 µS cm^{-1} (Milli-Q® Water Treatment System, Merck KGaA, Darmstadt, Germany). The stock solutions were stored in plug-sealed, gas tight glass serum bottles under nitrogen atmosphere in the dark at room temperature. pH was adjusted to 7 using HCl or NaOH. $CaCl_2$ as well as $MgCl_2$ were purchased from Carl Roth GmbH + Co. KG (Karlsruhe, Germany) in analytical grade.

Light source

For TMPyP, SAPYR, FLASH-02a and FLASH-06a a blue light source (blue_v, Waldmann GmbH, Villingen-Schwenningen, Germany) was used, while MB was irradiated under a red light source (PDT 1200, Waldmann GmbH, Villingen-Schwenningen, Germany). The applied irradiance for the blue light source was 18 mW cm^{-2} and for the red light source 20 mW cm^{-2}. The final radiant exposure depended on the time of the application and is represented the product of the applied irradiance in W cm^{-2} times the application time in s resulting in J cm^{-2}, which are the values given throughout the following.

Spectroscopic analysis

To investigate if aqueous solutions alter the chemical structure of the used photosensitizers, spectroscopic analysis was performed from 300 to 700 nm in a photometer (BMG Labtec, Ortenberg, Germany) with a 96-well microtiter plate (SARSTEDT AG & Co. KG, Nümbrecht, Germany). To rule out light induced reactions, the spectra were recorded before and after illumination with an appropriate light source with defined energy up to 5.4 J cm^{-2}. Each reaction was composed out of a total volume of 200 µl with PS concentrations ranging from 0 to 50 µmol l^{-1} and ionic solutions in concentrations of up to 75 mmol l^{-1}. The obtained transmission was then plotted with OriginLab 2019b (Northampton, USA).

Singlet oxygen production

To evaluate singlet oxygen production in qualitative manners, DPBF (1,3-Diphenylisobenzofurane) assays were carried out. DPBF was purchased from Sigma-Aldrich with a minimum dye content of 97%. DPBF reactions were composed in total as follows: a total volume of 200 µl contained either no PS (internal reference) or 1 to 50 µmol l^{-1} PS, 75 mmol l^{-1} $CaCl_2$ or $MgCl_2$ and 500 µmol l^{-1} DPBF which was dissolved in analytic grade ethanol. Assays were conducted as triplicates and measured after a total applied energy of 0, 0.018, 0.036, 0.054, 0.072, 0.09 and 0.18 J cm^{-2} with either the blue_v light source or the respective red light source. DPBF fluorescence was then measured utilizing a fluorescence plate reader from BMG Labtech with the excitation wavelength of 411 nm and emission detection at 451 nm. Values obtained for the internal reference (DPBF without PS) were set to 1, relative fluorescence was calculated as rations to the internal reference and the sample (DPBF with PS) and displayed in per cent using OriginLab 2019b software.

Evaluation of the logarithmic bacterial reduction

Bacterial cultures were harvested via centrifugation at 13,000 x g for 7 min. Afterwards, OD_{600} was adjusted to 0.6 with a cell density meter (Ultrospec 10, Ammersham Biosciences, Little Chalfont, UK). 1 ml of the cell suspension was transferred to 1.5 ml reaction tubes and centrifuged at 13,000 x g for 7 min. Supernatant was discarded and the remaining pellet was washed in H_2O three times. After the last washing step, the cells were mixed with 1 ml of either $CaCl_2$, $MgCl_2$ or H_2O in concentrations of 75 to 0.75 mmol l^{-1}. 25 µl of the bacterial cell suspension were mixed with the same volume of PS solutions in ascending concentrations, incubated for 10 min at room temperature under dark conditions with a maximum of 3 µW cm^{-2} and afterwards irradiated with a constant energy of 0.72 J cm^{-2}.

20 µl of the reaction were transferred into 180 µl Mueller Hinton bouillon after irradiation and cultivated at 37°C for 48 h. Optical density was measured at 600 nm using a plate reader. The obtained values were then used to calculate bacterial reduction as described elsewhere [467]. The method presented here was initially described as proliferation assay [497] and was adapted in the here presented study for liquid bacterial cultures. Doubling times were calculated for OD_{600} at 0.2 and 0.4.

Binding assays

To exclude interactions hindering photosensitizer attachment to bacterial cells, the bacterial cell suspensions were initially adjusted to an optical density of 0.6 at 600 nm. 500 µl thereof were transferred into 1.5 ml reaction tubes, centrifuged, and washed in water as described before. The washed pellet was mixed with 500 µl of the ionic solution and 500 µl of PS in a concentration of 100 µmol l^{-1}. The mixture was incubated for 10 min in absolute darkness and centrifuged at 4,500 x g for 10 min. The supernatant was collected and transferred into a cuvette and measured at 444 nm for FLASH-06a, 446 nm for FLASH-02a, 370 nm for SAPYR, 520 nm for TMPyP and 575 nm for MB.

Results

Photostability

Photosensitizers dissolved in H_2O did not show alterations in the transmission spectra after application of up to 5.4 J cm^{-2} radiant exposure, only a marginal loss of concentration of the photosensitizer was observed. (Supplementary Figure 1, Supplementary File 1). The transmission spectra for photosensitizers dissolved in 75 mmol l^{-1} $CaCl_2$ were also not altered after irradiation besides minor concentration losses (Supplementary Figure 2, Supplementary File 2). The concentration decreased in similar amounts as for the water controls. Photosensitizers dissolved in $MgCl_2$ solutions again showed low photodegradation not exceeding 2 % compared to the non-irradiated controls. Also, the photosensitizers maintained their chemical integrity (Supplementary Figure 3, Supplementary File 3), except for TMPyP as a bathochromic shift was observed. The transmission minimum (Soret band) was shifted to 435 nm and the Q bands were located at 520 to 521 nm and at 562 to 564 nm(Fig 27, Supplementary File 3).

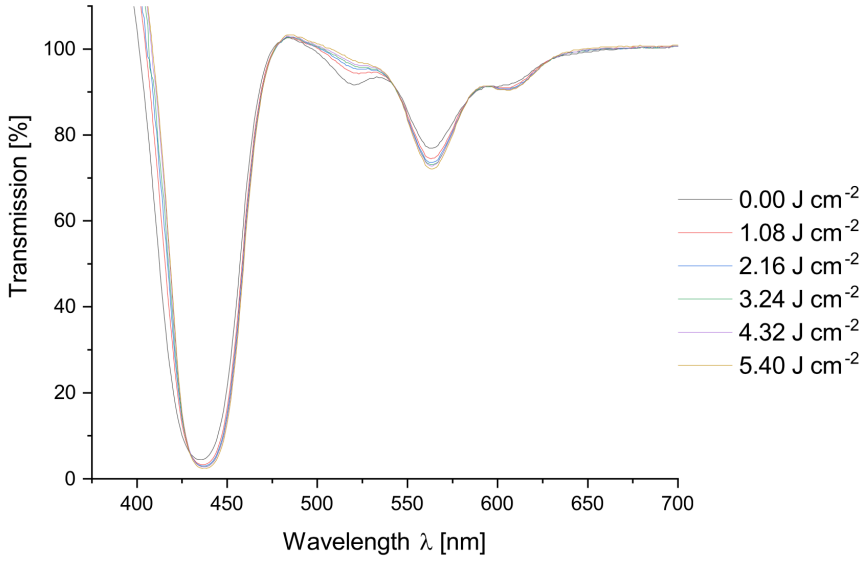

Figure 27: Transmission spectrum of TMPyP resuspended in 75 mmol l^{-1} $MgCl_2$.

The Y-axis indicates the transmission in %, the X-axis displays the corresponding wavelength in nm. The different line colors indicate the applied fluences.

Singlet oxygen production

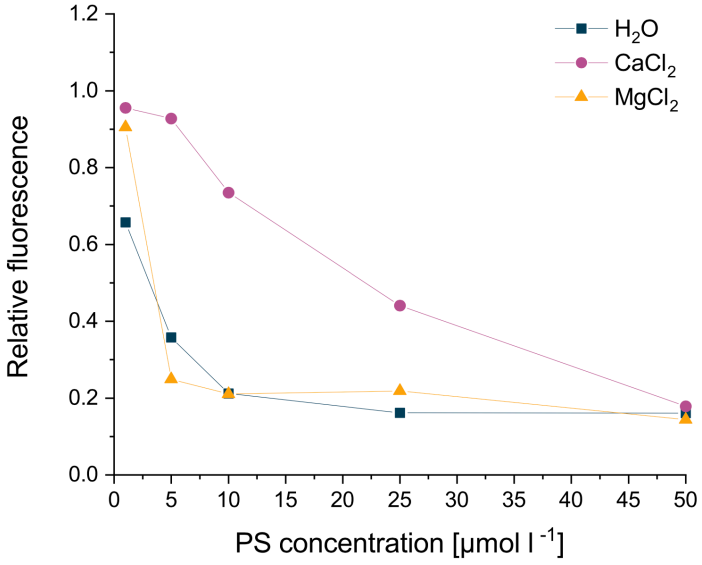

Figure 28: Results of DPBF assays for MB

Relative fluorescence is displayed on the Y-axis in dependence of the photosensitizer concentration shown on the X-axis in µmol l^{-1}. Blue lines and squares indicate H_2O as solvents, purple lines and dots $CaCl_2$ and yellow lines and triangles indicate $MgCl_2$.

As mentioned before, singlet oxygen production was measured as relative fluorescence of DPBF. The data are additionally given as a table in Supplementary File 4. Lower relative fluorescence hints at more efficient singlet oxygen production while values above 1 are measured, when the photobleaching effect of the reference exceeds the loss of the fluorescence caused by the photosensitizer. Relative fluorescence of DPBF for MB decreased at 10 µmol l^{-1} already to values around 0.2 for H_2O and $MgCl_2$ solution, while the same relative fluorescence value was achieved for $CaCl_2$ solution at the highest concentration of PS applied (Fig 28).

DPBF assays of TMPyP showed already drastically lowered relative fluorescence for 1 µmol l^{-1} of TMPyP. Application of concentrations as low as 5µmol l^{-1} of TMPyP already led to a relative fluorescence of around 0.1, indicating that all DPBF present in the reaction was readily depleted in all cases independent of the used solvents (Supplementary Figure 4B).

DPBF assays for SAPYR (Supplementary Figure 4C), FLASH-02a (Supplementary Figure 4D) and FLASH-06a (Supplementary Figure 4E) showed a similar reduction of the relative fluorescence mostly independent of the used solvents reaching minimal values of 0.1 to 0.2 for 50 µmol l^{-1} of applied PS.

Binding assays

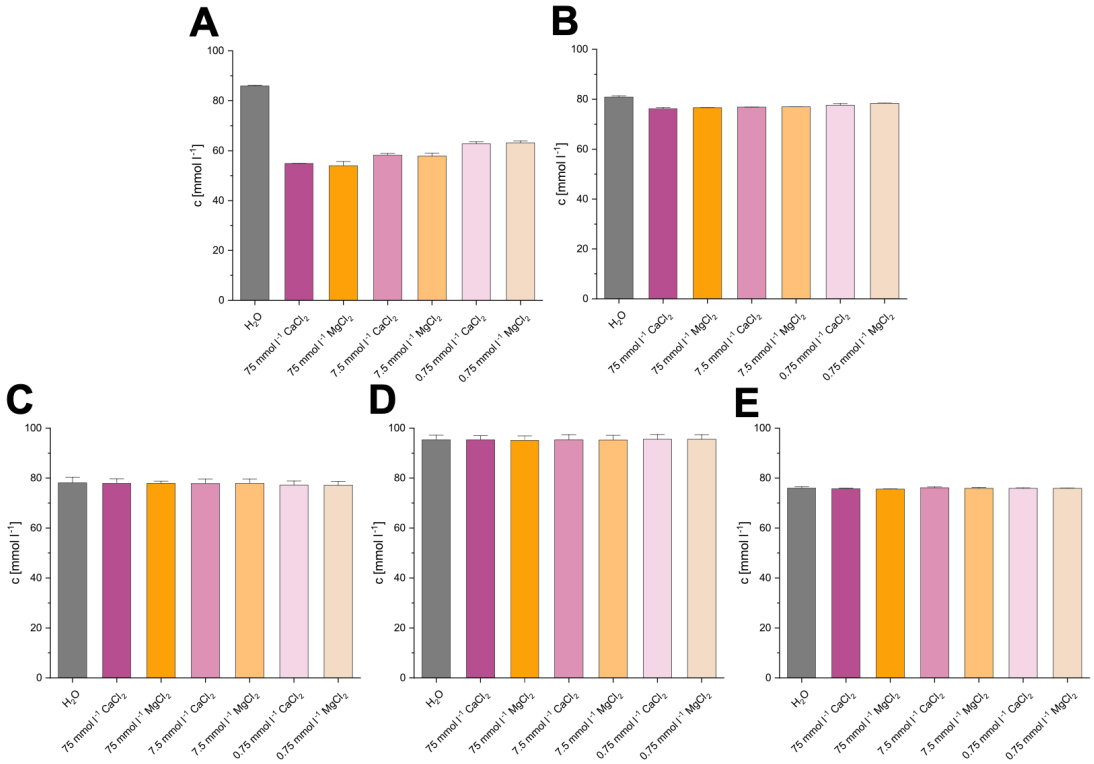

Figure 29: Binding assays of *Staphylococcus aureus*.

The graphs show the bound concentration of the PS to MRSA cells for (A) MB, (B) TMPyP, (C) SAPYR, (D) FLASH-02a and (E) FLASH-06a. The X-axis displays the various tested categories named accordingly, the Y-axis indicates the concentration of PS bound to MRSA cells in µmol l^{-1}. Error bars were calculated as standard error.

MB showed good binding behavior towards *S. aureus* cells in the presence of H_2O. However, the binding efficiency decreased with increasing ion concentration (Fig 29A). The measured concentrations for *S. aureus* are also given as a table in Supplementary File 5. The use of TMPyP showed a comparable but less pronounced effect (Fig 29B). The binding of SAPYR (Fig 29C), FLASH-02a (Fig 29D) and FLASH-06a (Fig 29E) was almost unaltered in the presence of divalent ions.

The highest amounts of bound PS were measured for FLASH-02a with or without 0.75 mmol l^{-1} $MgCl_2$ showing around 96 µmol l^{-1} or 95 µmol l^{-1}, respectively. MB bound with 86 µmol l^{-1} to *S. aureus* cells in the case of H_2O as a maximum value, followed by TMPyP with 81 µmol l^{-1} for H_2O. Most SAPYR was bound for the application of H_2O with 78 µmol l^{-1} and the least amount of PS was found for FLASH-06a with 76 µmol l^{-1} for 0.75 mmol l^{-1} $CaCl_2$ not differing significantly from the other measured values for the other experimental conditions.

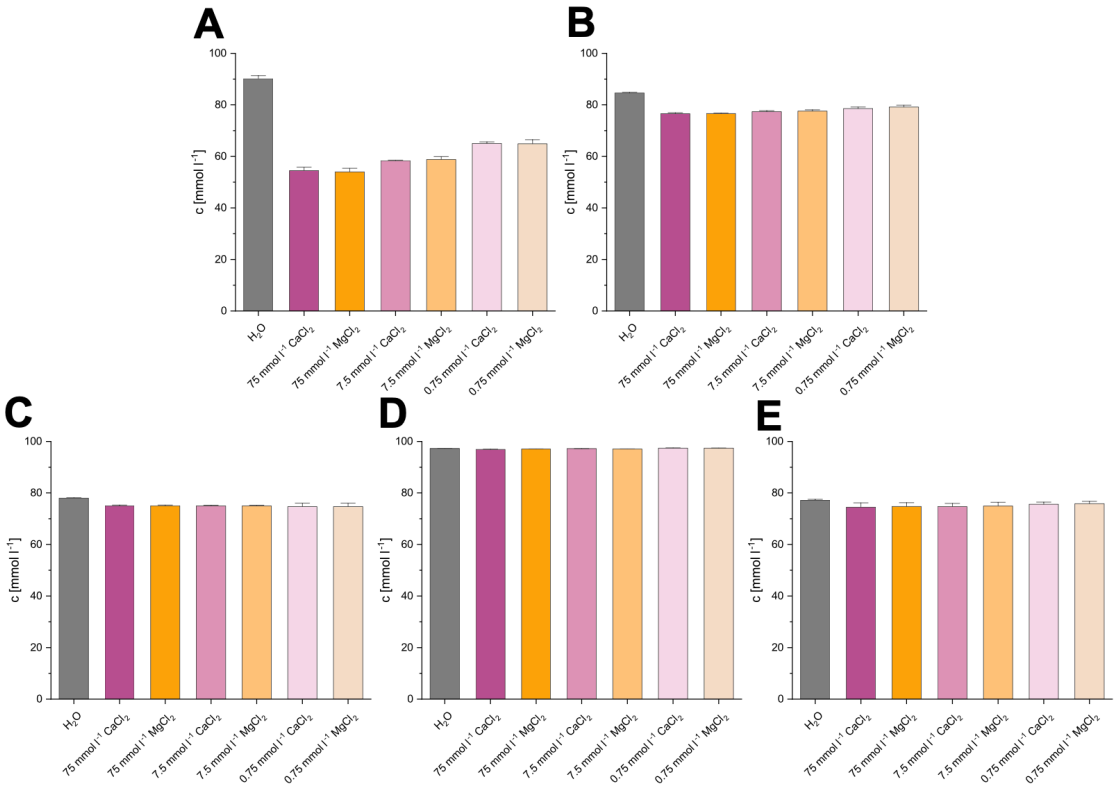

Figure 30. Binding assays of *Pseudomonas aeruginosa*.

The graphs show the bound concentration of the PS to *P. aeruginosa* cells for (A) MB, (B) TMPyP, (C) SAPYR, (D) FLASH-02a and (E) FLASH-06a. The X-axis displays the various tested categories named accordingly, the Y-axis indicates the concentration of PS bound to MRSA cells in µmol l^{-1}. Error bars were calculated as standard error.

The measured concentrations for *P. aeruginosa* are additionally displayed in Supplementary File 6 as a table. Again, MB bound well to *P. aeruginosa* cells in the presence of H_2O. As shown for *S. aureus*, $CaCl_2$ and $MgCl_2$ solutions inhibited the binding of MB to the cells drastically (Fig 30A). Descending ionic concentrations led to higher amounts of bound photosensitizer. Furthermore, TMPyP (Fig 30B) showed a similar effect but only in insignificant amounts. As observed for MRSA, the binding of SAPYR (Fig 30C), FLASH-02a (Fig 30D) and FLASH-06a (Fig 30E) did not change in the presence of $CaCl_2$ and $MgCl_2$ solutions. FLASH-02a showed the most PS bound to the cells with 97 µmol l^{-1} for 0.75 mmol l^{-1} $MgCl_2$ with minor fluctuations for the other applied ionic solutions indicating that nearly all used PS bound to the cells. The concentration of MB in the presence of H_2O was measured with 90 µmol l^{-1} and for TMPyP 85 µmol l^{-1}. SAPYR and FLASH-06a showed similar binding behavior with a maximum of 78 µmol l^{-1} for SAPYR in H_2O and 77 µmol l^{-1} for FLASH-06a in H_2O, respectively.

PDI of *Pseudomonas aeruginosa*

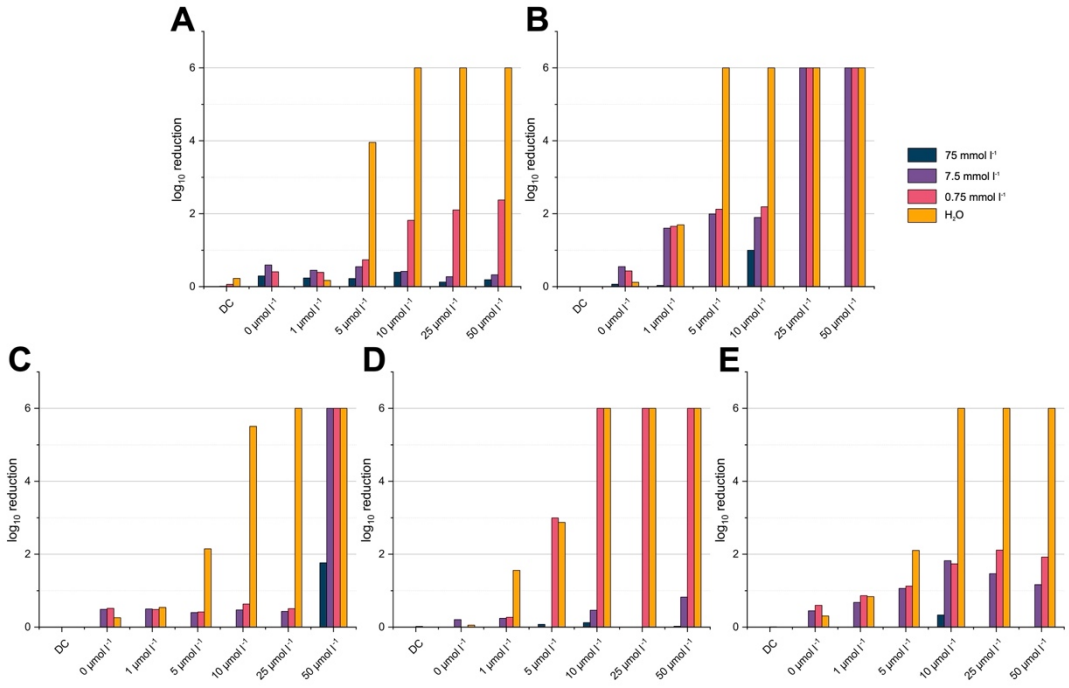

Figure 31: Diagrams of the calculated logarithmic reduction of *Pseudomonas aeruginosa* resuspended in $CaCl_2$ solutions in different concentrations.

The logarithmic reduction is displayed on the Y-axis while the dark control (DC) and applied PS concentrations are displayed on the X-axis. The different concentrations of the ions are symbolized by various colors indicated in the right corner. Panels A shows results for MB, B for TMPyP, C for SAPYR, D for FLASH-02a, E for FLASH-06a.

The mean logarithmic reduction values for *P. aeruginosa* resuspended in $CaCl_2$ are additionally provided as table in Supplementary File 7. PDI at 0.72 J cm^{-2} for MB in H_2O led to bacterial reduction of at least 6 log_{10} steps at a PS concentration as low as 10 µmol l^{-1}. 0.75 mmol l^{-1} $CaCl_2$ inhibited the PDI of MB and the PDI effect almost disappeared (< 1 log_{10} step) for concentrations of 75 or 7.5 mmol l^{-1} $CaCl_2$ (Fig 31A). In H_2O 5 µmol l^{-1} TMPyP and above led to a bacterial reduction of 6 log_{10} steps. $CaCl_2$ inhibited the photodynamic mechanism for 5 and 10 µmol l^{-1} as only a logarithmic reduction around 2 log_{10} steps was measured for 7.5 and 0.75 mmol l^{-1} $CaCl_2$. However, in none of the cases for 75 mmol l^{-1} $CaCl_2$ the efficacy exceeded 1 log_{10} step (Fig 31B). The application of SAPYR led to an efficient inactivation at concentrations as low as 10 µmol l^{-1} in H_2O. For 75 mmol l^{-1} $CaCl_2$ (Fig 31C) almost no bacterial reduction was observed. Lower concentrations of $CaCl_2$ led to an inactivation of 6 log_{10} steps for the application of 50 µmol l^{-1}

SAPYR. 10 µmol l^{-1} FLASH-02a and above led to an inactivation of 6 log_{10} steps (Fig 31D). Addition of 75 or 7.5 mmol l^{-1} $CaCl_2$ led to no efficient inactivation when FLASH-02a was applied under mentioned conditions, only 0.75 mmol l^{-1} showed similar efficacy to the water control (Fig 31D). In H_2O, concentrations of 10 µmol l^{-1} FLASH-06a and above yielded an efficacy of 6 log_{10} steps. The application of $CaCl_2$ did not lead to a reduction that exceeded 2 log_{10} steps in any cases (Fig 31E).

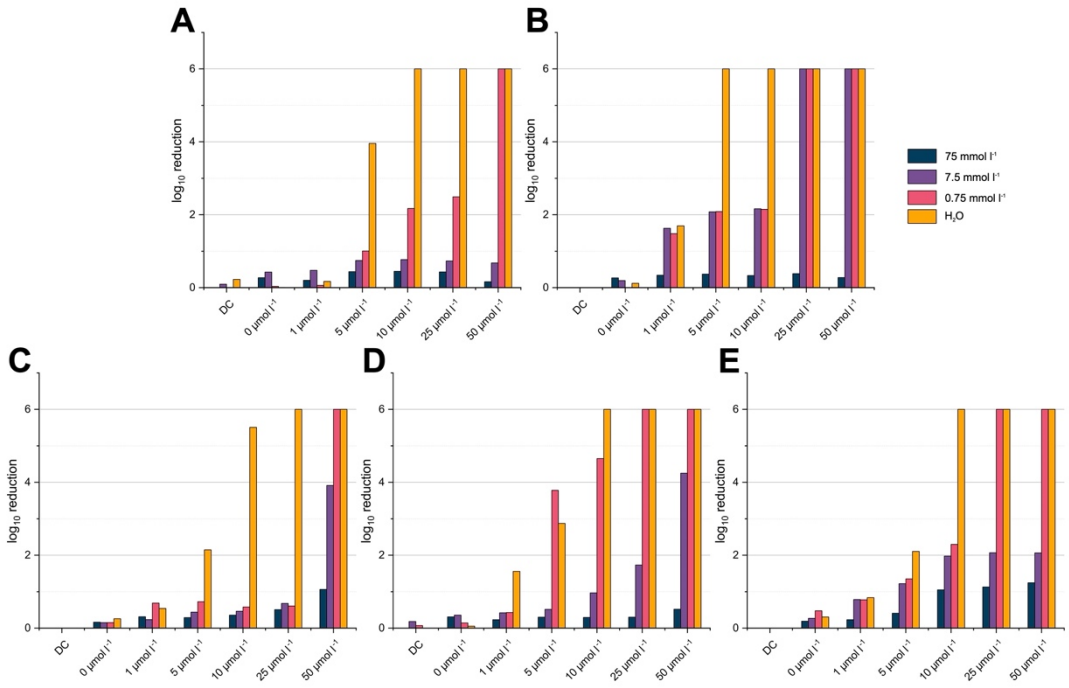

Figure 32: Diagrams of the calculated logarithmic reduction of *Pseudomonas aeruginosa* resuspended in $MgCl_2$ solutions in different concentrations.

The logarithmic reduction is displayed on the Y-axis while the dark control (DC) and applied PS concentrations are displayed on the X-axis. The different concentrations of the ions are symbolized by various colors indicated in the right corner. Panels A shows results for MB, B for TMPyP, C for SAPYR, D for FLASH-02a, E for FLASH-06a.

A table of the mean logarithmic reduction of *P. aeruginosa* resuspended $MgCl_2$ is provided in Supplementary File 8. The application of $MgCl_2$ had slightly less inhibitory effects on the PDI with MB (Fig 32A) than $CaCl_2$. Results obtained for TMPyP with bacteria resuspended in $MgCl_2$ solutions (Fig 32B) did not differ much from the beforehand presented results for $CaCl_2$. The application of 50 µmol l^{-1} SAPYR in 75 mmol l^{-1} $MgCl_2$ led to a maximum bacterial reduction of

about 1 log_{10} step. Lower $MgCl_2$ concentrations led to a maximum inactivation of around 4 log_{10} steps for 7.5 mmol l^{-1} $MgCl_2$ and 6 log_{10} steps for 0.75 mmol l^{-1} $MgCl_2$, respectively (Fig 32C). *P. aeruginosa* suspended in 7.5 mmol l^{-1} $MgCl_2$ solution were inactivated with an efficacy not exceeding 1 log_{10} step, 0.75 mmol l^{-1} $MgCl_2$ solution showed a bacterial reduction of around 4 log_{10} steps for 50 µmol l^{-1} FLASH-02a. 6 log_{10} steps were observed for 25 µmol l^{-1} FLASH-02a and above in 0.75 mmol l^{-1} $MgCl_2$ (Fig 32D). The experimental outcome of the application of $MgCl_2$ in combination with FLASH-06a showed a slightly higher inactivation efficacy for 75 mmol l^{-1} compared to $CaCl_2$. However, for 7.5 mmol l^{-1} $MgCl_2$ the efficacy did not exceed 2 log_{10} steps. 0.75 mmol l^{-1} $MgCl_2$ restored an efficacy of 6 log_{10} steps for 25 and 50 µmol l^{-1} FLASH-06a (Fig 32E).

PDI of *Staphylococcus aureus*

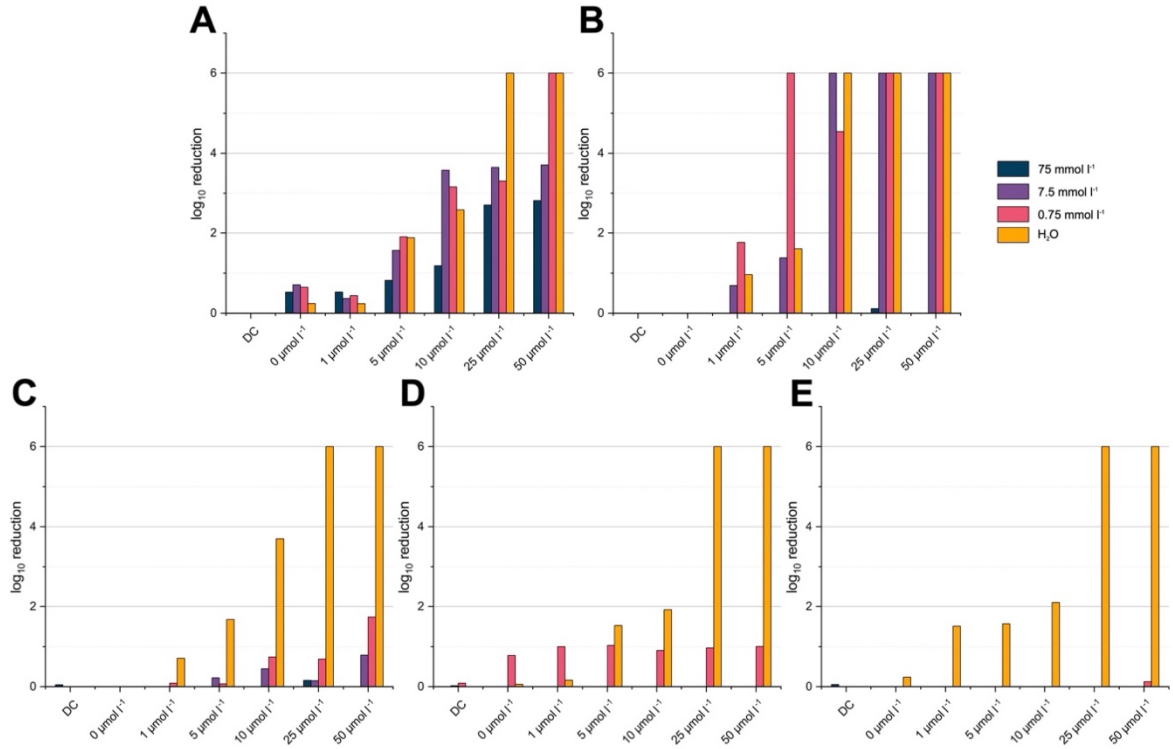

Figure 33: Diagrams of the calculated logarithmic reduction of *Staphylococcus aureus* resuspended in $CaCl_2$ solutions in different concentrations.

The logarithmic reduction is displayed on the Y-axis while the dark control (DC) and applied PS concentrations are displayed on the X-axis. The different concentrations of the ions are symbolized by various colors indicated in the right corner. Panels A shows results for MB, B for TMPyP, C for SAPYR, D for FLASH-02a, E for FLASH-06a.

Additionally, to the mentioned experiments with *P. aeruginosa*, the same set of conditions were tested for a methicillin resistant *S. aureus* strain (MRSA). A tabular presentation of the results is

provided in Supplementary File 9. The application of MB in H_2O led to an efficacy of 6 log_{10} steps for 25 and 50 µmol l^{-1}. 5 and 10 µmol l^{-1} led to an efficacy < 3 log_{10} steps (Fig 33A). In general, inactivation in the presence of $CaCl_2$ solution did not show any relevant reduction for 1 µmol l^{-1}. The application of 5 µmol l^{-1} MB showed a reduction < 2 log_{10} steps for 0.75 mmol l^{-1} $CaCl_2$. For 10 µmol l^{-1} MB, the application of 7.5 mmol l^{-1} $CaCl_2$ led to an efficacy of 3.5 log_{10} steps. 0.75 mmol l^{-1} $CaCl_2$ showed a reduction for 10 µmol l^{-1} MB with 3.1 log_{10} steps. 25 µmol l^{-1} MB achieved for 7.5 mmol l^{-1} $CaCl_2$ an efficacy of around 3 log_{10} steps at most. 50 µmol l^{-1} MB did not increase the efficacy for 75 and 7.5 mmol l^{-1} $CaCl_2$ while the application of 0.75 mmol l^{-1} $CaCl_2$ showed an efficacy of 6 log_{10} steps (Fig 33A). The photosensitizer TMPyP showed excellent efficacy in H_2O for 10 µmol l^{-1} and above with an efficacy 6 log_{10} steps (Fig 33B). 75 mmol l^{-1} $CaCl_2$ did not lead to efficient inactivation, 7.5 mmol l^{-1} $CaCl_2$ solution showed a reduction of 1.3 log_{10} steps for 5 µmol l^{-1} and 6 log_{10} steps for 10 µmol l^{-1} and above. Application of 0.75 mmol l^{-1} $CaCl_2$ showed better efficacy compared to the water control for 1 and 5 µmol l^{-1} TMPyP. 25 and 50 µmol l^{-1} restored the efficacy of the PDI with 6 log_{10} steps. (Fig 33B). SAYPR in H_2O was capable of an inactivation of 6 log_{10} steps for 25 µmol l^{-1} and above. However, the application of 75 mmol l^{-1} $CaCl_2$ led to no noteworthy reduction in bacterial viability (Fig 33C). The water control of FLASH-02a showed a reduction of 6 log_{10} steps for 25 and 50 µmol l^{-1} (Fig 33D), only minor efficacy was achieved for lower concentrations. However, when $CaCl_2$ solutions were applied, in none of the applied concentrations a noteworthy reduction was achieved (Fig 33D). While the water control for FLASH-06a (Fig 33E) did not differ in significant manners from the data for FLASH-02a, the addition of $CaCl_2$ aggravates the problems even more, no measurable reduction could be achieved (Fig 33E).

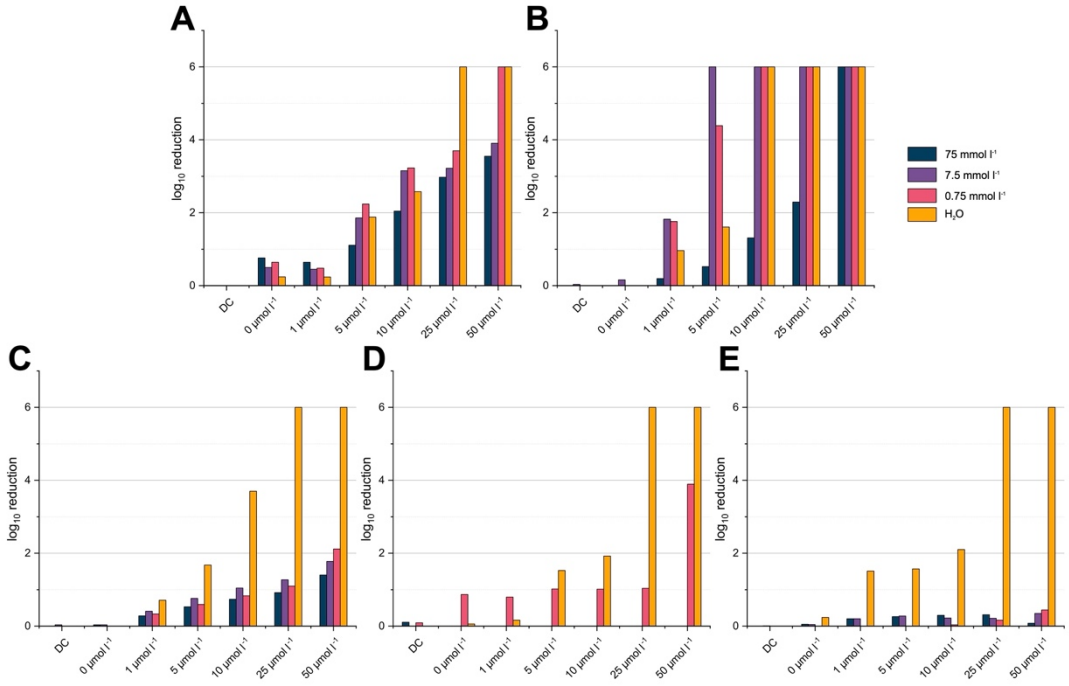

Figure 34: Diagrams of the calculated logarithmic reduction of *Staphylococcus aureus* resuspended in $MgCl_2$ solutions in different concentrations.

The logarithmic reduction is displayed on the Y-axis while the dark control (DC) and applied PS concentrations are displayed on the X-axis. The different concentrations of the ions are symbolized by various colors indicated in the right corner. Panels A shows results for MB, B for TMPyP, C for SAPYR, D for FLASH-02a, E for FLASH-06a.

The obtained results for *S. aureus* resuspended in $MgCl_2$ are also displayed as a table in Supplementary File 10. MB in the presence of $MgCl_2$ solutions had mediocre inactivation efficacy between 2 and 4 log_{10} steps for 5 to 25 µmol l^{-1} MB. 6 log_{10} steps of bacterial reduction were achieved for 0.75 mmol l^{-1} $MgCl_2$ for the highest applied MB concentration (Fig 34A). *S. aureus* resuspended in $MgCl_2$ solutions with TMPyP led to a good overall efficacy as 6 log_{10} steps were achieved even for the highest $MgCl_2$ concentration applied (Fig 34B). For the application of $MgCl_2$ solution in combination with SAPYR the maximum efficacy obtained was around 2 log_{10} steps for the highest SAPYR concentration (Fig 34C). Most dramatically influenced by the application of $MgCl_2$ were both FLASH-06a and FLASH-02a. For FLASH-02a, the only mentionable observed reduction was that at least for 0.75 mmol l^{-1} $MgCl_2$ at a concentration of 50 µmol l^{-1} FLASH-02a a reduction of around 4 log_{10} steps (Fig 34D). FLASH-06a in combination with $MgCl_2$ solutions led to no relevant observable reduction (Fig 34E).

Discussion

The presented results paint quite a clear picture concerning the role of $CaCl_2$ and $MgCl_2$ when performing PDI against the bacteria and photosensitizers used. Firstly, the absorption spectra showed that all photosensitizers in pure water were stable upon irradiation with up to 5.4 J cm^{-2}. Even the addition of the divalent ions at different concentrations showed no negative effect on photostability of photosensitizers, except for TMPyP in the presence of $MgCl_2$ (Fig 1). This is not surprising because a porphyrin structure is a pristine chelating agent for divalent ions [592]. The fact that the complexation of bivalent metal ions causes alterations in the spectrum of porphyrins has been described in literature before [593–595]. However, such chelating reactions of the porphyrin group are often influenced by specific reaction parameters such as defined pH [596–598] or temperatures [599,600]. This might also lead to incomplete complexation reactions, which could also be influenced upon light exposure explaining the different transmission spectra after irradiation. Further possible explanations of this change in absorption behavior in the Q bands might be potential partial cleavage of the methylpyrimidinum groups of TMPyP especially as the side chains of porphyrins seem to rather influence the absorption of the Q bands than of the Soret band [601,602]. The DPBF assays showed an efficient generation of singlet oxygen by all photosensitizers in combination with both divalent ions, except for MB in the presence of $CaCl_2$ (Fig 2). The singlet oxygen production of TMPyP is even at 1 µmol l^{-1} due to its high absorption coefficient so efficient that the relative fluorescence of DPBF dropped by nearly 0.5 for H_2O or even more for $CaCl_2$ and $MgCl_2$ solutions (Supplementary Figure 2B).

These two exceptions might not automatically reduce the efficacy of PDI. TMPyP has a rather high extinction coefficient [603] that even low amounts of functional PS can lead to efficient inactivation which is also reflected by the shown results for the biological inactivation as TMPyP showed the best inactivation efficacy under the given experimental conditions. It is also known that TMPyP with complexed metals is still capable of singlet oxygen production [582]. One of the possible explanations is that the complexation reaction might not be a process that takes place for all TMPyP molecules. Further, a change in pH value in the adjacency of bacterial cells might have stopped or even reverted the complexation.

In most of the PDI applications, the generation of singlet oxygen plays the major role in cell killing [309]. However, the photosensitizers may have the potential to generate not only singlet oxygen, as proven by DPBF assays in the present study. SAPYR shows a singlet oxygen quantum yield with a value of $\Phi = 0.99$ [230], TMPyP $\Phi = 0.77$ [604], the flavins $\Phi = 0.75$ to 0.78 [280], and MB $\Phi =$

0.52 [605]. In particular, the of MB could allow a simultaneous generation of other reactive oxygen species (ROS) that may also yield cell killing. A fact one should keep in mind is especially the potential photodemethylation of diaminomethylgroups as observed for example for photosensitizers like nocathoacin I [606] or methylene blue [607]. For the case of methylene blue, a degradation occurs to azure a or b, leading to reduced singlet oxygen yields and the potential increase of type I reactions [605,608]. However, it seems that calcium and magnesium ions do not favor such demethylation processes in an excessive manner as there are no hints that the spectra of the herein used methylene blue are altered in such ways.

At a glance, the microbial inactivation data, in the absence of the ions, showed an efficient PDI of all tested photosensitizers with a respective concentration of 25 µmol l^{-1} yielding a reduction of 6 log_{10} steps at low radiant exposure of light (Figs 5-8). Except for TMPyP, the efficacy of all photosensitizers is clearly lower in the presence of elevated concentrations of calcium and magnesium ions (Figs 5-8). A general observable trend was that increased concentrations of $CaCl_2$ and $MgCl_2$ led to inhibited inactivation. The effects were most severe for the tested flavins which are also affected by other ions such as carbonate or phosphate [564].

The applied concentrations of $CaCl_2$ and $MgCl_2$ resemble the concentrations present in several fields of application. The two lower $CaCl_2$ concentrations applied within this work, namely 7.5 and 0.75 mmol l^{-1} cover the usual calcium concentration in tap water [567–574,609]. Within this mentioned ranges, TMPyP is most efficient against Gram-negatives, followed by SAPYR and FLASH-02a. However, the findings in this study leads to an exclusion of FLASH-06a and MB from its potential use in such water applications. Gram-positives seem to be mostly inhibited by TMPyP again, but now followed by MB. SAPYR and the flavin based PS did not yield sufficient efficacy under the influence of calcium and magnesium ions. However, concerning drinking water applications, Gram-negatives such as *Shigella* sp., *Vibrio* sp., *Salmonella* sp. or *Escherichia coli* are the more crucial organisms as one of the main causes of contaminated drinking water [610].

The concentrations of magnesium ions usually present in drinking water [35–41] suggest that the magnesium ions poses less of a problem compared to calcium ion concentrations. Especially Gram-negatives might be readily inactivated in magnesium concentrations below 0.75 mmol l^{-1}.

Concerning food applications, potential use in dairy products are the most crucial applications in the light of the herein presented results due to their elevated calcium content [448,585,586]. Based on the results of this work, the use of TMPyP might show sufficient success concerning the reduction of the bacterial load while the other PS used here seem to be less promising. However, a publication

already observed reduced efficacy of applied PDI and the authors speculated that calcium and magnesium might take a part in the reduced efficacy besides further substances such as proteins or fatty acids [448].

Many researchers have already reported that the outermost layers of bacteria seem to be the target of PDI or at least play a major role in the uptake of the PS. A study by George, Hamblin and Kishen from 2009 revealed for MB that the PS showed lower uptake in the presence of divalent ions [611]. Although this study confirms the findings concerning MB, the other PS show no relevant difference in their uptake or binding behavior. Therefore, the sole differences in uptake and binding behavior of the PS do not explain the drastic differences observed in the microbial efficacy. Concerning cationic photosensitizers it is highly likely that negatively charged LPS molecules in the outer membrane that need calcium and magnesium ions for stability [612] form a positively charged layer surrounding the cell that electrostatically hinder the penetration of the PS up to the outer membrane but bind to outer sugar moieties of the LPS. Especially the fact that ions have a stabilizing effect has been reviewed extensively concerning the use of EDTA [613]. Further, this stability hypothesis is strengthened by a study demonstrating an efficacy-promoting effect of EDTA with zinc phthalocyanine against Gram-negative cells, which are without EDTA not effected by negatively or neutrally charged photosensitizers [614]. Similar might be true for Gram-positive cells as teichoic acids and wall teichoic acids have a certain metal ion binding capacity [615–617]. However, these calcium and magnesium ion interactions seem to be not fully understood yet [617].

Conclusion

Although the divalent ions calcium and magnesium have no direct effects on the investigated PS such as chemical degradation their levels for an application in PDI must be kept as low as possible. Therefore, appropriate dilution of the treated liquids or rinsing of surfaces like the human skin with distilled water prior to PDI treatment is highly recommended for future research. Furthermore, several suggestions for the application of photodynamic processes can be given: First, based on several studies that were performed under various conditions, it becomes clear that increased light intensity helps to overcome inhibitory processes, even those of calcium or magnesium ions. Second, higher PS concentrations seem to support the PDI in general. Under these predictions, PDI is an extremely promising antimicrobial treatment for the future, independently on the type of microorganisms or their antibiotic resistances.

Acknowledgement

We thank G. Gmeinwieser for technical assistance as well as L. Nißl for conducting preliminary experiments.

Funding

This work was funded by the Deutsche Forschungsgemeinschaft (DFG, German Research Foundation) – Projektnummer 415812443

Contributions

DBE: conceptualization, formal analysis, investigation, methodology, data curation, visualization, writing – original draft; NL: conceptualization, methodology, formal analysis, investigation, writing – original draft, visualization; AKH; validation, investigation, writing – review and editing; LS: validation, investigation, writing – review and editing; JD: validation, investigation, writing – review and editing; NW: validation, investigation, writing – review and editing; NW: validation, investigation, writing – review and editing; SSE: validation, investigation, writing – review and editing; PB: investigation; AE: validation, resources, writing – review and editing; HH: conceptualization, resources, writing – review and editing, supervision, project administration, funding acquisition; WB: conceptualization, resources, writing – review and editing, supervision, project administration, funding acquisition

The influence of citrate on photodynamic inactivation of bacteria in the presence of bivalent cations, tap water, and synthetic sweat

Daniel Bernhard Eckl[1,2,*], Nicole Landgraf[1,*], Anja Karen Hoffmann[1], Anja Eichner[2], Harald Huber[1], Wolfgang Bäumler[2]

1: University of Regensburg, Institute for Microbiology and Archaea Centre, Universitätsstrasse 31, 93053 Regensburg
2: University Hospital Regensburg, Department of Dermatology, Franz-Josef-Strauss-Allee 11, 93053 Regensburg
*Authors contributed equally

Correspondence: Daniel B. Eckl, email: Daniel.eckl@ur.de

Manuscript information:

Photochemistry and Photobiology (submitted)

Abstract

Many laboratory studies show that photodynamic inactivation (PDI) in general is a powerful tool in tackling multi resistant bacteria and in closing hygiene gaps in sensitive environments. However, the studies were frequently performed under standardized in vitro conditions comprising artificial laboratory settings. In contrast, applications of PDI under real life conditions will expect diverse settings that exhibit substances like ions, proteins, amino acids, and fatty acids, which may hamper PDI to an unpredictable extent.

Thus, PDI was investigated in the presence of calcium and magnesium solutions as well as synthetic sweat solutions to approach real life conditions like in tap water and on skin surface. The role of chelating citrate was studied that may counteract such ions.

The results indicate that the application of citrate can enhance PDI for certain ionic concentrations (e.g. $CaCl_2$ or $MgCl_2$ in concentrations of around 7.5 to 75 mmol l^{-1}) especially against Gram-negative bacteria. Citrate also improved PDI efficacy in tap water (especially for Gram-negative bacteria) and in synthetic sweat solution (especially for Gram-positive bacteria).

In conclusion, citrate is a potent agent that may antagonize effects, which hamper PDI in applications under real life conditions.

Introduction

Pathogenic viruses and antibiotic-resistant bacteria are serious threats to our society. Part of the dissemination of dangerous diseases are inter alia nosocomial infections. They can be defined as hospital-acquired infections (HAIs), occurring during or after hospital residence. Examples include surgical wound, primary bloodstream or urinary tract infections [618].

In Europe, roughly 63.5% of infections with antibiotic-resistant bacteria are originating from hospital and health care settings, resulting in 72.4% of attributable deaths [53]. With regards to its impact on the economy, these types of infections are causing significant losses of approximately EUR 7 billion per year for the EU [63]. Typical examples are infections with methicillin-resistant *Staphylococcus aureus* (MRSA), which were estimated to be responsible for costs up to EUR 1.55 billion in 2011 in Germany alone [64]. In the light of antibiotic resistances, multi-drug-resistant bacteria account for a prevalence of 5.7 to 19.1 per 100 patients concerning HAIs [619].

In health care settings, various measures against HAIs are designed such as adequate hand hygiene, proper usage of gloves and face masks, and standardized procedures for cleaning and disinfection of patient-near surfaces [620]. However, the compliance of hand hygiene (41 %) [409] and surface disinfection (48 %) [410] are persistently insufficient, contributing to HAIs and the spread of resistant pathogens. Another important topic is the hesitant implementation of the antimicrobial stewardship by which the use of antibiotics should be optimized [621]. Thus, the ongoing fight against HAIs and the increasing resistance of bacteria against antimicrobials requires new antimicrobials but also new technologies.

Photodynamic inactivation (PDI) offers a viable alternative to conventional disinfectants and medical drugs in many relevant application fields, and could thus slow the pace of resistance development [153,155,309]. PDI requires three harmless components, a photosensitizer (PS), visible light and molecular oxygen. Upon light absorption in the PS molecule, energy or charge may be transferred to adjacent molecules to generate reactive oxygen species (ROS), among which singlet oxygen should play an important role. In case the PS is in close contact with a bacterial cell, singlet oxygen can attack chemical double bonds of biomolecules like in lipids and proteins leading to cell killing [622]. Owing to its mechanisms of action, PDI should not contribute to bacterial resistance [309].

PDI should be considered a valuable component of new antimicrobial strategies, but PDI is inherently complex when compared to standard biocidal technologies. In contrast to a single, ready to use biocidal molecule, singlet oxygen and other ROS are produced in situ by the combined action

of light, photosensitizers and oxygen. The photosensitizers at different concentrations, with different absorption coefficients and quantum yields of ROS production are exposed to light at different wavelengths, intensities and times yielding different radiant exposures.

Firstly, that complexity of biocidal ROS generation in situ frequently hampers the comparison of laboratory experiments, exemplarily described for the well-known photosensitizer TMPyP. PDI of *E. coli* resuspended in H_2O led to 3 $\log_{10}$ steps of cell reduction in the presence of 10 µmol l^{-1} TMPyP at a very small radiant exposure of 0.079 J cm^{-2} [496]. On contrary, TMPyP immobilized on a chitosan membrane required a radiant exposure of up to 172.8 J cm^{-2} to achieve the same effect with *E. coli* resuspended in PBS [563]. Another study applied 0.73 µmol l^{-1} TMPyP only, which was exposed to 2,052 J cm^{-2} of light in order to reduce the cell count significantly [623]. Furthermore, for a study targeting several organisms in wastewater, 5 µmol l^{-1} TMPyP and 14.4 J cm^{-2} were applied to reach an inactivation of about 4 $\log_{10}$ steps [388].

Secondly, the situation may worsen when it comes to PDI applications beyond laboratory tests. The step from laboratory settings to real life frequently may unfold additional, technological problems, however, that step is necessary and worthwhile to leverage PDI, at least in some fields of environmental and medical applications.

Such a step was recently performed for a new application of PDI to act as an antimicrobial coating of frequently touched surfaces in health care settings and beyond [146,147,624]. After extensive and successful laboratory tests, a field study should verify whether that PDI technology keeps its efficacy under real life conditions. The field study was performed in two hospitals for several months and the results of the study clearly proved that the novel photodynamic coating significantly reduced the bacterial burden on patient-near surfaces, which may reduce the risk of nosocomial transmission of pathogens [147]. Unfortunately, despite the advantages of PDI coatings and its proven efficacy in field studies [146–148,625], the use of silver, copper and quaternary ammoniums are reported to be the major technologies so far, whereas the role of PDI is almost unmentioned [415,626].

For potential applications of PDI in environmental and medical fields, we developed three new classes of photosensitizers in the past years, which comprised some phenalenones, flavins, and curcumins. These photosensitizers showed a clear antimicrobial efficacy against various bacteria independent of their type and resistance profile [147,230,281,297,467,550,627–629]. The photosensitizers offer features, which are important when it should come to application in the environment and medicine. The molecules were patentable and its synthesis is economic. The usual

tests showed that the molecules have no toxic or mutagenic potential being bio-degradable and safe for the environment.

After the first successful tests of these photosensitizers in bacterial solutions, the use of phenalenones was tested as a potential skin antimicrobial, which might be applied in future to decontaminate large areas of human skin. The use of PDI to reduce the bacterial load in skin wounds was already studied using other photosensitizers [254,368,588]. *Ex vivo* skin was inoculated with *S. aureus*, MRSA, *E. coli*, or *P. aeruginosa*. The subsequent irradiation yielded a reduction of bacterial cells of up to 5 $\log_{10}$ steps [99]. However, the *ex vivo* study revealed that the photosensitizer concentration and the radiant exposure were clearly higher when compared to experiments in solution. Obviously, the skin surface may exhibit substances that hamper the photodynamic mechanisms to some extent and among others, different ions like Ca^{2+}, Mg^{2+}, and HCO_3^- might play a role [546,547,564]. Noteworthy, these ions are also ubiquitous in other environments like tap or waste water, in both, PDI was already studied to reduce their bacterial contamination [386,388,389,392,541,630].

Thus, for the present study, we focused on two potential applications of PDI, which still requires a better understanding of the parameters under real life conditions, skin decolonization and water disinfection. Decolonization of skin and mucosa is an important measure to reduce cross-contamination and surgical site infections [631]. The decolonization of skin usually involves biocidal substances like chlorhexidine, triclosan and iodine leading frequently to insufficient results [632]. The mucosa requires the use of antibiotics like mupirocin. Unfortunately, most of those substances already evolved a reduced sensitivity or resistance against typical skin pathogens [633].

Also the availability of safe tap water including its disinfection is an increasing challenge and the United Nations World Water Development Report stated that nearly 6 billion peoples will suffer from clean water scarcity by 2050 [634]. While water disinfection has effectively prevented waterborne diseases, an unintended consequence is the generation of disinfection byproducts [635], which may open the door to new and safe technologies like PDI.

Both potential application fields of PDI have in common that ions like Ca^{2+} and Mg^{2+} are ubiquitous in tap water and on skin surface. Some ions already showed a detrimental effect on PDI that was applied to inactivate *Pseudomonas aeruginosa* or *Staphylococcus aureus* [636]. It is assumed that such ions interact with the outer environment of the bacteria [636–638] possibly resulting in a protective layer.

To overcome the detrimental effects of ions, citrate was tested as chelating agent in bacterial solutions. VIS-spectroscopy and measurements of oxygen concentration in solutions was applied to

investigate any negative effect of citrate on the used photosensitizers. Subsequently, the results of the optimization with citrate obtained for calcium and magnesium ion solutions were transferred to solutions reflecting possible future fields of application for PDI. With citrate, an optimized PDI of *E. coli* and *S. aureus* was therefore targeted in tap water and in synthetic sweat solution.

Material and Methods

Bacterial strains

Escherichia coli (DSM 1103) as Gram-negative and *Staphylococcus aureus* (DSM 1104) as Gram-positive model organisms for this study were purchased from DSMZ (German Collection of Microorganisms and Cell Culture Lines, Braunschweig, Germany). All organisms were cultivated on Mueller-Hinton-Medium [527] (Carl Roth GmbH & Co. KG, Karlsruhe, Germany) at 37°C and 100 rpm overnight.

Preparation of ionic solutions, synthetic sweat, and tap water

Calcium chloride and magnesium chloride, both purchased from Carl Roth GmbH & Co. KG, Karlsruhe, Germany, were prepared in stock concentrations of 150, 15 and 1.5 mmol l^{-1}. Synthetic sweat solution [639,640] contained 85.56 mmol l^{-1} sodium chloride (Carl Roth GmbH & Co. KG, Karlsruhe, Germany), 0.72 mmol l^{-1} calcium chloride (Carl Roth GmbH & Co. KG, Karlsruhe, Germany), 0.13 mmol l^{-1} magnesium chloride (Carl Roth GmbH & Co. KG, Karlsruhe, Germany), 0.02 mmol l^{-1} zinc chloride (Merck KgaA, Darmstadt, Germany), 9.39 mmol l^{-1} L-histidine (Sigma-Aldrich Cooperation, St. Louis, Missouri, USA), 6.84 mmol l^{-1} sodium lactate (Carl Roth GmbH & Co. KG, Karlsruhe, Germany) and 19.65 mmol l^{-1} urea (Carl Roth GmbH & Co. KG, Karlsruhe, Germany). Additionally, the synthetic sweat solution was also prepared without histidine. In all cases, ultra-pure water was used as a solvent, hereafter simply referred to as H_2O. The pH value of calcium chloride and magnesium chloride solutions was adjusted to seven. Then, the solutions were filled into serum bottles, plugged, sealed, degassed and gassed with N_2 thrice and autoclaved at 121°C for 20 min at 2 bar. The solutions were then stored in the dark at room temperature. Synthetic sweat was produced freshly and sterile-filtered using 0.22 µm mixed cellulose ester based filters (Carl Roth GmbH & Co. KG, Karlsruhe, Germany) and stored at 4°C for a maximum of 2 days. Tap water was supplied by REWAG, Regensburg, Germany [641] and sterile filtered as mentioned before. The ionic composition of the tap water is provided in supplementary table 1.

Photosensitizers

SAPYR [230] – a phenalenone based photosensitizer with a quantum yield of at least 99% – was purchased from TriOptoTec GmbH Regensburg, Germany. The photosensitizer was dissolved in H_2O yielding concentrations of 10, 20 and 100 µmol l^{-1}. When experiments with sodium citrate (Merck KgaA, Darmstadt, Germany) were conducted, the photosensitizer was dissolved in sodium citrate solution (pH = 7) in concentrations of 3, 30 and 300 mmol l^{-1}.

Chemical assays via Vis-spectroscopy

To investigate the effect of the chelating agent in combination with different ion solutions on the PS SAPYR, chemical assays via vis-spectroscopy were conducted. 100 µl of 100 µmol l^{-1} PS dissolved in 300 mmol l^{-1} sodium citrate were mixed with 100 µl of 150 mmol l^{-1} of $CaCl_2$ or $MgCl_2$ solution, tap water, or synthetic sweat and pipetted into wells of a 96-well-plate. The absorption spectrum of the specimens at a wavelength range from 300 to 550 nm was determined using a spectral photometer (CLARIOStar, BMG, LABTECH GmbH, Ortenberg, Germany). The measurements were implemented once without exposure to light and subsequently after 30 s, 60 s, 300 s, and 600 s of illumination. For this process, a blue light source (blue_v, Waldmann GmbH, Villingen-Schweningen, Germany) with a radiant exposure of 18 mW cm^{-2} was used, resulting in a total applied energy of 0.54, 1.08, 5.4 and 10.8 J cm^{-2}.

Oxygen-concentration measurement

To examine, whether the chelating agents alone or in combination with different ion solutions influenced the singlet oxygen production of SAPYR, oxygen-concentration measurements were carried out. The samples were prepared as described in 2.4 with the exception that 1 µl of 5 mol l^{-1} imidazole, which served as a chemical singlet oxygen quencher, was added [642]. Additionally, to study oxygen consuming chemical processes, the measurements were also carried out without the addition of imidazole. This method ensured that produced singlet oxygen was readily depleted and the change of the oxygen concentration in the medium was detected with an optical sensor (Microx 4, Presens Precision Sensing GmbH, Regensburg Germany). After 1 min of measuring, the sample was illuminated with a blue light source (blue_v, Waldmann GmbH, Villingen-Schweningen, Germany) with a radiant exposure of 18 mW cm^{-2} for 40 s equal to 0.72 J cm^{-2}. Then, the quantification was continued for 540 s. The result was recorded as the relative oxygen saturation before and after illumination [%].

Photodynamic inactivation

The cells were harvested via centrifugation (13,000 x g, 7 min) and suspended in H_2O. The cells were washed twice and resuspended in ion solution, tap water, or synthetic sweat. The optical density of the specimens was measured using a photometer (Ultrospec 10, Amersham Biosciences, Little Chalfont, UK) at a wavelength of 600 nm and adjusted to an OD_{600} of 0.6. 25 µl of the bacterial suspension were subsequently mixed with 25 µl of PS solution in the desired concentration.

The mixture incubated for 10 min in absolute darkness and was later irradiated with the aforementioned light source at 18 mW cm^{-2} for 300 s, equal to 5.4 J cm^{-2}. 20 µl of the treated samples were transferred to 180 µl of prewarmed liquid MH-medium and incubated at 37°C for 48 h at 150 rpm. The optical density was monitored in a plate reader at 600 nm in 5 min intervals with subsequent calculation of the bacterial reduction as described in previous literature [467,564].

Results

Influence of bivalent cations on the PDI

To figure out, whether $CaCl_2$ or $MgCl_2$ solutions chemically modify the PS SAPYR, a mixture of ions and SAPYR was examined using vis-spectroscopy and oxygen concentration measurements. The obtained results show that $CaCl_2$ or $MgCl_2$ solutions slightly influence the absorption spectrum of the PS, independent on the duration of illumination (Fig. 35A-B). After 600 s of illumination, the loss of PS concentration is around 7.0 % for PS in 75 mmol l^{-1} $CaCl_2$ solutions and 9.3 % for 75 mmol l^{-1} $MgCl_2$. The change in oxygen concentration was likewise not strikingly altered by the addition of ions. Due to the production of singlet oxygen by SAPYR, the oxygen concentration decreased by approximately 40% after illumination (Fig. 35C-D). However, the oxygen depletion is solely based on singlet oxygen reacting with imidazole in the experimental setup, as control measurements without addition of a singlet oxygen quencher showed no decline in oxygen concentration in none of the cases where $CaCl_2$ or $MgCl_2$ was tested with or without citrate (Supplementary File Fig. S1-S4). This also indicates that the chemical reactions behind the observed PS concentration depletion described beforehand does not involve oxygen.

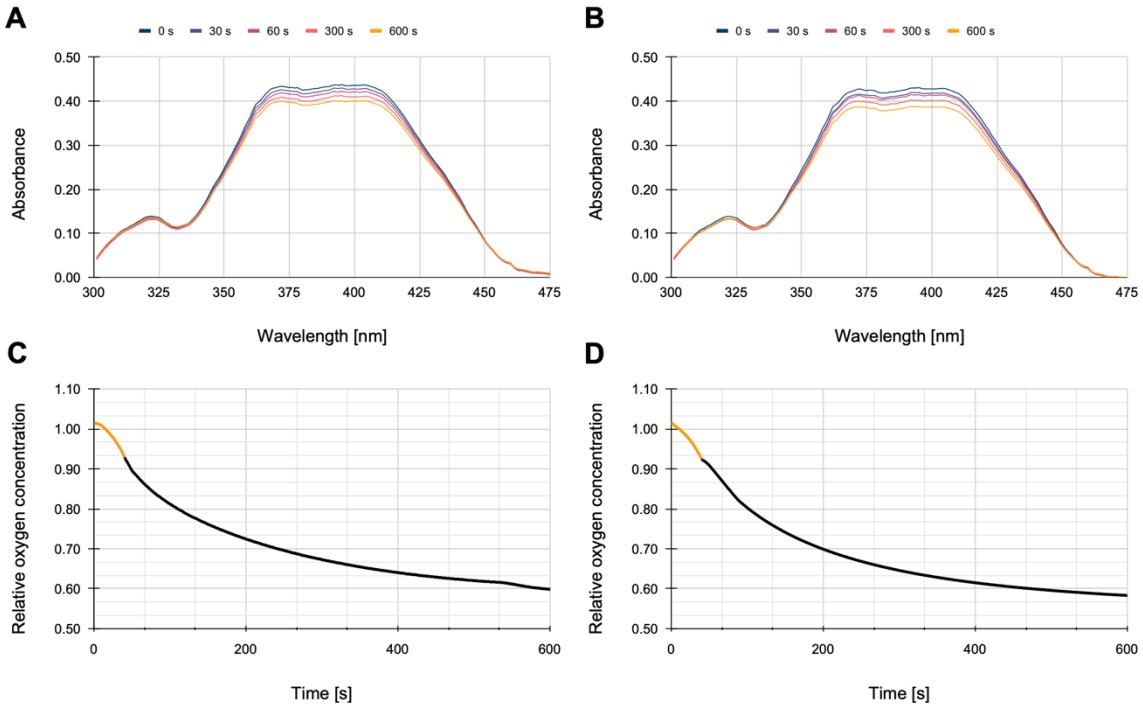

Figure 35: Effect of bivalent cations on the PS SAPYR. Absorption spectrum of SAPYR with $CaCl_2$ (A) or $MgCl_2$ (B) after different intervals of illumination. Change of the oxygen concentration after illumination of SAPYR with $CaCl_2$ (C) or $MgCl_2$ (D). The time in which the illumination was carried out is displayed as yellow datapoints.

For the optimization of the PDI, the subsequent setup of experiments was carried out with citrate. As shown in Fig. 36 the combination of citrate with $CaCl_2$ or $MgCl_2$ solutions had some detrimental effect on the absorption spectrum of the PS (Fig. 36A-B) as again a loss in PS concentration of around 6.8 % and 9.3 % were observed for $CaCl_2$ solutions and $MgCl_2$, respectively. The singlet oxygen production of SAPYR was not strikingly altered as compared to experiments conducted without citrate (Fig. 36C-D). Again, the oxygen depletion is only present when imidazole is added (Fig S3 and Fig S4).

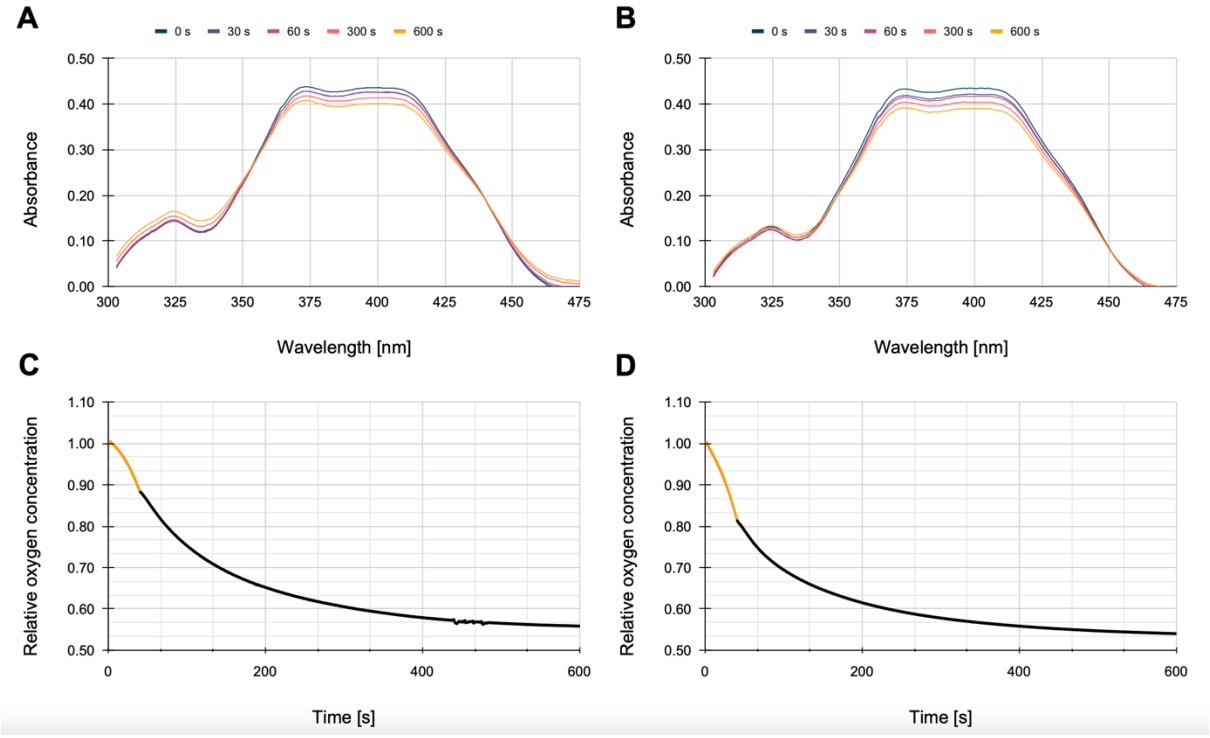

Figure 36: Effect of citrate in combination with bivalent cations on the PS SAPYR. Absorption spectrum of SAPYR with citrate and $CaCl_2$ (A) or $MgCl_2$ (B) after different intervals of illumination. Change of the oxygen concentration after illumination of SAPYR with citrate in combination with $CaCl_2$ (C) or $MgCl_2$ (D). The time in which the illumination was carried out is displayed as yellow datapoints.

Citrate might be a promising chelating agent to optimize PDI as exemplarily investigated in *E. coli* as a Gram-negative and *S. aureus* as a Gram-positive bacterium. Therefore, PDI was performed *in vitro* at different concentrations of citrate and $CaCl_2$ or $MgCl_2$. For 0.75 mmol l^{-1} $CaCl_2$ concentration, SAPYR concentrations of 5 and 10 µmol l^{-1} led to a reduction of less than 3 $\log_{10}$ steps without citrate, while the addition of citrate increased the efficacy by approximately 3 $\log_{10}$ steps (Fig. 37A). When increasing the SAPYR concentration to 50 µmol l^{-1} SAPYR, reduction of *E. coli* viability was 6 $\log_{10}$ steps, independent of the presence of citrate.

The 7.5 mmol l^{-1} $CaCl_2$ concentration revealed a clearer inhibition of the photodynamic inactivation *E. coli*. SAPYR concentrations of 5 and 10 µmol l^{-1} led to a reduction of less than 1 log_{10} steps without citrate, while the addition of citrate again increased the efficacy of PDI (Fig. 37B). The application of 50 µmol l^{-1} SAPYR led to an efficient inactivation of up to 6 log_{10} steps.

The highest $CaCl_2$ concentration of 75 mmol l^{-1} clearly hampered PDI for all SAPYR concentrations yielding a maximum of about 1.7 log_{10} steps for 50 µmol l^{-1} PS, while addition of citrate caused an increased efficacy of up to 3.2 log_{10} steps (Fig. 37C).

The use of $MgCl_2$ instead of $CaCl_2$ showed similar results of PDI against *E. coli*. However, the addition of citrate clearly increased the PDI efficacy (Fig. 37D-E). $MgCl_2$ in a concentration of 75 mmol l^{-1} again lowered the efficacy and experiments without citrate did not result in sufficient inactivation efficacies. On the contrary, experiments with added citrate achieved cell reductions of 4.5 log_{10} steps with 50 µmol l^{-1} of SAPYR. 10 µmol l^{-1} of the PS led to a bacterial reduction of at least 2.5 log_{10} steps, while lower concentrations did not result in noteworthy logarithmic reductions (Fig. 37F). Therefore, in all cases where *E. coli* was resuspended in $MgCl_2$ solutions the application of citrate and PS led to an enhanced photodynamic efficacy.

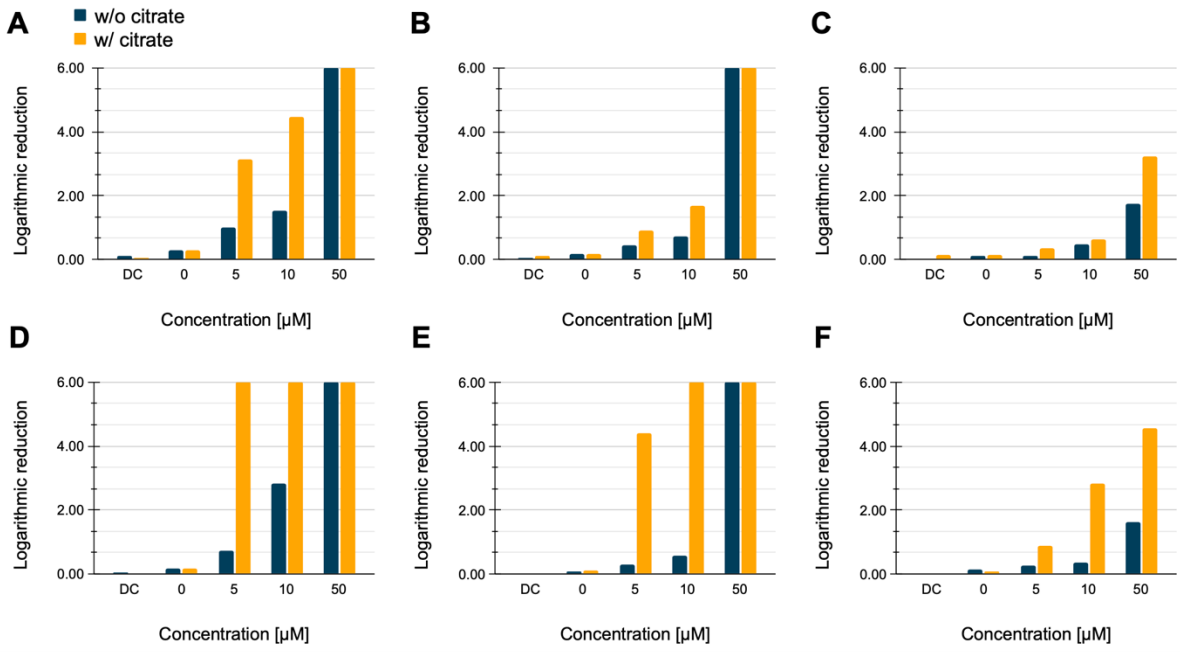

Figure 37: Calculated log_{10} reduction after the PDI of *E. coli* in presence of bivalent cations in different concentrations. PDI of *E. coli* with and without citrate in presence of $CaCl_2$ (A-C) or $MgCl_2$ (D-F). Blue bars indicate results obtained without the addition of citrate, yellow bars indicate the addition of the corresponding citrate concentration. A and D represent a salt concentration of 0.75 mmol l^{-1}, B and E 7.5 mmol l^{-1} and C and F 75 mmol l^{-1}.

In experiments using *S. aureus* cells quite different results were obtained. Even the lowest applied $CaCl_2$ concentrations of 0.75 mmol l^{-1} caused a bacterial reduction of 6 log_{10} steps for 50 µmol l^{-1} SAPYR, while the addition of citrate surprisingly reduced the efficacy and led to a reduction of only 4 log_{10} steps. The small PS concentrations resulted in small reductions of viability (Fig. 38A). Again, for 7.5 mmol l^{-1} $CaCl_2$, 5 and 10 µmol l^{-1} SAPYR did not lead to relevant bacterial reduction and a slightly increased efficacy was observed for 10 µmol l^{-1} when adding citrate. 50 µmol l^{-1} of SAPYR resulted in an efficient reduction of about 6 log_{10} steps without citrate and at least 6 log_{10} steps with citrate (Fig. 38B). For a $CaCl_2$ concentration of 75 mmol l^{-1} and without citrate, the bacterial reduction was below log_{10} step for all SAPYR concentrations. The addition of citrate clearly improved bacterial reduction, especially for the highest PS concentration, an increase in efficacy with over 5 log_{10} steps of bacterial reduction was observed (Fig. 38C).

When 0.75 mmol l^{-1} of $MgCl_2$ was added to *S. aureus* suspensions, the addition of citrate did not improve the PDI effect (Fig. 38D). For 7.5 mmol l^{-1} and 75 mmol l^{-1} $MgCl_2$, PDI improved in the presence of citrate (Fig. 38E-F).

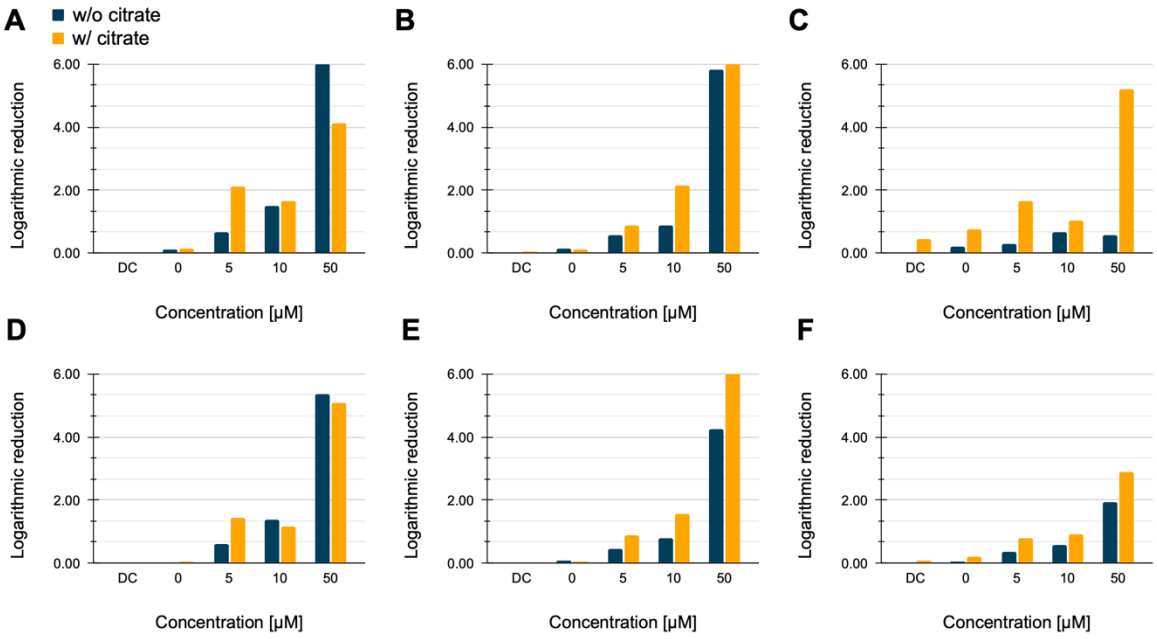

Figure 38: Calculated log_{10} reduction after the PDI of *S. aureus* in presence of bivalent cations with different concentrations. PDI of *S. aureus* with and without citrate in presence of $CaCl_2$ (A-C) and $MgCl_2$ (D-F). Blue bars indicate results obtained without the addition of citrate, yellow bars indicate the addition of the corresponding citrate concentration. A and D represent a salt concentration of 0.75 mmol l^{-1}, B and E 7.5 mmol l^{-1} and C and F 75 mmol l^{-1}.

Influence of tap water on PDI

A combination of different ions in solution could potentially inhibit the application of PDI outside any laboratory experiments and under real life conditions. These conditions were gradually approached by investigating how tap water might influence the process, since it contains a variety of ions. Vis-spectroscopy showed only small loss of concentration (9.3 %) in the spectrum of SAPYR when tap water was applied (Fig. 39A). However, when citrate was added to tap water the PS concentration decreased by 20.45 %. (Fig. 39B). Concerning the change of oxygen concentration after illuminating SAPYR in tap water, there is also no striking alteration without (Fig. 39C) or with citrate (Fig. 39D). Measurements conducted without the addition of the artificial singlet oxygen quencher imidazole show that the oxygen depletion is based on reactions of the produced singlet oxygen with imidazole, which does not occur in measurements without imidazole (Supplementary File Fig. S5 and S6). PDI against *E. coli*, being previously suspended in tap water, showed a better effect in the presence of citrate, achieving 6 $\log_{10}$ steps for 10 and 50 µmol l^{-1} SAPYR (Fig. 39E). With *S. aureus* as test organism, the result was similar except when 10 µmol l^{-1} of SAPYR were applied. Here, the antibacterial effect was partly less efficient when citrate was added. No difference was detected for the highest PS concentration. (Fig. 39F).

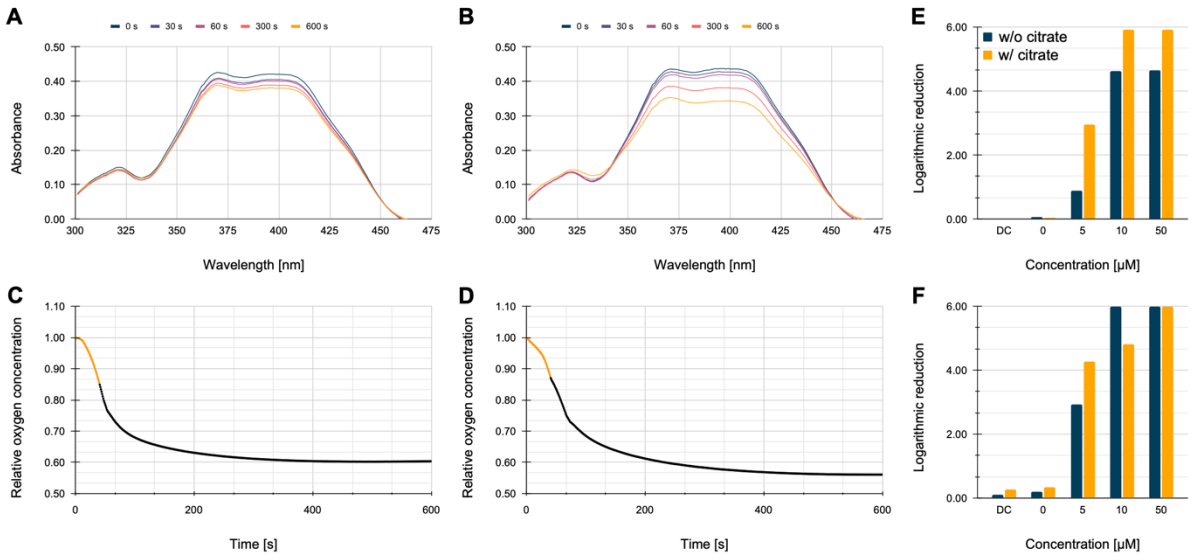

Figure 39: Investigation of the effect of tap water on the PDI. Absorption spectrum of SAPYR with tap water (A) or tap water combined with citrate (B) after different intervals of illumination. Change of the oxygen concentration after illumination (indicated by yellow data points) of SAPYR with tap water (C) or tap water combined with citrate (D). Calculated $\log_{10}$ reduction after the PDI of *E. coli* (E) and *S. aureus* (F) in tap water with or without the addition of citrate.

Influence of synthetic sweat on PDI

To further explore a potential clinical use of PDI on skin, the experiments were conducted in a synthetic sweat solution consisting of agents, which are typically present on human skin. The spectroscopic results indicate that the synthetic sweat severely interferes with the SAPYR, since its absorption spectrum is dramatically altered after illumination independent of whether citrate was added or not (Fig. 40A-B). The spectra do not form isosbestic points as the measured values do not meet the criteria described elsewhere [528]. The change of oxygen concentration after illuminating SAPYR was not altered (Fig. 40C-D). However, the decline in oxygen concentration is partly caused by the present histidine in the reaction as measurements without imidazole showed (Fig. S7 and S8). The PDI of *E. coli* suspended in synthetic sweat was not effective since the $\log_{10}$ reduction did not exceed 1 $\log_{10}$ step, independent of whether citrate was added or not (Fig. 40E). With *S. aureus* suspended in synthetic sweat, the bacterial reduction was slightly higher and with the addition of citrate more efficient than without (Fig. 40F). In none of the cases a bacterial reduction exceeding 3 $\log_{10}$ steps was measured.

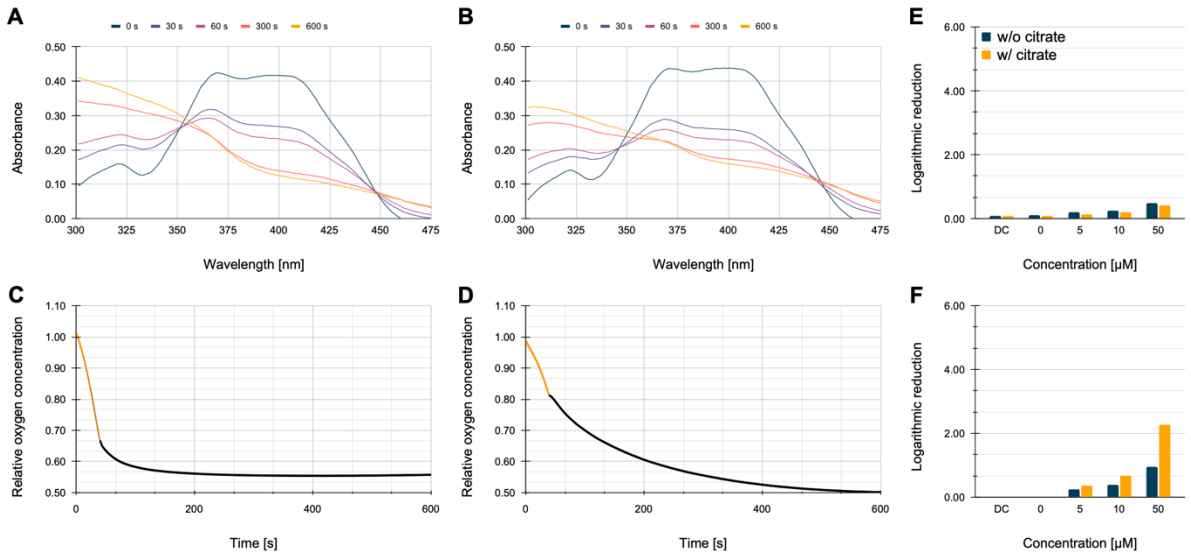

Figure 40: Investigation of the effect of synthetic sweat on the PDI. Absorption spectrum of SAPYR with synthetic sweat (A) or synthetic sweat combined with citrate (B) after different intervals of illumination. Change of the oxygen concentration after illumination (indicated by yellow data points) of SAPYR with synthetic sweat (C) and synthetic sweat combined with citrate (D). PDI of *E. coli* (E) and *S. aureus* (F) in synthetic sweat with and without the addition of citrate.

Influence of synthetic sweat without histidine on the PDI

To determine which component of the synthetic sweat solution was responsible for the inhibiting effect, histidine as a known chemical singlet oxygen quenching molecule was omitted from the mixture. Then, the experiments shown above were repeated accordingly. The absorption spectrum of SAPYR was not strikingly altered by the addition of synthetic sweat without histidine (Fig. 41A). When citrate was added, a slight loss of PS concentration occurred (Fig. 41B). The change of oxygen concentration after illuminating the PS was not influenced by the addition of synthetic sweat without histidine with or without citrate (Fig. 41C-D). In oxygen depletion measurements without imidazole no decline in relative oxygen concentration was measurable (Fig. S9 and S10). The PDI of *E. coli* suspended in synthetic sweat without histidine was effective with achieving at least 6 $\log_{10}$ steps of bacterial reduction with or without citrate at a PS concentration of 50 µmol l^{-1}. The addition of citrate improved the bacterial inactivation only slightly with a PS concentration of 5 µmol l^{-1} (Fig. 41E). When the PDI was conducted with *S. aureus*, cell reduction was enhanced when citrate was added to the highest concentrations of SAPYR achieving around 5.5 $\log_{10}$ steps of bacterial reduction (Fig. 41F).

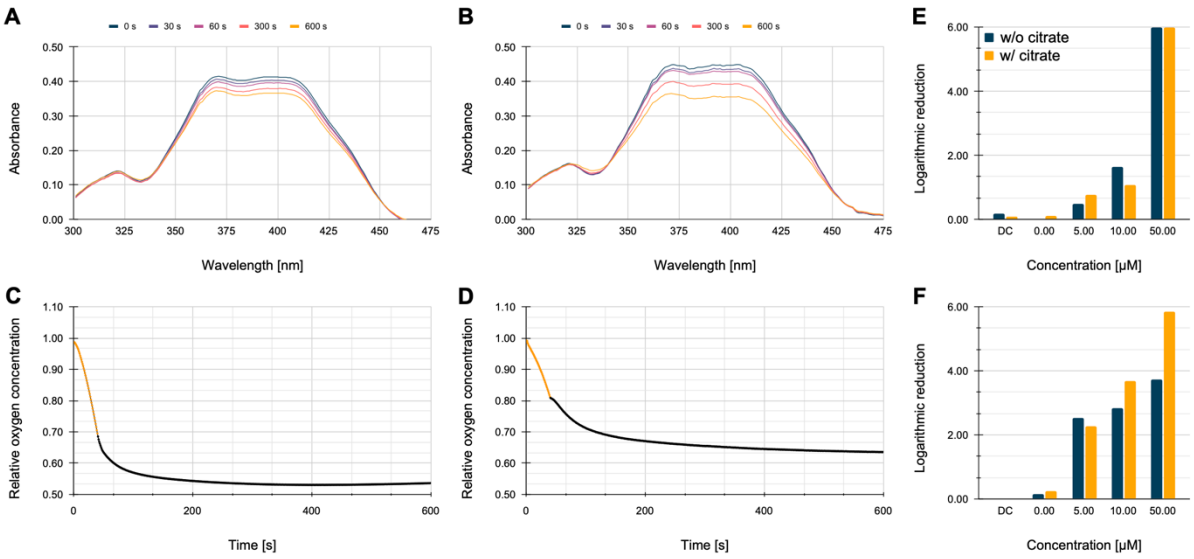

Figure 41: Investigation of the effect of synthetic sweat without histidine on the PDI. Absorption spectrum of SAPYR with synthetic sweat without histidine (A) or synthetic sweat without histidine combined with citrate (B) after different intervals of illumination. Change of the oxygen concentration after illumination of SAPYR with synthetic sweat without histidine (C) or synthetic sweat without histidine combined with citrate (D). Calculated $\log_{10}$ reduction after the PDI of *E. coli* (E) and *S. aureus* (F) in synthetic sweat without histidine with and without the addition of citrate.

Discussion

As it is known from several investigations, different ubiquitous ions like Ca^{2+} can hamper the effectiveness of the PDI [636–638]. Thus, the aim of this study was to investigate the influence of these ions in the presence of chelating molecules like citrate. The intention was that these agents generate complexes with bivalent cations, hence impeding their interaction with the outer membrane in the case for Gram-negative bacteria or the outer cell components for Gram-positive organisms.

For *E. coli*, the efficacy of PDI increased with increasing SAPYR concentrations to a maximum of 6 $\log_{10}$ steps in the presence of the low or moderate ion concentrations. However, PDI yielded less than 2 $\log_{10}$ steps in the presence of the high ion concentrations. The addition of citrate clearly improved PDI in all these settings.

For *S. aureus*, the efficacy of PDI also increased with increasing SAPYR concentrations and was less than 2 $\log_{10}$ steps in the presence of high ion concentrations. However, PDI yielded a maximum in the range of about 4 to 6 $\log_{10}$ steps in the presence of the low or moderate ion concentrations. In addition, the use of citrate showed now diverse results for low and moderate ion concentrations and only a clear improvement of PDI in case of the high ion concentrations.

All in all, higher concentrations of $CaCl_2$ and $MgCl_2$ solutions are more detrimental for the photodynamic inactivation in both cases for *E. coli* as well as for *S. aureus*. However, a clear tendency for enhanced photodynamic inactivation under the influence of citrate is only true for *E. coli*. In this case, citrate can increase the efficacy especially when cells are suspended in $MgCl_2$ solutions.

The results of the present study generally confirmed that PDI is hampered by the presence of calcium or magnesium ions, but the results were different for *E. coli* and *S. aureus*. Based on the findings here in combination with previous studies, PDI is most effective when the concentration of such divalent ions is low or is kept low by using chelating substances like citrate.

In the past, several attempts are published by which PDI efficacy should be enhanced using different substances. One of the most prominent examples for enhancing the photodynamic process is the addition of EDTA. The enhancing effect of EDTA was shown e.g., for *Burkholderia cepacia* by the application of a curcumin based PS [643]. Similar results were recently obtained by another research group with *Streptococcus mutans* [644]. An increase in efficacy with the application of EDTA was not only shown for curcumins but also for the commercially available PS Photosan [645]. Moreover, EDTA in general is often used to facilitate the uptake of other antimicrobial substances such as

antimicrobial peptides [646–648], chlorhexidine [649,650] or quaternary ammonium compounds [651] in several bacterial species. But optimization with EDTA seems not to be favorable in all cases [614,652].

The improved uptake by using chelating agents is due to the fact that they can destabilize the bacterial membrane [653,654]. On the other hand, calcium and magnesium ions are known as stabilizing factors of the outer membrane. Magnesium ions for example are also well known to bind to LPS and are the major stabilizing component [655,656]. Similar observations were made for calcium ions [657]. Both divalent ions are known to be necessary to a certain extent to the thermodynamic stability of the outer membrane of Gram-negative bacteria [612]. The outer environment of Gram-positive cells is also capable of binding magnesium or calcium ions to (wall) teichoic acids [617,658,659]. Based on the presented results, it is obvious that the effect of citrate in presence of magnesium leads to slightly more enhanced photodynamic inactivation compared to calcium chloride. This is further supported by the complex formation constants which were found to be 1.88 x 10^{-3} for calcium citrate complexes and 2.19 x 10^{-3} for magnesium citrate complexes [660].

Since the LPS is one of the outermost parts of a Gram-negative bacterial cell, electrostatic repulsion of the positively charged photosensitizer should be taken into consideration as well. It seems that membrane stability seems to be a major factor in Gram-negatives when it comes to the binding or the uptake of the PS. For Gram-positives on the other hand it seems more likely that electrostatic repulsions, caused by accumulation of divalent ions at teichoic acids, hinder the PS to efficiently damage the cells. Further attempts in optimizing photodynamic inactivation of bacteria were carried out by Hamblin and co-workers demonstrating a beneficial effect of iodide, thiocyanate, azide, and nitrite [554–556,661]. The addition of antimicrobial peptides in combination with photosensitizers has proven to be effective as well [662,663]. Nonetheless, the findings concerning the inhibitory effect seem not to be ubiquitous as some PS (especially negatively charged ones) appear to have increased antimicrobial efficacy in the presence of divalent ions [553].

The results of PDI in tap water clearly showed the potential of SAPYR to inactivate Gram-negative bacteria like *E. coli* that was additionally enhanced when using citrate (Fig. 5). Noteworthy, most of bacterial contaminants in drinking water are Gram-negative representatives [610,664]. In addition, the use of chelating substances allows the use of rather low SAPYR concentrations (e.g. 5 µmol l^{-1}) yielding about 3 $\log_{10}$ steps for *E. coli* although the applied tap water contained significant amounts of calcium and chloride ions. Typically, drinking water contains calcium ions

in a concentration of 0.03 to 10 mmol l^{-1} [570,573,574,609] and magnesium ions in a concentration of 0.065 to 0.62 $mmol^{-1}$ [575–577].

These differences, compared to the experiments carried out in calcium chloride solutions, could be explained by concurring effects of the other ions in tap water. They might bind to spaces around the bacterial envelope, consequently leading to diminished detrimental effects of the calcium ions in tap water. The efficient inactivation of microorganisms in drinking water was already shown by several researchers, however in most studies higher light doses were applied. Lesar *et al.* for example demonstrated efficient photodynamic inactivation towards *Legionella pneumophila* with porphyrin based photosensitizers applying light doses of around 12 J cm^{-2} [566,665] which is more than twice the light dose compared to our study (5.4 J cm^{-2}).

In case of PDI on skin, the photosensitizer and the singlet oxygen produced inevitably encounter not only bacteria on the skin surface but also other substances like sweat residues and terminally differentiated keratinocytes (corneocytes). These substances may comprise different ions, residual proteins, and amino acids. The results of the present study indicate that citrate can enhance PDI in the presence of synthetic sweat substances containing different ions, sodium lactate, urea, and amino acids in case of *S. aureus* (up to 2.5 $\log_{10}$ steps) but not *E. coli* (Fig. 6). Additionally, the presence of histidine in combination with SAPYR leads to a destruction of the photosensitizer when illuminated. When removing the singlet oxygen quencher histidine from the synthetic sweat solution, PDI effect clearly increased with increasing SAPYR concentration comparable to solutions with magnesium or calcium ions (Fig. 3 and 4) up to 6 $\log_{10}$ steps and the citrate showed again an enhancing effect. Noteworthy, the results were achieved with rather low radiant exposure (5.4 J cm^{-2}) and low SAPYR concentration ($\leq$ 50 µmol l^{-1}). Published studies already showed that PDI *in vivo* mouse models [588] or *ex vivo* human skin models [99] required higher radiant exposures and higher PS concentrations to accomplish efficient inactivation of bacteria. Nevertheless, the present results provide clear evidence that chelating substances like citrate should be added to PDI on skin to improve the antibacterial effect.

Conclusion

The presented results indicate that the application of citrate can enhance the photodynamic inactivation influenced by certain concentrations of ionic solutions. Especially when the most abundant species are expected to be Gram-negative and concentrations of around 7.5 to 75 mmol l^{-1} $CaCl_2$ or $MgCl_2$ are present, the application of citrate in PDI might be beneficial. Furthermore,

photodynamic treatment of tap water is efficiently feasible even without the presence of citrate. In synthetic sweat, the main inhibitory substance is not represented by ions but rather by singlet oxygen quenching amino acids. In the absence of amino acids in synthetic sweat an addition of citrate is beneficial if Gram-positive organisms are targeted.

Contributions

DBE: conceptualization, formal analysis, investigation, methodology, data curation, visualization, writing – original draft; NL: conceptualization, methodology, formal analysis, investigation, writing – original draft, visualization; AKH; validation, investigation, writing – review and editing; AE: validation, resources, writing – review and editing; HH: conceptualization, resources, writing – review and editing, supervision, project administration, funding acquisition; WB: conceptualization, resources, writing – review and editing, supervision, project administration, funding acquisition

Photodynamic inactivation of pathogenic bacteria on human skin by applying a potent photosensitizer in a hydrogel

Daniel Bernhard Eckl[1,2,*], Anja Karen Hoffmann[1,*], Nicole Landgraf[1], Larissa Kalb[2], Pauline Bäßler[2], Susanne Wallner[2], Anja Eichner[2], Harald Huber[1], Wolfgang Bäumler[2]

1: University of Regensburg, Institute for Microbiology and Archaea Centre, Universitätsstrasse 31, 93053 Regensburg
2: University Hospital Regensburg, Department of Dermatology, Franz-Josef-Strauss-Allee 11, 93053 Regensburg
*Authors contributed equally

Correspondence: Daniel B. Eckl, email: Daniel.eckl@ur.de

Manuscript information:

Submitted to bioRxiv as preprint: 10.04.2022

Available as preprint: 11.04.2022

DOI: 10.1101/2022.04.10.487760

Abstract

The antibiotic crisis increasingly threatens the health systems world-wide. Especially as there is an innovation gap in the development of novel antibiotics, treatment options for bacterial infections become fewer. The photodynamic inactivation (PDI) of bacteria appears to be a potent, new technology that may support the treatment of colonized or infected skin. In photodynamic inactivation, a dye – called photosensitizer – absorbs light and generates reactive singlet oxygen. This singlet oxygen is then capable of killing bacteria independent of species or strain and their antibiotic resistance profile. In order to provide a practical application for the skin surface, the photosensitizer was included in an aqueous hydrogel (photodynamically active hydrogel). The efficacy of this gel was initially tested on an inanimate surface and then on the human skin *ex vivo*. NBTC staining and TUNEL assays were carried out on skin biopsies to investigate potential harmful effects of the surface PDI to the underlying skin cells. The photosensitizer in the gel sufficienly produced singlet oxygen while showing only little photobleaching. On inanimate surfaces as well as on the human skin, the number of viable bacteria was reduced by over or nearly up to 4 log10 steps, equal to 99.99% reduction or even more. Furthermore, histological staining showed no harmful effects of the gel towards the tissue. The application of this hydrogel represents a valuablel method in decolonizing human skin including the potential to act against superficial skin infections. The presented results are promising and should lead to further investigation in a clinical study to check the effectivity of the photodynamically active hydrogel on patients.

Introduction

Bacteria resistant to multiple antibiotics are on their rise and pose a major threat to livestock, health, and health-care systems as well as economy. So-called multidrug-resistant bacteria – in brief MDR – were responsible for around 30,000 deaths and over 850,000 disability-adjusted life years according to an estimation by Cassini *et al.* [53]. However, a study by Abat *et al.* contradicts this estimations, terming it "alarmist predictions" [666]. When addressing economic losses, a report from the world bank group paints a dystopic picture where the GDP reduction caused by MDR bacteria might exceed the ones from the financial crisis 2008/2009 [667].

The reasons for emergence of these MDR bacteria are rather multifactorial [668] but might be deducted for example to the excessive use of antibiotics [669–671] as well as the lack of new innovations in antibiotic R&D; Several authors have come up with the catchphrase that the "antibiotic pipeline is dry" [65,67,672,673]. However, novel methods to circumvent the upcoming crisis are on their way such as vaccines against MDRs [74–77], bacteriophage therapy [92,93], or antimicrobial peptides [94,96–98] just to mention a few. It has been known for a long time that another method called photodynamic inactivation is capable of killing bacteria independent of their resistances [388,674–676]. Photodynamic inactivation is a method which requires essentially three components, namely a dye molecule – also termed photosensitizer, (visible) light, and oxygen. The absorption of a photon by the photosensitizer leads in its last consequence to the formation of either reactive oxygen species via a so-called type-I-reaction which subsequently can destruct organic matter [208–211] or singlet oxygen via a type-II-reaction being highly reactive towards organic matter [212,213]. Photodynamic inactivation might find its possible use in several fields of application from dentistry [313–317,645,677] over waste water disinfection [389,390,398] to food industry [430,435,439] or antimicrobial surfaces [147,148,424] but also in the treatment of infections or colonization of bacteria [99–101]. More in detail, *in vivo* evidence in mice exist describing the efficient inactivation of burn wounds infected with *S. aureus*. As a photosensitizer, the researches applied a cationic porphyrin derivative [101]. Also in an *in vivo* burn wound mouse model similar was shown for the critical germ *Acinetobacter baumannii* with chlorin e6 embedded in polyethylenimine [678]. *Ex vivo* experiments on the human skin with aqueous photosensitizer solution based on a cationic phenalene-1-one derivative yielded good efficacy of at least 3 $\log_{10}$ steps for *S. aureus* [99]. The photosensitizers used in aforementioned study are well known as pristine singlet oxygen generators with quantum yields of nearly 100% [220,230].

Based on the mentioned *in vivo* and *ex vivo* studies, it is known that photodynamic inactivation of bacteria works out quite well on the human skin based on an aqueous solution, past research has hinted at some problems that arise. Meanwhile, it is well known that certain ions can, sometimes even independent of the used photosensitizer, inhibit the photodynamic inactivation. The most important ions that must be mentioned here are calcium and magnesium. Both seem to accumulate in the vicinity of the bacterial cells producing a shielding effect that does not allow proper binding of cationic photosensitizers to the cells. It should be taken into account that such ions are present also on skin surface at certain concentrations due to sweat that may hamper bacteria killing on skin. Furthermore, other substances like amino acids, proteins and unsaturated lipids naturally occur on skin surface that may quench generated singlet oxygen and thereby affect photodynamic efficacy. Additionally, an aqueous solutions containing the photosensitizer are impractical for application on an usually dry skin surface. Therefore, the present study also tested the use of an amphiphilic gel suspension containing the photosensitizer at different concentrations. With the gained knowledge concerning inhibitory substances, the presented work anticipated for an optimization of the application.

Material and Methods

Preparation of the photodynamically active hydrogel

Initially, 100 ml of a solution containing 100 µmol l^{-1} SAPYR and 30 mmol l^{-1} sodium citrate was prepared; Ultrapure, MilliporeTM filtered H_2O (hereafter called H_2O) served as a solvent. The pH was adjusted to 5.5 to mimic the pH value of the human skin. The aqueous solution was sterile filtered using 0.22 µm mixed cellulose ester-based filters (Carl Roth GmbH & Co. KG, Karlsruhe, Germany) into a sterile container. The hydrogel was then prepared by slowly adding 5 g hydroxy ethyl cellulose (Sigma Aldrich, St. Louis, Missouri, USA) under constant, slow stirring at 60 rpm to avoid the formation of air inclusions. The gel was stored in the dark at 4°C no longer than 14 days. For experiments concerning oxygen concentration measurements, the gel contained an additional 100 µl of 9 mol l^{-1} imidazole solution which was used as an artificial singlet oxygen quencher. Additionally, a gel without photosensitizer was manufactured and used as a control for experiments with bacteria.

Vis-spectroscopy and oxygen concentration measurements

The chemical properties of the gel were investigated via vis spectroscopy before and after illumination with 10.8 J cm^{-2} with a blue light source (blue_v, Waldmann GmbH, Villingen-Schweningen), corresponding to 600 s of illumination at 18 mW cm^{-2}. The gel was slowly poured into a single use cuvette and the spectrum was recorded from 350 to 475 nm with a photometer (Spectrocord 50 plus, Analytik Jena GmbH, Jena, Germany).

The relative singlet oxygen concentration measurements were conducted with the imidazole supplemented gel as to indirectly detect singlet oxygen production, potentially produced singlet oxygen needs to be removed chemically from the gel. The detection was carried out with an oxygen concentration microsensor according to the manufacturer's instructions (PreSens GmbH, Regensburg, Germany). The illumination conditions were as described beforehand.

Cultivation of bacteria

As test organisms, *Staphylococcus aureus* DSM 13661 as well as *Pseudomonas aeruginosa* DSM 1117 were used, purchased from the Leibniz Institute DSMZ - German Collection of Microorganisms and Cell Cultures GmbH, Braunschweig, Germany. Bacteria were cultivated overnight in Mueller Hinton (MH) medium [527] at 37°C and harvested via centrifugation at 13,000 x g for 7 min. The supernatant was discarded, and the pellet was washed with Millipore-filtered H_2O and centrifuged again. This process was repeated thrice to remove any remaining material from the culture medium.

After the washing process, the pellet was resuspended in the solvent the experiment was carried out, the optical density at 600 nm of the reaction was adjusted to 0.6. corresponding to 10^8 cells per ml; For dilutions, the corresponding solvent was used.

Solvents

Bacteria were either resuspended in H_2O, tap water, synthetic sweat solution, or synthetic sweat solution without histidine. H_2O was sterilized via autoclaving while tap water and both synthetic sweat solutions were sterile filtered. All solutions were stored at 4°C in the dark for no longer than 7 days. The composition of the tap water from the local water supplier is provided in [641], the composition of the synthetic sweat with and without histidine was as follows: Synthetic sweat solution according to literature values [639,640] contained 85.56 mmol l^{-1} sodium chloride (Carl Roth GmbH & Co. KG, Karlsruhe, Germany), 0.72 mmol l^{-1} calcium chloride (Carl Roth GmbH & Co. KG, Karlsruhe, Germany), 0.13 mmol l^{-1} magnesium chloride (Carl Roth GmbH & Co. KG, Karlsruhe, Germany), 0.02 mmol l^{-1} zinc chloride (Merck KgaA, Darmstadt, Germany), 9.39 mmol l^{-1} L-histidine (Sigma-Aldrich Cooperation, St. Louis, Missouri, USA), 6.84 mmol l^{-1} sodium lactate (Carl Roth GmbH & Co. KG, Karlsruhe, Germany) and 19.65 mmol l^{-1} urea (Carl Roth GmbH & Co. KG, Karlsruhe, Germany).

Measuring the efficacy of the photodynamically active hydrogel on inanimate surfaces

Prior to experiments on the human skin, the efficacy of the photodynamically active gel was checked on glass slides. 50 µl of the bacterial suspension prepared as described above were placed on glass slides and kept at 37°C for 60 min in complete darkness until the droplet was macroscopically dried. Then, a sterile swab was used to apply a thin layer of gel to the surface covering the spot with the dried bacteria. After 10 min in complete darkness, the slide with the dried bacteria and the gel was illuminated for 10 min at 18 mW cm^{-2} resulting in an applied light dose of 10.8 J cm^{-2}. After the illumination process, the bacteria were recovered with a sterile swab into sterile MH broth, a tenfold dilution series was produced and subsequently plated with the drop-plate method. After 12 h of incubation, the colonies were counted, and the logarithmic reduction was calculated.

Measuring the efficacy of the photodynamically active hydrogel on human skin *ex vivo*

Tissue samples and annotated data were obtained and experimental procedures were performed within the framework of the nonprofit foundation HTCR, including the informed patient's consent [679]. The skin was of abdominal origin, arrived after a maximum of 12 h after surgical treatment

and was kept on ice during shipment. Immediately after arrival, the skin was thoroughly cleaned with H_2O to remove excess blood and cut into 2 x 2 cm large pieces with a surgical lancet. Any present adipose tissue was removed. The follow-up procedure was the same as described for inanimate surfaces.

Histology

To check for alterations in the human tissue, two different histological stainings were applied. To check for damage of skin cells, the viability of its mitochondria were perfomed, a NBT staining was performed as described elsewhere with minor adaptions [680]. As stock solutions, NADH was produced in a concentration of 2.5 mg ml^{-1}, aliquoted in 1 ml reaction tubes and stored at -20°C for further use and NBT stock solution was produced in a concentration of 2.0 mg ml^{-1} and stored in the dark at 4°C. The staining reaction was prepared immediately before the staining process was carried out as follows: 1 ml of NADH stock solution were mixed with 1 ml phosphate-buffered saline, 0.5 ml Ringer solution, and 2.5 ml NBT staining stock. The skin was submerged after the bacteriological processing in the staining solution for 30 min. Afterwards, the supernatant was discarded, and the skin was fixed in formaldehyde. For a positive control, skin was heated up for 10 min to 100°C and treated afterwards as described above.

All skin samples, either NBT stained or not, were fixed in 4 % formaldehyde solution for 18 h. Afterwards, an ascending isopropanol series was carried out in a tissue followed up by embedding in paraffin (Medite TES Valida, Burgdorf, Germany). After the paraffin hardened, sections were produced using a microtome (Rotation microtome HM 350 SV, MICROM Laborgeräte GmbH, Oberkochen, Germany), and the sections were placed on microscope slides (SuperfrostTMPlus Adhesion Microscope Slides, Gerhard Menzel GmbH, Braunschweig, Germany), followed by a xylol treatment and a descending ethanol row.

To evaluate apoptotic processes, an APO-BrdU-TUNEL assay was conducted. For this, the sections were placed on glass slides. The staining was then carried out according to the manufacturer's instructions. In brief, the sections were washed twice with the provided washing buffer and subsequently covered with reaction buffer, TdT enzyme, BrdUTP solution and H_2O prepared freshly before staining. The sections incubated with the staining solution for 60 min at 37°C, rinsed twice and stained with anti-BrdU-Alexa Fluor 488 for 30 min at room temperature protected from light. Propidium iodide was used to detect the cell nuclei for 30 min. The samples stained this way were

microscopically (Zeiss Axio Imager Z1, Carl Zeiss AG, Oberkochen, Germany) analyzed within three hours after staining.

Results

Chemical properties of the hydrogel

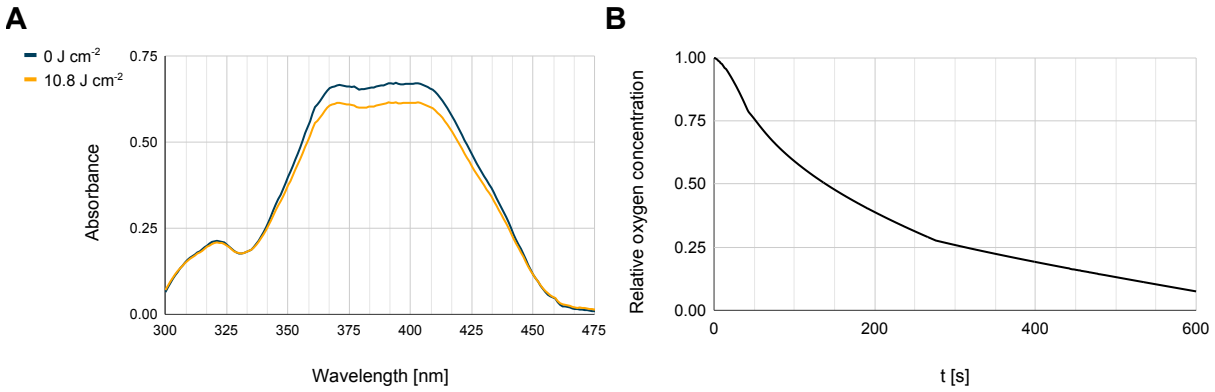

Figure 42: (A) Vis spectrum of the developed photodynamically active hydrogel with citrate before (blue) and after (yellow) light application of 10.8 J cm^{-2}. The Y-axis indicates the absorbance, and the wavelength is displayed by the X-axis in nm. (B) Oxygen concentration inside of the photodynamically active hydrogel in the process of illumination. Y-axis indicates the relative oxygen concentration, X-axis the time in seconds.

The vis spectroscopy of the developed photodynamically active hydrogel with citrate revealed that a certain photobleaching of the photosensitizer occurs (Fig. 42A). After the application of 10.8 J cm^{-2}, the concentration of the PS declined by around 8.2 %. Besides a loss in concentration, the spectrum is not drastically altered and the absence of hypsochromic or bathochromic effects as well as the lack of isosbestic points indicate that the chemical integrity of the remaining photosensitizer not subjected to photobleaching effects is not drastically altered.

The oxygen concentration measurements inside the gel hint at the fact that singlet oxygen is constantly generated efficiently throughout the illumination of the gel itself. Interestingly, nearly all oxygen is depleted in the reaction after the application of 10.8 J cm^{-2}, a relative oxygen concentration of around 7.5 % compared to the starting concentration remained in the gel (Fig. 42B).

Surface experiments

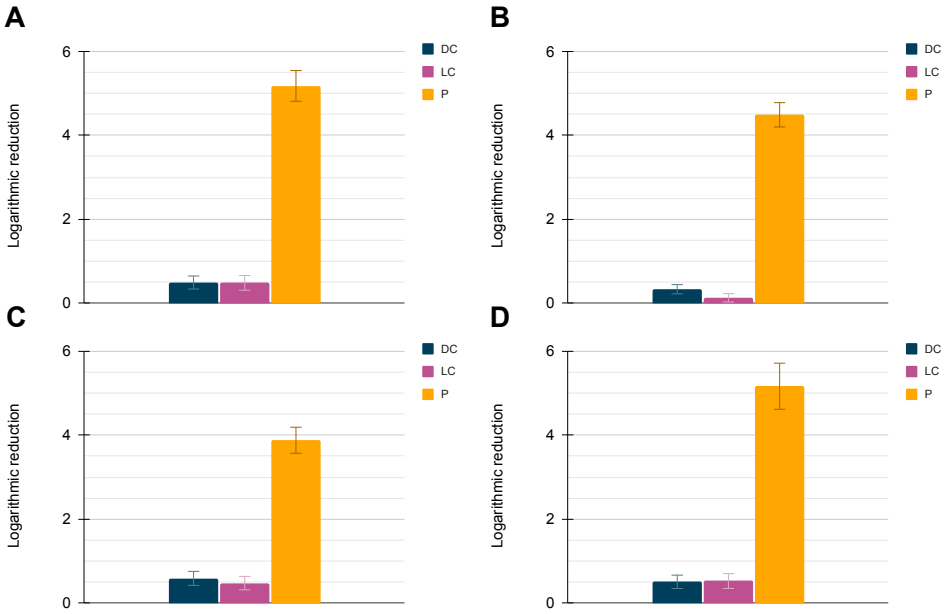

Figure 43: Results obtained for the photodynamic inactivation with the gel on *S. aureus* cells on inanimate surfaces. The Y-axis indicates the logarithmic reduction of the bacterial cells referenced to the reference surface where bacteria as well as a gel without the photosensitizer were applied and recovered subsequently. Blue bars indicate the logarithmic reduction determined for the dark control (DC, with photosensitizer, without light), pink bars represent the logarithmic reduction measured for the light control (LC, without photosensitizer, with light) and the yellow bars indicate the logarithmic reduction for the sample (P, with photosensitizer, with light). Error bars represent the calculated standard deviation based on three biological replicates. (A) depicts the result obtained for bacteria resuspended in H_2O, (B) shows the results for tap water, (C) for sweat and (D) for sweat without histidine.

Prior to an application of the gel to the human skin, experiments were conducted on inanimate surfaces to evaluate the gels antimicrobial potential . For *S. aureus*, in none of the tested controls, dark toxicity or reduction from light alone exceeded values above 1 $\log_{10}$ step. For H_2O (Fig. 43A), tap water (Fig. 43B) as well as sweat without histidine (Fig. 43D), logarithmic reduction exceeded 4 $\log_{10}$ steps, equal to 99.99% of inactivated bacteria corresponding to the reference sample. Only for the experiments with the artificial sweat solution (Fig. 43C) that contained histidine, the logarithmic reduction did not exceed 4 $\log_{10}$ steps on average. With the given conditions the bacteria were resuspended in, one can see that the antibacterial efficacy of the gel decreases for cells that were suspended in tap water or synthetic sweat. The detrimental effect was not present in sweat without histidine as reductions like those in H_2O were obtained.

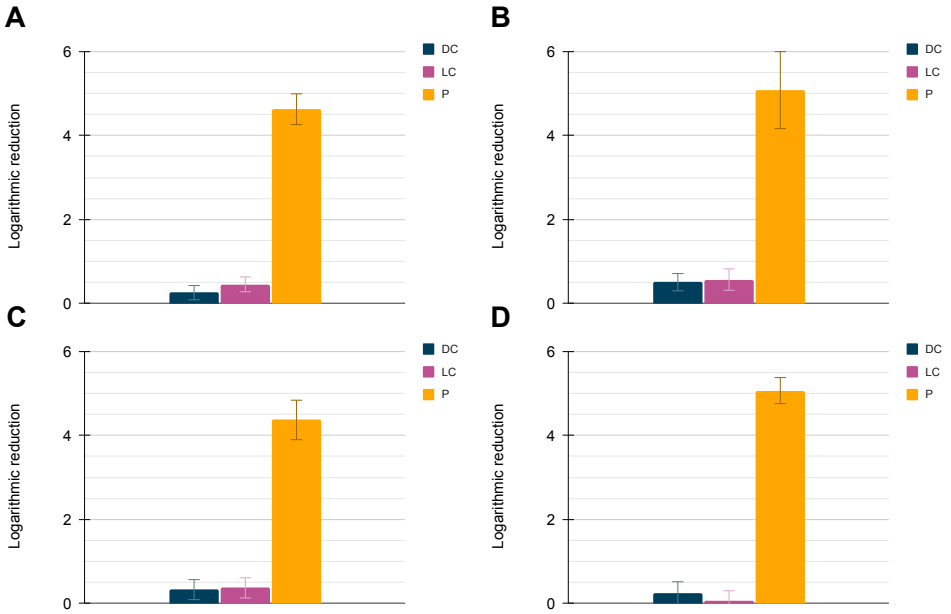

Figure 44: Results obtained for the photodynamic inactivation with the gel on *P. aeruginosa* cells on inanimate surfaces. The Y-axis indicates the logarithmic reduction of the bacterial cells referenced to the reference surface where bacteria as well as a gel without the photosensitizer were applied and recovered subsequently. Blue bars indicate the logarithmic reduction determined for the dark control (DC, with photosensitizer, without light), pink bars represent the logarithmic reduction measured for the light control (LC, without photosensitizer, with light) and the yellow bars indicate the logarithmic reduction for the sample (P, with photosensitizer, with light). Error bars represent the calculated standard deviation based on three biological replicates. (A) depicts the result obtained for bacteria resuspended in H_2O, (B) shows the results for tap water, (C) for sweat and (D) for sweat without histidine.

The results obtained for *P. aeruginosa* cells (Fig. 44) do not differ in noteworthy manners from the ones for *S. aureus*, except for the logarithmic reduction for *P. aeruginosa* cells resuspended in synthetic sweat solution with histidine which still achieved a logarithmic reduction of at least 4 $\log_{10}$ steps (Fig. 44D). Again, all controls in all cases did not lead to a logarithmic reduction exceeding 1 $\log_{10}$ step. The lowest inactivation efficacy was measured for cells resuspended in synthetic sweat containing histidine, yet still leading to good inactivation results.

Photodynamic efficacy on the human skin

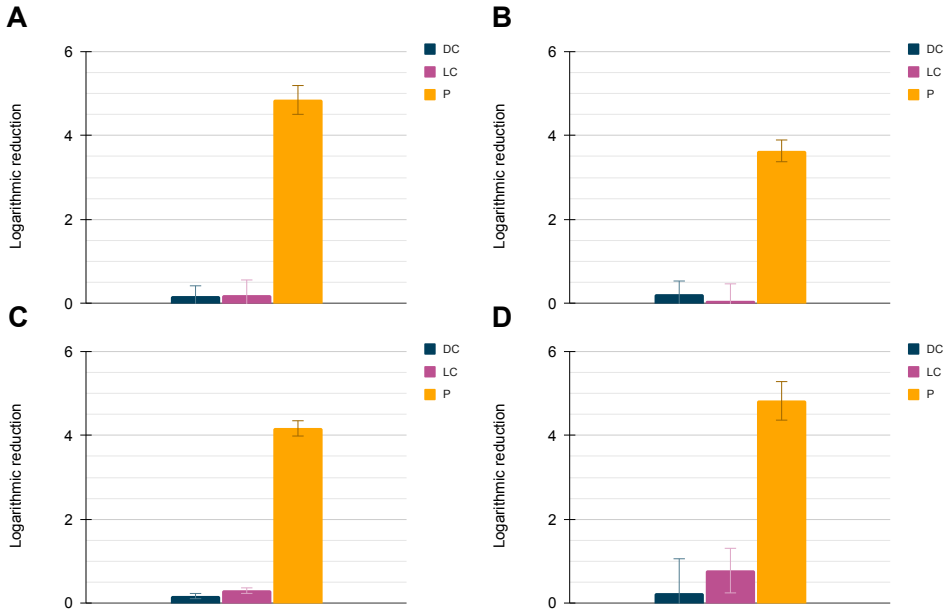

Figure 45: Results obtained for the photodynamic inactivation with the gel on *S. aureus* cells on the human skin. The Y-axis indicates the logarithmic reduction of the bacterial cells referenced to the reference surface where bacteria as well as a gel without the photosensitizer were applied and recovered subsequently. Blue bars indicate the logarithmic reduction determined for the dark control (DC, with photosensitizer, without light), pink bars represent the logarithmic reduction measured for the light control (LC, without photosensitizer, with light) and the yellow bars indicate the logarithmic reduction for the sample (P, with photosensitizer, with light). Error bars represent the calculated standard deviation based on three biological replicates. (A) depicts the result obtained for bacteria resuspended in H_2O, (B) shows the results for tap water, (C) for sweat and (D) for sweat without histidine.

On the human skin, the measured logarithmic reduction did not diverge greatly from the observations made on artificial surfaces for *S. aureus*. With exception of experiments with bacteria resuspended in tap water in which a logarithmic reduction of over 3.5 $\log_{10}$ steps was measured (Fig. 45B), the efficacy was determined to exceed 4 $\log_{10}$ steps. The application of synthetic sweat without histidine (Fig. 45D) led to a similar efficacy compared to H_2O (Fig. 45A). The means of all controls did not exceed 1 $\log_{10}$ step in reduction, therefore neither photosensitizer gel nor light alone have an antibacterial effect.

For inactivation experiments of *P. aeruginosa* on the human skin, a logarithmic reduction in the treated sample exceeded 4 $\log_{10}$ steps for experiments where bacteria were resuspended in H_2O (Fig. 46A) or synthetic sweat without histidine (Fig. 46D), while the mean logarithmic reduction was slightly below 4 $\log_{10}$ steps for tested conditions with tap water (Fig. 46B) and synthetic sweat (Fig. 46C).

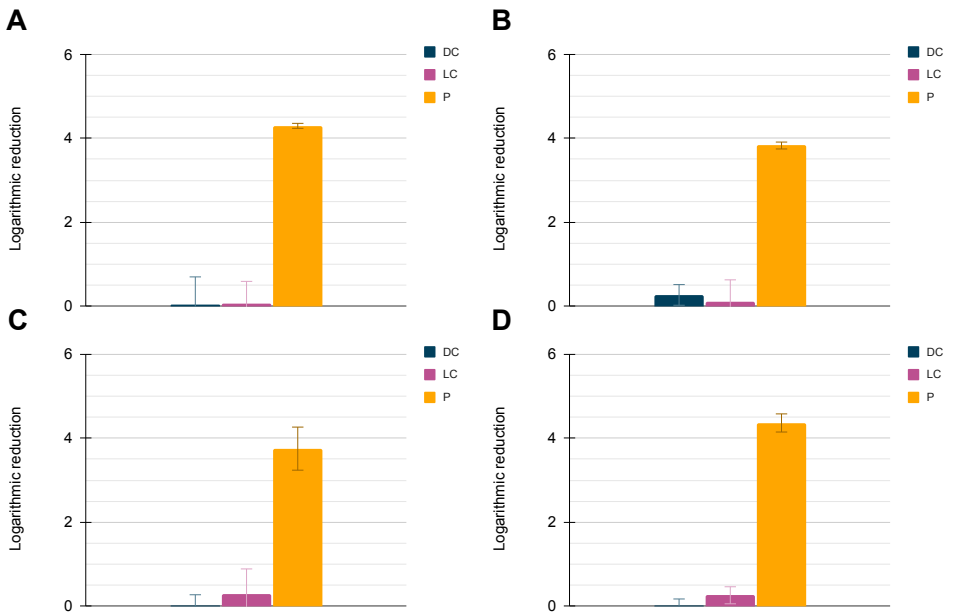

Figure 46: Results obtained for the photodynamic inactivation with the gel on *P. aeruginosa* cells on the human skin. The Y-axis indicates the logarithmic reduction of the bacterial cells referenced to the reference surface where bacteria as well as a gel without the photosensitizer were applied and recovered subsequently. Blue bars indicate the logarithmic reduction determined for the dark control (DC, with photosensitizer, without light), pink bars represent the logarithmic reduction measured for the light control (LC, without photosensitizer, with light) and the yellow bars indicate the logarithmic reduction for the sample (P, with photosensitizer, with light). Error bars represent the calculated standard deviation based on three biological replicates. (A) depicts the result obtained for bacteria resuspended in H_2O, (B) shows the results for tap water, (C) for sweat and (D) for sweat without histidine.

Histology

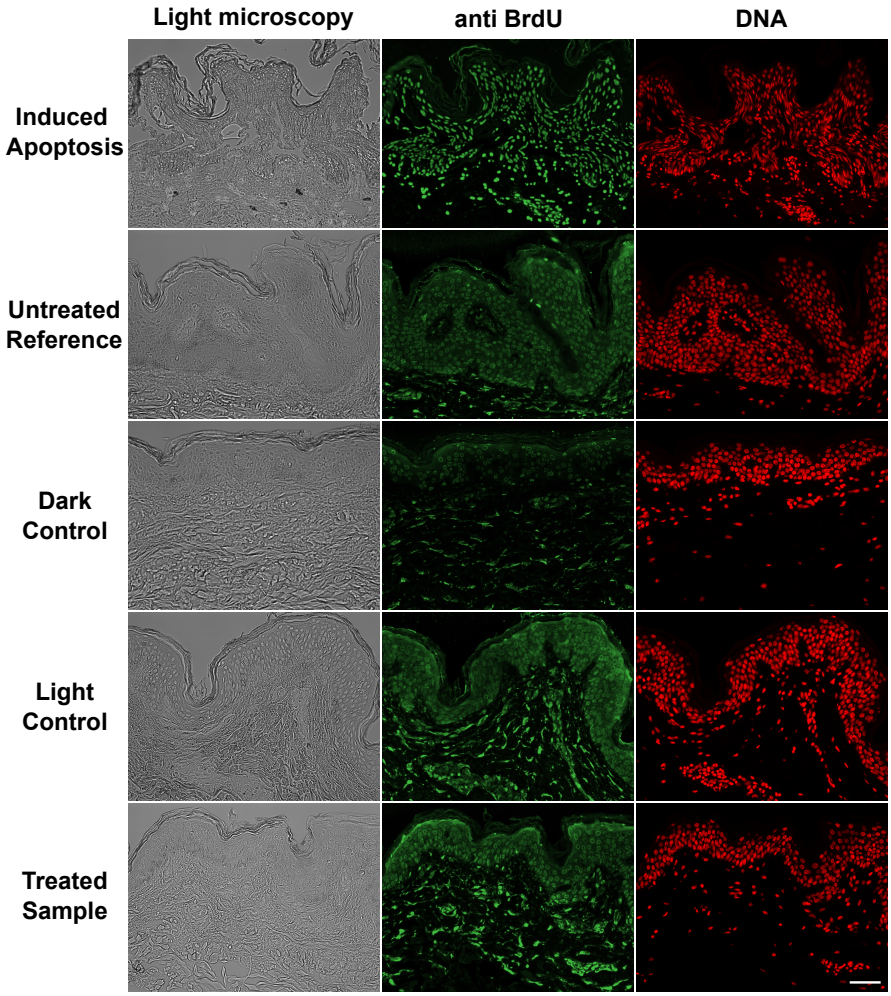

Figure 47: Results of the TUNEL assay. The left column displays the histological sample in the light microscope, the middle column indicates the anti BrdU staining which detects apoptosis when clearly present in the nucleus, and the right column displays the DNA specific staining corresponding the nuclei of the skin cells. The first line was a sample where apoptosis was induced as described earlier, second line displays an untreated control, the dark control sample (gel with photosensitizer, without light) is shown in the third line, fourth line shows a sample that was subjected to light and a gel without photosensitizer, and the last line depicts the results obtained for a treated sample (with light, with photosensitizer). The white scale bar in the lower right corner equals 25 µm.

The skin used for the experiments showed the typical cross section of a sample of abdominal skin. The results obtained for the TUNEL assay (Fig. 47) show that induced apoptosis leads to a clear, green staining of the nuclei in the histological sample that correlates with the DNA staining that was applied. The untreated reference lacks this specific staining of the nuclei but shows a certain – most likely unspecific – staining of the cytoplasm and possible membrane components. Similar is true for all other tested controls and the sample. An unspecific staining of the cytoplasm of *Stratum*

spinosum cells therefore does not indicate apoptosis, especially as the staining does not strictly accumulate as in the sample with induced apoptosis. Overall, the photodynamic killing of bacteria on the skin surface does not reach the underlying skin cells to induce apoptotic processes in any of the tested conditions.

Similar observations were made concerning the NBTC staining which indicates viability of mitochondria by the formation of an intracellular, deep blue precipitate. The inactivated skin sample showed no blue staining (negative control) (Fig. 48A), while the untreated reference sample (positive control) (Fig. 48B) as well as the dark control (Fig. 48C), light control (Fig. 48D) and the treated sample (Fig. 48E) clearly show viable mitochondria in the epidermis as well as in the dermis.

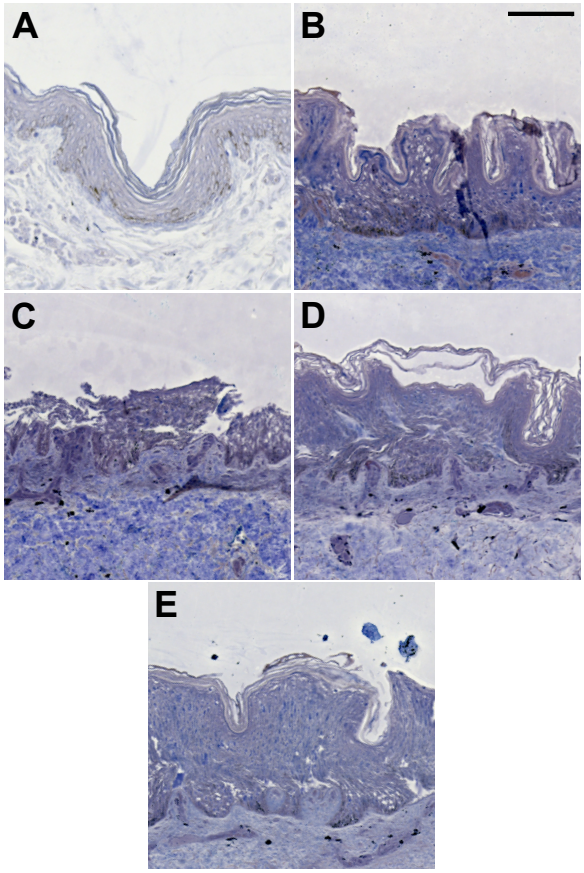

Figure 48: Micrographs of histological sections of the NBTC staining. A depicts the skin sample, which was heated, B shows a piece of untreated skin, C was skin treated with photosensitizer gel but without illumination (dark control), D displays a sample where the skin was treated with light and gel without photosensitizer (light control) and E shows a sample treated with light (10.8 J cm^{-2}) and the photodynamically active hydrogel. The scale bar in the upper right corner equals 100 µm.

Discussion

The present study impressively shows that the use of photosensitizer in the hydrogel clearly inactivated typical skin pathogens upon light activation with about 4 - 5 $\log_{10}$ steps, even in the presence of inhibitory substances like ions and sweat ingredients. The chemical structure of the photosensitizer was almost not affected and the action of singlet oxygen against the bacteria was obviously not hampered by the ingredients of the hydrogel. The observed loss in concentration might rather occur due to photobleaching effects [467]. This fact is also supported by the oxygen concentration measurements of the gel as the oxygen concentration declines due to quenching reactions of singlet oxygen in combination with the added imidazole. Importantly, the integrity of the human skin cells is almost not affected by the photodynamic bacteria killing on top of the skin. The studied photodynamic process along with the hydrogel represents an interesting addition to routine methods for skin decolonization and disinfection but should not replace them. When using the irradiation parameters of the present study, photodynamic inactivation currently required a treatment time of 10 min to achieve a bacteria inactivation of up to 5 $\log_{10}$ steps. At present, this somewhat hampers a fast disinfection process as compared to routine disinfectants but provides an opportunity of skin decolonization or the treatment of superficial skin infection. However, compared to conventional disinfectants, the photodynamic method shown here provides some major advantages. First of all, it should be mentioned that the hydrogel presented here is a water-based system. This means that excessive stress on the skin can be reduced compared with conventional disinfectants or decolonizing agents, as these are often relatively aggressive substances for human skin [632]. Furthermore, patients colonized with MDR bacteria could be additionally subjected to the treatment with the photodynamically active gel as it is known that photodynamic inactivation is highly unlikely to provoke resistances in bacteria [681] as shown by several researchers which exposed different organisms to sublethal photodynamic treatment [545,682,683]. However, this seems to be true at least for photosensitizers that mainly produce singlet oxygen, as there are observations that sublethal treatment with methylene blue might at least provoke a certain tolerance [684]. Additionally, photodynamic inactivation is also a method capable of killing bacteria independent of their antibiotic resistances [280,388,674].

Besides that, ethanol based disinfection for example are not capable of killing bacterial endospores efficiently – some species can even persist for months in such solutions [685]. Furthermore, alkylating agents, glutaraldehyde, formaldehyde, and peroxides do not pose much of a threat to

endospores [686–693]. Contrary to that, photodynamic inactivation performs well in the inactivation of bacterial endospores [281,694,695].

Meanwhile, there are also (hydro)gels available, which use silver ions as causative agent to kill bacteria [696–699]. While these aqueous formulations surely provide inactivation efficacies comparable with those provided in this work, one must consider the development of cross-resistances. It was for example shown for *P. aeruginosa* that the presence of silver also leads to a resistance towards carbapenem [700]; In various *Enterobacter* isolates resistances towards norfloxacin, imipenem, meropenem, ertapenem, gentamicin, ciprofloxacin, and tigecycline emerge under the influence of silver ions [701], and for *Escherichia coli* and *S. aureus* ampicillin resistance development was observed in combination with silver treatment [702]. Furthermore, plenty of reports exist on silver resistance in various microorganisms [703–706]. As antimicrobial zinc based hydrogels are also becoming more popular [707–709], one should also consider the possible development of antibiotic cross-resistances there against antibiotics like erythromycin, clindamycin, or carbapenem [710–712].

In general, the developed gel might impact the treatment of several medical conditions, one that is to mention is acne vulgaris, caused by *Propionibacterium acnes*. The topical treatment options at the moment mainly include the application of antimicrobial substances like clindamycin [713–716] or erythromycin [714,717–720]. More commonly, benzoyl peroxide formulations are used to treat acne [721–723], several commercial prescription free formulations are on the market, like Clerasil® distributed by Reckitt. The use of benzoyl peroxide is also favored when the *P. acnes* present on the skin show antibiotic resistance towards clindamycin or erythromycin. Furthermore, retinoids or azelaic acid may be used to treat *acne vulgaris*. However, as all of the mentioned methods have their very own drawbacks, the photodynamically active gel might represent an additional, supplementary pillar in treating severe *acne vulgaris* conditions, especially as it is known that photodynamic inactivation is successful against *P. acnes in vivo* with 5-ALA [381]. A methylene blue based hydrogel was also already shown to be effective against *P. acnes* [724] as well as other photosensitizers in *in vitro* experiments [725,726].

Another highly interesting field of application already mentioned is the treatment of burned skin. The undamaged human skin is an essential barrier to protect the human body against microorganisms and viruses. Any damage of this barrier frequently leads to skin infections and even beyond [727]. Burn wound sepsis is one of the main causes of burn wounds associated deaths [728]. Antimicrobial treatments for extensive burns are thus a highly interesting field for research, as

especially drug-resistant germs make it difficult to properly disinfect this type of wounds. As has already been shown, PDI might embody an efficient new method in this field of treatment [101,678]. A photodynamic active hydrogel with HEC as one of its main components, which is already used in well-established burn gels such as ocentilin® [729], should be considered as a possible pharmaceutical form in this context.

The analyzed gel used here contains 4 substances: H_2O, hydroxyethyl cellulose, sodium citrate and the phenalene-1-one based photosensitizer. Hydroxyethyl cellulose is well known and frequently used in cosmetics [730], pharmaceutical industry [731], and other industrial applications [732–735]. Sodium citrate is an approved food additive in the European Union, also known as E331 and might therefore considered to be safe for the use on the human skin if the pH is kept skin neutral. As shown in the *ex vivo* skin experiments, the hydrogel does not seem to have a detrimental influence on the human skin. However, experiments as requested by authorities would have to be conducted in the future to provide the photodynamically active gel for potential application on the human skin *in vivo*.

Conclusion

In general, the application of a hydrogel might represent an additional approach in disinfecting the human skin, not only for decolonization of the healthy skin but also when the skin barrier is damaged including burn wounds. The photodynamic approach is able to inactivate pathogenic bacteria regardless of their type and antibiotic resistance as well as dormant endospores. With the herein tested microorganisms, up to 5 $\log_{10}$ steps were achieved on human skin *ex vivo*. The presented results are promising and should lead to further investigation in a clinical study to check the effectivity of the photodynamically active hydrogel on patients.

Acknowledgement

We thank G. Gmeinwieser for technical support, L. Sax for conducting preliminary experiments and D. Grohmann for fruitful discussion. This work was supported by the German Research Foundation DFG [grant number 415812443]. The study was supported by HTCR, a non profit foundation under German civil law, which facilitates research with human tissue by providing an ethical and legal framework for prospective sample collection.

Contributions

DBE: conceptualization, formal analysis, investigation, methodology, data curation, visualization, writing – original draft; AKH: conceptualization, validation, investigation, writing – review and editing;; NL: investigation, validation, writing – review and editing; LK: validation, writing – review and editing; PB: validation, investigation; SW: investigation, visualization, writing – review and editing; AE: validation, resources, writing – review and editing; HH: conceptualization, resources, writing – review and editing, supervision, project administration, funding acquisition; WB: conceptualization, resources, writing – review and editing, supervision, project administration, funding acquisition

General Discussion

Brief Summary

The first manuscript of this thesis describes a new methodology in high-throughput manners to analyze the antimicrobial efficacy. It was the first step of this thesis to develop a quick and easy method that allows a high-throughput screening in the spotlight of antimicrobial efficacy in general as well as the photochemical and photophysical properties of a photosensitizer in various solutions in special. The proposed methodology was then analyzed with *Halobacterium salinarum*, which simultaneously was the first demonstration in literature that Archaea are affected by photodynamic inactivation as well.

Based on the published methodology that enables researchers for thorough investigation of the parameters applied in photodynamic inactivation, a screening of flavin based photosensitizers was conducted. The obtained results revealed that carbonate as well as phosphate led to a chemical destruction of the flavins when excitation by photons is given. The reaction product is consequently neither capable of producing singlet oxygen nor killing bacteria. The observed reaction is very specific for flavins and was not observed with other photosensitizers in combination with phosphate or carbonate and the inhibitory effects are not universal for other photosensitizers.

Other than for flavins in combination with carbonate or phosphate, it is striking that calcium and magnesium ions hamper photodynamic inactivation with methylene blue, TMPyP, FLASH-02a, FLASH-06a and SAPYR neither in chemical nor physical ways. Additionally, no changes in the binding behavior of the photosensitizer towards the bacterial cells were observed. It rather seems that these divalent ions accumulate in the vicinity of the bacterial envelope forming a positively charged area around the cell membrane forcing the photosensitizer to bind to distant cell structures such as antigen O moieties or teichoic acids.

However, further results indicate that this effect can be circumvented by a certain extent with the use of chelating agents especially for Gram-negative organisms. The application of citrate to calcium and magnesium ion solutions led in parts to better inactivation results, especially against Gram-negative bacteria. Furthermore, the impact of citrate was also investigated in more realistic environments like tap water or synthetic sweat. In these realistic environments, the addition of citrate improved PDI efficacy in tap water and in synthetic sweat solution.

Based on the results obtained *in vitro*, the last manuscript dealt with a more application-based theme. Results obtained *in vitro* were transferred to an *ex vivo* human skin model. The human skin was inoculated with bacteria resuspended in synthetic sweat solution containing numerous ions and

small organic molecules. In addition, to improve applicability, a hydroxyethyl cellulose gel was used, which contained a phenalene-based photosensitizer as well as citrate. The application of the hydrogel led to a bacterial reduction of up to 5 $\log_{10}$ steps on human skin *ex vivo*. Furthermore, no apoptotic processes of the human skin were observed, and mitochondrial activity was maintained.
Overall, the manuscripts provided within this thesis investigated on important factors in respect of photodynamic inactivation outside of the laboratory and might serve as guidance for future researchers and companies to improve their applications and products.

Potential impact on methodological concepts and test norms

Remarks on methodological concepts

Nowadays, we see the trend that the platform technology photodynamic inactivation is transferred more and more outside of the wet lab bench into environmental and medical applications. However, such environmental and medical applications often require a lot of effort in planning the experiments, in most cases additional engineering is needed to provide an appropriate treatment environment [541,561,565,736]. To minimize failure of such attempts, a quick and easy set of experiments that should be performed prior to application is proposed in the following.
First, the chemical integrity of the photosensitizer should be checked via spectroscopy or other even more accurate methods like HPLC. However, for an application it is extraneous what exact chemical alterations of the photosensitizer occur. Most importantly, dramatic loss of concentration as well as hypsochromic or bathochromic effects or the occurrence of isosbestic points serve as potential red flags for successful future application. Nevertheless, a differential look should be taken at some of these factors that do not necessarily exclude photosensitizers from their use in a specific field. Elevated photobleaching for example might not be of a great concern when the application time of the photosensitizer is only limited. For example curcumin derivatives bleach very fast but are still successfully used as photosensitizers [737], even in food applications [298,435]. Now whenever long lasting effects are desired, the photosensitizer needs to be extraordinary stable even in the presence of light to maintain the potential to kill bacteria [146,148]. Even hypsochromic or bathochromic effects especially for photosensitizers on a porphyrin base caused by chelation effects [593–595] may not necessarily be exclusive for future use as singlet oxygen is still produced.
Second, singlet oxygen production rates need to be investigated. Most of the techniques used to directly detect singlet oxygen are expensive and require highly specific components [215–221]. However, DPBF assays seem to represent an easy and sufficient alternative [738–741], especially

when supplemented with oxygen depletion assays. Of cause, the system comes with weaknesses on its own like the photobleaching of DPBF in the presence of light, specifity issues under certain conditions, or its limited water solubility [738,739]. Nevertheless, due to the affordability and the ease-of-use DBPF was used in the shown studies. In general, there are plenty of singlet oxygen detection molecules which could be used instead of DPBF, for example the commercially available Singlet Oxygen Sensor Green® [742], DPAX [743], ADPA [744], and many more which were reviewed in depth by You [745]. A direct measurement of singlet oxygen production is possible by detecting the phosphorescence that occurs when the singlet oxygen relaxes back to its triplet state at 1270 nm, which is a unique characteristic [512,746–751]. Nevertheless, this direct measurement method will not be easily implementable in R&D processes as due to the low intensity and the near infra-red wavelength a detection is highly complicated and requires refined apparatuses [752]. However, the photophysical quick check of the system seems to be very important, as in some cases even a chemically altered photosensitizer might still be capable of producing enough singlet oxygen as demonstrated in this work when TMPyP with a complexed magnesium ion was still capable of producing nearly the same amounts of singlet oxygen as the non-complexed counterpart.

Lastly, the growth curve method used to measure the bacterial logarithmic reduction potential is a great method to briefly scan through various parameters of the desired application for functionality such as light intensity, photosensitizer concentration, various bacteria, and different experimental environments. This comes in handy as parameters that need to be investigated quickly start to differentiate in an applied environment, thereby a certain automated high-throughput method will prove to be tremendously helpful. Considered a future application, the growth curve method cannot be implemented with ease as most applications will have fluctuating and complex bacterial populations. A constant doubling time, which is only given in defined bacterial monospecies solutions, is vital for the method itself. Therefore, conservative microbial analysis such as pour-plating, spread-plating [753], drop-plating [494], dilution series as well as the often commercially used dip slides by non-trained personnel [754] will still find its use. However, novel methods to investigate bacterial populations on a molecular basis on site or with little delay in the laboratory such as nanopore sequencing that also allow conclusions about the microbiome present in the investigated field of application should be taken into consideration in the future.

Up to date, most studies attempting to apply the antimicrobial photodynamic technology in aqueous environments already include parts of the prior mentioned set of experiments, especially chemical assays, and not so much singlet oxygen or ROS production analysis of the system

[101,386,389,439,440,755,756]. A study was recently published by Vecchio and colleagues that showed a thorough investigation on those factors, which may influence PDI [379].

By utilization of this proposed set of experiments, it was capable to demonstrate an optimized photodynamic inactivation on the human skin. Especially the use of a hydrogel as well as the addition of citrate led to an improved efficacy. However, in the context of surfaces it should be noted that inhibitory substances might play a minor role compared to experiments in solution, possibly due to precipitation of the salts as the water evaporates and in return are no longer able to bind as ions to the bacterial cells. This hypothesis is also strengthened by findings in field-study reports that document the activity of antimicrobial coatings in a realistic environment which are inevitably contaminated with ions and small organic molecules [147,148]. Although inhibitory substances seem to play only a minor role on surfaces, research that was not conducted in aqueous solution but rather on skin often misses out on these inhibitory problems. The chemical properties as well as the potential to generate singlet oxygen are investigated scarcely, even cultivation-based microbial methods are sometimes not applied [101,379,588,678]. Bacterial counting for example on skin experiments in photodynamic inactivation often uses fancy detection methods like measuring the relative fluorescence of genetically modified pathogens where one should be aware of the pitfalls of such experiments like limited detection sensitivity [101,379,588,678]. This problem might be closely entwined with a certain recovery problem that occurs for Gram-negative organisms. Without a sufficient methodology the organisms sometimes cannot be recovered from the surface anymore, thus, researchers have relied on other detection methods which are by no means as accurate when it comes to high logarithmic reductions compared to culture-based methods such as growth curves or plating [101,379,588,678].

The growth curve method for quantification of the microbial reduction rates was successfully proven within this work. This procedure allows a fast and precise assessment of the antimicrobial potential of a substance. The upcoming antibiotic crisis will intensify the need for the search of novel compounds that sufficiently can kill pathogenic bacteria. While nowadays *in silico* methods may greatly help in finding novel antibiotics [757,758] and therefore also help to reduce the amount of substances to be tested, it is still up to the wet lab scientists to demonstrate the antimicrobial efficacy. The growth curve method therefore has great advantages as it can save costs in human resources as well as in material. But besides the advantages of the growth curve method, some disadvantages should be mentioned, too. Obviously, anaerobic microorganisms cannot be investigated with ease as a plate reader would have to be placed inside an anaerobic chamber.

While from an engineering perspective this would be potentially possible, the limitations are more of practical nature as the process would have to be drastically altered. Therefore, anaerobic pathogens, especially such relevant in dentistry like *Porphyromonas gingivalis* [759] or *Prevotella melaninogenica* [760] are not accessible by the herein described method. Furthermore, the growth curve method is not applicable for organisms tending to heavy agglomeration or biofilm formation as this interferes with optical density measurements.

Re-thinking international test norms

Especially *in vitro* test procedures which are described throughout the scientific literature use highly artificial experimental surroundings for photodynamic inactivation that do not properly reflect reality and similar is true for some test norms. In the present work, the efficacy of PDI was investigated on skin surfaces, beforehand tested on inanimate surfaces. In 2000, the Japanese industrial standard JIS Z 2801-1 was introduced to evaluate antimicrobial properties of non-porous surfaces [761]. Seven years later, the standard became internationally recognized by the International Organziation of Standardization as ISO 22196 [762]. Now, taken into consideration that the method seeks to evaluate the efficacy of an antimicrobial surface, the test standard faces a major downside. The test is conducted constantly in wet conditions which do not reflect reality. Under real life conditions, inanimate surfaces are dry in nearly all cases and only exposed to the relative humidity of the air. Further, the experiment is conducted in diluted nutrient broth which may lead to the possibility of false-negative results in respect of the efficacy as depending on the doubling times of the used bacteria (*S. aureus* or *E. coli*) and the incubation time on the surface. The bacteria will metabolize the present nutrients, grow, and therefore distort the results. However, based on the manuscripts presented within the scope of this thesis, the ISO 22196 standard does not seem to represent a proper alternative for testing the antimicrobial properties of inanimate or skin surfaces in combination with photodynamic inactivation. A drying step should additionally be included in such testing. In general, it seems that parts of the scientific community are aware of the pitfalls the ISO22196 is bearing as it was found that there are also some critical points that, when modified, can have a huge impact on the outcome of the test [763]. Another possible test norm for surfaces, which reflects reality a little better than ISO 22196 is the German and European norm DIN EN 13697:2019-10 for non-porous surfaces [764,765]. Instead of using wet conditions, the bacterial suspensions are dried to the surface and additionally use high or low soiling conditions

mimicked by the addition of 0.03% albumin for low soiling as well as 0.3 % albumin and 0.3 % sheep erythrocytes for high soiling [764,765].

In this work, a rather scientific than normative approach was chosen to determine the antimicrobial efficacy of the photodynamic inactivation on the human skin – especially as the *ex vivo* experiments served for histology after photodynamic treatment. In order to check for the antimicrobial efficacy of any given substance on the human skin under real life conditions, there are some norms available like DIN EN 1500:2013-07 [765]. Thereby, 18 to 20 voluntary subjects are split up in two groups, one treated with a reference method and the other one with the actual substance to be tested. The controlled contamination is conducted by dipping the subjects' hands into an *E. coli* strain DSM 11250 suspension with casein soy broth containing around 10^8 colony forming units per ml. After a drying step, the reference treatment with 60% (v/v) isopropanol is compared to the actual treatment. While this experiment per se is well thought through, the procedure has a major downside from a photodynamic perspective: the resuspension of the bacteria in casein soy broth. By no means, casein soy broth reflects the real conditions on the human skin, as it contains way too much protein to resemble human sweat with in total 20 g peptone per 1000 ml. Further, the only salt present is NaCl with 0.5 % (w/v) in the inoculation medium. Further weaknesses especially from an accuracy point of view of tests like these have also already been discussed in literature [766].

For future test norms it might therefore be advisory to rethink the inoculation medium towards some more realistic solvents. In table 4 some proposed crucial points are listed that need consideration when it comes to creating novel normative test procedures. In a first step, the experiments should be carried out with no other solvent than ultrapure H_2O to exclude any interference caused by other substances. Additionally, the test should always include a realistic medium. While for example experiments targeting future applications in meat processing plants albumin and erythrocytes still might serve as a sufficiently realistic test medium, this is not true for the human skin or wastewater or other parts of food industry. As it is hard to provide a "carved-in-stone" like soiling solution to all fields of applications that sufficiently reflects reality, potential future norms and experimental procedures should include soiling protocols that are sufficient for the respective use. In addition, normative bodies should ensure that they are composed of a sufficiently broad range of experts so that the interests of all areas that are to be affected by the relevant standard are safeguarded. At least for applications on the human skin, the use of the herein

tested synthetic sweat solution as soiling reagent for future normative work is proposed on anything directly linked to antimicrobial action on the human skin.

Furthermore, in a second step it is advised to use an appropriate test surface, especially for testing on inanimate surfaces. Some normative procedures like USP 1072 testing for disinfection efficacy use stainless steel coupons submerged in liquid medium [767]. Stainless steel is a generic term for several different alloys that in their majority contain iron, but also various other substances like nickel, chromium, copper or molybdenum and it has been shown by several colleagues that especially high copper contents might already lead to a antibacterial effect caused solely by the stainless steel [768–770].

In a third step, it needs to be assured that the antimicrobial action of the respective technology is stopped at the end of the given exposure time. For photodynamic inactivation this might include turning off the used light source and reducing the ambient light conditions or highly inhibitory medium quenching potential singlet oxygen. For other antimicrobial substances, neutralization procedures need to be carried out, too. However, in literature there are some good existing concepts suitable for neutralization like Dey and Engley neutralizing broth effective against for example benzalkonium chloride or quaternary ammonium compounds [771,772]. Some other researchers also suggested the use of medium containing very high amounts of organic matter [773].

If tests are conducted on surfaces, it is also important to shed a light on the recovery of the microorganisms. A control sample of the solution applied to a surface needs to be compared to the bacteria dried to the surface without any antimicrobial substance to find out if bacteria cannot be recovered from the surface or die in the drying process. Lastly in the counting and calculation step, the researcher should consider the appropriate medium as well as the appropriate plating method.

Table 4: List of crucial steps in performing antimicrobial susceptibility tests in suspension and on surfaces

Step 1	**Remarks**
Choosing the right suspension medium	Tests for H_2O as well as more realistic media
Step 2 (if surfaces are tested)	
Using appropriate test surface	Inert test surfaces (glass, certain plastics)
Step 3 (if surfaces are tested)	
Drying the bacteria	Inanimate surfaces mostly not moist or wet
Step 4	
Applying the treating condition	Treatment should be stoppable
Step 5 (if surface is tested)	
Retrieving bacteria	Via swabs, potentially sonification
Step 6	
Counting and calculation	Appropriate medium and plating method

In addition, based on artificial laboratory test, many antimicrobial substances claim several orders of magnitude in reduction of the bacterial burden. It should be clear to the environmental microbiologist that these numbers do not reflect the real situation of human-made settings. While high bacterial counts are convenient for laboratory procedures as they allow a good estimation on the efficacy of antimicrobial substances, the microbial burden is in reality by several magnitudes lower. For example, only a few phones exceeded a bacterial load of 5 CFU cm^{-2}, whereat the majority had a lower microbial burden [774,775]. Keyboards on the other hand have bacterial loads of up to 430 CFU cm^{-2} [776]. In hospital settings, the average bacterial load on surfaces was found in one study to be at around 6 CFU cm^{-2} with values spanning from 0 to 480 CFU cm^{-2} [147]. Another study in buses determined the mean microbial burden to be at around 13 CFU cm^{-2}, whereas the values scattered from 0 to 209 CFU cm^{-2} [148]. Although various other studies report on slightly different values, these values represent the microbial load one can expect when sampling in human-built environments.

Therefore, it becomes obvious that the logarithmic detection limit is around 2 to 3 $\log_{10}$ steps, which is way lower than values achievable in the lab as most test norms for example use bacterial concentrations that allow a logarithmic detection limit of around 7 $\log_{10}$ steps [764,765]. This underlines the utter importance of real-life studies or field studies in addition to antimicrobial testing in suspension or laboratory surface testing [146]. This difference in logarithmic reduction however does not hint at the fact that the field test or the laboratory test is insufficient but rather it should be considered as two different measures which need to be evaluated separately from each other.

Prospects for future methodological advancements

Right now, for testing of antimicrobial substances, several other methods besides culture-based methods are additionally available for evaluating the antimicrobial efficacy but are far from being implemented into internationally recognized test norms. One of the most used methods is the ATP measurement present in a certain sample. The method is in principle based on the detection of a luminescence signal which is generated by a luciferase by converting ATP to AMP. However, ATP seems to possess only limited validity as ATP values and findings based on bacterial culture do not correlate [777–781], but the advantages of this methodology should be kept in mind for everyday usage by non-trained personnel especially as commercially available and simple to use systems are available on the market.

While ATP measurements might be used as rough estimates concerning the antimicrobial potential of substances when references are conducted in a sufficient manner, especially nucleic acid-based methods can help to gain tremendously deep insights into the microbial world before and after exposure to antimicrobial substances. One of the most advantageous methods is nanopore sequencing [782]. Briefly, in nanopore sequencing a DNA or RNA strand is translocated by an enzyme trough a MspA pore in a voltage-biased membrane. Current changes can then be used to identify the different bases that are being translocated through the membrane [783].

Using these methods in combination with photodynamic inactivation might account for one of the most important experiments in the upcoming years in photodynamic inactivation especially when photodynamic inactivation is applied in systems with vastly unknown microbial composition. Upcoming molecular methods such as nanopore sequencing might help to bridge the gap of knowledge between laboratory experiments and applications in different environments [784,785] or the skin [786,787].

Such methods provide insight into the abundance of microorganisms present in a specific sample (taking a certain bias into account, of cause), but also help in investigating how photodynamic inactivation will reshape the microbiota prior and after photodynamic treatments. Especially the microbiome analysis of the human skin could reveal which organisms are more affected by singlet oxygen or ROS than others, which would help to gain insight into important yet unknown processes. Furthermore, such a screening could help to solve the question of the potential emergence of resistance towards singlet oxygen, as a comparison of the genes found before and after a photodynamic treatment could possibly reveal some differences. A similar approach that could be used to study these differences was already found to be efficient for the identification of antibiotic resistance genes [788,789]. Besides, it should also be mentioned that nanopore sequencing might facilitate the investigations on the antiviral potential of antimicrobial substances as contrary to those commonly used methods nowadays are still based on culture-dependent analysis methods which are time-consuming and complex in their methodology.

In sum, especially for surface testing, it might be important to move away from highly artificial test procedures to more realistic protocols. Dry testing needs to be established in combination with inhibitory substances that mimic the environment of the targeted application better than current protocols. This includes the application of a synthetic sweat solution that in addition to the proposed one in this thesis might also include either amino acids or proteins as well as fatty acids. The addition of amino acids or fatty acids to a standardized synthetic sweat solution might also be

used as a differentiation between low and high soiling. However, a testing of both conditions – in suspension and on surfaces is highly recommended as demonstrated here. Suspension experiments with synthetic sweat and histidine clearly showed a strong inhibition of the photodynamic process, while experiments on artificial surfaces as well as the human skin still led to sufficient inactivation efficacy.

Future improvements for applied photodynamic inactivation

The herein demonstrated forms of optimization with citrate were by no means the first optimization attempts of its kind. Researchers have for example already used other chelators such as EDTA which is the most common one found in literature. Curcumin as a photosensitizer yielded for example a logarithmic reduction of around 0.4 while addition of 0.5% EDTA could increase the efficacy of up to 4 $\log_{10}$ steps [643]. Comparable results were obtained with *S. mutans* and curcumin [644]. Besides curcumins, an optimization via the addition of EDTA was also achieved for various bacteria relevant in dentistry in combination with a hematoporphyrin based photosensitizer [645]. Another study reported on the use of three different porphyrin based photosensitizers and were capable of showing an increased efficacy in the presence of EDTA [553]. All in all, the use of EDTA as well as related chelators such as EGTA should be carefully investigated as these chemicals might face degradation processes due to the singlet oxygen produced [790]. In consequence, such chelators would in return lead to increased light doses or elevated photosensitizer concentrations in order to circumvent the degradation effect at least to a certain extent. In preliminary screenings of this work, heavy degradation of the photosensitizers SAPYR (Fig. 49A) and TMPyP (Fig. 49B) were observed upon irradiation, which was the major reason why these chelating agents were excluded for further studies.

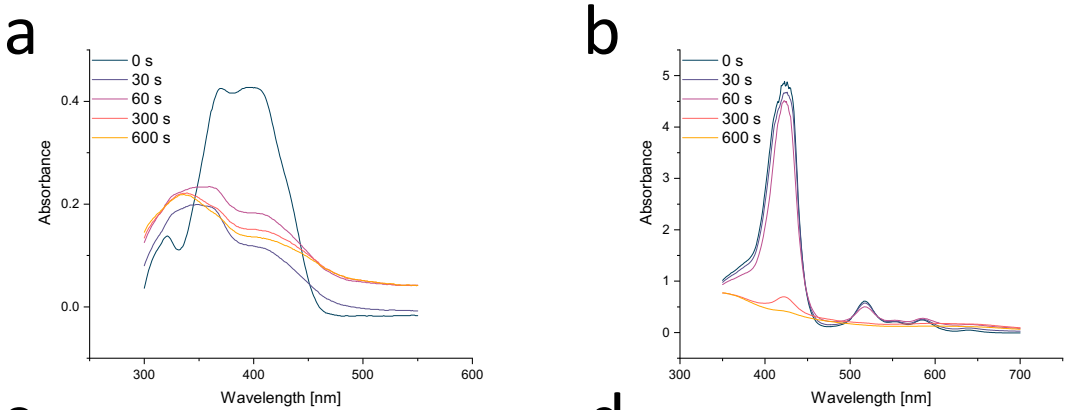

Figure 49: Absorption spectrum of SAPYR with EDTA (a) and TMPyP with EDTA (b) after different intervals of illumination indicated by differently colored lines. The Y-axis indicates the absorbance and the X-axis the wavelength in nm (Landgraf 2021, unpublished)

Further recent attempts in optimizing photodynamic inactivation include the addition of potassium iodide. It is speculated that potassium iodide most likely independent of the photosensitizer may enhance the generation of ROS due to a variety of reactions involving radicals [379,555,791,792]. Surprisingly, a similar effect occurs in the presence of sodium azide during photodynamic inactivation. This discovery from Michael Hamblin's lab is remarkable in two respects. First, sodium azide serves as a singlet oxygen quencher, so it should inhibit photodynamics. Secondly, this discovery also allows oxygen-independent photodynamic inactivation [554,661]. Especially with the emerging trend of photothermal therapy, this report could prove to be significant.

Besides the addition of ions, the chemical optimization of various photosensitizers is still a major topic within the photodynamic community. Just recently, a preprint reported on potential chemical alterations of flavin photosensitizers [292]. These researchers showed best success with a brominated flavin derivative containing a guanidino group. Bromine enhanced the efficacy of the intersystem crossing in the photosensitizer via the heavy atom effect while the guanidino moiety led to increased cellular uptake [292]. Also in the optimization of curcumins, a lot of research was done to optimize this chemical class for medical applications [297,793] or food associated treatments [298].

Furthermore, combinations between photodynamic inactivation and photothermal therapy – in brief PTT – are on the way right now. In photothermal therapy, a molecule or particle is illuminated and converts the absorbed light energy to thermal energy, which leads to a heating of the adjacency of such molecules or particles. The subsequent rise of temperature causes protein denaturation potentially leading to cell death or thermal lysis. Common nanoparticles (NP) used for PTT are Au-NPs [794–796], Ag-NPs [797], Pd-NPs [798,799], and graphene based NPs [800–803]. The photothermal reaction contrasts with the photodynamic inactivation independent of oxygen in the environment. While such coupling of both mechanisms has mostly been studied in tumor cells [804], antibacterial applications remain mostly underinvestigated [805], although synergistic effects probably fostered by Förster resonance energy transfer [741] might exist between the two mechanisms. Especially under certain conditions like tremendously high ion concentrations, when due to biological reasons photodynamic inactivation does not show sufficient efficacy, the combination with PTT systems might prove very beneficial. However, the fact that PTT has only little experience with bacterial inactivation makes it hard to predict how the method would perform under real-life conditions in for example wastewater applications. Nevertheless, the coupling of PDI and PTT should be intensified in the future.

Potential in medicine

Limiting factors

When PDI should be increasingly applied in clinical practice, the procedure must fulfil a set of prerequisites like harmless photosensitizers, checked by standard OECD norms (being e.g. non-toxic, non-mutagenic), and subsequently clinical trials involving patients with colonized or infected tissue. A routine use of PDI in humans requires then a clinical approval of the whole process, either as medical drug or as medical device. However, photodynamic applications on the human subject also have two major limitations, one of legal nature and another one due to the intrinsic properties of the photosensitizer. The first one, the legal limitation, is based on the German Technical Rules for the Occupational Health and Safety Ordinance on Artificial Optical Radiation, briefly called TROS [806]. Although visible light is present in our everyday lives, high doses of visible light can impact the human skin. Visible light, depending on the wavelength can even reach deeper tissue layers like the pulpa of the teeth or the dermis of the human skin. Although the energy of photons of visible light is too small to have ionizing properties, covalent bonds may be broken up by wavelengths of up to 550 nm. Further, high doses of visible light might also lead to a heating of tissue as radiation energy can be converted to heat energy by several tissue constituents like melanin or hemoglobin. Additionally, light dermatosis might be induced, leading to itching, burning, redness and wheals. However, these effects come into play when several mW cm^{-2} are applied over a short time. For example, the TROS defines exposure limits to be 598 mW cm^{-2} for 5 s, 351 mW cm^{-2} for 10 s and 87.5 mW cm^{-2} for 10 min of irradiation time. In this work, 18 mW cm^{-2} were used at highest for a maximum of 10 min and were therefore below this given exposure limits. As a side note, it should be mentioned that the risk for the human eye is higher, which includes thermal as well as photochemical effects which may lead to a loss of vision over time.

The second limitation factor is based on the physical and chemical properties of the photosensitizer. Due to the reaction principle, the photosensitizer needs to absorb light and therefore, most photosensitizers can do this quite efficiently. This property leads to a self-inhibiting effect as with an increasing thickness of photosensitizer deposit (e.g. in a hydrogel) on tissue surface, reduced light intensity reaches the bacteria in or under such a hydrogel deposit. In Fig 50 several TMPyP concentrations are plotted as layer thickness in cm against the transmission in per cent. For concentrations of around 50 µmol l^{-1}, the applied light is almost completely absorbed by a layer of a few mm and PDI is unlikely to happen for bacteria that are located under such a layer. (Fig. 50A). The effect for the Q band (Fig. 50B) is not that severe but in this case, it needs to be taken

into account that this is entwined with lower singlet oxygen production rates compared to the Soret band. Therefore, the concentration of a photosensitizer and the thickness of the gel should be adapted accordingly to avoid such negative effects.

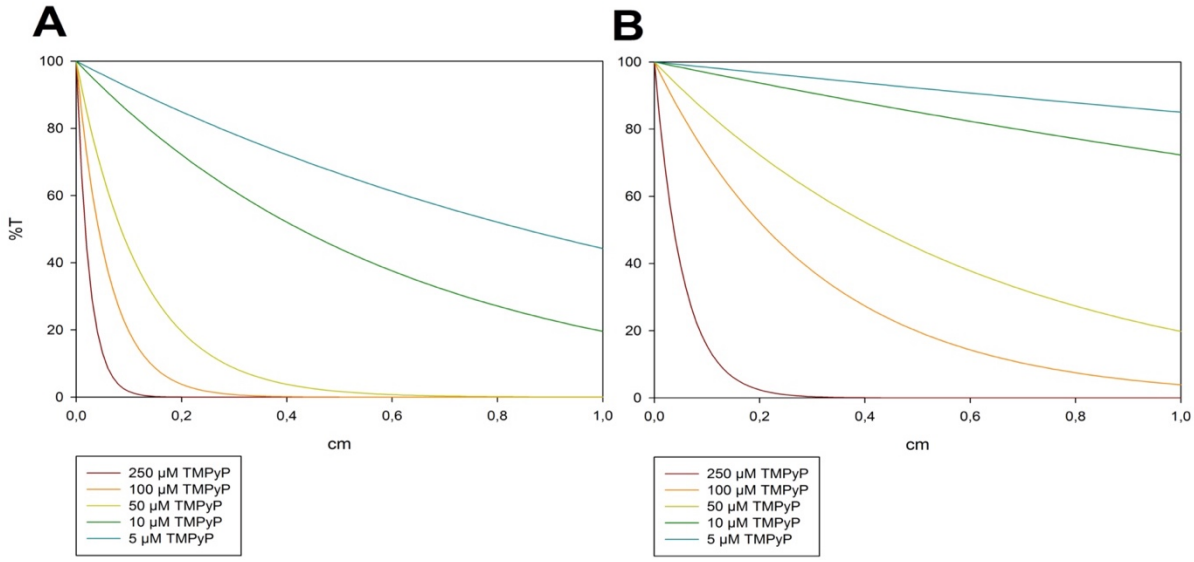

Figure 50: The transmission of light into the samples in the well plates using Lambert Beer law. The values are calculated for A light at 421 nm (Soret band) and for B 520 nm.

Remarks on the state-of-art in dental PDI

Photodynamic inactivation of bacteria is nowadays already applied in dentistry. Of cause, in this context the results are of great importance, especially as the environment in the oral cavity is generally wet. Therefore, photodynamic inactivation must deal with the exocrinically secreted saliva, which contains various chemical substances. When for example dentin becomes demineralized by for example cariotic processes, the release of calcium and phosphates is observed [807].

Due to this both mentioned potentially interfering factors, many studies clearly involve no rinsing process of the treatment area prior to photosensitizer application [677,808–819] or insufficient rinsing with ion containing solvents [820–824]. Only one study include rinsing with distilled water [825]. Interestingly, some studies included rinsing in their protocols after the photosensitizer was administered to prevent self-shielding effects due to the high extinction coefficients of the used photosensitizers [677,809,811,812,816,818,819]. While this rinsing might help in improving the efficacy concerning inhibitory amino acids or proteins, it is not likely that calcium and magnesium ions are flushed away by this rinsing procedure. As proposed in the discussions of two manuscripts presented here, calcium and magnesium stabilize the outer bacterial structures prior to photosensitizer exposure. Even the manual of a commercially available system, HELBO®, includes

only in two applications a rinsing, namely in endodontitis treatment and mucus membrane treatment [826]. Treatment of periodontitis, periimplantitis, alveolar disinfection, bone necrosis, and caries do not recommend rinsing steps currently [826]. The potential consideration of these interfering factors might improve the treatment success in dentistry greatly. Simple protocol optimizations involving chelating agents and rinsing steps could drastically boost the efficacy. However, this protocol changes would need to be specifically optimized for the different application fields in dentistry and would have to be checked for their successfulness in randomized double-blind clinical trials.

Two things must be addressed by dentists in the photodynamic field in the future: First, dentists should consider exchanging the intensively blue colored dyes such as phenothiazines used for photodynamic inactivation as these dyes do not only lead to microbial inactivation but also to potentially undesired staining of tissue or teeth in the oral cavity. Potential photodynamically active dyes which could be used as substituents are the flavins and phenalene-1-one derivatives. Both of the mentioned photosensitizer classes are of yellow color [220,230,276,280], which causes much less undesired staining than phenothiazines or porphyrins. Second, a change in the application form a formulation with a rather low viscosity to one with a higher viscosity will help to keep the photosensitizer in place while being applicated, therefore also allowing prolonged incubation times, which consequently might favor the inactivation process as this possibly might lead to more photosensitizer bound to the cells to be treated. Besides the photodynamically active gel based on hydroxy ethyl cellulose, the usage of so-called micro emulsions as drug delivery system might also be within the scope of applicability [827].

Future role of PDI in dermatology

While these points clearly have an implication on clinical practice as the method is already in-use, the following points are rather of a proposing nature as photodynamic inactivation of bacteria is not in clinical use on the human skin so far. However, the gained knowledge concerning ion-photosensitizer-bacteria interactions as well as in the light of the developed hydrogel are tremendously important in a variety of other medical fields. Probably the brightest future the photodynamic inactivation might face is in the light of skin and soft tissue infections (SSTIs) as well as surgical site infections (SSIs) and patient decolonization. For SSTIs, the photodynamic inactivation approach must be seen rather from an interventional point of view while the impact of

photodynamic inactivation for SSIs is rather of a preventive nature, which includes the decolonization of patients from MRSA [632,828].

From a microbiological point of view, SSTIs are most often caused either by *S. aureus* or *Strep. pyogenes*, whereas some SSTI risk factors also favor other microbial species causing SSTIs such as *P. aeruginosa* in the case of intravenous drug abuse or *Pasteurella multocida* in the case of cat and dog bite wounds [829]. Although only few evidence exist for the rational use of topic antibiotics [633,830], they are still prescribed by physicians especially in young and elderly patients [831]. In the following, some of the potential topic antibiotics are discussed which are state of the art right now, against all of which resistances are a frequently observed phenomenon.

P. fluorescens produces mupirocin as a secondary metabolite [832] which finds its use in topical application since the 1980s [833–837]. Up to date, the use of mupirocin is mostly indicated for *S. aureus* infections [838], scientific evidence clearly indicate also good efficacy against a variety of bacterial genera such as *Staphylococcus*, *Streptococcus*, *Haemophilus*, *Neisseria* and *Moraxella* [839]. The mode of action of the substance is based on interactions with the isoleucyl-tRNA synthetase due to structural similarities with isoleucine that consequently lead to the inhibition of the bacterial protein synthesis [840,841]. Resistance against mupirocin is either mediated by point mutations in the isoleucyl-tRNA synthetase gene (*ileS*) [841] or the *mupA* gene encoding for a new type of isoleucyl-tRNA synthetase [842,843].

In similar ways, sodium fusidate is used as a topic treatment option against *Staphylococcus* and *Streptococcus* SSTIs at it binds to EF-G and stalling the EF-G-GDP complex at the bacterial ribosome. Also for this substance, the occurrence of resistance is reported, either due to several point mutations [844–848] or acquired resistance genes [849–852].

Similarly, neomycin [853,854], bacitracin [855,856] and retapamulin [857,858] are used as antimicrobial substances. More novel substances like antimicrobial peptides seem promising for topical applications [859] and have been proven efficient clinical studies [860,861]

However, as already extensively elucidated in the introduction, antibiotic treatments pose a problem. Therefore, nowadays other biocidal substances find broad application in the treatment of SSTIs and the prevention of SSIs, representing major corner stones in the clinical routine.

One of the most prominent and broadly applied topical biocides is chlorhexidine, also abbreviated CHX, in various forms of application [862–864]. Side effects of chlorhexidine use are for example skin irritations or allergic reactions [865,866]. However, chlorhexidine is included in disinfecting hand washes [867], surgical site disinfectants [868] as well as in body washes for decolonization

[869,870] where it efficiently inactivates most bacteria by causing a leakage of potassium ions of the cells and the disruption of respiratory processes [871]. Bacterial endospores [689] as well as the genus *Mycoplasma* [872] are intrinsically resistant to the substance and biofilm formation leads to a certain tolerance at least [873]. Acquired resistance against CHX is mediated by the so-called *qac* genes which represent a group of efflux pumps that enable the cell to remove the toxic component [874], with qacA being the most important one [875,876]. The fact that CHX is a rather sub-optimal approach for decolonization of patients has also been demonstrated in randomized clinical trials where no treatment success could be demonstrated [828].

Another substance mainly used in the prevention of SSIs and in decolonization of patients is octenidine dihydrochloride [632]. Octenidine has a structural similarity to CHX [877] and is effective against bacteria [878,879] and several fungal species [880,881]. Until now, no resistance development was observed [882], contrary to CHX. However, the results from observational studies as some trials report on good decolonization efficacy of octenidine [883,884] while another trial did not report sufficient decolonization [885].

Further alternatives as topical disinfectants include also triclosan, which is broadly used in hand washes, oral hygiene [886] and sometimes even in several non-medical everyday objects [887]. From a mode-of-action point of view, triclosan interacts with FabI (the enoyl-acyl carrier protein reductase) of the fatty-acid biosynthesis pathway [888–890], which over time leads to defects in the bacterial membrane [891]. Unsurprisingly, also against triclosan resistances are known in several bacterial species such as *E. coli* [889], *S. aureus* [892], and *A. baumannii* [893], either due to point mutations in the upstream promotor region [893,894] or by horizontal gene transfer of genes encoding for alternative enzymes [895,896].

Since a long time, it is also known that iodine has a certain potential as topic antimicrobial [897,898]. Formulations nowadays consist out of complexed iodine in a PVP matrix [899] and is frequently used for disinfection prior to surgical treatment [900], or with far less importance in wound management [901,902], especially as the usefulness is debated [903]. Iodine has strong oxidizing potential of biological structures, consecutively leading to death of the bacterial cells, but the full set of actions have not been fully elucidated yet [633,689,900]. The substance has a tremendously broad activity spectrum [689,693,904,905] and the fact, that up to date no resistances were observed [906], makes it a very promising candidate for topical applications. Referring to that it needs to be stated, that scientific consensus is lacking on how to potentially detect resistances in this specific case [907].

Alcohol based formulations are nowadays often implemented in standard hygiene procedures in health care [908,909]. Although the chemical class of alcohols are effective against all bacteria, endospores are not or only little affected by the denaturation properties of alcohols [689], which yield optimal inactivation results in concentrations from 60 to 90 % [910]. While a certain tolerance against alcohols has been reported [911–913], up to date no true resistance is known. Additionally, biofilm formation might be triggered in increased manners in several clinically relevant organisms [914–916].

Lastly, there is also the use of 3 to 6 % hydrogen peroxide solution [917] for topical treatment to mention, which has from all the latter mentioned the most in common with the photodynamic inactivation. Similarly to photodynamic inactivation, hydrogen peroxide acts against all known life forms [918–922]. Hydrogen peroxide generates radicals intracellularly that inevitably lead to the destruction of all organic molecules [923,924]. However, due to the fact that reactive oxygen species always occur in normal metabolic processes [925,926], bacteria have developed mechanisms to cope with radicals and therefore certain tolerances exist in the microbial world.

In this list of treatment options for SSTIs and prevention techniques for SSIs, the photodynamic inactivation could be considered an innovative method that allows the reduction of pathogens on live skin. However, it should be stated here again that photodynamic inactivation does not aim for a complete substitution of the other substances for topical application, but PDI may support to close the gap of anti-infective procedures. Rather, discriminate use of the full set of possibilities will be the future way to go for medical staff. This will of cause increase the workload for the staff as single case decisions need to be made based on the individual microbiological situation of the patient. However, to prevent the spreading of resistances in the population as well as to provide the best possible outcome for the patient, a combination of at least two methods might be necessary – especially as no method is free of drawbacks. One major advantage of the method is that contrary to the long list of treatment options described before, no resistances exist and are also unlikely to develop. Nevertheless, photodynamic inactivation will not completely be capable of representing the gold standard for superficial infections one day but surely might find its use in a combinatory treatment of several options available.

Conclusions

This thesis clearly showed that PDI is a powerful tool to inactivate bacteria regardless of their species and resistance to antiseptics or antibiotics. The work elucidated the obstructive effects of

ions and amino acids hampering the efficacy of PDI in environmental and medical applications. However, it was also demonstrated that these inhibitory effects can be circumvented. Besides universal inhibitory processes observed for Ca^{2+} and Mg^{2+}, specific interactions were described between flavins and PO_4^{3-} or CO_3^{2-}.

Effects like these must be elucidated for real life applications by a screening of the photosensitizer and solvent on a chemical and physical basis. Especially the growth curve method helps to quickly scan plenty of variables relevant for PDI. However, on surfaces, inhibitory substances – especially divalent ions or histidine - might be of a minor problem. First, because the efficacy is still maintained on the surface and second, especially cleaning protocols can be adapted to render the surfaces more useful. However, the findings presented here make it inevitable to re-think current test norms concerning the antimicrobial efficacy as such methods are often integrated in highly artificial methodologies that cannot reflect the reality properly. Overall, the method itself is probably not capable of completely substitute certain measures but can help to close gaps between existing ones.

In sum, this work helps to improve existing PDI protocols in dentistry as some critical steps might be improved. A photodynamically active gel might prove as a versatile supplementary treatment of superficial skin infections especially with bacteria less susceptible or even resistant to several antibiotics. Due to the simple yet effective approach, the deployment of a photodynamically active gel in medical applications might prove tremendously useful in the future helping to face the dauting challenges of a post-antibiotic era.

Acknowledgement

Zuallererst möchte ich an dieser Stelle **Dr. Harald Huber** erwähnen, welcher als Mentor dieser Doktorarbeit fungierte. Harald, vielen Dank für deine immerwährende Unterstützung und deine stets offene Bürotür. Danke, für die zahlreichen Ratschläge und deine wertvollen Anmerkungen bei den Manuskripten. Ohne deine Bemühungen und dein Vertrauen in mich hätte diese Arbeit sicherlich so in dieser Form nicht durchgeführt werden können.

Weiterhin gilt es, **Prof. Dr. Wolfgang Bäumler,** Zweitgutachter und ebenfalls Mentor, zu danken. Vielen Dank für die zahllosen Treffen und Telefonate in den vergangenen Jahren, bei welchen du mir in allen nur erdenklichen Wegen mit Rat und Tat zur Seite gestanden bist, vor allem dann, wenn ich einmal nicht weiterwusste. Auch ohne deine Unterstützung vom Beginn dieses Projektes an hätte diese Arbeit nicht so entstehen können.

Besonders danken möchte ich auch **Prof. Dr. Dina Grohmann**, welche ebenfalls als Mentorin und Erstgutachterin eine tragende Rolle in dieser Arbeit einnahm. Hier möchte ich mich vor allem für den „Blick von außen“ auf mein Projekt bedanken, welcher stets für neue Ideen sorgte. Danke, dass ich mit allen Problemen, Wünschen und Fragen immer ins Büro platzen konnte. Besonders möchte ich mich auch für die Möglichkeit bedanken, dieses „exotische“ Projekt am Lehrstuhl für Mikrobiologie durchführen zu dürfen.

Für die Übernahme des Vorsitzenden des Prüfungsausschusses möchte ich mich auch bei **Prof. Dr. Stephan Schneuwly** recht herzlich bedanken und bei **Prof. Dr. Winfried Hausner** für die Bereitschaft, als Drittprüfer aufzutreten. Danke auch an **Prof. Dr. Oliver Bosch** für das Bereitstehen als Ersatzprüfer.

Ganz besonders bedanken möchte ich mich auch bei allen Studierenden, welche am PDI-Projekt mitgewirkt haben. Liebe **Nicole Landgraf**, vielen herzlichen Dank für deine engagierte Mitarbeit und deine großartigen Fortschritte bei der Optimierung mit Citrat. Bei der Entwicklung des Hydrogels hatte insbesondere **Anja Hofmann** großen Anteil am Erfolg dieses Vorhabens. Ein großes Dankeschön für deine genialen Ideen! **Laura Schottenhaml** gebührt größter Dank für die äußert mühevolle Mitarbeit beim Herausarbeiten der Flavin-Interaktionen. Für die unzähligen

Vorarbeiten und Experimente sei an dieser Stelle auch **Stefanie Eben, Johanna Niethammer, Julia Dirscherl, Nina Weber, Laura Nissl, Vanessa Mildenberger, Marina Vogl, Anne-Marie Hartl, Kay Knackfuß, Marie-Christin Falter** und **Lena Sax** gedankt. Auch, wenn viele eurer Experimente in diese Arbeit nicht miteingeflossen sind, so waren eure Erkenntnisse und Vorarbeiten für das Projekt sehr wertvoll. Ich bin mir sicher, dass noch das ein oder andere Experiment von euch in Zukunft gute Dienste leisten wird. Bei allen Studierenden, welche ich betreuen durfte, möchte ich mich auch entschuldigen, falls ich manchmal nicht der Betreuer war, den ihr in manchen Situationen gebraucht hättet oder ich uns auch mal zu viel aufgehalst hatte.

Auch im „H4“ am UKR durfte ich wunderbare Kollegen kennenlernen. **Dr. Anja Eichner** stand stets mit ihrer großartigen wissenschaftlichen Expertise in Sachen Mikrobiologie zur Verfügung. Danke, dass du dir für mich und mein Projekt die Zeit genommen hast. Besonders dafür, dass sie mich in den letzten Zügen dieser Arbeit ausgehalten hat, muss **Larissa Kalb** gedankt werden. Danke, dass du mir so vieles abgenommen hast und mir immer zugehört hast. Ohne die wunderbare und gewissenhafte Arbeit von **Ewa Kowalewski, Pauline Bäßler** und **Susanne Wallner** hätte das Projekt auch nicht in diesem Umfang so durchgeführt werden können. Danke, dass ihr euch so engagiert habt. Für die chemische Unterstützung möchte ich mich ganz besonders bei **Dr. Rudolf Vasold** und **Dr. Andreas Späth** bedanken, welche ihr Möglichstes taten, mich bei den chemischen Veränderungen der Farbstoffe zu unterstützen.

Ohne meine Kollegen am Lehrstuhl für Mikrobiologie wären die Tage sehr viel trister und weniger spaßig gewesen. Vielen Dank für die vielen guten Gespräche beim Mittagessen, beim Kaffee oder zum Feierabend. Danke für jegliche Unterstützung, die ihr mir immer wie selbstverständlich entgegenbrachtet. Einen ganz besonderen Dank möchte ich an dieser Stelle meiner langjährigen Büronachbarin **Gabi Gmeinwieser** aussprechen, welche für meine gelegentlich etwas wirre Art immer uneingeschränkt Verständnis zeigte. Gabi, ich kann dir für deine ganze Unterstützung und alles was du für mich getan hast und von mir anhören musstest, gar nicht genug danken. Es war mir eine Ehre, mit einem derart großartigen Menschen zusammenarbeiten zu dürfen. Auch **Dr. Annett Bellack** sei an dieser Stelle erwähnt, denn immer, wenn unvorhergesehene Probleme auftraten, war sie zur Stelle. Selbst wenn es manchmal nicht deine Aufgabe war, dich mit meinen Problemen zu plagen, hattest du immer Zeit für mich. Ich möchte mich auch bei den Sekretärinnen **Elisabeth Nagelfeld, Viola Janik-Erike, Rafaela Lemos-Schmid** und **Britt Morawetz**

bedanken, ohne euch ginge nichts. **Dr. Georg Schmid**, danke dass du immer zur Stelle warst, wenn ich mal ein gutes Gespräch oder Ablenkung brauchte. Danke auch an **Dr. Robert Reichelt** für die vielen Unterhaltungen, kurzen Pausen und wissenschaftlichen Diskussionen. Auch alle, die ich nun leider nicht erwähnen konnte, ihr wart wunderbare Kollegen!

Seit wir unsere ersten mikrobiologischen Schritte im Grundkurs zusammen gegangen sind, sind wir ein Stück dieses Weges gemeinsam gegangen, liebe **Linda Dengler**. Wir kämpften uns Seite an Seite, später auch mal Rücken an Rücken, durch das Studium und die Promotion. Auch an unsere allererste gemeinsame Publikation kann ich mich noch *dunkel* erinnern. Du nahmst dir immer Zeit für mich und meine Diskussionen und sagtest mir auch, wenn ich mal falsch lag. Danke für deine Freundschaft und alles was du für mich getan hast!

Sowohl bei den ernsten als auch den etwas weniger ernsten Problemen des Alltags stand auch immer **Andrea Böllmann** an meiner Seite. Danke für deine fröhliche Art, die auch mal half, durch etwas schwierigere Tage zu kommen. Für deine Arbeiten zur Photodynamik sei dir selbstverständlich auch gedankt, ohne dein großartiges Zutun wäre das Projekt heute nicht so weit gekommen. Auf noch viele weitere „Probleme“.

Auf keinen Fall selbstverständlich war auch die Unterstützung durch meine Freunde – auch wenn ich oftmals nicht die Zeit für euch hatte, die ihr gebraucht und verdient hattet, so hattet ihr doch stets Verständnis für mich und meine Arbeit. **Rich, Fred, Mich, Benny, Finn** und noch so viele mehr: Auch ihr habt Anteil an dieser Arbeit, denn wenn ich eure Freundschaft und Ablenkung am meisten gebraucht hatte, wart ihr stets zur Stelle.

Bedanken muss ich mich ebenfalls beim wunderbarsten Menschen in meinem Leben: **Carina**, danke, dass du mich immer ertragen hast, an mich geglaubt hast, wieder aufgebaut hast und immer Verständnis für mich hattest. Danke, dass du diesen Weg mit mir gegangen bist.

Die unermüdliche Unterstützung meiner **Eltern und Großeltern** machte mein Studium und dadurch diese Arbeit erst möglich. Danke, dass auch ihr immer an mich geglaubt habt und mich auch in schwierigen Zeiten materiell und immateriell unterstützt habt. Ich könnte mir keine bessere Familie vorstellen!

List of Figures

List of Tables

Bibliography

1. Schuenemann VJ, Bos K, Dewitte S, Schmedes S, Jamieson J, Mittnik A. Targeted enrichment of ancient pathogens yielding the pPCP1 plasmid of Yersinia pestis from victims of the Black Death. PNAS. 2011;108: 746–752. doi:10.1073/pnas.1105107108
2. WHO. WHO Report on Global Surveillance of Epidemic-prone Infectious Diseases. WHO. 2000.
3. WHO. Weekly epidemiological record. 2016.
4. Fleming SA. Nobel Lecture: Penicillin. Nobel Lect Physiol or Med 1942-1962. 1945; 83–93.
5. Fleming A. On the antibacterial action of cultures of a penicillium, with special reference to their use in the isolation of B. influenzae. Br J Exp Pathol. 1929;10: 223–236. doi:10.1038/146837a0
6. Chain E, Florey HW, Adelaide MB, Gardner AD, Oxfd DM, Heatley NG, et al. Penicillin as a chemotherapeutic agent. Lancet. 1940;236: 226–228. doi:10.1016/S0140-6736(01)08728-1
7. Kaiserliches Statistisches Amt. Statistisches Jahrbuch für das Deutsche Reich 1915. 1916.
8. Murray CK, Hinkle MK, Yun HC. History of infections associated with combat-related injuries. J Trauma. 2008;64: 221–231. doi:10.1097/TA.0b013e318163c40b
9. Gottfried J. History Repeating? Avoiding a Return to the Pre-Antibiotic Age. Harvard Law School. 2015: 1–73. Available: http://nrs.harvard.edu/urn-3:HUL.InstRepos:8889467%5CnThis
10. Statistisches Bundesamt. Statistisches Jahrbuch 1989 für die Bundesrepublik Deutschland. 1989.
11. Statistisches Bundesamt. Statistisches Jahrbuch 2014. 2014.
12. Coates ARM, Halls G, Hu Y. Novel classes of antibiotics or more of the same? Br J Pharmacol. 2011;163: 184–194. doi:10.1111/j.1476-5381.2011.01250.x
13. Frieden T. Antibiotic resistance threats in the United States, 2013. CDC. 2013. Available: http://www.cdc.gov/drugresistance/threat-report-2013/index.html
14. Abraham EP, Chain E. An Enzyme from Bacteria able to Destroy Penicillin. Nature. 1940;146: 837. doi:10.1038/146837a0
15. Rammelkamp CH, Maxon T. Resistance of *Staphylococcus aureus* to the Action of Penicillin. Proc Soc Exp Biol Med. 1942;51: 386–389. doi:10.3181/00379727-51-13986
16. Agouridas C, Bonnefoy A, Chantot JF. Antibacterial activity of RU 64004 (HMR 3004), a novel ketolide derivative active against respiratory pathogens. Antimicrob Agents Chemother. 1997;41: 2149–2158. doi:10.1128/AAC.41.10.2149
17. Ednie LM, Spangler SK, Jacobs MR, Appelbaum PC. Susceptibilities of 228 penicillin- and erythromycin-susceptible and -resistant pneumococci to RU 64004, a new ketolide, compared with susceptibilities to 16 other agents. Antimicrob Agents Chemother. 1997;41: 1033–1036. doi:10.1128/AAC.41.5.1033
18. Mason DJ, Dietz A, DeBoer C. Lincomycin, a new antibiotic. I. Discovery and biological properties. Antimicrob Agents Chemother. 1962;1962: 554–559.
19. Geddes AM, Sleet RA, Murdoch JM. Lincomycin hydrochloride: clinical and laboratory studies. Br Med J. 1964;2: 670.
20. Schatz A, Bugle E, Waksman SA. Streptomycin, a Substance Exhibiting Antibiotic Activity Against Gram-Positive and Gram-Negative Bacteria.∗†. Proc Soc Exp Biol Med. 1944;55: 66–69. doi:10.3181/00379727-55-14461
21. Demerec M. Origin of bacterial resistance to antibiotics. J Bacteriol. 1948;56: 63–74.
22. Stansly PG, Shepherd RG, White HJ. Polymyxin: a new chemotherapeutic agent. Bull Johns Hopkins Hosp. 1947;81: 43–54.
23. Jawetz E, Coleman VR. Laboratory and clinical observations on aerosporin (Polymyxin B). J Lab Clin Med. 1949;34: 751–760. doi:10.5555/uri:pii:0022214349902231
24. Debono M, Barnhart M, Carrell CB, Hoffmann JA, Occolowitz JL, Abbott BJ, et al. A21978C, a complex of new acidic peptide antibiotics: isolation, chemistry, and mass spectral structure elucidation. J Antibiot (Tokyo). 1987;40: 761–777.
25. Chow AW, Cheng N. In vitro activities of daptomycin (LY146032) and paldimycin (U-70,138F) against anaerobic gram-positive bacteria. Antimicrob Agents Chemother. 1988;32: 788–790. doi:10.1128/AAC.32.5.788
26. McCormick MH, Mcguire JM, Pittenger G, Pittenger RC, Stark WM. Vancomycin, a new antibiotic. I. Chemical and biologic properties. Antibiot Annu. 1955;3: 606–611.
27. Hendlin D, Stapley EO, Jackson M, Wallick H, Miller AK, Wolf FJ, et al. Phosphonomycin, a new antibiotic produced by strains of *Streptomyces*. Science (80-). 1969;166: 122–123.
28. Kadner RJ, Winkler HH. Isolation and Characterization of Mutations Affecting the Transport of Hexose Phosphates in Escherichia coli. J Bacteriol. 1973;113: 895–900. doi:10.1128/jb.113.2.895-900.1973
29. Lesher GY, Froelich EJ, Gruett MD, Bailey JH, Brundage RP. 1, 8-Naphthyridine derivatives. A new class of chemotherapeutic agents. J Med Chem. 1962;5: 1063–1065.
30. Barlow AM. Nalidixic Acid In Infections Of Urinary Tract. Laboratory And Clinical Investigations. Br Med J. 1963;2: 1308–1310. doi:10.1136/bmj.2.5368.1308
31. Fisher W, Machlowitz R, Tytell A. Streptogramin, a new antibiotic. Antibiot Chemother (Northfield, Ill). 1953;3: 1283–1286.
32. Jones WF, Nichols RL, Finland M. Development of Resistance and Cross-Resistance *in vitro* to Erythromycin, Carbomycin, Spiramycin, Oleandomycin and Streptogramin. Proc Soc Exp Biol Med. 1956;93: 388–393. doi:10.3181/00379727-93-22766
33. Domagk G. Ein Beitrag zur Chemotherapie der bakteriellen Infektionen. DMW-Deutsche Medizinische Wochenschrift.

1935;61: 250–253.
34. Maas WK, Davis BD. Production of an Altered Pantothenate-Synthesizing Enzyme by a Temperature-Sensitive Mutant of *Escherichia coli*. Proc Natl Acad Sci U S A. 1952;38: 785–797. doi:10.1073/pnas.38.9.785
35. Kurosawa H. The isolation of an antibiotic produced by a strain of *Streptomyces* K-300. Yokohama Med Bull. 1952;3: 386–399.
36. Barclay WR, Russe H. The *in vitro* Action of Cycloserine on *M. Tuberculosis*. Am Rev Tuberc Pulm Dis. 1955;72: 236–241. doi:10.1164/artpd.1955.72.2.236
37. Uttley AC. Vancomycin-resistant enterococci. Lancet. 1988;2: 57–58.
38. Margalith P, Beretta G. Rifomycin. XI. Taxonomic study on *Streptomyces mediterranei* nov. sp. Mycopathol Mycol Appl. 1960;13: 321–330. doi:10.1007/BF02089930
39. Rebstock MC, Crooks HM, Controulis J, Bartz QR. Chloramphenicol (Chloromycetin).1 IV.1a Chemical Studies. J Am Chem Soc. 1949;71: 2458–2462. doi:10.1021/ja01175a065
40. Colquhoun J, Weetch RS. Resistance to chloramphenicol developing during treatment of typhoid fever. Lancet. 1950; 621–623.
41. Aly R. Bacteriology of atopic dermatitis. Acta Derm Venereol Suppl. 1980;92: 16–18.
42. Casewell MW, Hill RLR. *In vitro* activity of mupirocin ('pseudomonic acid') against clinical isolates of *Staphylococcus aureus*. J Antimicrob Chemother. 1985;15: 523–531. doi:10.1093/jac/15.5.523
43. Duggar BM. Aureomycin: a product of the continuing search for new antibiotics. Ann N Y Acad Sci. 1948;51: 177–181.
44. Demerec M. Patterns of bacterial resistance to penicillin, aureomycin, and streptomycin. J Clin Invest. 1949;28: 891–893.
45. Sum P-E, Petersen P. Synthesis and structure-activity relationship of novel glycylcycline derivatives leading to the discovery of GAR-936. Bioorg Med Chem Lett. 1999;9: 1459–1462. doi:https://doi.org/10.1016/S0960-894X(99)00216-4
46. Henwood CJ, Gatward T, Warner M, James D, Stockdale MW, Spence RP, et al. Antibiotic resistance among clinical isolates of *Acinetobacter* in the UK, and *in vitro* evaluation of tigecycline (GAR-936). J Antimicrob Chemother. 2002;49: 479–487. doi:10.1093/jac/49.3.479
47. Bunch RL, Mcguire JM. Erythromycin, its salts, and method of preparation. Google Patents; 1953.
48. Haight TH, Finland M. Resistance of Bacteria to Erythromycin. Proc Soc Exp Biol Med. 1952;81: 183–188. doi:10.3181/00379727-81-19816
49. Harbarth S, Kahlmeter G, Kluytmans J, Mendelson M, Hospital GS, Town C, et al. Global priority list of antibiotic-resistant bacteria to guide research, discovery, and development of new antibiotics. WHO. 2017.
50. WHO. Critically important antimicrobials for human medicine. 6th rev. Geneva PP - Geneva: World Health Organization; Available: https://apps.who.int/iris/handle/10665/312266
51. WHO. Global antimicrobial resistance surveillance system (GLASS) report: early implementation 2016-2017. 2017.
52. ECDC. Antibiotic Resistance—An Increasing Threat to Human Health. 2021. Available: https://antibiotic.ecdc.europa.eu/en/publications-data/antibiotic-resistance-increasing-threat-human-health
53. Cassini A, Högberg LD, Plachouras D, Quattrocchi A, Hoxha A, Simonsen GS, et al. Attributable deaths and disability-adjusted life-years caused by infections with antibiotic-resistant bacteria in the EU and the European Economic Area in 2015: a population-level modelling analysis. Lancet Infect Dis. 2019;19: 56–66. doi:10.1016/S1473-3099(18)30605-4
54. Raoult D, Leone M, Roussel Y, Rolain J-M. Attributable deaths caused by infections with antibiotic-resistant bacteria in France. Lancet Infect Dis. 2019;19: 128–129. doi:10.1016/S1473-3099(18)30800-4
55. CDC. Antimicrobial Threats Report by the Center of Disease Control and Prevention. 2019. Available: https://www.cdc.gov/drugresistance/biggest-threats.html
56. Burnham JP, Olsen MA, Kollef MH. Re-estimating annual deaths due to multidrug-resistant organism infections. Infect Control Hosp Epidemiol. 2019;40: 112–113.
57. WHO. New report calls for urgent action to avert antimicrobial resistance crisis. 2019. Available: https://www.who.int/news/item/29-04-2019-new-report-calls-for-urgent-action-to-avert-antimicrobial-resistance-crisis
58. O'Neill J. Antimicrobial Resistance : Tackling a crisis for the health and wealth of nations. Review on Antimicrobial Resistance. 2014. pp. 1–16. doi:10.1038/510015a
59. Micael W, A. MC, W. CG, Tor M, J. CK. A Multidrug-Resistant *Staphylococcus epidermidis* Clone (ST2) Is an Ongoing Cause of Hospital-Acquired Infection in a Western Australian Hospital. J Clin Microbiol. 2012;50: 2147–2151. doi:10.1128/JCM.06456-11
60. Wang M, Wei H, Zhao Y, Shang L, Di L, Lyu C, et al. Analysis of multidrug-resistant bacteria in 3223 patients with hospital-acquired infections (HAI) from a tertiary general hospital in China. Bosn J basic Med Sci. 2019;19: 86.
61. Cornejo-Juárez P, Vilar-Compte D, Pérez-Jiménez C, Ñamendys-Silva SA, Sandoval-Hernández S, Volkow-Fernández P. The impact of hospital-acquired infections with multidrug-resistant bacteria in an oncology intensive care unit. Int J Infect Dis. 2015;31: 31–34. doi:https://doi.org/10.1016/j.ijid.2014.12.022
62. Zimlichman E, Henderson D, Tamir O, Franz C, Song P, Yamin CK, et al. Health care–associated infections: a meta-analysis of costs and financial impact on the US health care system. JAMA Intern Med. 2013;173: 2039–2046.
63. European centre for disease prevention and control. European Centre for Disease Prevention and Control: Annual epidemiological report on communicable diseases in Europe 2008. European centre for disease prevention and control. 2008.
64. Claus F, Sachse A, Ried W. Volkswirtschaftliche Kosten von MRSA in Deutschland. Gesundheitswesen. 2014;76: 800–

806. doi:10.1055/s-0034-1381987
65. Gupta SK, Nayak RP. Dry antibiotic pipeline: Regulatory bottlenecks and regulatory reforms. Journal of Pharmacology and Pharmacotherapeutics. 2014. pp. 4–7. doi:10.4103/0976-500X.124405
66. Morel CM, Mossialos E. Stoking the antibiotic pipeline. BMJ. 2010;340: c2115. doi:10.1136/bmj.c2115
67. Nelson R. Antibiotic development pipeline runs dry. Lancet. 2003;362: 1726–1727. doi:10.1016/s0140-6736(03)14885-4
68. Gould IM. Antibiotic resistance: the perfect storm. Int J Antimicrob Agents. 2009;34: S2–S5. doi:https://doi.org/10.1016/S0924-8579(09)70549-7
69. Burki T. Prospective antibacterial pipeline running dry. Lancet Infect Dis. 2009;9: 661.
70. McKellar MR, Fendrick AM. Innovation of novel antibiotics: an economic perspective. Clin Infect Dis. 2014;59: S104–S107.
71. Walsh C. Where will new antibiotics come from? Nat Rev Microbiol. 2003;1: 65–70. doi:10.1038/nrmicro727
72. CDC. One Health Basics.
73. Deutsche Gesellschaft für Infektiologie e.V. Antibiotic Stewardship (ABS).
74. Valneva. VLA84 – Valneva's *Clostridium difficile* vaccine candidate that remains on hold. Available: https://valneva.com/research-development/clostridium-difficile/
75. Pfizer. Safety and Efficacy of SA4Ag Vaccine in Adults Having Elective Open Posterior Spinal Fusion Procedures With Multilevel Instrumentation (STRIVE). 2021. Available: https://clinicaltrials.gov/ct2/show/study/NCT02388165?term=NCT02388165&draw=2&rank=1
76. Westritschnig K, Hochreiter R, Wallner G, Firbas C, Schwameis M, Jilma B. A randomized, placebo-controlled phase I study assessing the safety and immunogenicity of a *Pseudomonas aeruginosa* hybrid outer membrane protein OprF/I vaccine (IC43) in healthy volunteers. Hum Vaccin Immunother. 2013/09/24. 2014;10: 170–183. doi:10.4161/hv.26565
77. Matthews L, Reeve R, Gally DL, Low JC, Woolhouse MEJ, McAteer SP, et al. Predicting the public health benefit of vaccinating cattle against *Escherichia coli* O157. Proc Natl Acad Sci. 2013;110: 16265 LP – 16270. doi:10.1073/pnas.1304978110
78. Moriel DG, Bertoldi I, Spagnuolo A, Marchi S, Rosini R, Nesta B, et al. Identification of protective and broadly conserved vaccine antigens from the genome of extraintestinal pathogenic *Escherichia coli*. Proc Natl Acad Sci. 2010;107: 9072–9077.
79. Palliyil S, Downham C, Broadbent I, Charlton K, Porter AJ. High-sensitivity monoclonal antibodies specific for homoserine lactones protect mice from lethal *Pseudomonas aeruginosa* infections. Appl Environ Microbiol. 2014;80: 462–469.
80. Hua L, Hilliard JJ, Shi Y, Tkaczyk C, Cheng LI, Yu X, et al. Assessment of an anti-alpha-toxin monoclonal antibody for prevention and treatment of *Staphylococcus aureus*-induced pneumonia. Antimicrob Agents Chemother. 2014;58: 1108–1117.
81. Lu Q, Rouby J-J, Laterre P-F, Eggimann P, Dugard A, Giamarellos-Bourboulis EJ, et al. Pharmacokinetics and safety of panobacumab: specific adjunctive immunotherapy in critical patients with nosocomial *Pseudomonas aeruginosa* O11 pneumonia. J Antimicrob Chemother. 2011;66: 1110–1116.
82. Secher T, Fas S, Fauconnier L, Mathieu M, Rutschi O, Ryffel B, et al. The anti-*Pseudomonas aeruginosa* antibody Panobacumab is efficacious on acute pneumonia in neutropenic mice and has additive effects with meropenem. PLoS One. 2013;8: e73396.
83. DiGiandomenico A, Keller AE, Gao C, Rainey GJ, Warrener P, Camara MM, et al. A multifunctional bispecific antibody protects against *Pseudomonas aeruginosa*. Sci Transl Med. 2014;6: 262ra155-262ra155.
84. Morrison C. Antibacterial antibodies gain traction. Nat Rev Drug Discov. 2015;14: 737–739.
85. Hernandez LD, Racine F, Xiao L, DiNunzio E, Hairston N, Sheth PR, et al. Broad coverage of genetically diverse strains of *Clostridium difficile* by actoxumab and bezlotoxumab predicted by *in vitro* neutralization and epitope modeling. Antimicrob Agents Chemother. 2015;59: 1052–1060.
86. Gerding DN, Meyer T, Lee C, Cohen SH, Murthy UK, Poirier A, et al. Administration of spores of nontoxigenic *Clostridium difficile* strain M3 for prevention of recurrent *C difficile* infection: a randomized clinical trial. Jama. 2015;313: 1719–1727.
87. Jun SY, Jung GM, Yoon SJ, Choi Y-J, Koh WS, Moon KS, et al. Preclinical safety evaluation of intravenously administered SAL200 containing the recombinant phage endolysin SAL-1 as a pharmaceutical ingredient. Antimicrob Agents Chemother. 2014;58: 2084–2088.
88. Schuch R, Lee HM, Schneider BC, Sauve KL, Law C, Khan BK, et al. Combination therapy with lysin CF-301 and antibiotic is superior to antibiotic alone for treating methicillin-resistant *Staphylococcus aureus*-induced murine bacteremia. J Infect Dis. 2013/11/28. 2014;209: 1469–1478. doi:10.1093/infdis/jit637
89. Berber A, Del-Rio-Navarro BE, Flenady V, Sienra-Monge JJL. Immunostimulants for preventing respiratory tract infection in children. Cochrane Database Syst Rev. 2004.
90. Raqib R, Sarker P, Bergman P, Ara G, Lindh M, Sack DA, et al. Improved outcome in shigellosis associated with butyrate induction of an endogenous peptide antibiotic. Proc Natl Acad Sci. 2006;103: 9178–9183.
91. Bergman P, Norlin A-C, Hansen S, Rekha RS, Agerberth B, Björkhem-Bergman L, et al. Vitamin D3 supplementation in patients with frequent respiratory tract infections: a randomised and double-blind intervention study. BMJ Open. 2012;2: e001663.
92. Armata Pharmazeuticals. Pipeline Overview. Available: https://www.armatapharma.com/pipeline/pipeline-overview/
93. Phico Therapeutics. Phico Therapeutics Webpage. 2021. Available: https://www.phicotx.co.uk/

94. Jiang Y, Chen Y, Song Z, Tan Z, Cheng J. Recent advances in design of antimicrobial peptides and polypeptides toward clinical translation. Adv Drug Deliv Rev. 2021;170: 261–280. doi:https://doi.org/10.1016/j.addr.2020.12.016
95. Sarker P, Mily A, Mamun A Al, Jalal S, Bergman P, Raqib R, et al. Ciprofloxacin affects host cells by suppressing expression of the endogenous antimicrobial peptides cathelicidins and beta-defensin-3 in colon epithelia. Antibiotics. 2014;3: 353–374.
96. Fjell CD, Hiss JA, Hancock REW, Schneider G. Designing antimicrobial peptides: form follows function. Nat Rev Drug Discov. 2012;11: 37–51.
97. van der Velden WJFM, van Iersel TMP, Blijlevens NMA, Donnelly JP. Safety and tolerability of the antimicrobial peptide human lactoferrin 1-11 (hLF1-11). BMC Med. 2009;7: 1–8.
98. Papareddy P, Kasetty G, Kalle M, Bhongir RK V, Mörgelin M, Schmidtchen A, et al. NLF20: an antimicrobial peptide with therapeutic potential against invasive *Pseudomonas aeruginosa* infection. J Antimicrob Chemother. 2016;71: 170–180.
99. Schreiner M, Bäumler W, Eckl DB, Späth A, König B, Eichner A. Photodynamic inactivation of bacteria to decolonize meticillin-resistant *Staphylococcus aureus* from human skin. Br J Dermatol. 2018;179: 1358–1367. doi:10.1111/bjd.17152
100. Sun Y, Ogawa R, Xiao BH, Feng YX, Wu Y, Chen LH, et al. Antimicrobial photodynamic therapy in skin wound healing: A systematic review of animal studies. Int Wound J. 2020;17: 285–299. doi:10.1111/iwj.13269
101. Lambrechts SAG, Demidova TN, Aalders MCG, Hasan T, Hamblin MR. Photodynamic therapy for *Staphylococcus aureus* infected burn wounds in mice. Photochem Photobiol Sci. 2005;4: 503–509.
102. Kanamori H, Rutala WA, Weber DJ. The role of patient care items as a fomite in healthcare-associated outbreaks and infection prevention. Clin Infect Dis. 2017;65: 1412–1419.
103. Suleyman G, Alangaden G, Bardossy AC. The role of environmental contamination in the transmission of nosocomial pathogens and healthcare-associated infections. Curr Infect Dis Rep. 2018;20: 1–11.
104. Fujikura Y, Hamamoto T, Kanayama A, Kaku K, Yamagishi J, Kawana A. Bayesian reconstruction of a vancomycin-resistant *Enterococcus* transmission route using epidemiologic data and genomic variants from whole genome sequencing. J Hosp Infect. 2019;103: 395–403.
105. Kenters N, Huijskens EGW, de Wit SCJ, van Rosmalen J, Voss A. Effectiveness of cleaning-disinfection wipes and sprays against multidrug-resistant outbreak strains. Am J Infect Control. 2017;45: e69–e73. doi:https://doi.org/10.1016/j.ajic.2017.04.290
106. Rutala WA, Gergen MF, Weber DJ. Efficacy of Different Cleaning and Disinfection Methods against *Clostridium difficile* Spores: Importance of Physical Removal versus Sporicidal Inactivation. Infect Control Hosp Epidemiol. 2015/01/02. 2012;33: 1255–1258. doi:DOI: 10.1086/668434
107. Gonzalez EA, Nandy P, Lucas AD, Hitchins VM. Ability of cleaning-disinfecting wipes to remove bacteria from medical device surfaces. Am J Infect Control. 2015;43: 1331–1335. doi:https://doi.org/10.1016/j.ajic.2015.07.024
108. Sooklal S, Khan A, Kannangara S. Hospital *Clostridium difficile* outbreak linked to laundry machine malfunction. Am J Infect Control. 2014;42: 674–675. doi:https://doi.org/10.1016/j.ajic.2014.02.012
109. Sifuentes LY, Gerba CP, Weart I, Engelbrecht K, Koenig DW. Microbial contamination of hospital reusable cleaning towels. Am J Infect Control. 2013;41: 912–915. doi:https://doi.org/10.1016/j.ajic.2013.01.015
110. Rutala WA, Weber DJ. Best practices for disinfection of noncritical environmental surfaces and equipment in health care facilities: A bundle approach. Am J Infect Control. 2019;47: A96–A105. doi:https://doi.org/10.1016/j.ajic.2019.01.014
111. Havill NL. Best practices in disinfection of noncritical surfaces in the health care setting: creating a bundle for success. Am J Infect Control. 2013;41: S26–S30.
112. Rutala WA, Weber DJ. Selection of the Ideal Disinfectant. Infect Control Hosp Epidemiol. 2016/05/10. 2014;35: 855–865. doi:DOI: 10.1086/676877
113. Molinari JA, Gleason MJ, Cottone JA, Barrett ED. Comparison of dental surface disinfectants. Gen Dent. 1987;35: 171–175.
114. Desinfektionsmittel-Kommission im Verbund für Angewandte Hygiene. Desinfektionsmittel-Liste des VAH. Exner M, Gebel J, editors. Wiesbaden: mhp Verlag GmbH; 2018.
115. Donskey CJ. Does improving surface cleaning and disinfection reduce health care-associated infections? Am J Infect Control. 2013;41: S12–S19.
116. Datta R, Platt R, Yokoe DS, Huang SS. Environmental cleaning intervention and risk of acquiring multidrug-resistant organisms from prior room occupants. Arch Intern Med. 2011;171: 491–494.
117. Hayden MK, Bonten MJM, Blom DW, Lyle EA, van de Vijver DAMC, Weinstein RA. Reduction in Acquisition of Vancomycin-Resistant *Enterococcus* after Enforcement of Routine Environmental Cleaning Measures. Clin Infect Dis. 2006;42: 1552–1560. doi:10.1086/503845
118. Falk PS, Winnike J, Woodmansee C, Desai M, Mayhall CG. Outbreak of Vancomycin-Resistant Enterococci in a Burn Unit. Infect Control Hosp Epidemiol. 2015/01/02. 2000;21: 575–582. doi:DOI: 10.1086/501806
119. Denton M, Wilcox MH, Parnell P, Green D, Keer V, Hawkey PM, et al. Role of environmental cleaning in controlling an outbreak of *Acinetobacter baumannii* on a neurosurgical intensive care unit. J Hosp Infect. 2004;56: 106–110. doi:https://doi.org/10.1016/j.jhin.2003.10.017
120. Rampling A, Wiseman S, Davis L, Hyett AP, Walbridge AN, Payne GC, et al. Evidence that hospital hygiene is important in the control of methicillin-resistant *Staphylococcus aureus*. J Hosp Infect. 2001;49: 109–116. doi:https://doi.org/10.1053/jhin.2001.1013

121. Grabsch EA, Mahony AA, Cameron DRM, Martin RD, Heland M, Davey P, et al. Significant reduction in vancomycin-resistant *Enterococcus* colonization and bacteraemia after introduction of a bleach-based cleaning–disinfection programme. J Hosp Infect. 2012;82: 234–242. doi:https://doi.org/10.1016/j.jhin.2012.08.010
122. Eckstein BC, Adams DA, Eckstein EC, Rao A, Sethi AK, Yadavalli GK, et al. Reduction of *Clostridium difficile* and vancomycin-resistant *Enterococcus* contamination of environmental surfaces after an intervention to improve cleaning methods. BMC Infect Dis. 2007;7: 1–6.
123. Cooper RA, Griffith CJ, Malik RE, Obee P, Looker N. Monitoring the effectiveness of cleaning in four British hospitals. Am J Infect Control. 2007;35: 338–341. doi:https://doi.org/10.1016/j.ajic.2006.07.015
124. Lewis T, Griffith C, Gallo M, Weinbren M. A modified ATP benchmark for evaluating the cleaning of some hospital environmental surfaces. J Hosp Infect. 2008;69: 156–163. doi:https://doi.org/10.1016/j.jhin.2008.03.013
125. Dancer SJ. How do we assess hospital cleaning? A proposal for microbiological standards for surface hygiene in hospitals. J Hosp Infect. 2004;56: 10–15. doi:https://doi.org/10.1016/j.jhin.2003.09.017
126. Dancer SJ. Controlling hospital-acquired infection: focus on the role of the environment and new technologies for decontamination. Clin Microbiol Rev. 2014;27: 665–690.
127. Sierra Garcia JE, Guillen-Grima F, Garcia-Garcia MP, Cascajar L, Rodriguez-Merino FF. Evaluation of an UVC robot for terminal disinfection of hospital rooms. Antimicrob Resist Infect Control. 2021;10: 107.
128. Jan S, A. SH, Sandra D, Holger F, Michael E, P. TJ, et al. Airborne Disinfection by Dry Fogging Efficiently Inactivates Severe Acute Respiratory Syndrome Coronavirus 2 (SARS-CoV-2), Mycobacteria, and Bacterial Spores and Shows Limitations of Commercial Spore Carriers. Appl Environ Microbiol. 2021;87: e02019-20. doi:10.1128/AEM.02019-20
129. Buhl S, Stich A, Bulitta C. Efficiency of a dry-fog based decontamination method for the reduction of bacterial contamination. Antimicrob Resist Infect Control. 2021;10: 106.
130. Brill FHH, Burkhard T, Becker B, Paulmann D, Todt D, Bischoff B, et al. Virucidal efficacy of an ozone-generating system for automated room disinfection. Antimicrob Resist Infect Control. 2021;10: 105.
131. Feng Z, Wei F, Li H, Yu CW. Evaluation of indoor disinfection technologies for airborne disease control in hospital. Indoor Built Environ. 2021;30: 727–731. doi:10.1177/1420326X211002948
132. Matys J, Grzech-Leśniak K, Dominiak M. Disinfectants and devices for surface and air disinfection in dental offices. J Stomatol. 2020;73: 200–205.
133. Privett BJ, Youn J, Hong SA, Lee J, Han J, Shin JH, et al. Antibacterial fluorinated silica colloid superhydrophobic surfaces. Langmuir. 2011;27: 9597–9601.
134. Warnes SL, Caves V, Keevil CW. Mechanism of copper surface toxicity in *Escherichia coli* O157: H7 and *Salmonella* involves immediate membrane depolarization followed by slower rate of DNA destruction which differs from that observed for Gram-positive bacteria. Environ Microbiol. 2012;14: 1730–1743.
135. Bieser AM, Tiller JC. Mechanistic considerations on contact-active antimicrobial surfaces with controlled functional group densities. Macromol Biosci. 2011;11: 526–534.
136. Varghese S, Elfakhri S, Sheel DW, Sheel P, Bolton FJ, Foster HA. Novel antibacterial silver-silica surface coatings prepared by chemical vapour deposition for infection control. J Appl Microbiol. 2013;115: 1107–1116.
137. Scuri S, Petrelli F, Grappasonni I, Idemudia L, Marchetti F, Di Nicola C. Evaluation of the antimicrobial activity of novel composite plastics containing two silver (I) additives, acyl pyrazolonate and acyl pyrazolone. Acta Bio Medica Atenei Parm. 2019;90: 370.
138. Thukkaram M, Vaidulych M, Kylián O, Rigole P, Aliakbarshirazi S, Asadian M, et al. Biological activity and antimicrobial property of Cu/aC: H nanocomposites and nanolayered coatings on titanium substrates. Mater Sci Eng C. 2021;119: 111513.
139. Martinaga Pintarić L, Somogi Škoc M, Ljoljić Bilić V, Pokrovac I, Kosalec I, Rezić I. Synthesis, modification and characterization of antimicrobial textile surface containing ZnO nanoparticles. Polymers (Basel). 2020;12: 1210.
140. Druvari D, Koromilas ND, Lainioti GC, Bokias G, Vasilopoulos G, Vantarakis A, et al. Polymeric quaternary ammonium-containing coatings with potential dual contact-based and release-based antimicrobial activity. ACS Appl Mater Interfaces. 2016;8: 35593–35605.
141. Zhang R, Li Y, He Y, Qin D. Preparation of iodopropynyl butycarbamate loaded halloysite and its anti-mildew activity. J Mater Res Technol. 2020;9: 10148–10156.
142. Peng K, Dai X, Mao H, Zou H, Yang Z, Tu W, et al. Development of direct contact-killing non-leaching antimicrobial polyurethanes through click chemistry. J Coatings Technol Res. 2018;15: 1239–1250.
143. Nakano R, Hara M, Ishiguro H, Yao Y, Ochiai T, Nakata K, et al. Broad spectrum microbicidal activity of photocatalysis by TiO2. Catalysts. 2013;3: 310–323.
144. Fisher L, Ostovapour S, Kelly P, Whitehead KA, Cooke K, Storgårds E, et al. Molybdenum doped titanium dioxide photocatalytic coatings for use as hygienic surfaces: the effect of soiling on antimicrobial activity. Biofouling. 2014;30: 911–919.
145. Li R, Jin TZ, Liu Z, Liu L. Antimicrobial double-layer coating prepared from pure or doped-titanium dioxide and binders. Coatings. 2018;8: 41.
146. Bäumler W, Eckl D, Holzmann T, Schneider-Brachert W. Antimicrobial coatings for environmental surfaces in hospitals: a potential new pillar for prevention strategies in hygiene. Crit Rev Microbiol. 2021; 1–35. doi:10.1080/1040841X.2021.1991271
147. Eichner A, Holzmann T, Eckl DB, Zeman F, Koller M, Huber M, et al. Novel photodynamic coating reduces the

bioburden on near-patient surfaces thereby reducing the risk for onward pathogen transmission: a field study in two hospitals. J Hosp Infect. 2020;104: 85–91. doi:10.1016/j.jhin.2019.07.016
148. Kalb L, Bäßler P, Schneider-Brachert W, Eckl DB. Antimicrobial Photodynamic Coatings Reduce the Microbial Burden on Environmental Surfaces in Public Transportation - A Field Study in Buses. International Journal of Environmental Research and Public Health. 2022. doi:10.3390/ijerph19042325
149. Moan J, Peng Q. An outline of the history of PDT. In: Patrice T, editor. Photodynamic Therapy. The Royal Society of Chemistry; 2003. pp. 1–18. doi:10.1039/9781847551658-00001
150. University Leipzig. Papyrus Ebers. Available: https://papyrusebers.de
151. Daniell MD, Hill JS. A history of photodynamic therapy. Aust N Z J Surg. 1991;61: 340–348.
152. Abdel-kader MH. The journey of PDT throughout history: PDT from Pharos to present. 2016.
153. Raab O. Über die Wirkung fluorescierender Stoffe auf Infusorien. Z Biol. 1900;39: 524–546.
154. Tappeiner H von, Jodlbauer A. Über die Wirkung der photodynamischen (fluorescierenden) Stoffe auf Protozoen und Enzyme. Arch Klin Med. 1904;80: 427–487.
155. Tappeiner H von. Die photodynamische Erscheinung (Sensibilisierung durch fluoreszierende Stoffe). Ergeb Physiol. 1909;8: 698–741.
156. Tappeiner H von. Über die Wirkung fluorescierender Stoffe auf Infusorien nach Versuchen von Raab. Münch Med Wochenschr. 1900;1: 5–7.
157. Jodlbauer A, Von Tappeiner H. Über die Wirkung photodynamischer (fluoreszierender) Stoffe auf Bakterien. Munch Med Wochenschr. 1904;51: 1096–1097.
158. Jesionek A, Von Tappeiner H. Zur Behandlung der Hautcarcinome mit fluorescierenden Stoffen. Dtsch Arch Klin Med. 1905;85: 223–239.
159. Heidi A, Hamblin MR. New photosensitizers for photodynamic therapy. Biochem J. 2016;473: 347–364. doi:10.1042/BJ20150942
160. Browning CH, Cohen JB, Ellingworth S, Gulbransen R. The antiseptic action of compounds of the apocyanine, carbocyanine and isocyanine series. Proc R Soc London Ser B, Contain Pap a Biol Character. 1924;96: 317–333.
161. Schultz EW. Inactivation of *Staphyloccus* Bacteriophage by Methylene Blue. Proc Soc Exp Biol Med. 1928;26: 100–101.
162. Figge FHJ, Weiland GS, Manganiello LOJ. Cancer Detection and Therapy. Affinity of Neoplastic, Embryonic, and Traumatized Tissues for Porphyrins and Metalloporphyrins. Proc Soc Exp Biol Med. 1948;68: 640–641. doi:10.3181/00379727-68-16580
163. Rassmussen-Taxdal DS, Ward GE, Figge FHJ. Fluorescence of human lymphatic and cancer tissues following high doses of intravenous hematoporphyrin. Cancer. 1955;8: 78–81.
164. Lipson RL, Baldes EJ, Gray MJ. Hematoporphyrin derivative for detection and management of cancer. Cancer. 1967;20: 2255–2257.
165. Lipson RL, Baldes EJ, Olsen AM. The use of a derivative of hematoporphyrin in tumor detection. J Natl Cancer Inst. 1961;26: 1–11.
166. Diamond I, Mcdonagh A, Wilson C, Granelli S, Nielsen S, Jaenicke R. Photodynamic Therapy of Malignant Tumours. Lancet. 1972;300: 1175–1177. doi:https://doi.org/10.1016/S0140-6736(72)92596-2
167. Bockstahler LE, Coohill TP, Hellman KB, Lytle CD, Roberts JE. Photodynamic therapy for herpes simplex: a critical review. Pharmacol Ther. 1979;4: 473–499.
168. Felber TD, Smith EB, Knox JM, Wallis C, Melnick JL. Photodynamic inactivation of herpes simplex: report of a clinical trial. JAMA. 1973;223: 289–292.
169. Dougherty TJ, Grindey GB, Fiel R, Weishaupt KR, Boyle DG. Photoradiation therapy. II. Cure of animal tumors with hematoporphyrin and light. J Natl Cancer Inst. 1975;55: 115–121.
170. Dougherty TJ, Kaufmann JE, Goldfarb A, Weishaupt KR, Boyle D, Mittleman A. Photoradiation therapy for the treatment of malignant tumors. Cancer Res. 1978;38: 2628–2635.
171. Dougherty TJ, Lawrence G, Kaufman JH, Boyle D, Weishaupt KR, Goldfarb A. Photoradiation in the treatment of recurrent breast carcinoma. J Natl Cancer Inst. 1979;62: 231–237.
172. Dougherty TJ. Photoradiation therapy. Abstracts of the American Chemical Society Meeting Chicago. 1973.
173. Maisch T. Strategies to optimize photosensitizers for photodynamic inactivation of bacteria. J Photochem Photobiol B Biol. 2015;150: 2–10. doi:10.1016/j.jphotobiol.2015.05.010
174. Bertoloni G, Dall'Acqua M, Vazzoler M, Salvato B, Jori G. Bacterial and Yeast Cells as Models for Studying Hematoporphyrin Photosensitization. In: Andreoni A, Cubeddu R, editors. Porphyrins in Tumor Phototherapy. Boston, MA: Springer; 1984. pp. 177–183.
175. Malik Z, Gozhansky S, Nitzan Y. Effects of photoactivated haematoporphyrin derivative on bacteria and antibiotic resistance. 1982.
176. Nitzan Y, Gozhansky S, Malik Z. Effect of photoactivated hematoporphyrin derivative on the viability of *Staphylococcus aureus*. Curr Microbiol. 1983;8: 279–284.
177. Nitzan Y, Shainberg B, Malik Z. Photodynamic effects of deuteroporphyrin on Gram-positive bacteria. Curr Microbiol. 1987;15: 251–258.
178. Nitzan Y, Shainberg B, Malik Z. The mechanism of photodynamic inactivation of *Staphylococcus aureus* by deuteroporphyrin. Curr Microbiol. 1989;19: 265–269.
179. Ehrenberg B, Malik Z, Nitzan Y. Fluorescence spectral changes of hematoporphyrin derivative upon binding to lipid vesicles, *Staphylococcus aureus* and *Escherichia coli* cells. Photochem Photobiol. 1985;41: 429–435.

180. Vaara M, Vaara T. Sensitization of Gram-negative bacteria to antibiotics and complement by a nontoxic oligopeptide. Nature. 1983;303: 526–528.
181. Lam C, Hildebrandt J, Schütze E, Wenzel AF. Membrane-disorganizing property of polymyxin B nonapeptide. J Antimicrob Chemother. 1986;18: 9–15.
182. Nitzan Y. Photodynamic Inactivation. Photodyn Ther Basic Princ Clin Appl. 1992;10: 97.
183. Schmidt-Erfurth U, Miller J, Sickenberg M, Bunse A, Laqua H, Gragoudas E, et al. Photodynamic therapy of subfoveal choroidal neovascularization: clinical and angiographic examples. Graefe's Arch Clin Exp Ophthalmol. 1998;236: 365–374.
184. Agarwal ML, Clay ME, Harvey EJ, Evans HH, Antunez AR, Oleinick NL. Photodynamic therapy induces rapid cell death by apoptosis in L5178Y mouse lymphoma cells. Cancer Res. 1991;51: 5993–5996.
185. Kim H-RC, Luo Y, Li G, Kessel D. Enhanced apoptotic response to photodynamic therapy after bcl-2 transfection. Cancer Res. 1999;59: 3429–3432.
186. Xue L, Chiu S, Oleinick NL. Photochemical destruction of the Bcl-2 oncoprotein during photodynamic therapy with the phthalocyanine photosensitizer Pc 4. Oncogene. 2001;20: 3420–3427.
187. Kessel D, Vicente MGH, Reiners Jr JJ. Initiation of apoptosis and autophagy by photodynamic therapy. Lasers Surg Med Off J Am Soc Laser Med Surg. 2006;38: 482–488.
188. Buytaert E, Callewaert G, Vandenheede JR, Agostinis P. Deficiency in apoptotic effectors Bax and Bak reveals an autophagic cell death pathway initiated by photodamage to the endoplasmic reticulum. Autophagy. 2006;2: 238–240.
189. Kessel D, Oleinick NL. Cell death pathways associated with photodynamic therapy: an update. Photochem Photobiol. 2018;94: 213–218.
190. Malik Z, Lugaci H. Destruction of erythroleukaemic cells by photoactivation of endogenous porphyrins. Br J Cancer. 1987;56: 589–595.
191. Kennedy JC, Pottier RH, Pross DC. Photodynamic therapy with endogenous protoporphyrin. IX: Basic principles and present clinical experience. J Photochem Photobiol B Biol. 1990;6: 143–148. doi:10.1016/1011-1344(90)85083-9
192. EW J, JL M, GD W, al et. Photodynamic therapy of actinic keratosis with topical 5-aminolevulinic acid: A pilot dose-ranging study. Arch Dermatol. 1997;133: 727–732. Available: http://dx.doi.org/10.1001/archderm.1997.03890420065007
193. Lui H, Salasche S, Kollias N, Flotte T, McLean D, Anderson R. Photodynamic therapy of nonmelanoma skin cancer with topical aminolevulinic acid: A clinical and histologic study. Arch Dermatol. 1995;131: 737–738. Available: http://dx.doi.org/10.1001/archderm.1995.01690180117027
194. Reynolds T. Using lasers and light-activated drugs, researchers home in on early lung cancers. Oxford University Press; 1998.
195. Lustigman S, Ben-Hur E. Photosensitized inactivation of *Plasmodium falciparum* in human red cells by phthalocyanines. Transfusion. 1996;36: 543–546.
196. Gottlieb P, Shen L, Chimezie E, Bahng S, Kenney ME, Horowitz B, et al. Inactivation of *Trypanosoma cruzi* trypomastigote forms in blood components by photodynamic treatment with phthalocyanines. Photochem Photobiol. 1995;62: 869–874.
197. Gottlieb P, Margolis-Nunno H, Robinson R, Shen L, Chimezie E, Horowitz B, et al. Inactivation of *Trypanosoma cruzi* trypomastigote forms in blood components with a psoralen and ultraviolet A light. Photochem Photobiol. 1996;63: 562–565.
198. Merchat M, Bertolini G, Giacomini P, Villaneuva A, Jori G. Meso-substituted cationic porphyrins as efficient photosensitizers of gram-positive and gram-negative bacteria. J Photochem Photobiol B Biol. 1996;32: 153–157. doi:https://doi.org/10.1016/1011-1344(95)07147-4
199. Minnock A, Vernon DI, Schofield J, Griffiths J, Parish JH, Brown SB. Photoinactivation of bacteria. Use of a cationic water-soluble zinc phthalocyanine to photoinactivate both gram-negative and gram-positive bacteria. J Photochem Photobiol B Biol. 1996;32: 159–164.
200. Franck J, Dymond EG. Elementary processes of photochemical reactions. Trans Faraday Soc. 1926;21: 536–542. doi:10.1039/TF9262100536
201. Condon E. A Theory of Intensity Distribution in Band Systems. Phys Rev. 1926;28: 1182–1201. doi:10.1103/PhysRev.28.1182
202. Kasha M. Characterization of electronic transitions in complex molecules. Discuss Faraday Soc. 1950;9: 14–19. doi:10.1039/DF9500900014
203. Bensasson R V, Land EJ, Truscott TG. Excited states and free radicals in biology and medicine: contributions from flash photolysis and pulse radiolysis. Oxford University Press Oxford; 1993.
204. Oida T, Sako Y, Kusumi A. Fluorescence lifetime imaging microscopy (flimscopy). Methodology development and application to studies of endosome fusion in single cells. Biophys J. 1993;64: 676–685.
205. Kasha M. Phosphorescence and the Role of the Triplet State in the Electronic Excitation of Complex Molecules. Chem Rev. 1947;41: 401–419. doi:10.1021/cr60129a015
206. Koziar JC, Cowan DO. Photochemical heavy-atom effects. Acc Chem Res. 1978;11: 334–341.
207. Ji H-F, Shen L. Triplet excited state characters and photosensitization mechanisms of α-terthienyl: A theoretical study. J Photochem Photobiol B Biol. 2009;94: 51–53.
208. Plaetzer K, Krammer B, Berlanda J, Berr F, Kiesslich T. Photophysics and photochemistry of photodynamic therapy: fundamental aspects. Lasers Med Sci. 2009;24: 259–268.
209. Webster A, Britton D, Apap-Bologna A, Kemp G. A dye-photosensitized reaction that generates stable protein-protein

crosslinks. Anal Biochem. 1989;179: 154–157.
210. Vollers SS, Teplow DB, Bitan G. Determination of Peptide oligomerization state using rapid photochemical crosslinking. Amyloid Proteins. Springer; 2005. pp. 11–18.
211. Ifkovits JL, Burdick JA. Photopolymerizable and degradable biomaterials for tissue engineering applications. Tissue Eng. 2007;13: 2369–2385.
212. Aveline BM. Primary processes in photosensitization mechanisms. Comprehensive Series in Photosciences. Elsevier; 2001. pp. 17–37.
213. Foote CS. Definition of Type I and Type II Photosensitized Oxidation. Photochemistry and Photobiology. 199154: 659–659. doi:10.1111/j.1751-1097.1991.tb02071.x
214. Braslavsky SE. Glossary of terms used in photochemistry, 3rd edition (IUPAC Recommendations 2006). Pure Appl Chem. 2007;79: 293–465. doi:doi:10.1351/pac200779030293
215. Kuimova MK, Yahioglu G, Ogilby PR. Singlet oxygen in a cell: spatially dependent lifetimes and quenching rate constants. J Am Chem Soc. 2009;131: 332–340.
216. Jensen RL, Arnbjerg J, Ogilby PR. Reaction of singlet oxygen with tryptophan in proteins: a pronounced effect of the local environment on the reaction rate. J Am Chem Soc. 2012;134: 9820–9826.
217. Baier J, Maisch T, Maier M, Landthaler M, Bäumler W. Direct detection of singlet oxygen generated by UVA irradiation in human cells and skin. J Invest Dermatol. 2007;127: 1498–1506.
218. Jarvi MT, Niedre MJ, Patterson MS, Wilson BC. Singlet oxygen luminescence dosimetry (SOLD) for photodynamic therapy: current status, challenges and future prospects. Photochem Photobiol. 2006;82: 1198–1210.
219. Maisch T, Baier J, Franz B, Maier M, Landthaler M, Szeimies RM, et al. The role of singlet oxygen and oxygen concentration in photodynamic inactivation of bacteria. Proc Natl Acad Sci U S A. 2007;104: 7223–7228. doi:10.1073/pnas.0611328104
220. Nonell S, Gonzalez M, Trull FR. 1H-Phenalen-1-One-2-Sulfonic Acid-An extremely efficient singlet molecular-oxygen sensitizer for aqueous-media. Afinidad. 1993;50: 445–450.
221. Hackbarth S, Schlothauer J, Preuß A, Röder B. New insights to primary photodynamic effects–Singlet oxygen kinetics in living cells. J Photochem Photobiol B Biol. 2010;98: 173–179.
222. Howard JA, Mendenhall GD. Autoxidation and Photooxidation of 1,3-Diphenylisobenzofuran: A Kinetic and Product Study. Can J Chem. 1975;53: 2199–2201. doi:10.1139/v75-307
223. Gollmer A, Arnbjerg J, Blaikie FH, Pedersen BW, Breitenbach T, Daasbjerg K, et al. Singlet Oxygen Sensor Green®: photochemical behavior in solution and in a mammalian cell. Photochem Photobiol. 2011;87: 671–679.
224. Hamblin MR, Abrahamse H. Oxygen-Independent Antimicrobial Photoinactivation: Type III Photochemical Mechanism? Antibiotics . 2020. doi:10.3390/antibiotics9020053
225. Maisch T. Strategies to optimize photosensitizers for photodynamic inactivation of bacteria. J Photochem Photobiol B Biol. 2015;150: 2–10. doi:10.1016/j.jphotobiol.2015.05.010
226. Castano AP, Demidova TN, Hamblin MR. Mechanisms in photodynamic therapy: Part one - Photosensitizers, photochemistry and cellular localization. Photodiagnosis and Photodynamic Therapy. 2004. pp. 279–293. doi:10.1016/S1572-1000(05)00007-4
227. Moan J. On the diffusion length of singlet oxygen in cells and tissues. J Photochem Photobiol B. 1990;6: 343–347. doi:10.1016/1011-1344(90)85104-5
228. Nitzan Y, Dror R, Ladan H, Malik Z, Kimel S, Gottfried V. Structure-Activity Relationship of Porphines for Photoinactivation of Bacteria. Photochem Photobiol. 1995;62: 342–347. doi:10.1111/j.1751-1097.1995.tb05279.x
229. Alves E, Costa L, Carvalho CMB, Tomé JPC, Faustino MA, Neves MGPMS, et al. Charge effect on the photoinactivation of Gram-negative and Gram-positive bacteria by cationic meso-substituted porphyrins. BMC Microbiol. 2009;9: 70. doi:10.1186/1471-2180-9-70
230. Cieplik F, Späth A, Regensburger J, Gollmer A, Tabenski L, Hiller KA, et al. Photodynamic biofilm inactivation by SAPYR - An exclusive singlet oxygen photosensitizer. Free Radic Biol Med. 2013;65: 477–487. doi:10.1016/j.freeradbiomed.2013.07.031
231. Kiesslich T, Gollmer A, Maisch T, Berneburg M, Plaetzer K. A comprehensive tutorial on *in vitro* characterization of new photosensitizers for photodynamic antitumor therapy and photodynamic inactivation of microorganisms. Biomed Res Int. 2013;2013.
232. Redmond RW, Gamlin JN. A Compilation of Singlet Oxygen Yields from Biologically Relevant Molecules. Photochem Photobiol. 1999;70: 391–475. doi:https://doi.org/10.1111/j.1751-1097.1999.tb08240.x
233. Wainwright M. Methylene blue derivatives—suitable photoantimicrobials for blood product disinfection? Int J Antimicrob Agents. 2000;16: 381–394.
234. Wainwright M, Phoenix DA, Laycock SL, Wareing DRA, Wright PA. Photobactericidal activity of phenothiazinium dyes against methicillin-resistant strains of *Staphylococcus aureus*. FEMS Microbiol Lett. 1998;160: 177–181.
235. Wainwright M, Phoenix DA, Marland J, Wareing DRA, Bolton FJ. A study of photobactericidal activity in the phenothiazinium series. FEMS Immunol Med Microbiol. 1997;19: 75–80.
236. Felgenträger A, Maisch T, Dobler D, Späth A. Hydrogen bond acceptors and additional cationic charges in methylene blue derivatives: photophysics and antimicrobial efficiency. Biomed Res Int. 2013;2013.
237. Gunther WHH, Searle R, Sieber F. Structure-activity relationships in the antiviral and antileukemic photoproperties of merocyanine dyes. Seminars in hematology. 1992. pp. 88–94.
238. Krieg M, Bilitz JM, Srichai MB, Redmond RW. Effects of structural modifications on the photosensitizing properties of

dialkylcarbocyanine dyes in homogeneous and heterogeneous solutions. Biochim Biophys Acta (BBA)-General Subj. 1994;1199: 149–156.

239. Redmond RW, Srichai MB, Bilitz JM, Schlomer DD, Krieg M. Merocyanine dyes: effect of structural modifications on photophysical properties and biological activity. Photochem Photobiol. 1994;60: 348–355.
240. Anderson GS, Günther WHH, Searle R, Bilitz JM, Krieg M, Sieber F. Inactivation of photosensitizing merocyanine dyes by plasma, serum and serum components. Photochem Photobiol. 1996;64: 683–687.
241. Kadish KM, Maiya BG, Araullo-McAdams C. Spectroscopic characterization of meso-tetrakis (1-methylpyridinium-4-yl) porphyrins,[(TMpyP) H2] 4+ and [(TMpyP) M] 4+, in aqueous micellar media, where M= VO2+, Cu (II), and Zn (II). J Phys Chem. 1991;95: 427–431.
242. Kadish KM, Araullo C, Maiya GB, Sazou D, Barbe JM, Guilard R. Electrochemical and spectral characterization of copper, zinc, and vanadyl meso-tetrakis (1-methylpyridinium-4-yl) porphyrin complexes in dimethylformamide. Inorg Chem. 1989;28: 2528–2533.
243. Soret J-L. Analyse spectrale: Sur le spectre d'absorption du sang dans la partie violette et ultra-violette. Compt Rend. 1883;97: 1269–1270.
244. Dayer MR, Moosavi-Movahedi AA, Dayer MS. Band assignment in hemoglobin porphyrin ring spectrum: Using four-orbital model of Gouterman. Protein Pept Lett. 2010;17: 473–479.
245. Nitzan Y, Malik Z, Ehrenberg B. Photosensitization of microbial cells. Photobiology. Springer; 1991. pp. 815–820.
246. Reddi E, Ceccon M, Valduga G, Jori G, Bommer JC, Elisei F, et al. Photophysical Properties and Antibacterial Activity of Meso-substituted Cationic Porphyrins. Photochem Photobiol. 2002;75: 462–470.
247. Cowsert LM. Treatment of papillomavirus infections: recent practice and future approaches. Intervirology. 1994;37: 226–230.
248. Grandadam M, Ingrand D, Huraux J-M, Aveline B, Delgado O, Vever-Bizet C, et al. Photodynamic inactivation of cell-free HIV strains by a red-absorbing chlorin-type photosensitizer. J Photochem Photobiol B Biol. 1995;31: 171–177.
249. North J, Neyndorff H, Levy JG. New trends in photobiology: Photosensitizers as virucidal agents. J Photochem Photobiol B Biol. 1993;17: 99–108.
250. Wilkinson F, Helman WP, Ross AB. Quantum Yields for the Photosensitized Formation of the Lowest Electronically Excited Singlet State of Molecular Oxygen in Solution. J Phys Chem Ref Data. 1993;22: 113–262. doi:10.1063/1.555934
251. Maisch T, Bosl C, Szeimies R-M, Lehn N, Abels C. Photodynamic effects of novel XF porphyrin derivatives on prokaryotic and eukaryotic cells. Antimicrob Agents Chemother. 2005;49: 1542–1552.
252. Park J-H, Ahn M-Y, Kim Y-C, Kim S-A, Moon Y-H, Ahn S-G, et al. *In Vitro* and *in Vivo* Antimicrobial Effect of Photodynamic Therapy Using a Highly Pure Chlorin e_6 against *Staphylococcus aureus* Xen29. Biol Pharm Bull. 2012;35: 509–514. doi:10.1248/bpb.35.509
253. Berthiaume F, Reiken SR, Toner M, Tompkins RG, Yarmush ML. Antibody-targeted photolysis of bacteria *in vivo*. Bio/technology. 1994;12: 703–706.
254. Hamblin MR, O'Donnell DA, Murthy N, Contag CH, Hasan T. Rapid Control of Wound Infections by Targeted Photodynamic Therapy Monitored by *In Vivo* Bioluminescence Imaging. Photochem Photobiol. 2002;75: 51. doi:10.1562/0031-8655(2002)075<0051:rcowib>2.0.co;2
255. Griffiths J, Schofield J, Wainwright M, Brown SB. Some observations on the synthesis of polysubstituted zinc phthalocyanine sensitisers for photodynamic therapy. Dye Pigment. 1997;33: 65–78.
256. Rywkin S, Ben-Hur E, Malik Z, Prince AM, Li Y, Kenney ME, et al. New phthalocyanines for photodynamic virus inactivation in red blood cell concentrates. Photochem Photobiol. 1994;60: 165–170.
257. Smetana Z, Mendelson E, Manor J, Van Lier JE, Ben-Hur E, Salzberg S, et al. Photodynamic inactivation of herpes viruses with phthalocyanine derivatives. J Photochem Photobiol B Biol. 1994;22: 37–43.
258. Ben-Hur E, Moor ACE, Margolis-Nunno H, Gottlieb P, Zuk MM, Lustigman S, et al. The photodecontamination of cellular blood components: mechanisms and use of photosensitization in transfusion medicine. Transfus Med Rev. 1996;10: 15–22.
259. Ben-Hur E, Rywkin S, Rosenthal I, Geacintov NE, Horowitz B. Virus inactivation in red cell concentrates by photosensitization with phthalocyanines: protection of red cells but not of vesicular stomatitis virus with a water-soluble analogue of vitamin E. Transfusion. 1995;35: 401–406.
260. Margolis-Nunno H, Ben-Hur E, Gottlieb P, Robinson R, Oetjen J, Horowitz B. Inactivation by phthalocyanine photosensitization of multiple forms of human immunodeficiency virus in red cell concentrates. Transfusion. 1996;36: 743–750.
261. Wilson M, Burns T, Pratten J. Killing of *Streptococcus sanguis* in biofilms using a light-activated antimicrobial agent. J Antimicrob Chemother. 1996;37: 377–381.
262. Wilson M, Pratten J. Lethal photosensitisation of *Staphylococcus aureus in vitro*: Effect of growth phase, serum, and pre-irradiation time. Lasers Surg Med. 1995;16: 272–276.
263. Aslam BB, PhindaáSongca S. Photobactericidal materials based on porphyrins and phthalocyanines. J Mater Chem. 1993;3: 323–324.
264. Bertoloni G, Rossi F, Valduga G, Jori G, Ali H, Van Lier JE. Photosensitizing activity of water-and lipid-soluble phthalocyanines on prokaryotic and eukaryotic microbial cells. Microbios. 1992;71: 33–46.
265. Vecchio D, Dai T, Huang L, Fantetti L, Roncucci G, Hamblin MR. Antimicrobial photodynamic therapy with RLP068 kills methicillin-resistant *Staphylococcus aureus* and improves wound healing in a mouse model of infected skin abrasion PDT with RLP068/Cl in infected mouse skin abrasion. J Biophotonics. 2013;6: 733–742.

266. Boyd DB, Slanina Z. Introduction and foreword to the special issue commemorating the thirtieth anniversary of Eiji Osawa's C60 paper. J Mol Graph Model. 2001;19: 181–184. doi:https://doi.org/10.1016/S1093-3263(00)00106-6
267. Tegos GP, Demidova TN, Arcila-Lopez D, Lee H, Wharton T, Gali H, et al. Cationic fullerenes are effective and selective antimicrobial photosensitizers. Chem Biol. 2005;12: 1127–1135.
268. Huang L, Terakawa M, Zhiyentayev T, Huang Y-Y, Sawayama Y, Jahnke A, et al. Innovative cationic fullerenes as broad-spectrum light-activated antimicrobials. Nanomedicine Nanotechnology, Biol Med. 2010;6: 442–452. doi:https://doi.org/10.1016/j.nano.2009.10.005
269. Yin R, Wang M, Huang Y-Y, Huang H-C, Avci P, Chiang LY, et al. Photodynamic therapy with decacationic [60] fullerene monoadducts: effect of a light absorbing electron-donor antenna and micellar formulation. Nanomedicine Nanotechnology, Biol Med. 2014;10: 795–808.
270. Huang L, Wang M, Sharma S, Sperandio F, Maragani S, Nayka S, et al. Decacationic [70] fullerene approach for efficient photokilling of infectious bacteria and cancer cells. ECS Trans. 2013;45: 65.
271. Yin R, Wang M, Huang Y-Y, Landi G, Vecchio D, Chiang LY, et al. Antimicrobial photodynamic inactivation with decacationic functionalized fullerenes: Oxygen-independent photokilling in presence of azide and new mechanistic insights. Free Radic Biol Med. 2015;79: 14–27.
272. Oliveros E, Suardi-Murasecco P, Aminian-Saghafi T, Braun AM, Hansen H. 1H-Phenalen-1-one: photophysical properties and singlet-oxygen production. Helv Chim Acta. 1991;74: 79–90.
273. Busscher HJ, White DJ, Atema-Smit J, Geertsema-Doornbusch G, De Vries J, Van Der Mei HC. Surfactive and antibacterial activity of cetylpyridinium chloride formulations *in vitro* and *in vivo*. J Clin Periodontol. 2008;35: 547–554.
274. Bäumler W, Maisch T, Späth A. 10H-benzo[g]pteridine-2,4-dione derivatives, method for the production thereof, and use thereof. WO2012/175729 A1, 2012.
275. Gadda G. Flavins. In: Roberts CKG, editor. Encyclopedia of Biophysics. Berlin: Springer; 2013. pp. 771–771.
276. Massey V. The chemical and biological versatility of riboflavin. Biochemical Society Transactions. 2000. pp. 283–296. doi:10.1042/bst0280283
277. Mansoorabadi SO, Thibodeaux CJ, Liu HW. The diverse roles of flavin coenzymes - Nature's most versatile thespians. Journal of Organic Chemistry. 2007. pp. 6329–6342. doi:10.1021/jo0703092
278. Ohnishi T. Iron-sulfur clusters/semiquinones in Complex I. Biochim Biophys Acta - Bioenerg. 1998;1364: 186–206. doi:10.1016/S0005-2728(98)00027-9
279. Engebrecht J, Nealson K, Silverman M. Bacterial bioluminescence: Isolation and genetic analysis of functions from *Vibrio fischeri*. Cell. 1983;32: 773–781. doi:10.1016/0092-8674(83)90063-6
280. Maisch T, Eichner A, Späth A, Gollmer A, König B, Regensburger J, et al. Fast and effective photodynamic inactivation of multiresistant bacteria by cationic riboflavin derivatives. PLoS One. 2014;9: e111792. doi:10.1371/journal.pone.0111792
281. Eichner A, Gollmer A, Späth A, Bäumler W, Regensburger J, König B, et al. Fast and effective inactivation of *Bacillus atrophaeus* endospores using light-activated derivatives of vitamin B2. Photochem Photobiol Sci. 2015;14: 387–396. doi:10.1039/C4PP00285G
282. Galston AW. Riboflavin-sensitized photooxidation of indoleacetic acid and related compounds. Proc Natl Acad Sci U S A. 1949;35: 10–17. doi:10.1073/pnas.35.1.10
283. Eichler M, Lavi R, Shainberg A, Lubart R. Flavins are source of visible-light-induced free radical formation in cells. Lasers Surg Med. 2005;37: 314–319. doi:10.1002/lsm.20239
284. Posthuma J, Berends W. Triplet-triplet transfer as a mechanism of a photodynamic reaction. BBA - Biochim Biophys Acta. 1960;41: 538–541. doi:10.1016/0006-3002(60)90058-5
285. Chacon JN, McLearie J, Sinclair RS. Singlet oxygen yields and radical contributions in the dye-sensitised photo-oxidation in methanol of esters of polyunsaturated fatty acids (oleic, linoleic, linolenic and arachnidonic). Photochem Photobiol. 1988;47: 647–656. doi:10.1111/j.1751-1097.1988.tb02760.x
286. Bäumler W, Regensburger J, Knak A, Felgenträger A, Maisch T. UVA and endogenous photosensitizers - The detection of singlet oxygen by its luminescence. Photochemical and Photobiological Sciences. 2012. pp. 107–117. doi:10.1039/c1pp05142c
287. Regensburger J, Knak A, Maisch T, Landthaler M, Bäumler W. Fatty acids and vitamins generate singlet oxygen under UVB irradiation. Exp Dermatol. 2012;21: 135–139. doi:10.1111/j.1600-0625.2011.01414.x
288. Baier J, Maisch T, Maier M, Engel E, Landthaler M, Bäumler W. Singlet oxygen generation by UVA light exposure of endogenous photosensitizers. Biophys J. 2006;91: 1452–1459. doi:10.1529/biophysj.106.082388
289. Remucal CK, McNeill K. Photosensitized amino acid degradation in the presence of riboflavin and its derivatives. Environ Sci Technol. 2011;45: 5230–5237. doi:10.1021/es200411a
290. Kashiwabuchi RT, Khan Y, Carvalho FRDS, Hirai F, Campos MS, McDonnell PJ. Antimicrobial susceptibility of photodynamic therapy (UVA/riboflavin) against *Staphylococcus aureus*. Arq Bras Oftalmol. 2012;75: 423–426. doi:10.1590/S0004-27492012000600011
291. Thakuri PS, Joshi R, Basnet S, Pandey S, Taujale SD, Mishra N. Antibacterial photodynamic therapy on *Staphylococcus aureus* and *Pseudomonas aeruginosa in-vitro*. Nepal Med Coll J. 2011;13: 281–284.
292. Fruk L, Crocker L, Lee JH, Mital S, Mills G, Schack S, et al. Tuning Riboflavin Derivatives For Photodynamic Inactivation of Pathogens. 2021.
293. Chignell CF, Bilskj P, Reszka KJ, Motten AG, Sik RH, Dahl TA. Spectral and photochemical properties of curcumin.

Photochem Photobiol. 1994;59: 295–302.
294. Ansari MJ, Ahmad S, Kohli K, Ali J, Khar RK. Stability-indicating HPTLC determination of curcumin in bulk drug and pharmaceutical formulations. J Pharm Biomed Anal. 2005;39: 132–138. doi:https://doi.org/10.1016/j.jpba.2005.03.021
295. Ribeiro APD, Pavarina AC, Dovigo LN, Brunetti IL, Bagnato VS, Vergani CE, et al. Phototoxic effect of curcumin on methicillin-resistant *Staphylococcus aureus* and L929 fibroblasts. Lasers Med Sci. 2013;28: 391–398.
296. Araújo NC, Fontana CR, Bagnato VS, Gerbi MEM. Photodynamic antimicrobial therapy of curcumin in biofilms and carious dentine. Lasers Med Sci. 2014;29: 629–635. doi:10.1007/s10103-013-1369-3
297. Späth A, Graeler A, Maisch T, Plaetzer K. CureCuma–cationic curcuminoids with improved properties and enhanced antimicrobial photodynamic activity. Eur J Med Chem. 2018;159: 423–440. doi:10.1016/j.ejmech.2017.09.072
298. Glueck M, Schamberger B, Eckl P, Plaetzer K. New horizons in microbiological food safety: Photodynamic Decontamination based on a curcumin derivative. Photochem Photobiol Sci. 2017;16: 1784–1791. doi:10.1039/c7pp00165g
299. Glueck M, Hamminger C, Fefer M, Liu J, Plaetzer K. Save the crop: Photodynamic Inactivation of plant pathogens I: Bacteria. Photochem Photobiol Sci. 2019;18: 1700–1708. doi:10.1039/c9pp00128j
300. Caruso E, Banfi S, Barbieri P, Leva B, Orlandi VT. Synthesis and antibacterial activity of novel cationic BODIPY photosensitizers. J Photochem Photobiol B Biol. 2012;114: 44–51.
301. Orlandi VT, Rybtke M, Caruso E, Banfi S, Tolker-Nielsen T, Barbieri P. Antimicrobial and anti-biofilm effect of a novel BODIPY photosensitizer against *Pseudomonas aeruginosa* PAO1. Biofouling. 2014;30: 883–891.
302. Kamkaew A, Lim SH, Lee HB, Kiew LV, Chung LY, Burgess K. BODIPY dyes in photodynamic therapy. Chem Soc Rev. 2012/09/26. 2013;42: 77–88. doi:10.1039/c2cs35216h
303. Usui Y. Determination of quantum yield of singlet oxygen formation by photosensitization. Chem Lett. 1973;2: 743–744.
304. Singh RJ, Feix JIMB, Pintar TJ, Girotti AW, Kalyanaraman B. Photodynamic action of merocyanine 540 in artificial bilayers and natural membranes: action spectra and quantum yields. Photochem Photobiol. 1991;53: 493–500.
305. Mathai S, Smith TA, Ghiggino KP. Singlet oxygen quantum yields of potential porphyrin-based photosensitisers for photodynamic therapy. Photochem Photobiol Sci. 2007;6: 995–1002.
306. Prat F, Martí C, Nonell S, Zhang X, Foote CS, Moreno RG, et al. C 60 fullerene-based materials as singlet oxygen O2 (1Δg) photosensitizers: a time-resolved near-IR luminescence and optoacoustic study. Phys Chem Chem Phys. 2001;3: 1638–1643.
307. Epelde-Elezcano N, Martínez-Martínez V, Pena-Cabrera E, Gómez-Durán CFA, Arbeloa IL, Lacombe S. Modulation of singlet oxygen generation in halogenated BODIPY dyes by substitution at their meso position: towards a solvent-independent standard in the vis region. RSC Adv. 2016;6: 41991–41998.
308. Adarsh N, Avirah RR, Ramaiah D. Tuning photosensitized singlet oxygen generation efficiency of novel aza-BODIPY dyes. Org Lett. 2010;12: 5720–5723.
309. Wainwright M, Maisch T, Nonell S, Plaetzer K, Almeida A, Tegos GP, et al. Photoantimicrobials - are we afraid of the light? Lancet Infect Dis. 2017;17: e49–e55. doi:10.1016/S1473-3099(16)30268-7
310. Schwarz SR, Hirsch S, Hiergeist A, Kirschneck C, Muehler D, Hiller K-A, et al. Limited antimicrobial efficacy of oral care antiseptics in microcosm biofilms and phenotypic adaptation of bacteria upon repeated exposure. Clin Oral Investig. 2021;25: 2939–2950.
311. Cieplik F, Jakubovics NS, Buchalla W, Maisch T, Hellwig E, Al-Ahmad A. Resistance toward chlorhexidine in oral bacteria–is there cause for concern? Front Microbiol. 2019;10: 587.
312. de Oliveira RR, Schwartz-Filho HO, Novaes Jr AB, Taba Jr M. Antimicrobial photodynamic therapy in the non-surgical treatment of aggressive periodontitis: A preliminary randomized controlled clinical study. J Periodontol. 2007;78: 965–973.
313. Qin YL, Luan XL, Bi LJ, Sheng YQ, Zhou CN, Zhang ZG. Comparison of toluidine blue-mediated photodynamic therapy and conventional scaling treatment for periodontitis in rats. J Periodontal Res. 2008;43: 162–167.
314. Paschoal MA, Lin M, Santos-Pinto L, Duarte S. Photodynamic antimicrobial chemotherapy on *Streptococcus mutans* using curcumin and toluidine blue activated by a novel LED device. Lasers Med Sci. 2015;30: 885–890.
315. Dovigo LN, Pavarina AC, Carmello JC, Machado AL, Brunetti IL, Bagnato VS. Susceptibility of clinical isolates of *Candida* to photodynamic effects of curcumin. Lasers Surg Med. 2011;43: 927–934.
316. Shrestha A, Hamblin MR, Kishen A. Photoactivated rose bengal functionalized chitosan nanoparticles produce antibacterial/biofilm activity and stabilize dentin-collagen. Nanomedicine Nanotechnology, Biol Med. 2014;10: 491–501.
317. Pfitzner A, Sigusch BW, Albrecht V, Glockmann E. Killing of periodontopathogenic bacteria by photodynamic therapy. J Periodontol. 2004;75: 1343–1349.
318. Wilson M, Dobson J, Harvey W. Sensitization of oral bacteria to killing by low-power laser radiation. Curr Microbiol. 1992;25: 77–81. doi:10.1007/BF01570963
319. Mogens K, Mikkelsen L, Henrichsen Jø. Taxonomic Study of Viridans Streptococci: Description of *Streptococcus gordonii* sp. nov. and Emended Descriptions of *Streptococcus sanguis* (White and Niven 1946), *Streptococcus oralis* (Bridge and Sneath 1982), and <i>Streptococcus mit. Int J Syst Evol Microbiol. 1989;39: 471–484. doi:https://doi.org/10.1099/00207713-39-4-471
320. Lopez R, Flavell S, Thomas C. A not very NICE case of endocarditis. Case Reports. 2013;2013: bcr2012007918.
321. Coykendall AL, Kaczmarek FS, Slots Jø. Genetic Heterogeneity in *Bacteroides asaccharolyticus* (Holdeman and Moore

1970) Finegold and Barnes 1977 (Approved Lists, 1980) and Proposal of *Bacteroides gingivalis* sp. nov. and *Bacteroides macacae* (Slots and Genco) comb. nov. Int J Syst Evol Microbiol. 1980;30: 559–564. doi:https://doi.org/10.1099/00207713-30-3-559

322. Signat B, Roques C, Poulet P, Duffaut D. Role of *Fusobacterium nucleatum* in Periodontal Health and Disease. Current Issues in Molecular Biology. 2011. doi:10.21775/cimb.013.025
323. Nørskov-Lauritsen N, Kilian M. Reclassification of *Actinobacillus actinomycetemcomitans, Haemophilus aphrophilus, Haemophilus paraphrophilus* and *Haemophilus segnis* as *Aggregatibacter actinomycetemcomitans* gen. nov., comb. nov., *Aggregatibacter aphrophilus* co. Int J Syst Evol Microbiol. 2006;56: 2135–2146. doi:https://doi.org/10.1099/ijs.0.64207-0
324. Burns T, Wilson M, Pearson GJ. Killing of cariogenic bacteria by light from a gallium aluminium arsenide diode laser. J Dent. 1994;22: 273–278. doi:https://doi.org/10.1016/0300-5712(94)90056-6
325. Burns T, Wilson M, Pearson GJ. Effect of Dentine and Collagen on the Lethal Photosensitization of *Streptococcus mutans*. Caries Res. 1995;29: 192–197. doi:10.1159/000262068
326. Cieplik F, Pummer A, Leibl C, Regensburger J, Schmalz G, Buchalla W, et al. Photodynamic Inactivation of Root Canal Bacteria by Light Activation through Human Dental Hard and Simulated Surrounding Tissue . Frontiers in Microbiology . 2016. p. 929. Available: https://www.frontiersin.org/article/10.3389/fmicb.2016.00929
327. Peng P-C, Hsieh C-M, Chen C-P, Tsai T, Chen C-T. Assessment of Photodynamic Inactivation against Periodontal Bacteria Mediated by a Chitosan Hydrogel in a 3D Gingival Model. International Journal of Molecular Sciences . 2016. doi:10.3390/ijms17111821
328. Stranadko EP, Riabov M V, Volkova NN, Spaniol S, Rauschning W, Nifantiev NE. Testing of efficacy of photodynamic therapy with a new photosensitizer: a derivative of chlorin e6 (BLC 1010). Laser-Tissue Interactions, Therapeutic Applications, and Photodynamic Therapy. International Society for Optics and Photonics; 2001. pp. 155–157.
329. Sigusch BW, Pfitzner A, Albrecht V, Glockmann E. Efficacy of photodynamic therapy on inflammatory signs and two selected periodontopathogenic species in a beagle dog model. J Periodontol. 2005;76: 1100–1105.
330. Greenstein G. Periodontal response to mechanical non-surgical therapy: A review. J Periodontol. 1992;63: 118–130.
331. Moore J, Wilson M, Kieser JB. The distribution of bacterial lipopolysaccharide (endotoxin) in relation to periodontally involved root surfaces. J Clin Periodontol. 1986;13: 748–751.
332. Badersten A, Niveus R, Egelberg J. 4-year observations of basic periodontal therapy. J Clin Periodontol. 1987;14: 438–444.
333. Fontana CR, Abernethy AD, Som S, Ruggiero K, Doucette S, Marcantonio RC, et al. The antibacterial effect of photodynamic therapy in dental plaque-derived biofilms. J Periodontal Res. 2009;44: 751–759.
334. Schneider M, Kirfel G, Berthold M, Frentzen M, Krause F, Braun A. The impact of antimicrobial photodynamic therapy in an artificial biofilm model. Lasers Med Sci. 2012;27: 615–620.
335. Bulit F, Grad I, Manoil D, Simon S, Wataha JC, Filieri A, et al. Antimicrobial Activity and Cytotoxicity of 3 Photosensitizers Activated with Blue Light. J Endod. 2014;40: 427–431. doi:https://doi.org/10.1016/j.joen.2013.12.001
336. Voos AC, Kranz S, Tonndorf-Martini S, Voelpel A, Sigusch H, Staudte H, et al. Photodynamic antimicrobial effect of safranine O on an *ex vivo* periodontal biofilm. Lasers Surg Med. 2014;46: 235–243.
337. Melo MAS, Rolim JPML, Passos VF, Lima RA, Zanin ICJ, Codes BM, et al. Photodynamic antimicrobial chemotherapy and ultraconservative caries removal linked for management of deep caries lesions. Photodiagnosis Photodyn Ther. 2015;12: 581–586. doi:https://doi.org/10.1016/j.pdpdt.2015.09.005
338. Nielsen HK, Garcia J, Væth M, Schlafer S. Comparison of Riboflavin and Toluidine Blue O as Photosensitizers for Photoactivated Disinfection on Endodontic and Periodontal Pathogens *In Vitro*. PLoS One. 2015;10: e0140720. Available: https://doi.org/10.1371/journal.pone.0140720
339. Poli PP, Souza FÁ, Damiani G, Hadad H, Maiorana C, Beretta M. Adjunctive use of antimicrobial photodynamic therapy in the surgical treatment of periapical lesions: A case series. Photodiagnosis Photodyn Ther. 2022;37: 102598. doi:https://doi.org/10.1016/j.pdpdt.2021.102598
340. Al-Hamoudi N, Alali Y, Al-Aali K, Alhumaidan AA, Heer E, Tanveer SA, et al. Peri-implant parameters and bone metabolic markers among water-pipe users treated with photodynamic therapy. Photodiagnosis Photodyn Ther. 2022;37: 102655. doi:https://doi.org/10.1016/j.pdpdt.2021.102655
341. Sivieri-Araujo G, Strazzi-Sahyon HB, Jacomassi DP, dos Santos PH, Cintra LTA, Kurachi C, et al. Effects of methylene blue and curcumin photosensitizers on the color stability of endodontically treated intraradicular dentin. Photodiagnosis Photodyn Ther. 2022;37: 102650. doi:https://doi.org/10.1016/j.pdpdt.2021.102650
342. Persoon IF, Özok AR. Definitions and epidemiology of endodontic infections. Curr oral Heal reports. 2017;4: 278–285.
343. Li C, Cui Y, Zhou C, Sun J, Zhou X. Epigenetics in Odontogenesis and its Influences. Curr Stem Cell Res Ther. 2018;13: 110–117.
344. Okamoto CB, Motta LJ, Prates RA, da Mota ACC, Gonçalves MLL, Horliana ACRT, et al. Antimicrobial Photodynamic Therapy as a Co-adjuvant in Endodontic Treatment of Deciduous Teeth: Case Series. Photochem Photobiol. 2018;94: 760–764.
345. Demidova TN, Hamblin MR. Effect of cell-photosensitizer binding and cell density on microbial photoinactivation. Antimicrob Agents Chemother. 2005;49: 2329–2335.
346. Petersen J, Glaßl E-M, Nasseri P, Crismani A, Luger AK, Schoenherr E, et al. The association of chronic apical periodontitis and endodontic therapy with atherosclerosis. Clin Oral Investig. 2014;18: 1813–1823.
347. Garcez AS, Nuñez SC, Hamblin MR, Ribeiro MS. Antimicrobial effects of photodynamic therapy on patients with

necrotic pulps and periapical lesion. J Endod. 2008;34: 138–142.
348. Aas JA, Griffen AL, Dardis SR, Lee AM, Olsen I, Dewhirst FE, et al. Bacteria of dental caries in primary and permanent teeth in children and young adults. J Clin Microbiol. 2008;46: 1407–1417.
349. Faragó I, Nagy G, Márton S, Túry F, Szabó E, Hopcraft M, et al. Dental caries experience in a Hungarian police student population. Caries Res. 2012;46: 95–101.
350. Stájer A, Urban E, Mihalik E, Rakonczay Z, Nagy E, Fazekas A, et al. *Streptococcus mutans* colonization on titanium surfaces treated with various fluoride-containing preventive solutions. Fogorv Sz. 2009;102: 117–122.
351. Barrak I, Urbán E, Turzó K, Nagy K, Braunitzer G, Stájer A. Short-and long-term influence of fluoride-containing prophylactics on the growth of *Streptococcus mutans* on titanium surface. Implant Dent. 2015;24: 675–679.
352. Stájer A, Urbán E, Pelsõczi I, Mihalik E, Rakonczay Z, Nagy K, et al. Effect of caries preventive products on the growth of bacterial biofilm on titanium surface. Acta Microbiol Immunol Hung. 2012;59: 51–61.
353. Ricatto LGO, Conrado LAL, Turssi CP, França FMG, Basting RT, Amaral FLB. Comparative evaluation of photodynamic therapy using LASER or light emitting diode on cariogenic bacteria: an *in vitro* study. Eur J Dent. 2014;8: 509–514.
354. Bevilacqua IM, Nicolau RA, Khouri S, Brugnera Jr. A, Teodoro GR, Zângaro RA, et al. The Impact of Photodynamic Therapy on the Viability of *Streptococcus mutans* in a Planktonic Culture. Photomed Laser Surg. 2007;25: 513–518. doi:10.1089/pho.2007.2109
355. Khammissa RAG, Feller L, Meyerov R, Lemmer J. Peri-implant mucositis and periimplantitis: bacterial infection. South African Dent J. 2012;67: 70–74.
356. Prathapachandran J, Suresh N. Management of peri-implantitis. Dent Res J (Isfahan). 2012;9: 516.
357. Dörtbudak O, Haas R, Bernhart T, Mailath-Pokorny G. Lethal photosensitization for decontamination of implant surfaces in the treatment of peri-implantitis. Clin Oral Implants Res. 2001;12: 104–108.
358. Esposito M, Grusovin MG, De Angelis N, Camurati A, Campailla M, Felice P. The adjunctive use of light-activated disinfection (LAD) with FotoSan is ineffective in the treatment of peri-implantitis: 1-year results from a multicentre pragmatic randomised controlled trial. Eur J Oral Implant. 2013;6: 109–119.
359. Stulberg DL, Penrod MA, Blatny RA. Common bacterial skin infections. Am Fam Physician. 2002;66: 119.
360. Perry AL, Lambert PA. *Propionibacterium acnes*. Lett Appl Microbiol. 2006;42: 185–188.
361. Banerjee S, Ghosh D, Vishakha K, Das S, Mondal S, Ganguli A. Photodynamic antimicrobial chemotherapy (PACT) using riboflavin inhibits the mono and dual species biofilm produced by antibiotic resistant *Staphylococcus aureus* and *Escherichia coli*. Photodiagnosis Photodyn Ther. 2020;32: 102002.
362. Liu S, Mai B, Jia M, Lin D, Zhang J, Liu Q, et al. Synergistic antimicrobial effects of photodynamic antimicrobial chemotherapy and gentamicin on *Staphylococcus aureus* and multidrug-resistant *Staphylococcus aureus*. Photodiagnosis Photodyn Ther. 2020;30: 101703.
363. Gao Y, Mai B, Wang A, Li M, Wang X, Zhang K, et al. Antimicrobial properties of a new type of photosensitizer derived from phthalocyanine against planktonic and biofilm forms of *Staphylococcus aureus*. Photodiagnosis Photodyn Ther. 2018;21: 316–326.
364. Zeina B, Greenman J, Purcell WM, Das B. Killing of cutaneous microbial species by photodynamic therapy. Br J Dermatol. 2001;144: 274–278.
365. Soares JM, Inada NM, Bagnato VS, Blanco KC. Evolution of surviving *Streptoccocus pyogenes* from pharyngotonsillitis patients submit to multiple cycles of antimicrobial photodynamic therapy. J Photochem Photobiol B Biol. 2020;210: 111985.
366. Tsai T, Yang Y, Wang T, Chien H, Chen C. Improved photodynamic inactivation of gram-positive bacteria using hematoporphyrin encapsulated in liposomes and micelles. Lasers Surg Med Off J Am Soc Laser Med Surg. 2009;41: 316–322.
367. Xiao-Ming L, Fischman AJ, Stevens E, Lee TT, Strong L, Tompkins RG, et al. Sn-chlorin e6 antibacterial immunoconjugates: An *in vitro* and *in vivo* analysis. J Immunol Methods. 1992;156: 85–99. doi:https://doi.org/10.1016/0022-1759(92)90014-K
368. Zolfaghari PS, Packer S, Singer M, Nair SP, Bennett J, Street C, et al. *In vivo* killing of *Staphylococcus aureus* using a light-activated antimicrobial agent. BMC Microbiol. 2009;9: 1–8. doi:10.1186/1471-2180-9-27
369. Paolillo FR, Rodrigues PGS, Bagnato VS, Alves F, Pires L, Corazza AV. The effect of combined curcumin-mediated photodynamic therapy and artificial skin on *Staphylococcus aureus*–infected wounds in rats. Lasers Med Sci. 2021;36: 1219–1226. doi:10.1007/s10103-020-03160-6
370. Qiu L, Wang C, Lan M, Guo Q, Du X, Zhou S, et al. Antibacterial Photodynamic Gold Nanoparticles for Skin Infection. ACS Appl Bio Mater. 2021;4: 3124–3132. doi:10.1021/acsabm.0c01505
371. Akhtar F, Khan AU, Misba L, Akhtar K, Ali A. Antimicrobial and antibiofilm photodynamic therapy against vancomycin resistant *Staphylococcus aureus* (VRSA) induced infection *in vitro* and *in vivo*. Eur J Pharm Biopharm. 2021;160: 65–76. doi:https://doi.org/10.1016/j.ejpb.2021.01.012
372. Zhao Z, Ma J, Wang Y, Xu Z, Zhao L, Zhao J, et al. Antimicrobial Photodynamic Therapy Combined With Antibiotic in the Treatment of Rats With Third-Degree Burns. Front Microbiol. 2021;12: 48. doi:10.3389/fmicb.2021.622410
373. Ishiwata N, Tsunoi Y, Sarker RR, Haruyama Y, Kawauchi S, Sekine Y, et al. Control of Burn Wound Infection by Methylene Blue-Mediated Photodynamic Treatment With Light-Emitting Diode Array Illumination in Rats. Lasers Surg Med. 2021.
374. Sarker RR, Tsunoi Y, Haruyama Y, Sato S, Nishidate I. Antimicrobial photodynamic therapy for burn wound infection

with *P. aeruginosa* in rats. Photonic Diagnosis, Monitoring, Prevention, and Treatment of Infections and Inflammatory Diseases 2021. International Society for Optics and Photonics; 2021. p. 116260Q.

375. Dai T, Tegos GP, Lu Z, Huang L, Zhiyentayev T, Franklin MJ, et al. Photodynamic therapy for *Acinetobacter baumannii* burn infections in mice. Antimicrob Agents Chemother. 2009;53: 3929–3934.
376. Hashimoto MCE, Prates RA, Kato IT, Nunez SC, Courrol LC, Ribeiro MS. Antimicrobial photodynamic therapy on drug-resistant *Pseudomonas aeruginosa*-induced infection. An *in vivo* study. Photochem Photobiol. 2012;88: 590–595.
377. Oyama J, Ramos-Milaré ÁCFH, Lera-Nonose DSSL, Nesi-Reis V, Demarchi IG, Aristides SMA, et al. Photodynamic therapy in wound healing *in vivo*: a systematic review. Photodiagnosis Photodyn Ther. 2020;30: 101682.
378. Ragàs X, Dai T, Tegos GP, Agut M, Nonell S, Hamblin MR. Photodynamic inactivation of *Acinetobacter baumannii* using phenothiazinium dyes: *In vitro* and *in vivo* studies. Lasers Surg Med. 2010;42: 384–390. doi:https://doi.org/10.1002/lsm.20922
379. Daniela V, Asheesh G, Liyi H, Giacomo L, Pinar A, Andrea R, et al. Bacterial Photodynamic Inactivation Mediated by Methylene Blue and Red Light Is Enhanced by Synergistic Effect of Potassium Iodide. Antimicrob Agents Chemother. 2022;59: 5203–5212. doi:10.1128/AAC.00019-15
380. Itoh Y, Ninomiya Y, Tajima S, Ishibashi A. Photodynamic therapy of acne vulgaris with topical δ-aminolaevulinic acid and incoherent light in Japanese patients. Br J Dermatol. 2001;144: 575–579.
381. Hongcharu W, Taylor CR, Aghassi D, Suthamjariya K, Anderson RR, Chang Y. Topical ALA-photodynamic therapy for the treatment of acne vulgaris. J Invest Dermatol. 2000;115: 183–192.
382. Pollock B, Turner D, Stringer MR, Bojar RA, Goulden V, Stables GI, et al. Topical aminolaevulinic acid-photodynamic therapy for the treatment of acne vulgaris: a study of clinical efficacy and mechanism of action. Br J Dermatol. 2004;151: 616–622.
383. Fabbrocini G, Cacciapuoti S, De Vita V, Fardella N, Pastore F, Monfrecola G. The effect of aminolevulinic acid photodynamic therapy on microcomedones and macrocomedones. Dermatology. 2009;219: 322–328.
384. Kim BJ, Lee HG, Woo SM, Youn J Il, Suh DH. Pilot study on photodynamic therapy for acne using indocyanine green and diode laser. J Dermatol. 2009;36: 17–21.
385. Li B, Fang X, Hu X, Hua H, Wei P. Successful treatment of chronic hyperplastic candidiasis with 5-aminolevulinic acid photodynamic therapy: A case report. Photodiagnosis Photodyn Ther. 2022;37: 102633. doi:https://doi.org/10.1016/j.pdpdt.2021.102633
386. Gerba CP, Wallis C, Melnick JL. Disinfection of Wastewater by Photodynamic Oxidation. J (Water Pollut Control Fed. 1977;49: 575–583. Available: http://www.jstor.org/stable/25039316
387. Jori G. Photodynamische Therapien in der Mikrobiologie. Klin fluoreszenzdiagnostik und Photodyn Ther Berlin Blackwell verlag. 2003; 360–371.
388. Almeida J, Tomé JPC, Neves MGPMS, Tomé AC, Cavaleiro JAS, Cunha Â, et al. Photodynamic inactivation of multidrug-resistant bacteria in hospital wastewaters: Influence of residual antibiotics. Photochem Photobiol Sci. 2014;13: 626–633. doi:10.1039/c3pp50195g
389. Bartolomeu M, Reis S, Fontes M, Neves MGPMS, Faustino MAF, Almeida A. Photodynamic Action against Wastewater Microorganisms and Chemical Pollutants: An Effective Approach with Low Environmental Impact. Water . 2017. doi:10.3390/w9090630
390. Carvalho CMB, Gomes ATPC, Fernandes SCD, Prata ACB, Almeida MA, Cunha MA, et al. Photoinactivation of bacteria in wastewater by porphyrins: Bacterial β-galactosidase activity and leucine-uptake as methods to monitor the process. J Photochem Photobiol B Biol. 2007;88: 112–118. doi:10.1016/j.jphotobiol.2007.04.015
391. Costa L, Carvalho CMB, Faustino MAF, Neves MGPMS, Tomé JPC, Tomé AC, et al. Sewage bacteriophage inactivation by cationic porphyrins: influence of light parameters. Photochem Photobiol Sci. 2010;9: 1126–1133. doi:10.1039/C0PP00051E
392. Bartolomeu M, Oliveira C, Pereira C, Neves MGPMS, Faustino MAF, Almeida A. Antimicrobial Photodynamic Approach in the Inactivation of Viruses in Wastewater: Influence of Alternative Adjuvants. Antibiotics . 2021. doi:10.3390/antibiotics10070767
393. Schrader KK, Bommer JC, Jori G. In vitro evaluation of the antimicrobial agent AquaFrin as a bactericide and selective algicide for use in channel catfish aquaculture. N Am J Aquac. 2010;72: 304–308.
394. Newton JC, Wood TM, Hartley MM. Isolation and partial characterization of extracellular proteases produced by isolates of *Flavobacterium columnare* derived from channel catfish. J Aquat Anim Health. 1997;9: 75–85.
395. Hawke JP, McWhorter AC, SteigerwaltT AG, Brenner DONJ. *Edwardsiella ictaluri* sp. nov., the causative agent of enteric septicemia of catfish. Int J Syst Evol Microbiol. 1981;31: 396–400.
396. Magaraggia M, Faccenda F, Gandolfi A, Jori G. Treatment of microbiologically polluted aquaculture waters by a novel photochemical technique of potentially low environmental impact. J Environ Monit. 2006;8: 923–931.
397. Alouini Z, Jemli M. Destruction of helminth eggs by photosensitized porphyrin. J Environ Monit. 2001;3: 548–551.
398. Jemli M, Alouini Z, Sabbahi S, Gueddari M. Destruction of fecal bacteria in wastewater by three photosensitizers. J Environ Monit. 2002;4: 511–516. doi:10.1039/b204637g
399. Magaraggia M, Jori G. Photodynamic approaches to water disinfection. CRC Handbook of Organic Photochemistry and Photobiology, Third Edition-Two Volume Set. CRC Press; 2019. pp. 1543–1556.
400. Van Doremalen N, Bushmaker T, Morris DH, Holbrook MG, Gamble A, Williamson BN, et al. Aerosol and surface stability of SARS-CoV-2 as compared with SARS-CoV-1. N Engl J Med. 2020;382: 1564–1567.
401. Kramer A, Assadian O. Survival of microorganisms on inanimate surfaces. Use of Biocidal Surfaces for Reduction of

Healthcare Acquired Infections. Springer; 2014. pp. 7–26.
402. Thompson K-A, Bennett AM. Persistence of influenza on surfaces. J Hosp Infect. 2017;95: 194–199.
403. Kampf G, Todt D, Pfaender S, Steinmann E. Persistence of coronaviruses on inanimate surfaces and their inactivation with biocidal agents. J Hosp Infect. 2020;104: 246–251.
404. Ong SWX, Tan YK, Chia PY, Lee TH, Ng OT, Wong MSY, et al. Air, surface environmental, and personal protective equipment contamination by severe acute respiratory syndrome coronavirus 2 (SARS-CoV-2) from a symptomatic patient. Jama. 2020;323: 1610–1612.
405. Oxford J, Berezin EN, Courvalin P, Dwyer DE, Exner M, Jana LA, et al. The survival of influenza A (H1N1) pdm09 virus on 4 household surfaces. Am J Infect Control. 2014;42: 423–425.
406. Song X, Vossebein L, Zille A. Efficacy of disinfectant-impregnated wipes used for surface disinfection in hospitals: a review. Antimicrob Resist Infect Control. 2019;8: 1–14.
407. Goodman ER, Piatt R, Bass R, Onderdonk AB, Yokoe DS, Huang SS. Impact of an environmental cleaning intervention on the presence of methicillin-resistant *Staphylococcus aureus* and vancomycin-resistant enterococci on surfaces in intensive care unit rooms. Infect Control Hosp Epidemiol. 2008;29: 593–599.
408. Doidge M, Allworth AM, Woods M, Marshall P, Terry M, O'Brien K, et al. Control of an outbreak of carbapenem-resistant *Acinetobacter baumannii* in Australia after introduction of environmental cleaning with a commercial oxidizing disinfectant. Infect Control Hosp Epidemiol. 2010;31: 418–420.
409. Clancy C, Delungahawatta T, Dunne CP. Hand hygiene-related clinical trials reported between 2014 and 2020: a comprehensive systematic review. J Hosp Infect. 2021.
410. Carling PC, Parry MM, Rupp ME, Po JL, Dick B, Von Beheren S, et al. Improving cleaning of the environment surrounding patients in 36 acute care hospitals. Infect Control Hosp Epidemiol. 2008;29: 1035–1041.
411. Weber DJ, Rutala WA, Miller MB, Huslage K, Sickbert-Bennett E. Role of hospital surfaces in the transmission of emerging health care-associated pathogens: norovirus, *Clostridium difficile*, and *Acinetobacter* species. Am J Infect Control. 2010;38: S25–S33.
412. Otter JA, Yezli S, Salkeld JAG, French GL. Evidence that contaminated surfaces contribute to the transmission of hospital pathogens and an overview of strategies to address contaminated surfaces in hospital settings. Am J Infect Control. 2013;41: S6–S11.
413. Russotto V, Cortegiani A, Raineri SM, Giarratano A. Bacterial contamination of inanimate surfaces and equipment in the intensive care unit. J intensive care. 2015;3: 1–8.
414. Adams CE, Dancer SJ. Dynamic transmission of *Staphylococcus aureus* in the intensive care unit. Int J Environ Res Public Health. 2020;17: 2109.
415. Adlhart C, Verran J, Azevedo NF, Olmez H, Keinänen-Toivola MM, Gouveia I, et al. Surface modifications for antimicrobial effects in the healthcare setting: A critical overview. J Hosp Infect. 2018;99: 239–249.
416. Muller MP, Macdougall C, Lim M, Armstrong I, Bialachowski A, Callery S, et al. Antimicrobial surfaces to prevent healthcare-associated infections: a systematic review. J Hosp Infect. 2016;92: 7–13.
417. Chyderiotis S, Legeay C, Verjat-Trannoy D, Le Gallou F, Astagneau P, Lepelletier D. New insights on antimicrobial efficacy of copper surfaces in the healthcare environment: a systematic review. Clin Microbiol Infect. 2018;24: 1130–1138.
418. Palza H, Nuñez M, Bastías R, Delgado K. *In situ* antimicrobial behavior of materials with copper-based additives in a hospital environment. Int J Antimicrob Agents. 2018;51: 912–917.
419. Mitra D, Kang E-T, Neoh KG. Antimicrobial copper-based materials and coatings: potential multifaceted biomedical applications. ACS Appl Mater Interfaces. 2019;12: 21159–21182.
420. Grass G, Rensing C, Solioz M. Metallic copper as an antimicrobial surface. Appl Environ Microbiol. 2011;77: 1541–1547.
421. Varghese N, Yang S, Sejwal P, Luk Y-Y. Surface control of blastospore attachment and ligand-mediated hyphae adhesion of *Candida albicans*. Chem Commun. 2013;49: 10418–10420.
422. Ortí-Lucas RM, Muñoz-Miguel J. Effectiveness of surface coatings containing silver ions in bacterial decontamination in a recovery unit. Antimicrob Resist Infect Control. 2017;6: 1–7.
423. Yao T, Wang J, Xue Y, Yu W, Gao Q, Ferreira L, et al. A photodynamic antibacterial spray-coating based on the host–guest immobilization of the photosensitizer methylene blue. J Mater Chem B. 2019;7: 5089–5095.
424. Ghareeb CR, Peddinti BST, Kisthardt SC, Scholle F, Spontak RJ, Ghiladi RA. Toward Universal Photodynamic Coatings for Infection Control. Front Med. 2021;8.
425. Gram L, Ravn L, Rasch M, Bruhn JB, Christensen AB, Givskov M. Food spoilage—interactions between food spoilage bacteria. Int J Food Microbiol. 2002;78: 79–97. doi:https://doi.org/10.1016/S0168-1605(02)00233-7
426. Silva AF, Borges A, Freitas CF, Hioka N, Mikcha JMG, Simões M. Antimicrobial photodynamic inactivation mediated by rose bengal and erythrosine is effective in the control of food-related bacteria in planktonic and biofilm states. Molecules. 2018;23: 2288.
427. Mazaheri T, Cervantes-Huamán BRH, Bermúdez-Capdevila M, Ripolles-Avila C, Rodríguez-Jerez JJ. *Listeria monocytogenes* biofilms in the food industry: is the current hygiene program sufficient to combat the persistence of the pathogen? Microorganisms. 2021;9: 181.
428. Møretrø T, Langsrud S. Residential bacteria on surfaces in the food industry and their implications for food safety and quality. Compr Rev Food Sci Food Saf. 2017;16: 1022–1041.
429. Wainwright M, Maisch T, Nonell S, Plaetzer K, Almeida A, Tegos GP, et al. Photoantimicrobials—are we afraid of the

light? Lancet Infect Dis. 2017;17: e49–e55.
430. Kreitner M, Wagner K-H, Alth G, Ebermann R, Foißy H, Elmadfa I. Haematoporphyrin-and sodium chlorophyllin-induced phototoxicity towards bacteria and yeasts–a new approach for safe foods. Food Control. 2001;12: 529–533.
431. Buchovec I, Vaitonis Z, Luksiene Z. Novel approach to control *Salmonella enterica* by modern biophotonic technology: photosensitization. J Appl Microbiol. 2009;106: 748–754.
432. Murdoch LE, Maclean M, Endarko E, MacGregor SJ, Anderson JG. Bactericidal effects of 405 nm light exposure demonstrated by inactivation of *Escherichia, Salmonella, Shigella, Listeria*, and *Mycobacterium* species in liquid suspensions and on exposed surfaces. Sci World J. 2012;2012.
433. Ghate VS, Ng KS, Zhou W, Yang H, Khoo GH, Yoon W-B, et al. Antibacterial effect of light emitting diodes of visible wavelengths on selected foodborne pathogens at different illumination temperatures. Int J Food Microbiol. 2013;166: 399–406.
434. Kumar A, Ghate V, Kim M-J, Zhou W, Khoo GH, Yuk H-G. Kinetics of bacterial inactivation by 405 nm and 520 nm light emitting diodes and the role of endogenous coproporphyrin on bacterial susceptibility. J Photochem Photobiol B Biol. 2015;149: 37–44.
435. Bonifácio D, Martins C, David B, Lemos C, Neves M, Almeida A, et al. Photodynamic inactivation of *Listeria innocua* biofilms with food-grade photosensitizers: a curcumin-rich extract of *Curcuma longa* vs commercial curcumin. J Appl Microbiol. 2018;125: 282–294.
436. Maisch T, Spannberger F, Regensburger J, Felgenträger A, Bäumler W. Fast and effective: Intense pulse light photodynamic inactivation of bacteria. J Ind Microbiol Biotechnol. 2012;39: 1013–1021. doi:10.1007/s10295-012-1103-3
437. Painter JA, Hoekstra RM, Ayers T, Tauxe R V, Braden CR, Angulo FJ, et al. Attribution of foodborne illnesses, hospitalizations, and deaths to food commodities by using outbreak data, United States, 1998–2008. Emerg Infect Dis. 2013;19: 407.
438. Randazzo W, Aznar R, Sánchez G. Curcumin-mediated photodynamic inactivation of norovirus surrogates. Food Environ Virol. 2016;8: 244–250.
439. Luksiene Z, Paskeviciute E. Microbial control of food-related surfaces: Na-Chlorophyllin-based photosensitization. J Photochem Photobiol B Biol. 2011;105: 69–74.
440. Buchovec I, Lukseviciute V, Marsalka A, Reklaitis I, Luksiene Z. Effective photosensitization-based inactivation of Gram (−) food pathogens and molds using the chlorophyllin–chitosan complex: Towards photoactive edible coatings to preserve strawberries. Photochem Photobiol Sci. 2016;15: 506–516.
441. Paskeviciute E, Luksiene Z. Novel approach to decontaminate fruits and vegetables: Combined treatment of pulsed light and photosensitization. Environ friendly safe Technol Qual fruit Veg. 2010; 220–222.
442. Tortik N, Spaeth A, Plaetzer K. Photodynamic decontamination of foodstuff from *Staphylococcus aureus* based on novel formulations of curcumin. Photochem Photobiol Sci. 2014;13: 1402–1409.
443. Guffey JS, Payne WC, Motts SD, Towery P, Hobson T, Harrell G, et al. Inactivation of *Salmonella* on tainted foods: using blue light to disinfect cucumbers and processed meat products. Food Sci Nutr. 2016;4: 878–887.
444. Kim M-J, Bang WS, Yuk H-G. 405±5 nm light emitting diode illumination causes photodynamic inactivation of *Salmonella* spp. on fresh-cut papaya without deterioration. Food Microbiol. 2017;62: 124–132.
445. Ghate V, Kumar A, Kim M-J, Bang W-S, Zhou W, Yuk H-G. Effect of 460 nm light emitting diode illumination on survival of *Salmonella* spp. on fresh-cut pineapples at different irradiances and temperatures. J Food Eng. 2017;196: 130–138.
446. Kingsley DH, Perez-Perez RE, Boyd G, Sites J, Niemira BA. Evaluation of 405-nm monochromatic light for inactivation of Tulane virus on blueberry surfaces. J Appl Microbiol. 2018;124: 1017–1022.
447. Srimagal A, Ramesh T, Sahu JK. Effect of light emitting diode treatment on inactivation of *Escherichia coli* in milk. LWT-Food Sci Technol. 2016;71: 378–385.
448. Galstyan A, Dobrindt U. Determining and unravelling origins of reduced photoinactivation efficacy of bacteria in milk. J Photochem Photobiol B Biol. 2019;197. doi:10.1016/j.jphotobiol.2019.111554
449. Gunther IV NW, Phillips JG, Sommers C. The effects of 405-nm visible light on the survival of *Campylobacter* on chicken skin and stainless steel. Foodborne Pathog Dis. 2016;13: 245–250.
450. Josewin SW, Ghate V, Kim M-J, Yuk H-G. Antibacterial effect of 460 nm light-emitting diode in combination with riboflavin against *Listeria monocytogenes* on smoked salmon. Food Control. 2018;84: 354–361.
451. Liu F, Li Z, Cao B, Wu J, Wang Y, Xue Y, et al. The effect of a novel photodynamic activation method mediated by curcumin on oyster shelf life and quality. Food Res Int. 2016;87: 204–210.
452. Luksiene Z, Buchovec I, Paskeviciute E. Inactivation of *Bacillus cereus* by Na-chlorophyllin-based photosensitization on the surface of packaging. J Appl Microbiol. 2010;109: 1540–1548.
453. Luksiene Z, Paskeviciute E. Novel approach to the microbial decontamination of strawberries: chlorophyllin-based photosensitization. J Appl Microbiol. 2011;110: 1274–1283. doi:https://doi.org/10.1111/j.1365-2672.2011.04986.x
454. Luksiene Z, Buchovec I, Paskeviciute E. Inactivation of several strains of *Listeria monocytogenes* attached to the surface of packaging material by Na-chlorophyllin-based photosensitization. J Photochem Photobiol B Biol. 2010;101: 326–331.
455. Su L, Huang J, Li H, Pan Y, Zhu B, Zhao Y, et al. Chitosan-riboflavin composite film based on photodynamic inactivation technology for antibacterial food packaging. Int J Biol Macromol. 2021;172: 231–240. doi:https://doi.org/10.1016/j.ijbiomac.2021.01.056
456. Martínez-Suárez J V, Ortiz S, López-Alonso V. Potential impact of the resistance to quaternary ammonium

disinfectants on the persistence of *Listeria monocytogenes* in food processing environments. Front Microbiol. 2016;7: 638.

457. Rodriguez-Melcon C, Capita R, Rodríguez-Jerez JJ, Martinez-Suarez J V, Alonso-Calleja C. Effect of low doses of disinfectants on the biofilm-forming ability of *Listeria monocytogenes*. Foodborne Pathog Dis. 2019;16: 262–268.
458. Mavri A, Možina SS. Development of antimicrobial resistance in *Campylobacter jejuni* and *Campylobacter coli* adapted to biocides. Int J Food Microbiol. 2013;160: 304–312.
459. Cadena M, Kelman T, Marco ML, Pitesky M. Understanding antimicrobial resistance (AMR) profiles of *Salmonella* biofilm and planktonic bacteria challenged with disinfectants commonly used during poultry processing. Foods. 2019;8: 275.
460. Giacometti F, Shirzad-Aski H, Ferreira S. Antimicrobials and Food-Related Stresses as Selective Factors for Antibiotic Resistance along the Farm to Fork Continuum. Antibiotics. 2021;10: 671.
461. Liao X, Ma Y, Daliri EB-M, Koseki S, Wei S, Liu D, et al. Interplay of antibiotic resistance and food-associated stress tolerance in foodborne pathogens. Trends Food Sci Technol. 2020;95: 97–106.
462. Usacheva MN, Teichert MC, Biel MA. Comparison of the methylene blue and toluidine blue photobactericidal efficacy against gram-positive and gram-negative microorganisms. Lasers Surg Med Off J Am Soc Laser Med Surg. 2001;29: 165–173.
463. Caires CSA, Leal CRB, Ramos CAN, Bogo D, Lima AR, Arruda EJ, et al. Photoinactivation effect of eosin methylene blue and chlorophyllin sodium-copper against *Staphylococcus aureus* and *Escherichia coli*. Lasers Med Sci. 2017;32: 1081–1088. doi:10.1007/s10103-017-2210-1
464. Capella M, Coelho AM, Menezes S. Effect of glucose on photodynamic action of methylene blue in *Escherichia coli* cells. Photochem Photobiol. 1996;64: 205–210.
465. Peloi LS, Soares RRS, Biondo CEG, Souza VR, Hioka N, Kimura E. Photodynamic effect of light-emitting diode light on cell growth inhibition induced by methylene blue. J Biosci. 2008;33: 231–237.
466. Salmon-Divon M, Nitzan Y, Malik Z. Mechanistic aspects of *Escherichia coli* photodynamic inactivation by cationic tetra-meso(N-methylpyridyl)porphine. Photochem Photobiol Sci. 2004;3: 423–429. doi:10.1039/b315627n
467. Eckl DB, Huber H, Bäumler W. First Report on Photodynamic Inactivation of Archaea Including a Novel Method for High-Throughput Reduction Measurement. Photochem Photobiol. 2020;96: 883–889. doi:10.1111/php.13229
468. Nitzan Y, Ashkenazi H. Photoinactivation of *Acinetobacter baumannii* and *Escherichia coli* B by a cationic hydrophilic porphyrin at various light wavelengths. Curr Microbiol. 2001;42: 408–414. doi:10.1007/s002840010238
469. Kossakowska-Zwierucho M, Szewczyk G, Sarna T, Nakonieczna J. Farnesol potentiates photodynamic inactivation of *Staphylococcus aureus* with the use of red light-activated porphyrin TMPyP. J Photochem Photobiol B Biol. 2020;206: 111863. doi:https://doi.org/10.1016/j.jphotobiol.2020.111863
470. Allen L, O'Connell A, Kiermer V. How can we ensure visibility and diversity in research contributions? How the Contributor Role Taxonomy (CRediT) is helping the shift from authorship to contributorship. Learn Publ. 2019;32: 71–74.
471. Robertson CA, Evans DH, Abrahamse H. Photodynamic therapy (PDT): A short review on cellular mechanisms and cancer research applications for PDT. Journal of Photochemistry and Photobiology B: Biology. 2009. pp. 1–8. doi:10.1016/j.jphotobiol.2009.04.001
472. Yin R, R. Hamblin M. Antimicrobial Photosensitizers: Drug Discovery Under the Spotlight. Curr Med Chem. 2015;22: 2159–2185. doi:10.2174/0929867322666150319120134
473. Rywkin S, Lenny L, Goldstein J, Geacintov NE, Margolis-Nunno H, Horowitz B. Importance of type I and type II mechanisms in the photodynamic inactivation of viruses in blood with aluminium phthalocyanine derivates. Photochem Photobiol. 1992;56: 463–469. doi:10.1111/j.1751-1097.1992.tb02189.x
474. Lenard J, Vanderoef R. Photoinactivation of influenza virus fusion and infectivity bay rose bengal. Photochem Photobiol. 1993;58: 527–531. doi:10.1111/j.1751-1097.1993.tb04926.x
475. Degar S, Prince AM, Pascual D, Lavie G, Levin B, Mazur Y, et al. Inactivation of the Human Immunodeficiency Virus by Hypericin: Evidence for Photochemical Alterations of p24 and a Block in Uncoating. AIDS Res Hum Retroviruses. 2009;8: 1929–1936. doi:10.1089/aid.1992.8.1929
476. Egyeki M, Turóczy G, Majer Z, Tóth K, Fekete A, Maillard P, et al. Photosensitized inactivation of T7 phage as surrogate of non-enveloped DNA viruses: Efficiency and mechanism of action. Biochim Biophys Acta - Gen Subj. 2003;1624: 115–124. doi:10.1016/j.bbagen.2003.10.003
477. Gábor F, Szolnoki J, Tóth K, Fekete A, Maillard P, Csík G. Photoinduced Inactivation of T7 Phage Sensitized by Symmetrically and Asymmetrically Substituted Tetraphenyl Porphyrin: Comparison of Efficiency and Mechanism of Action. Photochem Photobiol. 2004;73: 304. doi:https://doi.org/10.1562/0031-8655(2001)0730304PIOTPS2.0.CO2
478. Badireddy AR, Hotze EM, Chellam S, Alvarez P, Wiesner MR. Inactivation of bacteriophages via photosensitization of fullerol nanoparticles. Environ Sci Technol. 2007;41: 6627–6632. doi:10.1021/es0708215
479. Pereira Gonzales F, Maisch T. Photodynamic inactivation for controlling *Candida albicans* infections. Fungal Biol. 2012;116: 1–10. doi:10.1016/j.funbio.2011.10.001
480. Quiroga ED, Alvarez MG, Durantini EN. Susceptibility of Candida albicans to photodynamic action of 5,10,15,20-tetra(4-N-methylpyridyl)porphyrin in different media. FEMS Immunol Med Microbiol. 2010;60: 123–131. doi:10.1111/j.1574-695X.2010.00725.x
481. Eichner A, Gonzales FP, Felgenträger A, Regensburger J, Holzmann T, Schneider-Brachert W, et al. Dirty hands: photodynamic killing of human pathogens like EHEC, MRSA and *Candida* within seconds. Photochem Photobiol Sci.

2013;12: 135–147. doi:10.1039/C2PP25164G

482. Gonzales FP, Da Silva SH, Roberts DW, Braga GUL. Photodynamic inactivation of conidia of the fungi *Metarhizium anisopliae* and *Aspergillus nidulans* with methylene blue and toluidine blue. Photochem Photobiol. 2010;86: 653–661. doi:10.1111/j.1751-1097.2009.00689.x
483. Soares BM, Alves OA, Ferreira MVL, Amorim JCF, Sousa GR, De Barros Silveira L, et al. *Cryptococcus gattii*: *In vitro* susceptibility to photodynamic inactivation. Photochem Photobiol. 2011;87: 357–364. doi:10.1111/j.1751-1097.2010.00868.x
484. Gardlo K, Horska Z, Enk CD, Rauch L, Megahed M, Ruzicka T, et al. Treatment of cutaneous leishmaniasis by photodynamic therapy. J Am Acad Dermatol. 2003;48: 893–896. doi:10.1067/mjd.2003.218
485. Horz HP. Archaeal lineages within the human microbiome: Absent, rare or elusive? Life. 2015. pp. 1333–1345. doi:10.3390/life5021333
486. Probst AJ, Auerbach AK, Moissl-Eichinger C. Archaea on Human Skin. PLoS One. 2013;8: e65388. doi:10.1371/journal.pone.0065388
487. Dridi B, Raoult D, Drancourt M. Archaea as emerging organisms in complex human microbiomes. Anaerobe. 2011. pp. 56–63. doi:10.1016/j.anaerobe.2011.03.001
488. Jolivet E, L'Haridon S, Corre E, Forterre P, Prieur D. *Thermococcus gammatolerans* sp. nov., a hyperthermophilic archeon from a deep-sea hydrothermal vent that resists ionizing radiation. Int J Syst Evol Microbiol. 2003;53: 847–851. doi:10.1099/ijs.0.02503-0
489. Schleper C, Pühler G, Klenk HP, Zillig W. *Picrophilus oshimae* and *Picrophilus torridus* fam. nov., gen. nov., sp. nov., two species of hyperacidophilic, thermophilic, heterotrophic, aerobic archaea. Int J Syst Bacteriol. 1996;46: 814–816. doi:10.1099/00207713-46-3-814
490. Mora M, Wink L, Kögler I, Mahnert A, Rettberg P, Schwendner P, et al. Space Station conditions are selective but do not alter microbial characteristics relevant to human health. Nat Commun. 2019;10: 3990. doi:10.1038/s41467-019-11682-z
491. Ranck RO. Some reactions of phenothiazine and its derivatives. Iowa State College. 1957.
492. Harrison FC, Kennedy ME. The red discolouration of cured codfish. Proc R Soc Canada. 1922;5: 101–152.
493. Elazari-Volcani B. Bergey's Manual of Determinative Bacteriology Genus XII *Halobacterium*. Murray, Smith, editors. 1957.
494. Miles AA, Misra SS, Irwin JO. the Estimation of the Bactericidal Power of the Blood. J Hyg (Lond). 1938;38: 732–749. doi:10.1017/S002217240001158X
495. Herigstad B, Hamilton M, Heersink J. How to optimize the drop plate method for enumerating bacteria. J Microbiol Methods. 2001;44: 121–129. doi:10.1016/S0167-7012(00)00241-4
496. Eckl DB, Dengler L, Nemmert M, Eichner A, Bäumler W, Huber H. A Closer Look at Dark Toxicity of the Photosensitizer TMPyP in Bacteria. Photochem Photobiol. 2018;94: 165–172. doi:10.1111/php.12846
497. Bechert T, Steinrücke P, Guggenbichler JP. A new method for screening anti-infective biomaterials. Nature Medicine. 2000. pp. 1053–1056. doi:10.1038/79568
498. Upasani VN, Desai SG, Moldoveanu N, Kates M. Lipids of extremely halophilic archaeobacteria from saline environments in India: A novel glycolipid in *Natronobacterium* strains. Microbiology. 1994;140: 1959–1966. doi:10.1099/13500872-140-8-1959
499. Kate M. Membrane lipids of archaea. New Compr Biochem. 1993;26: 261–295. doi:10.1016/S0167-7306(08)60258-6
500. Oesterhelt D, Stoeckenius W. Rhodopsin-like protein from the purple membrane of *Halobacterium halobium*. Nat New Biol. 1971;233: 149–152. doi:10.1038/newbio233149a0
501. Schobert B, Cupp-Vickery J, Hornak V, Smith SO, Lanyi JK. Crystallographic structure of the K intermediate of bacteriorhodopsin: Conservation of free energy after photoisomerization of the retinal. J Mol Biol. 2002;321: 715–726. doi:10.1016/S0022-2836(02)00681-2
502. Oesterhelt D, Stoeckenius W. Functions of a new photoreceptor membrane. Proc Natl Acad Sci U S A. 1973;70: 2853–2857. doi:10.1073/pnas.70.10.2853
503. Rubio MA, Mártire DO, Braslavsky SE, Lissi EA. Influence of the ionic strength on O2(1Δg) quenching by azide. J Photochem Photobiol A Chem. 1992;66: 153–157. doi:10.1016/1010-6030(92)85209-D
504. Starostin A V, Fedorovich IB, Ostrovskii MA. Photooxidation of rhodopsin. Oxygen consumption and action spectrum. Biofizika. 1988;33: 452–455.
505. Krasnovsky AA, Kagan VE. Photosensitization and quenching of singlet oxygen by pigments and lipids of photoreceptor cells of the retina. FEBS Lett. 1979;108: 152–154. doi:10.1016/0014-5793(79)81198-9
506. Wilkinson F, Helman WP, Ross AB. Rate Constants for the Decay and Reactions of the Lowest Electronically Excited Singlet State of Molecular Oxygen in Solution. An Expanded and Revised Compilation. Am Chem Soc. 1995.
507. Caforio A, Siliakus MF, Exterkate M, Jain S, Jumde VR, Andringa RLH, et al. Converting *Escherichia coli* into an archaebacterium with a hybrid heterochiral membrane. Proc Natl Acad Sci U S A. 2018;115: 3704–3709. doi:10.1073/pnas.1721604115
508. Sumper M. S-Layer Glycoproteins from Moderately and Extremely Halophilic Archaeobacteria. Advances in Bacterial Paracrystalline Surface Layers. 1993. pp. 109–117. doi:10.1007/978-1-4757-9032-0_11
509. Sleytr UB, Pum D, Egelseer EM, Ilk N, Schuster B. S-layer proteins. Handbook of Biofunctional Surfaces. 2013. pp. 507–568.
510. Mescher MF, Strominger JL. Purification and characterization of a prokaryotic glycoprotein from the cell envelope of

Halobacterium salinarium. J Biol Chem. 1976;251: 2005–2014.

511. Cieplik F, Pummer A, Regensburger J, Hiller KA, Späth A, Tabenski L, et al. The impact of absorbed photons on antimicrobial photodynamic efficacy. Front Microbiol. 2015;6. doi:10.3389/fmicb.2015.00706
512. Baier J, Maisch T, Regensburger J, Loibl M, Vasold R, Bäumler W. Time dependence of singlet oxygen luminescence provides an indication of oxygen concentration during oxygen consumption. J Biomed Opt. 2007;12: 064008. doi:10.1117/1.2821153
513. Tang HM, Hamblin MR, Yow CMN. A comparative *in vitro* photoinactivation study of clinical isolates of multidrug-resistant pathogens. J Infect Chemother. 2007;13: 87–91. doi:10.1007/s10156-006-0501-8
514. Pérez-Laguna V, Pérez-Artiaga L, Lampaya-Pérez V, García-Luque I, Ballesta S, Nonell S, et al. Bactericidal effect of photodynamic therapy, alone or in combination with mupirocin or linezolid, on *Staphylococcus aureus*. Front Microbiol. 2017;8. doi:10.3389/fmicb.2017.01002
515. Koskinen K, Pausan MR, Perras AK, Beck M, Bang C, Mora M, et al. First insights into the diverse human archaeome: Specific detection of Archaea in the gastrointestinal tract, lung, and nose and on skin. MBio. 2017;8: e00824-17. doi:10.1128/mBio.00824-17
516. Nkamga VD, Henrissat B, Drancourt M. Archaea: Essential inhabitants of the human digestive microbiota. Human Microbiome Journal. 2017. pp. 1–8. doi:10.1016/j.humic.2016.11.005
517. Lurie-Weinberger MN, Gophna U. Archaea in and on the Human Body: Health Implications and Future Directions. PLoS Pathogens. 2015. p. e1004833. doi:10.1371/journal.ppat.1004833
518. Miller TL, Wolin MJ, De Macario EC, Macario AJL. Isolation of *Methanobrevibacter smithii* from human feces. Appl Environ Microbiol. 1982;43: 227–232.
519. Belay N, Johnson R, Rajagopal BS, De Macario EC, Daniels L. Methanogenic bacteria from human dental plaque. Appl Environ Microbiol. 1988;54: 600–603.
520. Belay N, Mukhopadhyay B, Conway de Macario E, Galask R, Daniels L. Methanogenic bacteria in human vaginal samples. J Clin Microbiol. 1990;28: 1666–1668.
521. Ferrari A, Brusa T, Rutili A, Canzi E, Biavati B. Isolation and characterization of *Methanobrevibacter oralis* sp. nov. Curr Microbiol. 1994;29: 7–12. doi:10.1007/BF01570184
522. Drancourt M, Nkamga VD, Lakhe NA, Régis JM, Dufour H, Fournier PE, et al. Evidence of Archaeal Methanogens in Brain Abscess. Clin Infect Dis. 2017;65: 1–5. doi:10.1093/cid/cix286
523. Bundesministerium für Gesundheit. Verordnung über die Zulassung von Zusatzstoffen zu Lebensmitteln zu technologischen Zwecken (Zusatzstoff- Zulassungsverordnung - ZZulV). Bundesgesetzblatt 1998.
524. Blyth AW. LVI. - The composition of cows' milk in health and disease. Journal of the Chemical Society. 1879. pp. 530–539. doi:10.1039/CT8793500530
525. Morrison PWJ, Connon CJ, Khutoryanskiy V V. Cyclodextrin-mediated enhancement of riboflavin solubility and corneal permeability. Mol Pharm. 2013;10: 756–762. doi:10.1021/mp3005963
526. Schoenen J, Jacquy J, Lenaerts M. Effectiveness of high-dose riboflavin in migraine prophylaxis: A randomized controlled trial. Neurology. 1998;50: 466–470. doi:10.1212/WNL.50.2.466
527. Mueller JH, Hinton J. A Protein-Free Medium for Primary Isolation of the *Gonoeceus* and *Meningococcus*. Proc Soc Exp Biol Med. 1941;48: 330–33. doi:10.3181/00379727-48-13311
528. Thomas O, Cerda V. From Spectra to Qualitative and Quantitative Results. In: Thomas O, Burgess C, editors. UV-Visible Spectrophotometry of Water and Wastewater. Amsterdam: Elsevier B.V.; 2007. pp. 31–33.
529. Fabritius M, Al-Munajjed AA, Freytag C, Jülke H, Zehe M, Lemarchand T, et al. Antimicrobial silver multilayer coating for prevention of bacterial colonization of orthopedic implants. Materials (Basel). 2020;13. doi:10.3390/ma13061415
530. Ahmad I, Vaid FHM. Photochemistry of Flavins in Aqueous and Organic Solvents. In: Silva E, Edwards AM, editors. Flavins: Photochemistry and Photobiology. Cambridge: RSC Publishing; 2007. pp. 13–40. doi:10.1039/9781847555397-00013
531. Ahmad I, Fasihullah Q, Vaid FHM. A study of simultaneous photolysis and photoaddition reactions of riboflavin in aqueous solution. J Photochem Photobiol B Biol. 2004;75: 13–20. doi:10.1016/j.jphotobiol.2004.04.001
532. Gallot S, Thomas O. Fast and easy interpretation of a set of absorption spectra: theory and qualitative applications for UV examination of waters and wastewaters. Fresenius J Anal Chem. 1993. doi:10.1007/BF00322762
533. Berlett BS, Levine RL, Stadtman ER. Use of isosbestic point wavelength shifts to estimate the fraction of a precursor that is converted to a given product. Anal Biochem. 2000. doi:10.1006/abio.2000.4876
534. Poole RK, Bashford CL. Spectrophotometry and Spectrofluorimetry: A Practical Approach. In: Harris DA, Bashford CL, editors. Oxford: IRL Press; 1987. pp. 23–489.
535. Penzkofer A. Reduction-oxidation photocycle dynamics of flavins in starch films. Int J Mol Sci. 2012;13: 9157–9183. doi:10.3390/ijms13079157
536. Kottke T, Heberle J, Hehn D, Dick B, Hegemannt P. Phot-LOV1: Photocycle of a blue-light receptor domain from the green alga *Chlamydomonas reinhardtii*. Biophys J. 2003;84: 1192–1201. doi:10.1016/S0006-3495(03)74933-9
537. Song SH, Dick B, Penzkofer A, Hegemann P. Photo-reduction of flavin mononucleotide to semiquinone form in LOV domain mutants of blue-light receptor phot from *Chlamydomonas reinhardtii*. J Photochem Photobiol B Biol. 2007;87: 37–48. doi:10.1016/j.jphotobiol.2006.12.007
538. Tagliaferri E, Bosset JO, Eberhard P, Bütikofer U, Sieber R. Untersuchung einiger Kriterien zum Nachweis von Veränderungen der Vollmilch nach thermischen und mechanischen Behandlungen sowie nach verschieden langen

Belichtungszeiten. II: Bestimmung des Vitamins B1 mit hilfe eine neuentwickelten RP-HPLC-Methode. Mitteilungen aus dem Gebiete der Leb und Hyg. 1992;83: 435–452.

539. Vaid FHM, Gul W, Faiyaz A, Anwar Z, Ejaz MA, Zahid S, et al. Divalent anion catalyzed photodegradation of riboflavin: A kinetic study. J Photochem Photobiol A Chem. 2019;371: 59–66. doi:10.1016/j.jphotochem.2018.10.048
540. Kainz QM, Späth A, Weiss S, Michl TD, Schätz A, Stark WJ, et al. Magnetic Nanobeads as Support for Zinc(II)-Cyclen Complexes: Selective and Reversible Extraction of Riboflavin. ChemistryOpen. 2012;1: 125–129. doi:10.1002/open.201200008
541. Kuznetsova NA, Makarov DA, Kaliya OL, Vorozhtsov GN. Photosensitized oxidation by dioxygen as the base for drinking water disinfection. J Hazard Mater. 2007;146: 487–491. doi:10.1016/j.jhazmat.2007.04.064
542. Jori G, Magaraggia M, Fabris C, Soncin M, Camerin M, Tallandini L, et al. Photodynamic inactivation of microbial pathogens: Disinfection of water and prevention of water-borne diseases. J Environ Pathol Toxicol Oncol. 2011;30: 261–271. doi:10.1615/JEnvironPatholToxicolOncol.v30.i3.90
543. Engelhardt V, Krammer B, Plaetzer K. Antibacterial photodynamic therapy using water-soluble formulations of hypericin or mTHPC is effective in inactivation of *Staphylococcus aureus*. Photochem Photobiol Sci. 2010;9: 365–369. doi:10.1039/b9pp00144a
544. Lambrechts SAG, Aalders MCG, Van Marle J. Mechanistic study of the photodynamic inactivation of *Candida albicans* by a cationic porphyrin. Antimicrob Agents Chemother. 2005;49: 2026–2034. doi:10.1128/AAC.49.5.2026-2034.2005
545. Tavares A, Carvalho CMB, Faustino MA, Neves MGPMS, Tomé JPC, Tomé AC, et al. Antimicrobial photodynamic therapy: Study of bacterial recovery viability and potential development of resistance after treatment. Mar Drugs. 2010;8: 91–105. doi:10.3390/md8010091
546. Sato K, Kang WH, Saga K, Sato KT. Biology of sweat glands and their disorders. I. Normal sweat gland function. J Am Acad Dermatol. 1989;20: 537–563. doi:10.1016/S0190-9622(89)70063-3
547. Patterson MJ, Galloway SDR, Nimmo MA. Variations in regional sweat composition in normal human males. Exp Physiol. 2000;85: 869–875. doi:10.1111/j.1469-445X.2000.02058.x
548. Yang MY, Chang KC, Chen LY, Hu A. Low-dose blue light irradiation enhances the antimicrobial activities of curcumin against *Propionibacterium acnes*. J Photochem Photobiol B Biol. 2018;189: 21–28. doi:10.1016/j.jphotobiol.2018.09.021
549. Hamblin MR. Polycationic photosensitizer conjugates: effects of chain length and Gram classification on the photodynamic inactivation of bacteria. J Antimicrob Chemother. 2002;49: 941–951. doi:10.1093/jac/dkf053
550. Späth A, Leibl C, Cieplik F, Lehner K, Regensburger J, Hiller KA, et al. Improving photodynamic inactivation of bacteria in dentistry: Highly effective and fast killing of oral key pathogens with novel tooth-colored type-II photosensitizers. J Med Chem. 2014;57: 5157–5168. doi:10.1021/jm4019492
551. Dharmaratne P, Wang B, Wong RCH, Chan BCL, Lau KM, Ke MR, et al. Monosubstituted tricationic Zn(II) phthalocyanine enhances antimicrobial photodynamic inactivation (aPDI) of methicillin-resistant *Staphylococcus aureus* (MRSA) and cytotoxicity evaluation for topical applications: *in vitro* and *in vivo*. Emerg Microbes Infect. 2020; 1–29. doi:10.1080/22221751.2020.1790305
552. Bhavya ML, Umesh Hebbar H. Efficacy of blue LED in microbial inactivation: Effect of photosensitization and process parameters. Int J Food Microbiol. 2019;290: 296–304. doi:10.1016/j.ijfoodmicro.2018.10.021
553. Gsponer NS, Spesia MB, Durantini EN. Effects of divalent cations, EDTA and chitosan on the uptake and photoinactivation of *Escherichia coli* mediated by cationic and anionic porphyrins. Photodiagnosis Photodyn Ther. 2015;12: 67–75. doi:10.1016/j.pdpdt.2014.12.004
554. Huang L, St. Denis TG, Xuan Y, Huang YY, Tanaka M, Zadlo A, et al. Paradoxical potentiation of methylene blue-mediated antimicrobial photodynamic inactivation by sodium azide: Role of ambient oxygen and azide radicals. Free Radic Biol Med. 2012;53: 2062–2071. doi:10.1016/j.freeradbiomed.2012.09.006
555. Huang L, Szewczyk G, Sarna T, Hamblin MR. Potassium Iodide Potentiates Broad-Spectrum Antimicrobial Photodynamic Inactivation Using Photofrin. ACS Infect Dis. 2017;3: 320–328. doi:10.1021/acsinfecdis.7b00004
556. Yuan L, Lyu P, Huang YY, Du N, Qi W, Hamblin MR, et al. Potassium iodide enhances the photobactericidal effect of methylene blue on *Enterococcus faecalis* as planktonic cells and as biofilm infection in teeth. J Photochem Photobiol B Biol. 2020;203: 111730. doi:10.1016/j.jphotobiol.2019.111730
557. Watts RJ, Kong S, Orr MP, Miller GC, Henry BE. Photocatalytic inactivation of coliform bacteria and viruses in secondary wastewater effluent. Water Res. 1995;29: 95–100. doi:https://doi.org/10.1016/0043-1354(94)E0122-M
558. Santos MRE, Mendonça P V, Branco R, Sousa R, Dias C, Serra AC, et al. Light-Activated Antimicrobial Surfaces Using Industrial Varnish Formulations to Mitigate the Incidence of Nosocomial Infections. ACS Appl Mater Interfaces. 2021;13: 7567–7579. doi:10.1021/acsami.0c18930
559. Corrêa TQ, Blanco KC, Garcia ÉB, Perez SML, Chianfrone DJ, Morais VS, et al. Effects of ultraviolet light and curcumin-mediated photodynamic inactivation on microbiological food safety: A study in meat and fruit. Photodiagnosis Photodyn Ther. 2020;30: 101678. doi:https://doi.org/10.1016/j.pdpdt.2020.101678
560. Penha CB, Bonin E, da Silva AF, Hioka N, Zanqueta ÉB, Nakamura TU, et al. Photodynamic inactivation of foodborne and food spoilage bacteria by curcumin. LWT - Food Sci Technol. 2017;76: 198–202. doi:https://doi.org/10.1016/j.lwt.2016.07.037
561. Foschi F, Fontana CR, Ruggiero K, Riahi R, Vera A, Doukas AG, et al. Photodynamic inactivation of *Enterococcus faecalis* in dental root canals *in vitro*. Lasers Surg Med. 2007;39: 782–787. doi:https://doi.org/10.1002/lsm.20579

562. Santezi C, Tanomaru JMG, Bagnato VS, Júnior OBO, Dovigo LN. Potential of curcumin-mediated photodynamic inactivation to reduce oral colonization. Photodiagnosis Photodyn Ther. 2016;15: 46–52. doi:https://doi.org/10.1016/j.pdpdt.2016.04.006
563. Majiya H, Chowdhury KF, Stonehouse NJ, Millner P. TMPyP functionalised chitosan membrane for efficient sunlight driven water disinfection. J Water Process Eng. 2019;30: 100475. doi:https://doi.org/10.1016/j.jwpe.2017.08.013
564. Eckl DB, Eben SS, Schottenhaml L, Eichner A, Vasold R, Späth A, et al. Interplay of phosphate and carbonate ions with flavin photosensitizers in photodynamic inactivation of bacteria. PLoS One. 2021;16: e0253212. Available: https://doi.org/10.1371/journal.pone.0253212
565. Kuznetsova NA, Kaliya OL. Photodynamic water disinfection. Russ J Gen Chem. 2015;85: 321–332. doi:10.1134/S1070363215010466
566. Lesar A, Begić G, Malatesti N, Gobin I. Innovative approach in *Legionella* water treatment with photodynamic cationic amphiphilic porphyrin. Water Supply. 2019;19: 1473–1479. doi:10.2166/ws.2019.012
567. USGS. Hardness of Water.
568. Gesetz über die Umweltverträglichkeit von Wasch- und Reinigungsmitteln. Bundesgesetzblatt. 2013;1: 2539–2542.
569. Sjörs H, Gunnarsson U. Calcium and pH in north and central Swedish mire waters. J Ecol. 2002;90: 650–657. doi:https://doi.org/10.1046/j.1365-2745.2002.00701.x
570. Azoulay A, Garzon P, Eisenberg MJ. Comparison of the mineral content of tap water and bottled waters. J Gen Intern Med. 2001;16: 168–175. doi:10.1111/j.1525-1497.2001.04189.x
571. Olajire AA, Imeokparia FE. Water Quality Assessment of Osun River: Studies on Inorganic Nutrients. Environ Monit Assess. 2001;69: 17–28. doi:10.1023/A:1010796410829
572. Kumar A, Roberts D, Wood KE, Light B, Parrillo JE, Sharma S, et al. Duration of hypotension before initiation of effective antimicrobial therapy is the critical determinant of survival in human septic shock. Crit Care Med. 2006;34: 1589–1596. doi:10.1097/01.CCM.0000217961.75225.E9
573. Kumar M, Singh S, Mahajan RK. Trace Level Determination of U, Zn, Cd, Pb and Cu in Drinking Water Samples. Environ Monit Assess. 2006;112: 283–292. doi:10.1007/s10661-006-1069-6
574. Al-Saleh I, Al-Doush I. Survey of trace elements in household and bottled drinking water samples collected in Riyadh, Saudi Arabia. Sci Total Environ. 1998;216: 181–192. doi:https://doi.org/10.1016/S0048-9697(98)00137-5
575. Rylander R, Bonevik H, Rubenowitz E. Magnesium and calcium in drinking water and cardiovascular mortality. Scand J Work Environ Health. 1991;17: 91–94. Available: http://www.jstor.org/stable/40965866
576. Rubenowitz E, Axelsson G, Rylander R. Magnesium in drinking water and body magnesium status measured using an oral loading test. Scand J Clin Lab Invest. 1998;58: 423–428. doi:10.1080/00365519850186409
577. Rubenowitz E, Axelsson G, Rylander R. Magnesium in drinking water and death from acute myocardial infarction. Am J Epidemiol. 1996;143: 456–462.
578. Flaten TP, Bølviken B. Geographical associations between drinking water chemistry and the mortality and morbidity of cancer and some other diseases in Norway. Sci Total Environ. 1991;102: 75–100.
579. Peder Flaten T. A nation-wide survey of the chemical composition of drinking water in Norway. Sci Total Environ. 1991;102: 35–73. doi:https://doi.org/10.1016/0048-9697(91)90307-Z
580. Maheswaran R, Morris S, Falconer S, Grossinho A, Perry I, Wakefield J, et al. Magnesium in drinking water supplies and mortality from acute myocardial infarction in north west England. Heart. 1999;82: 455 LP – 460. doi:10.1136/hrt.82.4.455
581. Leary Reyes, AJ, Lockett, CJ, Arbuckle, DD & van der Byl, K WP. Magnesium and deaths ascribed to ischaemic heart disease in South Africa-a preliminary report. South African Med J. 1983;64: 775–776.
582. Tang J, Tang G, Niu J, Yang J, Zhou Z, Gao Y, et al. Preparation of a Porphyrin Metal–Organic Framework with Desirable Photodynamic Antimicrobial Activity for Sustainable Plant Disease Management. J Agric Food Chem. 2021;69: 2382–2391. doi:10.1021/acs.jafc.0c06487
583. Jesus V, Martins D, Branco T, Valério N, Neves MGPMS, Faustino MAF, et al. An insight into the photodynamic approach versus copper formulations in the control of *Pseudomonas syringae pv. actinidiae* in kiwi plants. Photochem Photobiol Sci. 2018;17: 180–191. doi:10.1039/C7PP00300E
584. Martins D, Mesquita MQ, Neves MGPMS, Faustino MAF, Reis L, Figueira E, et al. Photoinactivation of *Pseudomonas syringae pv. actinidiae* in kiwifruit plants by cationic porphyrins. Planta. 2018;248: 409–421. doi:10.1007/s00425-018-2913-y
585. Armstrong T V. Variations in the Gross Composition of Milk as Related to the Breed of the Cow: A Review and Critical Evaluation of Literature of the United States and Canada1. J Dairy Sci. 1959;42: 1–19. doi:https://doi.org/10.3168/jds.S0022-0302(59)90518-1
586. Hibbs JW. Principles of dairy chemistry (Jenness, Robert; Patton, Stuart). J Chem Educ. 1960;37: 274. doi:10.1021/ed037p274.4
587. Posati, Linda P, Orr, Martha L. Composition of Foods - Dairy and Egg Products - Raw - Processed - Prepared. Washington, DC: United States Department of Agriculture; 1976.
588. Ragàs X, Dai T, Tegos GP, Agut M, Nonell S, Hamblin MR. Photodynamic inactivation of *Acinetobacter baumannii* using phenothiazinium dyes: *In vitro* and *in vivo* studies. Lasers Surg Med. 2010;42: 384–390. doi:10.1002/lsm.20922
589. Robinson S, Robinson AH. Chemical composition of sweat. Physiol Rev. 1954;34: 202–220. doi:10.1152/physrev.1954.34.2.202
590. Foster KG. Relation between the colligative properties and chemical composition of sweat. J Physiol. 1961;155: 490–

497. doi:10.1113/jphysiol.1961.sp006641
591. Wilkinson F, Helman WP, Ross AB. Rate Constants for the Decay and Reactions of the Lowest Electronically Excited Singlet State of Molecular Oxygen in Solution. An Expanded and Revised Compilation. J Phys Chem Ref Data. 1995;24: 663–677. doi:10.1063/1.555965
592. Zamadar M, Orr C, Uherek M. Water Soluble Cationic Porphyrin Sensor for Detection of Hg^{2+}, Pb^{2+}, Cd^{2+}, and Cu^{2+}. Khan SB, editor. J Sensors. 2016;2016: 1905454. doi:10.1155/2016/1905454
593. Li J, Wei Y, Guo L, Zhang C, Jiao Y, Shuang S, et al. Study on spectroscopic characterization of Cu porphyrin/Co porphyrin and their interactions with ctDNA. Talanta. 2008;76: 34–39. doi:https://doi.org/10.1016/j.talanta.2008.01.065
594. Igarashi S, Suzuki H, Yotsuyanagi T. The equilibrium constants of cadmium (II)-, lead (II)-, magnesium (II)-, and zinc (II)-α, β, γ, δ-tetrakis (1-methylpyridinium-4-yl) porphine complexes. Talanta. 1995;42: 1171–1177.
595. Gouterman M. Spectra of porphyrins. J Mol Spectrosc. 1961;6: 138–163. doi:https://doi.org/10.1016/0022-2852(61)90236-3
596. Di Costanzo L, Geremia S, Randaccio L, Purrello R, Lauceri R, Sciotto D, et al. Calixarene–Porphyrin Supramolecular Complexes: pH-Tuning of the Complex Stoichiometry. Angew Chemie Int Ed. 2001;40: 4245–4247. doi:https://doi.org/10.1002/1521-3773(20011119)40:22<4245::AID-ANIE4245>3.0.CO;2-#
597. Wolak M, van Eldik R. pH Controls the Rate and Mechanism of Nitrosylation of Water-Soluble FeIII Porphyrin Complexes. J Am Chem Soc. 2005;127: 13312–13315. doi:10.1021/ja052855n
598. Fleischer EB, Choi EI, Hambright P, Stone A. Porphyrin studies: kinetics of metalloporphyrin formation. Inorg Chem. 1964;3: 1284–1287.
599. Caughey WS, Deal RM, McLees BD, Alben JO. Species equilibria in nickel (II) porphyrin solutions: Effect of porphyrin structure, solvent and temperature. J Am Chem Soc. 1962;84: 1735–1736.
600. Seth J, Palaniappan V, Bocian DF. Oxidation of nickel (II) tetraphenylporphyrin revisited. Characterization of stable nickel (III) complexes at room temperature. Inorg Chem. 1995;34: 2201–2206.
601. Lazzeri D, Rovera M, Pascual L, Durantini EN. Photodynamic Studies and Photoinactivation of *Escherichia coli* Using meso-Substituted Cationic Porphyrin Derivatives with Asymmetric Charge Distribution. Photochem Photobiol. 2004;80: 286–293. doi:10.1562/2004-03-08-ra-105.1
602. Mahajan PG, Dige NC, Vanjare BD, Phull AR, Kim SJ, Hong S-K, et al. Synthesis, photophysical properties and application of new porphyrin derivatives for use in photodynamic therapy and cell imaging. J Fluoresc. 2018;28: 871–882.
603. Pasternack RF, Huber PR, Boyd P, Engasser G, Francesconi L, Gibbs E, et al. Aggregation of meso-substituted water-soluble porphyrins. J Am Chem Soc. 1972;94: 4511–4517. doi:10.1021/ja00768a016
604. Frederiksen PK, McIlroy SP, Nielsen CB, Nikolajsen L, Skovsen E, Jørgensen M, et al. Two-Photon Photosensitized Production of Singlet Oxygen in Water. J Am Chem Soc. 2005;127: 255–269. doi:10.1021/ja0452020
605. Usui Y, Kamogawa K. A Standard System To Determine The Quantum Yield Of Singlet Oxygen Formation In Aqueous Solution. Photochem Photobiol. 1974;19.
606. Li W, Huang S, Liu X, Leet JE, Cantone JL, Lam KS. N-Demethylation of nocathiacin I via photo-oxidation. Bioorg Med Chem Lett. 2008;18: 4051–4053. doi:https://doi.org/10.1016/j.bmcl.2008.05.112
607. Zhang T, Oyama T ki, Horikoshi S, Hidaka H, Zhao J, Serpone N. Photocatalyzed N-demethylation and degradation of methylene blue in titania dispersions exposed to concentrated sunlight. Sol Energy Mater Sol Cells. 2002;73: 287–303. doi:https://doi.org/10.1016/S0927-0248(01)00215-X
608. Hirakawa K. Fluorometry of singlet oxygen generated via a photosensitized reaction using folic acid and methotrexate. Anal Bioanal Chem. 2009;393: 999–1005. doi:10.1007/s00216-008-2522-x
609. Cotruvo J, Bartram J. Calcium and Magnesium in Drinking-water : Public health significance. Geneva; 2009.
610. Cabral JPS. Water microbiology. Bacterial pathogens and water. Int J Environ Res Public Health. 2010/10/15. 2010;7: 3657–3703. doi:10.3390/ijerph7103657
611. George S, Hamblin MR, Kishen A. Uptake pathways of anionic and cationic photosensitizers into bacteria. Photochem Photobiol Sci. 2009/03/31. 2009;8: 788–795. doi:10.1039/b809624d
612. Hancock REW. Alterations In Outer Membrane Permeability. Annu Rev Microbiol. 1984;38: 237–264. doi:10.1146/annurev.mi.38.100184.001321
613. Finnegan S, Percival SL. EDTA: An Antimicrobial and Antibiofilm Agent for Use in Wound Care. Adv Wound Care. 2014;4: 415–421. doi:10.1089/wound.2014.0577
614. Bertolini G, Rossi F, Valduga G, Jori G, Van Lier J. Photosensitizing activity of water- and lipid-soluble phthalocyanines on *Escherichia coli*. FEMS Microbiol Lett. 1990;71: 149–155. doi:10.1111/j.1574-6968.1990.tb03814.x
615. Doyle RJ, Matthews TH, Streips UN. Chemical basis for selectivity of metal ions by the *Bacillus subtilis* cell wall. J Bacteriol. 1980;143: 471–480. doi:10.1128/jb.143.1.471-480.1980
616. Yee N, Fowle DA, Ferris FG. A Donnan potential model for metal sorption onto *Bacillus subtilis*. Geochim Cosmochim Acta. 2004;68: 3657–3664.
617. Thomas 3rd KJ, Rice C V. Revised model of calcium and magnesium binding to the bacterial cell wall. Biometals. 2014/10/15. 2014;27: 1361–1370. doi:10.1007/s10534-014-9797-5
618. Garner JS, Jarvis WR, Emori TG, Horan TC, Hughes JM. CDC definitions for nosocomial infections, 1988. AJIC Am J Infect Control. 1988;16: 128–140. doi:10.1016/0196-6553(88)90053-3
619. Allegranzi B, Nejad SB, Combescure C, Graafmans W, Attar H, Donaldson L, et al. Burden of endemic health-care-

associated infection in developing countries: systematic review and meta-analysis. Lancet. 2011;377: 228–241. doi:https://doi.org/10.1016/S0140-6736(10)61458-4

620. Mehta Y, Gupta A, Todi S, Myatra SN, Samaddar DP, Patil V, et al. Guidelines for prevention of hospital acquired infections. Indian J Crit Care Med. 2014;18: 149–163. doi:10.4103/0972-5229.128705
621. Klein EY, Milkowska-Shibata M, Tseng KK, Sharland M, Gandra S, Pulcini C, et al. Assessment of WHO antibiotic consumption and access targets in 76 countries, 2000–15: an analysis of pharmaceutical sales data. Lancet Infect Dis. 2021;21: 107–115. doi:https://doi.org/10.1016/S1473-3099(20)30332-7
622. Hamblin MR. Antimicrobial photodynamic inactivation: a bright new technique to kill resistant microbes. Curr Opin Microbiol. 2016;33: 67–73. doi:10.1016/j.mib.2016.06.008
623. Ergaieg K, Seux R. A comparative study of the photoinactivation of bacteria by meso-substituted cationic porphyrin, rose Bengal and methylene blue. Desalination. 2009;246: 353–362. doi:10.1016/j.desal.2008.03.060
624. Humphreys H. Self-disinfecting and microbiocide-impregnated surfaces and fabrics: What potential in interrupting the spread of healthcare-associated infection? Clin Infect Dis. 2014;58: 848–853. doi:10.1093/cid/cit765
625. Baigorria E, Durantini JE, Martínez SR, Milanesio ME, Palacios YB, Durantini AM. Potentiation Effect of Iodine Species on the Antimicrobial Capability of Surfaces Coated with Electroactive Phthalocyanines. ACS Appl Bio Mater. 2021;4: 8559–8570. doi:10.1021/acsabm.1c01029
626. Rosenberg M, Ilić K, Juganson K, Ivask A, Ahonen M, Vrček IV, et al. Potential ecotoxicological effects of antimicrobial surface coatings: a literature survey backed up by analysis of market reports. PeerJ. 2019;7: e6315.
627. Tabenski I, Cieplik F, Tabenski L, Regensburger J, Hiller K-A, Buchalla W, et al. The impact of cationic substituents in phenalen-1-one photosensitizers on antimicrobial photodynamic efficacy. Photochem Photobiol Sci. 2016;15: 57. doi:10.1039/c5pp00262a
628. Muehler D, Sommer K, Wennige S, Hiller K-A, Cieplik F, Maisch T, et al. Light-activated phenalen-1-one bactericides: efficacy, toxicity and mechanism compared with benzalkonium chloride. Future Microbiol. 2017;12: 1297–1310. doi:10.2217/fmb-2016-0229
629. Cieplik F, Wimmer F, Muehler D, Thurnheer T, Belibasakis GN, Hiller K-A, et al. Phenalen-1-one-mediated antimicrobial photodynamic therapy and chlorhexidine applied to a novel caries biofilm model. Caries Res. 2018;52: 447–453.
630. Rossi G, Goi D, Comuzzi C. The photodynamic inactivation of *Staphylococcus aureus* in water using visible light with a new expanded porphyrin. J Water Health. 2012;10: 390–399. doi:10.2166/wh.2012.034
631. Obara H, Takeuchi M, Kawakubo H, Shinoda M, Okabayashi K, Hayashi K, et al. Aqueous olanexidine versus aqueous povidone-iodine for surgical skin antisepsis on the incidence of surgical site infections after clean-contaminated surgery: a multicentre, prospective, blinded-endpoint, randomised controlled trial. Lancet Infect Dis. 2020;20: 1281–1289. doi:https://doi.org/10.1016/S1473-3099(20)30225-5
632. Krishna BVS, Gibb AP. Use of octenidine dihydrochloride in meticillin-resistant *Staphylococcus aureus* decolonisation regimens: a literature review. J Hosp Infect. 2010;74: 199–203. doi:https://doi.org/10.1016/j.jhin.2009.08.022
633. Williamson DA, Carter GP, Howden BP. Current and emerging topical antibacterials and antiseptics: agents, action, and resistance patterns. Clin Microbiol Rev. 2017;30: 827–860.
634. Boretti A, Rosa L. Reassessing the projections of the world water development report. NPJ Clean Water. 2019;2: 1–6.
635. Li X-F, Mitch WA. Drinking Water Disinfection Byproducts (DBPs) and Human Health Effects: Multidisciplinary Challenges and Opportunities. Environ Sci Technol. 2018;52: 1681–1689. doi:10.1021/acs.est.7b05440
636. Lambrechts SAG, Aalders MCG, Langeveld-Klerks DH, Khayali Y, Lagerberg JWM. Effect of Monovalent and Divalent Cations on the Photoinactivation of Bacteria with meso-Substituted Cationic Porphyrins. Photochem Photobiol. 2004;79: 297. doi:10.1562/sa-03-15.1
637. Kato N, Ohta M, Kido N, Ito H, Naito S. Formation of a Hexagonal Lattice Structure by an R-Form Lipopolysaccharide of *Klebsiella* sp. Microbiol Immunol. 1988;32: 481–490. doi:10.1111/j.1348-0421.1988.tb01408.x
638. Rojas ER, Billings G, Odermatt PD, Auer GK, Zhu L, Miguel A, et al. The outer membrane is an essential load-bearing element in Gram-negative bacteria. Nature. 2018;559: 617–621. doi:10.1038/s41586-018-0344-3
639. Schaal S, Kunsch K, Kunsch S. Der Mensch in Zahlen. Der Mensch in Zahlen. 2016. doi:10.1007/978-3-642-55399-8
640. Callewaert C, Buysschaert B, Vossen E, Fievez V, Van de Wiele T, Boon N. Artificial sweat composition to grow and sustain a mixed human axillary microbiome. J Microbiol Methods. 2014;103: 6–8. doi:10.1016/j.mimet.2014.05.005
641. REWAG. Unser Trinkwasser und seine Bestandteile.
642. Hartman PE, Hartman Z, Ault KT. Scavening of singlet molecular oxygen by imidazole compounds: high and sustained activities of carboxy terminal histidine dipeptides and exceptional activity of imidazole-4-acetic acid. Photochem Photobiol. 1990;51: 59–66. doi:10.1111/j.1751-1097.1990.tb01684.x
643. Hu J, Lin S, Tan BK, Hamzah SS, Lin Y, Kong Z, et al. Photodynamic inactivation of *Burkholderia cepacia* by curcumin in combination with EDTA. Food Res Int. 2018;111: 265–271. doi:https://doi.org/10.1016/j.foodres.2018.05.042
644. Nima G, Soto-Montero J, Alves LA, Mattos-Graner RO, Giannini M. Photodynamic inactivation of *Streptococcus mutans* by curcumin in combination with EDTA. Dent Mater. 2021;37: e1–e14. doi:https://doi.org/10.1016/j.dental.2020.09.015
645. Maisch T, Wagner J, Papastamou V, Nerl H-J, Hiller K-A, Szeimies R-M, et al. Combination of 10% EDTA, Photosan, and a blue light hand-held photopolymerizer to inactivate leading oral bacteria in dentistry *in vitro*. J Appl Microbiol. 2009;107: 1569–1578. doi:https://doi.org/10.1111/j.1365-2672.2009.04342.x

646. Khan A, Vu KD, Riedl B, Lacroix M. Optimization of the antimicrobial activity of nisin, Na-EDTA and pH against gram-negative and gram-positive bacteria. LWT - Food Sci Technol. 2015;61: 124–129. doi:https://doi.org/10.1016/j.lwt.2014.11.035
647. Mastromatteo M, Lucera A, Sinigaglia M, Corbo MR. Synergic Antimicrobial Activity of Lysozyme, Nisin, and EDTA against *Listeria Monocytogenes* in Ostrich Meat Patties. J Food Sci. 2010;75: M422–M429. doi:https://doi.org/10.1111/j.1750-3841.2010.01732.x
648. Sawer IK, Berry MI, Ford JL. Effect of medium composition, agitation and the presence of EDTA on the antimicrobial activity of cryptolepine. Lett Appl Microbiol. 1997;25: 207–211. doi:https://doi.org/10.1046/j.1472-765X.1997.00206.x
649. Guardabassi L, Ghibaudo G, Damborg P. *In vitro* antimicrobial activity of a commercial ear antiseptic containing chlorhexidine and Tris–EDTA. Vet Dermatol. 2010;21: 282–286. doi:https://doi.org/10.1111/j.1365-3164.2009.00812.x
650. Jalil A, Asim MH, Akkus ZB, Schoenthaler M, Matuszczak B, Bernkop-Schnürch A. Self-emulsifying drug delivery systems comprising chlorhexidine and alkyl-EDTA: A novel approach for augmented antimicrobial activity. J Mol Liq. 2019;295: 111649. doi:https://doi.org/10.1016/j.molliq.2019.111649
651. Lambert RJW, Hanlon GW, Denyer SP. The synergistic effect of EDTA/antimicrobial combinations on *Pseudomonas aeruginosa*. J Appl Microbiol. 2004;96: 244–253. doi:https://doi.org/10.1046/j.1365-2672.2004.02135.x
652. Bertoloni G, Salvato B, Dall'Acqua M, Vazzoler M, Jori G. HEMATOPORPHYRIN-SENSITIZED PHOTOINACTIVATION OF *Streptococcus faecalis*. Photochem Photobiol. 1984;39: 811–816. doi:https://doi.org/10.1111/j.1751-1097.1984.tb08864.x
653. Birdsell DC, Cota-Robles EH. Production and ultrastructure of lysozyme and ethylenediaminetetraacetate-lysozyme spheroplasts of *Escherichia coli*. J Bacteriol. 1967;93: 427–437. doi:10.1128/jb.93.1.427-437.1967
654. Costerton W, Cecil J, Forsberg I, Matula Tibor A, Buckmire FL, MacLeod Robert A. Nutrition and Metabolism of Marine Bacteria XVI. Formation of Protoplasts, Spheroplasts, and Related Forms from a Gram-negative Marine Bacterium. J Bacteriol. 1967;94: 1764–1777. doi:10.1128/jb.94.5.1764-1777.1967
655. Hughes MN, Poole RK. Metal speciation and microbial growth—the hard (and soft) facts. Microbiology. 1991;137: 725–734. doi:https://doi.org/10.1099/00221287-137-4-725
656. Walker GM. The Roles of Magnesium in Biotechnology. Crit Rev Biotechnol. 1994;14: 311–354. doi:10.3109/07388559409063643
657. Clifton LA, Skoda MWA, Le Brun AP, Ciesielski F, Kuzmenko I, Holt SA, et al. Effect of Divalent Cation Removal on the Structure of Gram-Negative Bacterial Outer Membrane Models. Langmuir. 2015;31: 404–412. doi:10.1021/la504407v
658. Lambert PA, Hancock IC, Baddiley J. Influence of alanyl ester residues on the binding of magnesium ions to teichoic acids. Biochem J. 1975;151: 671–676. doi:10.1042/bj1510671
659. Thomas KJ, Rice C V. Equilibrium binding behavior of magnesium to wall teichoic acid. Biochim Biophys Acta - Biomembr. 2015;1848: 1981–1987. doi:https://doi.org/10.1016/j.bbamem.2015.05.003
660. Meyer JL. Formation constants for interaction of citrate with calcium and magnesium lons. Anal Biochem. 1974;62: 295–300. doi:https://doi.org/10.1016/0003-2697(74)90391-1
661. Hamblin MR. Potentiation of antimicrobial photodynamic inactivation by inorganic salts. Expert Rev Anti Infect Ther. 2017;15: 1059–1069. doi:10.1080/14787210.2017.1397512
662. de Freitas LM, Lorenzón EN, Santos-Filho NA, Zago LH de P, Uliana MP, de Oliveira KT, et al. Antimicrobial Photodynamic therapy enhanced by the peptide aurein 1.2. Sci Rep. 2018;8: 4212. doi:10.1038/s41598-018-22687-x
663. Zhou J, Qi G-B, Wang H. A purpurin-peptide derivative for selective killing of Gram-positive bacteria via insertion into cell membrane. J Mater Chem B. 2016;4: 4855–4861. doi:10.1039/C6TB00406G
664. Ford TE. Microbiological safety of drinking water: United States and global perspectives. Environ Health Perspect. 1999;107: 191–206. doi:10.1289/ehp.99107s1191
665. Lesar A, Mušković M, Begić G, Lončarić M, Tomić Linšak D, Malatesti N, et al. Cationic Porphyrins as Effective Agents in Photodynamic Inactivation of Opportunistic Plumbing Pathogen *Legionella pneumophila*. International Journal of Molecular Sciences. 2020. doi:10.3390/ijms21155367
666. Abat C, Fournier P-E, Jimeno M-T, Rolain J-M, Raoult D. Extremely and pandrug-resistant bacteria extra-deaths: myth or reality? Eur J Clin Microbiol Infect Dis. 2018;37: 1687–1697. doi:10.1007/s10096-018-3300-0
667. World Bank. Drug-Resistant Infections: A Threat to Our Economic Future. Washington, DC; 2017.
668. Tenover FC, McGowan JE. Reasons for the Emergence of Antibiotic Resistance. Am J Med Sci. 1996;311: 9–16. doi:https://doi.org/10.1016/S0002-9629(15)41625-8
669. Lewis MAO. Why we must reduce dental prescription of antibiotics: European Union Antibiotic Awareness Day. Br Dent J. 2008;205: 537–538. doi:10.1038/sj.bdj.2008.984
670. Gross M. Antibiotics in crisis. Curr Biol. 2013;23: R1063–R1065. doi:https://doi.org/10.1016/j.cub.2013.11.057
671. Laxminarayan R, Heymann DL. Challenges of drug resistance in the developing world. BMJ Br Med J. 2012;344: e1567. doi:10.1136/bmj.e1567
672. Clarke T. Drug companies snub antibiotics as pipeline threatens to run dry. Nature. 2003. p. 225. doi:10.1038/425225a
673. Forsyth C. Repairing the antibiotic pipeline: can the gain act do it. Wash JL Tech Arts. 2013;9: 1.
674. Maisch T, Hackbarth S, Regensburger J, Felgenträger A, Bäumler W, Landthaler M, et al. Photodynamic inactivation of multi-resistant bacteria (PIB)–a new approach to treat superficial infections in the 21st century. JDDG J der Dtsch Dermatologischen Gesellschaft. 2011;9: 360–366.
675. Gulías Ò, McKenzie G, Bayó M, Agut M, Nonell S. Effective photodynamic inactivation of 26 *Escherichia coli* strains with different antibiotic susceptibility profiles: A planktonic and biofilm study. Antibiotics. 2020;9: 98.

676. Dai T, Tegos GP, Zhiyentayev T, Mylonakis E, Hamblin MR. Photodynamic therapy for methicillin-resistant *Staphylococcus aureus* infection in a mouse skin abrasion model. Lasers Surg Med Off J Am Soc Laser Med Surg. 2010;42: 38–44.
677. Novaes AB, Schwartz-Filho HO, de Oliveira RR, Feres M, Sato S, Figueiredo LC. Antimicrobial photodynamic therapy in the non-surgical treatment of aggressive periodontitis: microbiological profile. Lasers Med Sci. 2012;27: 389–395. doi:10.1007/s10103-011-0901-6
678. Dai T, Tegos George P, Zongshun L, Liyi H, Timur Z, J. FM, et al. Photodynamic Therapy for Acinetobacter baumannii Burn Infections in Mice. Antimicrob Agents Chemother. 2009;53: 3929–3934. doi:10.1128/AAC.00027-09
679. Thasler WE, Weiss TS, Schillhorn K, Stoll P-T, Irrgang B, Jauch K-W. Charitable state-controlled foundation human tissue and cell research: ethic and legal aspects in the supply of surgically removed human tissue for research in the academic and commercial sector in Germany. Cell Tissue Bank. 2003;4: 49–56.
680. Neumann RA, Leonhartsberger H, Pieczkowski F, Knobler RM, Gebhart W. Accurate Histochemical Definition of Argon-Laser-Induced Tissue Necrosis. Dermatology. 1992;184: 202–204. doi:10.1159/000247541
681. Maisch T. Resistance in antimicrobial photodynamic inactivation of bacteria. Photochem Photobiol Sci. 2015;14: 1518–1526. doi:10.1039/c5pp00037h
682. Amin RM, Bhayana B, Hamblin MR, Dai T. Antimicrobial blue light inactivation of *Pseudomonas aeruginosa* by photo-excitation of endogenous porphyrins: *In vitro* and *in vivo* studies. Lasers Surg Med. 2016;48: 562–568.
683. Zhang Y, Zhu Y, Gupta A, Huang Y, Murray CK, Vrahas MS, et al. Antimicrobial blue light therapy for multidrug-resistant *Acinetobacter baumannii* infection in a mouse burn model: implications for prophylaxis and treatment of combat-related wound infections. J Infect Dis. 2014;209: 1963–1971.
684. Cassidy CM, Donnelly RF, Tunney MM. Effect of sub-lethal challenge with Photodynamic Antimicrobial Chemotherapy (PACT) on the antibiotic susceptibility of clinical bacterial isolates. J Photochem Photobiol B Biol. 2010;99: 62–66. doi:10.1016/j.jphotobiol.2010.02.004
685. Thomas P. Long-Term Survival of *Bacillus* Spores in Alcohol and Identification of 90% Ethanol as Relatively More Spori/Bactericidal. Curr Microbiol. 2012;64: 130–139. doi:10.1007/s00284-011-0040-0
686. Bloomfield SF, Arthur M. Mechanisms of inactivation and resistance of spores to chemical biocides. J Appl Bacteriol. 1994;76: 91S-104S.
687. Loshon CA, Genest PC, Setlow B, Setlow P. Formaldehyde kills spores of *Bacillus subtilis* by DNA damage and small, acid-soluble spore proteins of the αααααααα/ββββββββ-type protect spores against this DNA damage. J Appl Microbiol. 1999;87: 8–14.
688. Marquis RE, Shin SY. Mineralization and responses of bacterial spores to heat and oxidative agents. FEMS Microbiol Rev. 1994;14: 375–379. doi:10.1111/j.1574-6976.1994.tb00111.x
689. Gerald M, Denver RA. Antiseptics and Disinfectants: Activity, Action, and Resistance. Clin Microbiol Rev. 1999;12: 147–179. doi:10.1128/CMR.12.1.147
690. Popham DL, Sengupta S, Setlow P. Heat, hydrogen peroxide, and UV resistance of *Bacillus subtilis* spores with increased core water content and with or without major DNA-binding proteins. Appl Environ Microbiol. 1995;61: 3633–3638. doi:10.1128/aem.61.10.3633-3638.1995
691. Riesenman P, Nicholson W. Role of the Spore Coat Layers in Bacillus subtilis Spore Resistance to Hydrogen Peroxide, Artificial UV-C, UV-B, and Solar UV Radiation. Appl Environ Microbiol. 2000;66: 620–626. doi:10.1128/AEM.66.2.620-626.2000
692. Russell AD. Bacterial spores and chemical sporicidal agents. Clin Microbiol Rev. 1990;3: 99–119. doi:10.1128/CMR.3.2.99
693. Tennen R, Setlow B, Davis KL, Loshon CA, Setlow P. Mechanisms of killing of spores of *Bacillus subtilis* by iodine, glutaraldehyde and nitrous acid. J Appl Microbiol. 2000;89: 330–338.
694. da Silva RN, Tome AC, Tome JPC, Neves MG, Faustino MAF, Cavaleiro JAS, et al. Photo-inactivation of *Bacillus* endospores: Inter-specific variability of inactivation efficiency. Microbiol Immunol. 2012;56: 692–699.
695. Oliveira A, Almeida A, Carvalho CMB, Tomé JPC, Faustino MAF, Neves M, et al. Porphyrin derivatives as photosensitizers for the inactivation of *Bacillus cereus* endospores. J Appl Microbiol. 2009;106: 1986–1995.
696. Jain J, Arora S, Rajwade JM, Omray P, Khandelwal S, Paknikar KM. Silver Nanoparticles in Therapeutics: Development of an Antimicrobial Gel Formulation for Topical Use. Mol Pharm. 2009;6: 1388–1401. doi:10.1021/mp900056g
697. Thomas V, Yallapu MM, Sreedhar B, Bajpai SK. A versatile strategy to fabricate hydrogel–silver nanocomposites and investigation of their antimicrobial activity. J Colloid Interface Sci. 2007;315: 389–395. doi:https://doi.org/10.1016/j.jcis.2007.06.068
698. Boonkaew B, Kempf M, Kimble R, Supaphol P, Cuttle L. Antimicrobial efficacy of a novel silver hydrogel dressing compared to two common silver burn wound dressings: Acticoat™ and PolyMem Silver®. Burns. 2014;40: 89–96. doi:https://doi.org/10.1016/j.burns.2013.05.011
699. Zakia M, Koo JM, Kim D, Ji K, Huh P, Yoon J, et al. Development of silver nanoparticle-based hydrogel composites for antimicrobial activity. Green Chem Lett Rev. 2020;13: 34–40. doi:10.1080/17518253.2020.1725149
700. Li Z, Cai Z, Cai Z, Zhang Y, Fu T, Jin Y, et al. Molecular genetic analysis of an XDR *Pseudomonas aeruginosa* ST664 clone carrying multiple conjugal plasmids. J Antimicrob Chemother. 2020;75: 1443–1452.
701. Andrade LN, Siqueira TES, Martinez R, Darini ALC. Multidrug-Resistant CTX-M-(15, 9, 2)- and KPC-2-Producing *Enterobacter hormaechei* and *Enterobacter asburiae* Isolates Possessed a Set of Acquired Heavy Metal Tolerance Genes

Including a Chromosomal *sil* Operon (for Acquired Silver Resis. Frontiers in Microbiology. 2018. Available: https://www.frontiersin.org/article/10.3389/fmicb.2018.00539

702. Kaweeteerawat C, Na Ubol P, Sangmuang S, Aueviriyavit S, Maniratanachote R. Mechanisms of antibiotic resistance in bacteria mediated by silver nanoparticles. J Toxicol Environ Heal Part A. 2017;80: 1276–1289. doi:10.1080/15287394.2017.1376727
703. Panáček A, Kvítek L, Smékalová M, Večeřová R, Kolář M, Röderová M, et al. Bacterial resistance to silver nanoparticles and how to overcome it. Nat Nanotechnol. 2018;13: 65–71. doi:10.1038/s41565-017-0013-y
704. Deshpande LM, Chopade BA. Plasmid mediated silver resistance in *Acinetobacter baumannii*. Biometals. 1994;7: 49–56. doi:10.1007/BF00205194
705. Hendry AT, Stewart IO. Silver-resistant *Enterobacteriaceae* from hospital patients. Can J Microbiol. 1979;25: 915–921. doi:10.1139/m79-136
706. Hosny AE-DM, Rasmy SA, Aboul-Magd DS, Kashef MT, El-Bazza ZE. The increasing threat of silver-resistance in clinical isolates from wounds and burns. Infect Drug Resist. 2019;12: 1985–2001. doi:10.2147/IDR.S209881
707. Schwartz VB, Thétiot F, Ritz S, Pütz S, Choritz L, Lappas A, et al. Antibacterial surface coatings from zinc oxide nanoparticles embedded in poly (n-isopropylacrylamide) hydrogel surface layers. Adv Funct Mater. 2012;22: 2376–2386.
708. Straccia MC, d'Ayala GG, Romano I, Laurienzo P. Novel zinc alginate hydrogels prepared by internal setting method with intrinsic antibacterial activity. Carbohydr Polym. 2015;125: 103–112.
709. Baghaie S, Khorasani MT, Zarrabi A, Moshtaghian J. Wound healing properties of PVA/starch/chitosan hydrogel membranes with nano Zinc oxide as antibacterial wound dressing material. J Biomater Sci Polym Ed. 2017;28: 2220–2241.
710. Mata MT, Baquero F, Pérez-Díaz JC. A multidrug efflux transporter in *Listeria monocytogenes*. FEMS Microbiol Lett. 2000;187: 185–188. doi:10.1111/j.1574-6968.2000.tb09158.x
711. Hayashi S, Abe M, Kimoto M, Furukawa S, Nakazawa T. The DsbA-DsbB Disulfide Bond Formation System of *Burkholderia cepacia* Is Involved in the Production of Protease and Alkaline Phosphatase, Motility, Metal Resistance, and Multi-Drug Resistance. Microbiol Immunol. 2000;44: 41–50.
712. Perron K, Caille O, Rossier C, Van Delden C, Dumas J-L, Köhler T. CzcR-CzcS, a two-component system involved in heavy metal and carbapenem resistance in *Pseudomonas aeruginosa*. J Biol Chem. 2004;279: 8761–8768.
713. Becker LE, Bergstresser PR, Whiting DA, Clendenning WE, Dobson RL, Jordan WP, et al. Topical Clindamycin Therapy for Acne Vulgaris: A Cooperative Clinical Study. Arch Dermatol. 1981;117: 482–485. doi:10.1001/archderm.1981.01650080036024
714. Leyden JJ, Hickman JG, Jarratt MT, Stewart DM, Levy SF. The Efficacy and Safety of a CombinationBenzoyl Peroxide/Clindamycin Topical Gel Compared with Benzoyl Peroxide Alone anda Benzoyl Peroxide/Erythromycin Combination Product. J Cutan Med Surg Inc Med Surg Dermatology. 2001;5: 37–42. doi:10.1007/s102270000008
715. Ellis CN, Leyden J, Katz HI, Goldfarb MT, Hickman J, Jones TM, et al. Therapeutic studies with a new combination benzoyl peroxide/clindamycin topical gel in acne vulgaris. Cutis. 2001;67: 13–20.
716. Cunliffe WJ, Holland KT, Bojar R, Levy SF. A randomized, double-blind comparison of a clindamycin phosphate/benzoyl peroxide gel formulation and a matching clindamycin gel with respect to microbiologic activity and clinical efficacy in the topical treatment of acne vulgaris. Clin Ther. 2002;24: 1117–1133. doi:https://doi.org/10.1016/S0149-2918(02)80023-6
717. Dobson RL, Belknap BS. Topical erythromycin solution in acne: Results of a multiclinic trial. J Am Acad Dermatol. 1980;3: 478–482. doi:https://doi.org/10.1016/S0190-9622(80)80113-7
718. Lesher JL, Chalker DK, Smith JG, Guenther LC, Ellis CN, Voorhees JJ, et al. An evaluation of a 2% erythromycin ointment in the topical therapy of acne vulgaris. J Am Acad Dermatol. 1985;12: 526–531. doi:https://doi.org/10.1016/S0190-9622(85)70074-6
719. Jones EL, Crumley AF. Topical Erythromycin vs Blank Vehicle in a Multiclinic Acne Study. Arch Dermatol. 1981;117: 551–553. doi:10.1001/archderm.1981.01650090033020
720. Habbema L, Koopmans B, Menke HE, Doornweerd S, De Boulle K. A 4% erythromycin and zinc combination (Zineryt®) versus 2% erythromycin (Eryderm®) in acne vulgaris: a randomized, double-blind comparative study. Br J Dermatol. 1989;121: 497–502.
721. Burkhart CG, Burkhart CN. Treatment of acne vulgaris without antibiotics: tertiary amine–benzoyl peroxide combination vs. benzoyl peroxide alone (Proactiv Solution™). Int J Dermatol. 2007;46: 89–93.
722. Leyden JJ, Wortzman M, Baldwin EK. Antibiotic-resistant *Propionibacterium acnes* suppressed by a benzoyl peroxide cleanser 6%. Cutis. 2008;82: 417–421.
723. Mills Jr OH, Kligman AM, Pochi P, Comite H. Comparing 2.5%, 5%, and 10% benzoyl peroxide on inflammatory acne vulgaris. Int J Dermatol. 1986;25: 664–667.
724. Frade ML, De Annunzio SR, Calixto GM, Victorelli FD, Chorilli M, Fontana CR. Assessment of Chitosan-Based Hydrogel and Photodynamic Inactivation against *Propionibacterium acnes*. Molecules. 2018. doi:10.3390/molecules23020473
725. de Annunzio SR, de Freitas LM, Blanco AL, da Costa MM, Carmona-Vargas CC, de Oliveira KT, et al. Susceptibility of *Enterococcus faecalis* and *Propionibacterium acnes* to antimicrobial photodynamic therapy. J Photochem Photobiol B Biol. 2018;178: 545–550. doi:https://doi.org/10.1016/j.jphotobiol.2017.11.035
726. Wainwright M, Smalley H, Scully O, Lotfipour E. Comparative photodynamic evaluation of new phenothiazinium derivatives against *Propionibacterium acnes*. Photochem Photobiol. 2012;88: 523–526.

727. Gallo RL. Human Skin Is the Largest Epithelial Surface for Interaction with Microbes. J Invest Dermatol. 2017/04/08. 2017;137: 1213–1214. doi:10.1016/j.jid.2016.11.045
728. Tiwari VK. Burn wound: How it differs from other wounds? Indian J Plast Surg. 2012;45: 364–373.
729. Schülke & Mayr GmbH. octenilin® Wundgel.
730. Lochhead RY. The Role of Polymers in Cosmetics: Recent Trends. Cosmetic Nanotechnology. American Chemical Society; 2007. pp. 1–3. doi:doi:10.1021/bk-2007-0961.ch001
731. Chang C, Zhang L. Cellulose-based hydrogels: Present status and application prospects. Carbohydr Polym. 2011;84: 40–53. doi:https://doi.org/10.1016/j.carbpol.2010.12.023
732. Kroon G. Associative behavior of hydrophobically modified hydroxyethyl celluloses (HMHECs) in waterborne coatings. Prog Org Coatings. 1993;22: 245–260. doi:https://doi.org/10.1016/0033-0655(93)80027-8
733. Sun W, Sun D, Wei Y, Liu S, Zhang S. Oil-in-water emulsions stabilized by hydrophobically modified hydroxyethyl cellulose: Adsorption and thickening effect. J Colloid Interface Sci. 2007;311: 228–236. doi:https://doi.org/10.1016/j.jcis.2007.02.082
734. Cannazza G, Cataldo A, De Benedetto E, Demitri C, Madaghiele M, Sannino A. Experimental Assessment of the Use of a Novel Superabsorbent polymer (SAP) for the Optimization ofWater Consumption in Agricultural Irrigation Process. Water . 2014. doi:10.3390/w6072056
735. Liu M, Liang R, Zhan F, Liu Z, Niu A. Synthesis of a slow-release and superabsorbent nitrogen fertilizer and its properties. Polym Adv Technol. 2006;17: 430–438.
736. Kassab G, Cheburkanov V, Willis J, Moule MG, Kurachi C, Yakovlev V, et al. Safety and delivery efficiency of a photodynamic treatment of the lungs using indocyanine green and extracorporeal near infrared illumination. J Biophotonics. 2020;13: e202000176.
737. Rego-Filho FG, de Araujo MT, de Oliveira KT, Bagnato VS. Validation of Photodynamic Action via Photobleaching of a New Curcumin-Based Composite with Enhanced Water Solubility. J Fluoresc. 2014;24: 1407–1413. doi:10.1007/s10895-014-1422-z
738. Entradas T, Waldron S, Volk M. The detection sensitivity of commonly used singlet oxygen probes in aqueous environments. J Photochem Photobiol B Biol. 2020;204: 111787.
739. Wu H, Song Q, Ran G, Lu X, Xu B. Recent developments in the detection of singlet oxygen with molecular spectroscopic methods. TrAC Trends Anal Chem. 2011;30: 133–141. doi:https://doi.org/10.1016/j.trac.2010.08.009
740. Rossi LM, Silva PR, Vono LLR, Fernandes AU, Tada DB, Baptista MS. Protoporphyrin IX Nanoparticle Carrier: Preparation, Optical Properties, and Singlet Oxygen Generation. Langmuir. 2008;24: 12534–12538. doi:10.1021/la800840k
741. Zou Y, Long S, Xiong T, Zhao X, Sun W, Du J, et al. Single-Molecule Förster Resonance Energy Transfer-Based Photosensitizer for Synergistic Photodynamic/Photothermal Therapy. ACS Cent Sci. 2021;7: 327–334. doi:10.1021/acscentsci.0c01551
742. Ragàs X, Jiménez-Banzo A, Sánchez-García D, Batllori X, Nonell S. Singlet oxygen photosensitisation by the fluorescent probe Singlet Oxygen Sensor Green®. Chem Commun. 2009; 2920–2922.
743. Umezawa N, Tanaka K, Urano Y, Kikuchi K, Higuchi T, Nagano T. Novel fluorescent probes for singlet oxygen. Angew Chemie Int Ed. 1999;38: 2899–2901.
744. Lindig BA, Rodgers MAJ, Schaap AP. Determination of the lifetime of singlet oxygen in water-d2 using 9, 10-anthracenedipropionic acid, a water-soluble probe. J Am Chem Soc. 1980;102: 5590–5593.
745. You Y. Chemical tools for the generation and detection of singlet oxygen. Org Biomol Chem. 2018;16: 4044–4060.
746. Schweitzer C, Schmidt R. Physical Mechanisms of Generation and Deactivation of Singlet Oxygen. Chem Rev. 2003;103: 1685–1758. doi:10.1021/cr010371d
747. Ogilby PR. Solvent Effects on the Radiative Transitions of Singlet Oxygen. Acc Chem Res. 1999;32: 512–519. doi:10.1021/ar980005p
748. Snyder JW, Zebger I, Gao Z, Poulsen L, Frederiksen PK, Skovsen E, et al. Singlet Oxygen Microscope: From Phase-Separated Polymers to Single Biological Cells. Acc Chem Res. 2004;37: 894–901. doi:10.1021/ar040075y
749. Krasnovsky Jr AA. Photoluminescence of singlet oxygen in pigment solutions. Photochem Photobiol. 1979;29: 29–36.
750. Baier J, Fuß T, Pöllmann C, Wiesmann C, Pindl K, Engl R, et al. Theoretical and experimental analysis of the luminescence signal of singlet oxygen for different photosensitizers. J Photochem Photobiol B Biol. 2007;87: 163–173. doi:10.1016/j.jphotobiol.2007.02.006
751. Regensburger J, Maisch T, Felgenträger A, Santarelli F, Bäumler W. A helpful technology - The luminescence detection of singlet oxygen to investigate photodynamic inactivation of bacteria (PDIB). J Biophotonics. 2010;3: 319–327. doi:10.1002/jbio.200900106
752. Ragàs X, Gallardo A, Zhang Y, Massad W, Geddes CD, Nonell S. Singlet Oxygen Phosphorescence Enhancement by Silver Islands Films. J Phys Chem C. 2011;115: 16275–16281. doi:10.1021/jp202095a
753. Sanders ER. Aseptic laboratory techniques: plating methods. J Vis Exp. 2012; e3064–e3064. doi:10.3791/3064
754. Ellner PD, Papachristos T. Detection of bacteriuria by dip-slide: routine use in a large general hospital. Am J Clin Pathol. 1975;63: 516–521.
755. Sarker MAR, Ahn Y-H. Green phytoextracts as natural photosensitizers in LED-based photodynamic disinfection of multidrug-resistant bacteria in wastewater effluent. Chemosphere. 2022;297: 134157. doi:https://doi.org/10.1016/j.chemosphere.2022.134157
756. Lambrechts SAG, Aalders MCG, Verbraak FD, Lagerberg JWM, Dankert JB, Schuitmaker JJ. Effect of albumin on

the photodynamic inactivation of microorganisms by a cationic porphyrin. J Photochem Photobiol B Biol. 2005;79: 51–57. doi:https://doi.org/10.1016/j.jphotobiol.2004.11.020

757. Weber T. *In silico* tools for the analysis of antibiotic biosynthetic pathways. Int J Med Microbiol. 2014;304: 230–235. doi:https://doi.org/10.1016/j.ijmm.2014.02.001
758. Snow Setzer M, Sharifi-Rad J, Setzer WN. The Search for Herbal Antibiotics: An *In-Silico* Investigation of Antibacterial Phytochemicals. Antibiotics. 2016. doi:10.3390/antibiotics5030030
759. Mysak J, Podzimek S, Sommerova P, Lyuya-Mi Y, Bartova J, Janatova T, et al. *Porphyromonas gingivalis*: Major Periodontopathic Pathogen Overview. Riera CM, editor. J Immunol Res. 2014;2014: 476068. doi:10.1155/2014/476068
760. Baumgartner JC, Watkins BJ, Bae K-S, Xia T. Association of black-pigmented bacteria with endodontic infections. J Endod. 1999;25: 413–415. doi:https://doi.org/10.1016/S0099-2399(99)80268-4
761. Association JS. Test of Antimicrobial activity and efficacy. JIS Z 2801. 2000.
762. ISO 22196:2011-08. Measurement of antibacterial activity on plastics and other non-porous surfaces. 2011.
763. Wiegand C, Völpel A, Ewald A, Remesch M, Kuever J, Bauer J, et al. Critical physiological factors influencing the outcome of antimicrobial testing according to ISO 22196/JIS Z 2801. PLoS One. 2018;13: e0194339.
764. DIN EN 13697:2019-10. Chemische Desinfektionsmittel und Antiseptika - Quantitativer Oberflächen-Versuch zur Bestimmung der bakteriziden und/oder fungiziden Wirkung chemischer Desinfektionsmittel auf nicht porösen Oberflächen in den Bereichen Lebensmittel, Industrie, Haushalt u. 2019. doi:https://dx.doi.org/10.31030/3054767
765. The Members of the Disinfection Committee. Anforderungen und Methoden zur VAH-Zertifizierung chemischer Desinfektionsverfahren. Desinfektionsmittel-Kommission im VAH, editor. Wiesbaden: mhp Verlag GmbH; 2019.
766. Kampf G, Ostermeyer C. Intra-laboratory reproducibility of the hand hygiene reference procedures of EN 1499 (hygienic handwash) and EN 1500 (hygienic hand disinfection). J Hosp Infect. 2002;52: 219–224. doi:https://doi.org/10.1053/jhin.2002.1299
767. Convention USP. United States Pharmacopeia USP 35< 1072> Disinfectants and Antiseptics. United States Pharmacopeial Convention North Bethesda, MD, USA; 2012.
768. Nan L, Yang WC, Liu YQ, Xu H, Li Y, Lu MQ, et al. Antibacterial mechanism of copper-bearing antibacterial stainless steel against *E. coli*. 2008.
769. Hong IT, Koo CH. Antibacterial properties, corrosion resistance and mechanical properties of Cu-modified SUS 304 stainless steel. Mater Sci Eng A. 2005;393: 213–222.
770. Faure E, Lecomte P, Lenoir S, Vreuls C, Van De Weerdt C, Archambeau C, et al. Sustainable and bio-inspired chemistry for robust antibacterial activity of stainless steel. J Mater Chem. 2011;21: 7901–7904.
771. Dey BP, Engley FB. Neutralization of antimicrobial chemicals by recovery media. J Microbiol Methods. 1994;19: 51–58. doi:https://doi.org/10.1016/0167-7012(94)90025-6
772. Dey BP, Engley FB. Methodology for recovery of chemically treated *Staphylococcus aureus* with neutralizing medium. Appl Environ Microbiol. 1983;45: 1533–1537. doi:10.1128/aem.45.5.1533-1537.1983
773. Gelinas P, Goulet J. Neutralization of the activity of eight disinfectants by organic matter. J Appl Bacteriol. 1983;54: 243–247.
774. Misgana GM, Abdissa K, Abebe G. Bacterial contamination of mobile phones of health care workers at Jimma University Specialized Hospital, Jimma, South West Ethiopia. Int J Infect Control. 2015;11.
775. Mark D, Leonard C, Breen H, Graydon R, O'Gorman C, Kirk S. Mobile phones in clinical practice: reducing the risk of bacterial contamination. Int J Clin Pract. 2014;68: 1060–1064.
776. Messina G, Quercioli C, Burgassi S, Nisticò F, Lupoli A, Nante N. How many bacteria live on the keyboard of your computer? Am J Infect Control. 2011;39: 616–618. doi:10.1016/j.ajic.2010.12.023
777. Venkateswaran K, Hattori N, La Duc MT, Kern R. ATP as a biomarker of viable microorganisms in clean-room facilities. J Microbiol Methods. 2003;52: 367–377. doi:https://doi.org/10.1016/S0167-7012(02)00192-6
778. Kovach CR, Taneli Y, Neiman T, Dyer EM, Arzaga AJA, Kelber ST. Evaluation of an ultraviolet room disinfection protocol to decrease nursing home microbial burden, infection and hospitalization rates. BMC Infect Dis. 2017;17: 186. doi:10.1186/s12879-017-2275-2
779. Deshpande A, Dunn AN, Fox J, Cadnum JL, Mana TSC, Jencson A, et al. Monitoring the effectiveness of daily cleaning practices in an intensive care unit (ICU) setting using an adenosine triphosphate (ATP) bioluminescence assay. Am J Infect Control. 2020;48: 757–760. doi:https://doi.org/10.1016/j.ajic.2019.11.031
780. La Duc MT, Kern R, Venkateswaran K. Microbial Monitoring of Spacecraft and Associated Environments. Microb Ecol. 2004;47: 150–158. doi:10.1007/s00248-003-1012-0
781. Shama G, Malik DJ. The uses and abuses of rapid bioluminescence-based ATP assays. Int J Hyg Environ Health. 2013;216: 115–125. doi:https://doi.org/10.1016/j.ijheh.2012.03.009
782. Leggett RM, Clark MD. A world of opportunities with nanopore sequencing. J Exp Bot. 2017;68: 5419–5429. doi:10.1093/jxb/erx289
783. Deamer D, Akeson M, Branton D. Three decades of nanopore sequencing. Nat Biotechnol. 2016;34: 518–524. doi:10.1038/nbt.3423
784. Urban L, Holzer A, Baronas JJ, Hall MB, Braeuninger-Weimer P, Scherm MJ, et al. Freshwater monitoring by nanopore sequencing. Zambrano MM, Kana BD, Zambrano MM, Sanchez-Flores A, editors. Elife. 2021;10: e61504. doi:10.7554/eLife.61504
785. Brandt C, Bongcam-Rudloff E, Müller B. Abundance Tracking by Long-Read Nanopore Sequencing of Complex Microbial Communities in Samples from 20 Different Biogas/Wastewater Plants. Applied Sciences . 2020.

doi:10.3390/app10217518
786. Cuscó A, Catozzi C, Viñes J, Sanchez A, Francino O. Microbiota profiling with long amplicons using Nanopore sequencing: full-length 16S rRNA gene and the 16S-ITS-23S of the rrn operon. F1000Research. 2018;7: 1755. doi:10.12688/f1000research.16817.2
787. Cuscó A, Viñes J, D'Andreano S, Riva F, Casellas J, Sánchez A, et al. Using MinION^{TM} to characterize dog skin microbiota through full-length 16S rRNA gene sequencing approach. BioRxiv. 2017; 167015.
788. Cao MD, Ganesamoorthy D, Elliott AG, Zhang H, Cooper MA, Coin LJM. Streaming algorithms for identification of pathogens and antibiotic resistance potential from real-time MinION(TM) sequencing. Gigascience. 2016;5: 32. doi:10.1186/s13742-016-0137-2
789. Ferreira FA, Helmersen K, Visnovska T, Jørgensen SB, Aamot HV. Rapid nanopore-based DNA sequencing protocol of antibiotic-resistant bacteria for use in surveillance and outbreak investigation. Microb genomics. 2021;7: 557. doi:10.1099/mgen.0.000557
790. Hessler DP, Frimmel FH, Oliveros E, Braun AM. Solvent Isotope Effect on the Rate Constants of Singlet-Oxygen Quenching by edta and Its Metal Complexes. Helv Chim Acta. 1994;77: 859–868.
791. Wen X, Zhang X, Szewczyk G, El-Hussein A, Huang Y-Y, Sarna T, et al. Potassium iodide potentiates antimicrobial photodynamic inactivation mediated by rose bengal *in in vitro* and *in vivo* studies. Antimicrob Agents Chemother. 2017;61: e00467-17.
792. Reynoso E, Quiroga ED, Agazzi ML, Ballatore MB, Bertolotti SG, Durantini EN. Photodynamic inactivation of microorganisms sensitized by cationic BODIPY derivatives potentiated by potassium iodide. Photochem Photobiol Sci. 2017;16: 1524–1536.
793. Dai C, Lin J, Li H, Shen Z, Wang Y, Velkov T, et al. The Natural Product Curcumin as an Antibacterial Agent: Current Achievements and Problems. Antioxidants . 2022. doi:10.3390/antiox11030459
794. Li C, Chen T, Ocsoy I, Zhu G, Yasun E, You M, et al. Gold-coated Fe3O4 nanoroses with five unique functions for cancer cell targeting, imaging, and therapy. Adv Funct Mater. 2014;24: 1772–1780.
795. Sun T, Wang Y, Wang Y, Xu J, Zhao X, Vangveravong S, et al. Using SV119-Gold Nanocage Conjugates to Eradicate Cancer Stem Cells Through a Combination of Photothermal and Chemo Therapies. Adv Healthc Mater. 2014;3: 1283–1291.
796. Shi P, Ju E, Ren J, Qu X. Near-Infrared Light-Encoded Orthogonally Triggered and Logical Intracellular Release Using Gold Nanocage@ Smart Polymer Shell. Adv Funct Mater. 2014;24: 826–834.
797. Di Corato R, Palumberi D, Marotta R, Scotto M, Carregal-Romero S, Rivera_Gil P, et al. Magnetic nanobeads decorated with silver nanoparticles as cytotoxic agents and photothermal probes. Small. 2012;8: 2731–2742.
798. Xiao J-W, Fan S-X, Wang F, Sun L-D, Zheng X-Y, Yan C-H. Porous Pd nanoparticles with high photothermal conversion efficiency for efficient ablation of cancer cells. Nanoscale. 2014;6: 4345–4351.
799. Tang S, Chen M, Zheng N. Sub-10-nm Pd Nanosheets with renal clearance for efficient near-infrared photothermal cancer therapy. Small. 2014;10: 3139–3144.
800. Yang K, Feng L, Shi X, Liu Z. Nano-graphene in biomedicine: theranostic applications. Chem Soc Rev. 2013;42: 530–547.
801. Antaris AL, Robinson JT, Yaghi OK, Hong G, Diao S, Luong R, et al. Ultra-low doses of chirality sorted (6, 5) carbon nanotubes for simultaneous tumor imaging and photothermal therapy. ACS Nano. 2013;7: 3644–3652.
802. Zhang Z, Wang Z, Wang F, Ren J, Qu X. Programmable Downregulation of Enzyme Activity Using a Fever and NIR-Responsive Molecularly Imprinted Nanocomposite. Small. 2015;11: 6172–6178.
803. Li M, Yang X, Ren J, Qu K, Qu X. Using graphene oxide high near-infrared absorbance for photothermal treatment of Alzheimer's disease. Adv Mater. 2012;24: 1722–1728.
804. Lin J, Wang S, Huang P, Wang Z, Chen S, Niu G, et al. Photosensitizer-Loaded Gold Vesicles with Strong Plasmonic Coupling Effect for Imaging-Guided Photothermal/Photodynamic Therapy. ACS Nano. 2013;7: 5320–5329. doi:10.1021/nn4011686
805. Huang X, Chen G, Pan J, Chen X, Huang N, Wang X, et al. Effective PDT/PTT dual-modal phototherapeutic killing of pathogenic bacteria by using ruthenium nanoparticles. J Mater Chem B. 2016;4: 6258–6270.
806. Laserstrahlung T. Technische Regeln zur Arbeitsschutzverordnung zu künstlicher optischer Strahlung. 2016.
807. ten Cate JM, Damen JJM, Buijs MJ. Inhibition of Dentin Demineralization by Fluoride *in vitro*. Caries Res. 1998;32: 141–147. doi:10.1159/000016444
808. Martins SHL, Novaes Jr AB, Taba Jr M, Palioto DB, Messora MR, Reino DM, et al. Effect of surgical periodontal treatment associated to antimicrobial photodynamic therapy on chronic periodontitis: A randomized controlled clinical trial. J Clin Periodontol. 2017;44: 717–728.
809. Lulic M, Leiggener Görög I, Salvi GE, Ramseier CA, Mattheos N, Lang NP. One-year outcomes of repeated adjunctive photodynamic therapy during periodontal maintenance: a proof-of-principle randomized-controlled clinical trial. J Clin Periodontol. 2009;36: 661–666.
810. Christodoulides N, Nikolidakis D, Chondros P, Becker J, Schwarz F, Rössler R, et al. Photodynamic therapy as an adjunct to non-surgical periodontal treatment: a randomized, controlled clinical trial. J Periodontol. 2008;79: 1638–1644.
811. Braun A, Dehn C, Krause F, Jepsen S. Short-term clinical effects of adjunctive antimicrobial photodynamic therapy in periodontal treatment: a randomized clinical trial. J Clin Periodontol. 2008;35: 877–884.
812. Moreira AL, Novaes Jr AB, Grisi MF, Taba Jr M, Souza SL, Palioto DB, et al. Antimicrobial photodynamic therapy

as an adjunct to non-surgical treatment of aggressive periodontitis: A split-mouth randomized controlled trial. J Periodontol. 2015;86: 376–386.

813. Petelin M, Perkič K, Seme K, Gašpirc B. Effect of repeated adjunctive antimicrobial photodynamic therapy on subgingival periodontal pathogens in the treatment of chronic periodontitis. Lasers Med Sci. 2015;30: 1647–1656. doi:10.1007/s10103-014-1632-2
814. Bassetti M, Schär D, Wicki B, Eick S, Ramseier CA, Arweiler NB, et al. Anti-infective therapy of peri-implantitis with adjunctive local drug delivery or photodynamic therapy: 12-month outcomes of a randomized controlled clinical trial. Clin Oral Implants Res. 2014;25: 279–287.
815. Thierbach R, Eger T. Clinical outcome of a nonsurgical and surgical treatment protocol in different types of peri-implantitis: a case series. Quintessence Int. 2013;44: 137–148.
816. Alwaeli HA, Al-Khateeb SN, Al-Sadi A. Long-term clinical effect of adjunctive antimicrobial photodynamic therapy in periodontal treatment: a randomized clinical trial. Lasers Med Sci. 2015;30: 801–807. doi:10.1007/s10103-013-1426-y
817. Arweiler NB, Pietruska M, Skurska A, Dolińska E, Pietruski JK, Bläs M, et al. Nonsurgical treatment of aggressive periodontitis with photodynamic therapy or systemic antibiotics. Three-month results of a randomized, prospective, controlled clinical study. Schweizer Monatsschrift für Zahnmedizin. 2013;123: 532–544.
818. de Oliveira RR, Novaes AB, Garlet GP, de Souza RF, Taba M, Sato S, et al. The effect of a single episode of antimicrobial photodynamic therapy in the treatment of experimental periodontitis. Microbiological profile and cytokine pattern in the dog mandible. Lasers Med Sci. 2011;26: 359–367. doi:10.1007/s10103-010-0864-z
819. Sigusch BW, Engelbrecht M, Völpel A, Holletschke A, Pfister W, Schütze J. Full-Mouth Antimicrobial Photodynamic Therapy in Fusobacterium nucleatum–Infected Periodontitis Patients. J Periodontol. 2010;81: 975–981.
820. Rakašević D, Lazić Z, Rakonjac B, Soldatović I, Janković S, Magić M, et al. Efficiency of photodynamic therapy in the treatment of peri-implantitis: A three-month randomized controlled clinical trial. Srp Arh Celok Lek. 2016;144: 478–484.
821. Ahad A, Lamba AK, Faraz F, Tandon S, Chawla K, Yadav N. Effect of Antimicrobial Photodynamic Therapy as an Adjunct to Nonsurgical Treatment of Deep Periodontal Pockets: A Clinical Study. J lasers Med Sci. 2016/10/27. 2016;7: 220–226. doi:10.15171/jlms.2016.39
822. Jurič IB, Plečko V, Pandurić DG, Anić I. The antimicrobial effectiveness of photodynamic therapy used as an addition to the conventional endodontic re-treatment: a clinical study. Photodiagnosis Photodyn Ther. 2014;11: 549–555.
823. Silva LAB, Novaes AB, de Oliveira RR, Nelson-Filho P, Santamaria M, Silva RAB. Antimicrobial Photodynamic Therapy for the Treatment of Teeth with Apical Periodontitis: A Histopathological Evaluation. J Endod. 2012;38: 360–366. doi:https://doi.org/10.1016/j.joen.2011.12.023
824. Chondros P, Nikolidakis D, Christodoulides N, Rössler R, Gutknecht N, Sculean A. Photodynamic therapy as adjunct to non-surgical periodontal treatment in patients on periodontal maintenance: a randomized controlled clinical trial. Lasers Med Sci. 2009;24: 681–688.
825. Macedo G de O, Novaes AB, Souza SLS, Taba M, Palioto DB, Grisi MFM. Additional effects of aPDT on nonsurgical periodontal treatment with doxycycline in type II diabetes: a randomized, controlled clinical trial. Lasers Med Sci. 2014;29: 881–886. doi:10.1007/s10103-013-1285-6
826. HELBO GmbH. HELBO (R) Manual. Available: https://www.helbo.de/blaetterkatalog/epaper-Helbo_Manual_deutsch/index.html#22
827. Lawrence MJ, Rees GD. Microemulsion-based media as novel drug delivery systems. Adv Drug Deliv Rev. 2000;45: 89–121. doi:https://doi.org/10.1016/S0169-409X(00)00103-4
828. Huang SS, Septimus E, Kleinman K, Moody J, Hickok J, Heim L, et al. Chlorhexidine versus routine bathing to prevent multidrug-resistant organisms and all-cause bloodstream infections in general medical and surgical units (ABATE Infection trial): a cluster-randomised trial. Lancet (London, England). 2019/03/05. 2019;393: 1205–1215. doi:10.1016/S0140-6736(18)32593-5
829. Ki V, Rotstein C. Bacterial skin and soft tissue infections in adults: A review of their epidemiology, pathogenesis, diagnosis, treatment and site of care. Can J Infect Dis Med Microbiol = J Can des Mal Infect la Microbiol medicale. 2008;19: 173–184. doi:10.1155/2008/846453
830. Lapolla WJ, Levender MM, Davis SA, Yentzer BA, Williford PM, Feldman SR. Topical antibiotic trends from 1993 to 2007: use of topical antibiotics for non-evidence-based indications. Dermatologic Surg. 2011;37: 1427–1433.
831. Williamson D, Ritchie SR, Best E, Upton A, Leversha A, Smith A, et al. A bug in the ointment: topical antimicrobial usage and resistance in New Zealand. NZ Med J. 2015;128: 103–109.
832. Wuite J, Davies BI, Go M, Lambers J, Jackson D, Mellows G. Pseudomonic Acid: A New Topical Antimicrobial Agent. Lancet. 1983;322: 394. doi:10.1016/S0140-6736(83)90358-6
833. Dacre JE, Emmerson AM, Jenner EA. Nasal Carriage Of Gentamicin And Methicillin Resistant Staphylococcus aureus Treated With Topical Pseudomonic Acid. Lancet. 1983;322: 1036. doi:10.1016/S0140-6736(83)91029-2
834. Reilly GD, Spencer RC. Pseudomonic acid—a new antibiotic for skin infections. J Antimicrob Chemother. 1984;13: 295–298. doi:10.1093/jac/13.3.295
835. Phillips LM, Yogev RAM, Esterly NB. The efficacy of mupirocin (pseudomonic acid) in the treatment of pyoderma in children. Pediatr Emerg Care. 1985;1. Available: https://journals.lww.com/pec-online/Fulltext/1985/12000/The_efficacy_of_mupirocin___pseudomonic_acid___in.2.aspx
836. Rumsfield J, West DP, Aronson IK. Topical Mupirocin in the Treatment of Bacterial Skin Infections. Drug Intell Clin Pharm. 1986;20: 943–948. doi:10.1177/106002808602001204

837. Eells LD, Mertz PM, Piovanetti Y, Pekoe GM, Eaglstein WH. Topical Antibiotic Treatment of Impetigo With Mupirocin. Arch Dermatol. 1986;122: 1273–1276. doi:10.1001/archderm.1986.01660230065012
838. Koning S, van der Sande R, Verhagen AP, van Suijlekom-Smit LWA, Morris AD, Butler CC, et al. Interventions for impetigo. Cochrane Database Syst Rev. 2012. doi:10.1002/14651858.CD003261.pub3
839. Sutherland R, Boon RJ, Griffin KE, Masters PJ, Slocombe B, White AR. Antibacterial activity of mupirocin (pseudomonic acid), a new antibiotic for topical use. Antimicrob Agents Chemother. 1985;27: 495–498. doi:10.1128/AAC.27.4.495
840. Thomas CM, Hothersall J, Willis CL, Simpson TJ. Resistance to and synthesis of the antibiotic mupirocin. Nat Rev Microbiol. 2010;8: 281–289. doi:10.1038/nrmicro2278
841. Antonio M, McFerran N, Pallen MJ. Mutations affecting the Rossman fold of isoleucyl-tRNA synthetase are correlated with low-level mupirocin resistance in *Staphylococcus aureus*. Antimicrob Agents Chemother. 2002;46: 438–442.
842. Hodgson JE, Curnock SP, Dyke KG, Morris R, Sylvester DR, Gross MS. Molecular characterization of the gene encoding high-level mupirocin resistance in *Staphylococcus aureus* J2870. Antimicrob Agents Chemother. 1994;38: 1205–1208. doi:10.1128/AAC.38.5.1205
843. Lima de Castro Nunes E, dos Santos KRN, Mondino PJJ, de Freire Bastos M do C, Giambiagi-deMarval M. Detection of ileS-2 gene encoding mupirocin resistance in methicillin-resistant *Staphylococcus aureus* by multiplex PCR. Diagn Microbiol Infect Dis. 1999;34: 77–81. doi:https://doi.org/10.1016/S0732-8893(99)00021-8
844. Laurberg M, Kristensen O, Martemyanov K, Gudkov AT, Nagaev I, Hughes D, et al. Structure of a mutant EF-G reveals domain III and possibly the fusidic acid binding site11Edited by I. A. Wilson. J Mol Biol. 2000;303: 593–603. doi:https://doi.org/10.1006/jmbi.2000.4168
845. Norström T, Lannergård J, Hughes D. Genetic and Phenotypic Identification of Fusidic Acid-Resistant Mutants with the Small-Colony-Variant Phenotype in *Staphylococcus aureus*. Antimicrob Agents Chemother. 2007;51: 4438–4446. doi:10.1128/AAC.00328-07
846. Mariana C, A. WA, M. BJ, D. TJ, N. JR. Fusidic Acid Resistance Rates and Prevalence of Resistance Mechanisms among *Staphylococcus* spp. Isolated in North America and Australia, 2007-2008. Antimicrob Agents Chemother. 2010;54: 3614–3617. doi:10.1128/AAC.01390-09
847. Besier S, Ludwig A, Brade V, Wichelhaus TA. Molecular analysis of fusidic acid resistance in *Staphylococcus aureus*. Mol Microbiol. 2003;47: 463–469.
848. Besier S, Albrecht L, Brade T, Wichelhaus T. Compensatory Adaptation to the Loss of Biological Fitness Associated with Acquisition of Fusidic Acid Resistance in *Staphylococcus aureus*. Antimicrob Agents Chemother. 2005;49: 1426–1431. doi:10.1128/AAC.49.4.1426-1431.2005
849. Koripella RK, Chen Y, Peisker K, Koh CS, Selmer M, Sanyal S. Mechanism of Elongation Factor-G-mediated Fusidic Acid Resistance and Fitness Compensation in Staphylococcus aureus*. J Biol Chem. 2012;287: 30257–30267. doi:10.1074/jbc.M112.378521
850. Cox G, Thompson GS, Jenkins HT, Peske F, Savelsbergh A, Rodnina M V, et al. Ribosome clearance by FusB-type proteins mediates resistance to the antibiotic fusidic acid. Proc Natl Acad Sci. 2012;109: 2102 LP – 2107. doi:10.1073/pnas.1117275109
851. Huang J, Ye M, Ding H, Guo Q, Ding B, Wang M. Prevalence of fusB in *Staphylococcus aureus* clinical isolates. J Med Microbiol. 2013;62: 1199–1203. doi:https://doi.org/10.1099/jmm.0.058305-0
852. Farrell DJ, Castanheira M, Chopra I. Characterization of Global Patterns and the Genetics of Fusidic Acid Resistance. Clin Infect Dis. 2011;52: S487–S492. doi:10.1093/cid/cir164
853. Waksman SA, Lechevalier HA. Neomycin, a new antibiotic active against streptomycin-resistant bacteria, including tuberculosis organisms. Science (80-). 1949;109: 305–307.
854. Magnet S, Blanchard JS. Molecular Insights into Aminoglycoside Action and Resistance. Chem Rev. 2005;105: 477–498. doi:10.1021/cr0301088
855. Jones RN, Li Q, Kohut B, Biedenbach DJ, Bell J, Turnidge JD. Contemporary antimicrobial activity of triple antibiotic ointment: a multiphased study of recent clinical isolates in the United States and Australia. Diagn Microbiol Infect Dis. 2006;54: 63–71. doi:https://doi.org/10.1016/j.diagmicrobio.2005.08.009
856. Evans FL. A note on the susceptibility of *Hemophilus influenzae* type B to bacitracin. J Bacteriol. 1948;56: 507.
857. M. TM, D. BS. Proposed MIC and Disk Diffusion Microbiological Cutoffs and Spectrum of Activity of Retapamulin, a Novel Topical Antimicrobial Agent. Antimicrob Agents Chemother. 2008;52: 3863–3867. doi:10.1128/AAC.00399-08
858. Gentry D, Rittenhouse S, McCloskey L, Holmes D. Stepwise Exposure of *Staphylococcus aureus* to Pleuromutilins Is Associated with Stepwise Acquisition of Mutations in *rplC* and Minimally Affects Susceptibility to Retapamulin. Antimicrob Agents Chemother. 2007;51: 2048–2052. doi:10.1128/AAC.01066-06
859. Joakim H, Camilla B, Kerstin L, Emma S, Veronika S, Margit M. Efficacy of the Novel Topical Antimicrobial Agent PXL150 in a Mouse Model of Surgical Site Infections. Antimicrob Agents Chemother. 2014;58: 2982–2984. doi:10.1128/AAC.00143-14
860. Flamm RK, Rhomberg PR, Farrell DJ, Jones RN. *In vitro* spectrum of pexiganan activity; bactericidal action and resistance selection tested against pathogens with elevated MIC values to topical agents. Diagn Microbiol Infect Dis. 2016;86: 66–69. doi:https://doi.org/10.1016/j.diagmicrobio.2016.06.012
861. Flamm R, Rhomberg P, Simpson K, Farrell D, Sader H, Jones R. *In Vitro* Spectrum of Pexiganan Activity When Tested against Pathogens from Diabetic Foot Infections and with Selected Resistance Mechanisms. Antimicrob Agents Chemother. 2022;59: 1751–1754. doi:10.1128/AAC.04773-14

862. Silvestri DL, McEnery-Stonelake M. Chlorhexidine: Uses and Adverse Reactions. Dermatitis®. 2013;24. Available: https://journals.lww.com/dermatitis/Fulltext/2013/05000/Chlorhexidine___Uses_and_Adverse_Reactions.6.aspx
863. Loftus MJ, Florescu CJ, Stuart RL. *Staphylococcus aureus* bacteraemia associated with peripherally inserted central catheters: the role of chlorhexidine gluconate-impregnated sponge dressings. Med J Aust. 2014;200: 317–318.
864. Rupp ME, Lisco SJ, Lipsett PA, Perl TM, Keating K, Civetta JM, et al. Effect of a Second-Generation Venous Catheter Impregnated with Chlorhexidine and Silver Sulfadiazine on Central Catheter–Related Infections. Ann Intern Med. 2005;143: 570–580. doi:10.7326/0003-4819-143-8-200510180-00007
865. Sijbesma T, Röckmann H, Van Der Weegen W. Severe Anaphylactic Reaction to Chlorhexidine during Total Hip Arthroplasty Surgery. A Case Report. HIP Int. 2011;21: 630–632. doi:10.5301/HIP.2011.8644
866. Parkes AW, Harper N, Herwadkar A, Pumphrey R. Anaphylaxis to the chlorhexidine component of Instillagel®: a case series. BJA Br J Anaesth. 2009;102: 65–68. doi:10.1093/bja/aen324
867. Maki DG. The Use of Antiseptics for Handwashing by Medical Personnel. J Chemother. 1989;1: 3–11. doi:10.1080/1120009X.1989.11738936
868. Mangram AJ, Horan TC, Pearson ML, Silver LC, Jarvis WR. Guideline for Prevention of Surgical Site Infection, 1999. Infect Control Hosp Epidemiol. 2015/01/02. 1999;20: 247–280. doi:DOI: 10.1086/501620
869. Horner C, Mawer D, Wilcox M. Reduced susceptibility to chlorhexidine in staphylococci: is it increasing and does it matter? J Antimicrob Chemother. 2012;67: 2547–2559. doi:10.1093/jac/dks284
870. Climo MW, Sepkowitz KA, Zuccotti G, Fraser VJ, Warren DK, Perl TM, et al. The effect of daily bathing with chlorhexidine on the acquisition of methicillin-resistant *Staphylococcus aureus*, vancomycin-resistant *Enterococcus*, and healthcare-associated bloodstream infections: Results of a quasi-experimental multicente. Crit Care Med. 2009;37. Available: https://journals.lww.com/ccmjournal/Fulltext/2009/06000/The_effect_of_daily_bathing_with_chlorhexidine_on.4.aspx
871. Russell AD, Path FRC. Chlorhexidine: Antibacterial action and bacterial resistance. Infection. 1986;14: 212–215. doi:10.1007/BF01644264
872. Best M, Sattar SA, Springthorpe VS, Kennedy ME. Efficacies of selected disinfectants against *Mycobacterium tuberculosis*. J Clin Microbiol. 1990;28: 2234–2239. doi:10.1128/jcm.28.10.2234-2239.1990
873. Bonez PC, dos Santos Alves CF, Dalmolin TV, Agertt VA, Mizdal CR, Flores V da C, et al. Chlorhexidine activity against bacterial biofilms. Am J Infect Control. 2013;41: e119–e122. doi:https://doi.org/10.1016/j.ajic.2013.05.002
874. Wassenaar T, Ussery D, Nielsen L, Ingmer H. Review and phylogenetic analysis of qac genes that reduce susceptibility to quaternary ammonium compounds in *Staphylococcus* species. Eur J Microbiol Immunol. 2015;5: 44–61. doi:10.1556/eujmi-d-14-00038
875. Smith K, Gemmell CG, Hunter IS. The association between biocide tolerance and the presence or absence of *qac* genes among hospital-acquired and community-acquired MRSA isolates. J Antimicrob Chemother. 2008;61: 78–84. doi:10.1093/jac/dkm395
876. Lu Z, Chen Y, Chen W, Liu H, Song Q, Hu X, et al. Characteristics of *qacA/B*-positive *Staphylococcus aureus* isolated from patients and a hospital environment in China. J Antimicrob Chemother. 2015;70: 653–657. doi:10.1093/jac/dku456
877. Block SS. Disinfection, sterilization, and preservation. Lippincott Williams & Wilkins; 2001.
878. Sedlock DM, Bailey DM. Microbicidal activity of octenidine hydrochloride, a new alkanediylbis [pyridine] germicidal agent. Antimicrob Agents Chemother. 1985;28: 786–790.
879. Bailey DM, DeGrazia CG, Hoff SJ, Schulenberg PL, O'Connor JR, Paris DA, et al. Bispyridinamines: a new class of topical antimicrobial agents as inhibitors of dental plaque. J Med Chem. 1984;27: 1457–1464.
880. Ghannoum MA, Elteen KA, Ellabib M, Whittaker PA. Antimycotic effects of octenidine and pirtenidine. J Antimicrob Chemother. 1990;25: 237–245.
881. Harke HP. Octenidine dihydrochloride, properties of a new antimicrobial agent. Zentralblatt fur Hyg und Umweltmedizin= Int J Hyg Environ Med. 1989;188: 188–193.
882. Al-Doori Z, Goroncy-Bermes P, Gemmell CG, Morrison D. Low-level exposure of MRSA to octenidine dihydrochloride does not select for resistance. J Antimicrob Chemother. 2007;59: 1280–1281.
883. Rohr U, Mueller C, Wilhelm M, Muhr G, Gatermann S. Methicillin-resistant *Staphylococcus aureus* whole-body decolonization among hospitalized patients with variable site colonization by using mupirocin in combination with octenidine dihydrochloride. J Hosp Infect. 2003;54: 305–309.
884. Sloot N, Siebert J, Höffler U. Eradication of MRSA from carriers by means of whole-body washing with an antiseptic in combination with mupirocin nasal ointment. Zentralblatt für Hyg und Umweltmedizin. 1999;202: 513–523.
885. Hansen D, Patzke P-I, Werfel U, Benner D, Brauksiepe A, Popp W. Success of MRSA eradication in hospital routine: depends on compliance. Infection. 2007;35: 260–264.
886. Jones RD, Jampani HB, Newman JL, Lee AS. Triclosan: A review of effectiveness and safety in health care settings. Am J Infect Control. 2000;28: 184–196. doi:https://doi.org/10.1067/mic.2000.102378
887. Russell AD. Whither triclosan? J Antimicrob Chemother. 2004;53: 693–695. doi:10.1093/jac/dkh171
888. Stewart MJ, Parikh S, Xiao G, Tonge PJ, Kisker C. Structural basis and mechanism of enoyl reductase inhibition by triclosan11Edited by P. E. Wright. J Mol Biol. 1999;290: 859–865. doi:https://doi.org/10.1006/jmbi.1999.2907
889. Heath RJ, Rubin JR, Holland DR, Zhang E, Snow ME, Rock CO. Mechanism of Triclosan Inhibition of Bacterial Fatty Acid Synthesis *. J Biol Chem. 1999;274: 11110–11114. doi:10.1074/jbc.274.16.11110

890. McMurry LM, Oethinger M, Levy SB. Triclosan targets lipid synthesis. Nature. 1998;394: 531–532. doi:10.1038/28970
891. Schweizer HP. Triclosan: a widely used biocide and its link to antibiotics. FEMS Microbiol Lett. 2001;202: 1–7. doi:10.1111/j.1574-6968.2001.tb10772.x
892. Brenwald NP, Fraise AP. Triclosan resistance in methicillin-resistant *Staphylococcus aureus* (MRSA). J Hosp Infect. 2003;55: 141–144. doi:https://doi.org/10.1016/S0195-6701(03)00222-6
893. Chen Y, Pi B, Zhou H, Yu Y, Li L. Triclosan resistance in clinical isolates of *Acinetobacter baumannii*. J Med Microbiol. 2009;58: 1086–1091. doi:https://doi.org/10.1099/jmm.0.008524-0
894. Grandgirard D, Furi L, Ciusa ML, Baldassarri L, Knight DR, Morrissey I, et al. Mutations upstream of *fabI* in triclosan resistant *Staphylococcus aureus* strains are associated with elevated *fabI* gene expression. BMC Genomics. 2015;16: 345. doi:10.1186/s12864-015-1544-y
895. Ciusa ML, Furi L, Knight D, Decorosi F, Fondi M, Raggi C, et al. A novel resistance mechanism to triclosan that suggests horizontal gene transfer and demonstrates a potential selective pressure for reduced biocide susceptibility in clinical strains of *Staphylococcus aureus*. Int J Antimicrob Agents. 2012;40: 210–220. doi:https://doi.org/10.1016/j.ijantimicag.2012.04.021
896. Furi L, Haigh R, Al Jabri ZJH, Morrissey I, Ou H-Y, León-Sampedro R, et al. Dissemination of Novel Antimicrobial Resistance Mechanisms through the Insertion Sequence Mediated Spread of Metabolic Genes. Front Microbiol. 2016;7. doi:10.3389/fmicb.2016.01008
897. Durani P, Leaper D. Povidone–iodine: use in hand disinfection, skin preparation and antiseptic irrigation. Int Wound J. 2008;5: 376–387.
898. Hugo WB. A brief history of heat and chemical preservation and disinfection. J Appl Bacteriol Oxford. 1991;71: 9–18.
899. Shelanski HA. PVP-iodine: history, toxicity and therapeutic uses. J Inter Coll Surg. 1956.
900. Zamora JL. Chemical and microbiologic characteristics and toxicity of povidone-iodine solutions. Am J Surg. 1986;151: 400–406. doi:https://doi.org/10.1016/0002-9610(86)90477-0
901. Mitani O, Nishikawa A, Kurokawa I, Gabazza EC, Ikeda M, Mizutani H. Enhanced wound healing by topical application of ointment containing a low concentration of povidone-iodine. J Wound Care. 2016;25: 521–529. doi:10.12968/jowc.2016.25.9.521
902. Goldenheim PD. An appraisal of povidone-iodine and wound healing. Postgrad Med J. 1993;69 Suppl 3: S97—105. Available: http://europepmc.org/abstract/MED/8290466
903. O'Meara S, Al-Kurdi D, Ologun Y, Ovington LG, Martyn-St James M, Richardson R. Antibiotics and antiseptics for venous leg ulcers. Cochrane Database Syst Rev. 2014.
904. Eggers M, Eickmann M, Kowalski K, Zorn J, Reimer K. Povidone-iodine hand wash and hand rub products demonstrated excellent in vitro virucidal efficacy against Ebola virus and modified vaccinia virus Ankara, the new European test virus for enveloped viruses. BMC Infect Dis. 2015;15: 375. doi:10.1186/s12879-015-1111-9
905. Sabracos L, Romanou S, Dontas I, Coulocheri S, Ploumidou K, Perrea D. The *in vitro* effective antiviral action of povidone–iodine (PVP–I) may also have therapeutic potential by its intravenous administration diluted with Ringer's solution. Med Hypotheses. 2007;68: 272–274. doi:https://doi.org/10.1016/j.mehy.2006.07.039
906. Capriotti K, Capriotti JA. Topical iodophor preparations: chemistry, microbiology, and clinical utility. Dermatol Online J. 2012;18.
907. Hill RLR, Casewell MW. The *in-vitro* activity of povidone–iodinecream against *Staphylococcus aureus* and its bioavailability in nasal secretions. J Hosp Infect. 2000;45: 198–205. doi:https://doi.org/10.1053/jhin.2000.0733
908. Bolon M. Hand Hygiene. Infect Dis Clin. 2011;25: 21–43. doi:10.1016/j.idc.2010.11.001
909. Sroka S, Gastmeier P, Meyer E. Impact of alcohol hand-rub use on meticillin-resistant *Staphylococcus aureus*: an analysis of the literature. J Hosp Infect. 2010;74: 204–211. doi:https://doi.org/10.1016/j.jhin.2009.08.023
910. Morton HE. The relationship of concentration and germicidal efficiency of ethyl alcohol. Ann N Y Acad Sci. 1950;53: 191–196.
911. Woodruff LBA, Pandhal J, Ow SY, Karimpour-Fard A, Weiss SJ, Wright PC, et al. Genome-scale identification and characterization of ethanol tolerance genes in *Escherichia coli*. Metab Eng. 2013;15: 124–133. doi:https://doi.org/10.1016/j.ymben.2012.10.007
912. Gérando HM de, Fayolle-Guichard F, Rudant L, Millah SK, Monot F, Ferreira NL, et al. Improving isopropanol tolerance and production of *Clostridium beijerinckii* DSM 6423 by random mutagenesis and genome shuffling. Appl Microbiol Biotechnol. 2016;100: 5427–5436. doi:10.1007/s00253-016-7302-5
913. Akinosho H, Rydzak T, Borole A, Ragauskas A, Close D. Toxicological challenges to microbial bioethanol production and strategies for improved tolerance. Ecotoxicology. 2015;24: 2156–2174. doi:10.1007/s10646-015-1543-4
914. Luther MK, Bilida S, Mermel LA, LaPlante KL. Ethanol and Isopropyl Alcohol Exposure Increases Biofilm Formation in *Staphylococcus aureus* and *Staphylococcus epidermidis*. Infect Dis Ther. 2015;4: 219–226. doi:10.1007/s40121-015-0065-y
915. Knobloch JK-M, Horstkotte MA, Rohde H, Kaulfers P-M, Mack D. Alcoholic ingredients in skin disinfectants increase biofilm expression of *Staphylococcus epidermidis*. J Antimicrob Chemother. 2002;49: 683–687. doi:10.1093/jac/49.4.683
916. Nwugo CC, Arivett BA, Zimbler DL, Gaddy JA, Richards AM, Actis LA. Effect of Ethanol on Differential Protein Production and Expression of Potential Virulence Functions in the Opportunistic Pathogen *Acinetobacter baumannii*. PLoS One. 2012;7: e51936. Available: https://doi.org/10.1371/journal.pone.0051936
917. Linley E, Denyer SP, McDonnell G, Simons C, Maillard J-Y. Use of hydrogen peroxide as a biocide: new consideration of its mechanisms of biocidal action. J Antimicrob Chemother. 2012;67: 1589–1596. doi:10.1093/jac/dks129

918. Omidbakhsh N, Sattar SA. Broad-spectrum microbicidal activity, toxicologic assessment, and materials compatibility of a new generation of accelerated hydrogen peroxide-based environmental surface disinfectant. Am J Infect Control. 2006;34: 251–257. doi:https://doi.org/10.1016/j.ajic.2005.06.002

919. Horn K, Otter JA. Hydrogen peroxide vapor room disinfection and hand hygiene improvements reduce *Clostridium difficile* infection, methicillin-resistant *Staphylococcus aureus*, vancomycin-resistant enterococci, and extended-spectrum β-lactamase. Am J Infect Control. 2015;43: 1354–1356. doi:https://doi.org/10.1016/j.ajic.2015.06.029

920. Barbut F, Menuet D, Verachten M, Girou E. Comparison of the Efficacy of a Hydrogen Peroxide Dry-Mist Disinfection System and Sodium Hypochlorite Solution for Eradication of *Clostridium difficile* Spores. Infect Control Hosp Epidemiol. 2015/01/02. 2009;30: 507–514. doi:DOI: 10.1086/597232

921. Hiti K, Walochnik J, Faschinger C, Haller-Schober E-M, Aspöck H. One- and two-step hydrogen peroxide contact lens disinfection solutions against *Acanthamoeba*: How effective are they? Eye. 2005;19: 1301–1305. doi:10.1038/sj.eye.6701752

922. Rogez-Kreuz C, Yousfi R, Soufflet C, Quadrio I, Yan Z-X, Huyot V, et al. Inactivation of Animal and Human Prions by Hydrogen Peroxide Gas Plasma Sterilization. Infect Control Hosp Epidemiol. 2015/01/02. 2009;30: 769–777. doi:DOI: 10.1086/598342

923. Repine JE, Fox RB, Berger EM. Hydrogen peroxide kills *Staphylococcus aureus* by reacting with staphylococcal iron to form hydroxyl radical. J Biol Chem. 1981;256: 7094–7096. doi:10.1016/S0021-9258(19)68927-1

924. Imlay J, Chin S, Stuart L. Toxic DNA Damage by Hydrogen Peroxide Through the Fenton Reaction *in Vivo* and *in Vitro*. Science (80-). 1988;240: 640–642. doi:10.1126/science.2834821

925. Eason MM, Fan X. The role and regulation of catalase in respiratory tract opportunistic bacterial pathogens. Microb Pathog. 2014;74: 50–58. doi:https://doi.org/10.1016/j.micpath.2014.07.002

926. Binesse J, Lindgren H, Lindgren L, Conlan W, Sjöstedt A, Payne MS. Roles of Reactive Oxygen Species-Degrading Enzymes of *Francisella tularensis* SCHU S4. Infect Immun. 2015;83: 2255–2263. doi:10.1128/IAI.02488-14

Web resources were accessed on 11.04.2022